JAERI-Conf--98-016

JAERI-Conf
98-016

PROCEEDINGS OF THE THIRD SPECIALISTS' MEETING ON HIGH ENERGY NUCLEAR DATA, MARCH 30-31, 1998, JAERI, TOKAI, JAPAN

November 1998

(Ed.) Tokio FUKAHORI

日本原子力研究所
Japan Atomic Energy Research Institute

本レポートは，日本原子力研究所が不定期に公刊している研究報告書です。
入手の問合わせは，日本原子力研究所研究情報部研究情報課（〒319-1195　茨城県那珂郡東海村）あて，お申し越しください。なお，このほかに財団法人原子力弘済会資料センター〒319-1195　茨城県那珂郡東海村日本原子力研究所内）で複写による実費領布をおこなっております。

This report is issued irregularly.
Inquiries about availability of the reports should be addressed to Research Information Division, Department of Intellectual Resources, Japan Atomic Energy Research Institute, Tokai-mura, Naka-gun, Ibaraki-ken 319-1195, Japan.

編集兼発行　日本原子力研究所

JAERI−Conf 98−016

Proceedings of the Third Specialists' Meeting on High Energy Nuclear Data March 30-31, 1998, JAERI, Tokai, Japan

(Ed.) Tokio FUKAHORI

Japanese Nuclear Data Committee and Nuclear Data Center
Tokai Research Establishment
Japan Atomic Energy Research Institute
Tokai-mura, Naka-gun, Ibaraki-ken

(Received October 7, 1998)

This report is the Proceedings of the Third Specialists' Meeting on High Energy Nuclear Data. The meeting was held on March 30-31, 1998, at the Tokai Research Establishment of Japan Atomic Energy Research Institute with the participation of forty-odd specialists, who were the evaluators, theorists, experimentalists and users of high energy nuclear data including the members of the Japanese Nuclear Data Committee. The need of the high energy nuclear data up to a few Gev has been stressed in the meeting for many applications, such as spallation neutron sources for radioactive waste treatment, accelerator shielding design, medical isotope production, radiation therapy, the effects of space radiation on astronauts and their equipments, and the cosmic history of meteorites and other galactic substances. Since the Second Specialists' Meeting in 1995, such an evaluation activity in Japan has been grown and the results are accumulated. Foreign activities of high energy nuclear data evaluation are also being increased. According to the above situation, with the view point of reviewing and validating an evaluated high energy nuclear data file, project of high energy nuclear data file production, differential and integral experiments, status of evaluation and reviewing methods, processing and transport calculation methods, benchmark tests, international trends, etc. were discussed.

Keywords: Proceedings, Nuclear Data, High Energy, Evaluation, Experiment, Applicative Review, Theoretical Review

JAERI－Conf 98－016

第3回高エネルギー核データ専門家会議報文集
1998年3月30日～31日、東海研究所、東海村

日本原子力研究所東海研究所
シグマ研究委員会・核データセンター
（編）深掘　智生

（1998年10月7日受理）

本報文集は、第3回高エネルギー核データ専門家会議の報文を収録したものである。専門家会議は、1998年3月30日と31日の両日、日本原子力研究所東海研究所において、40数名の専門家の出席のもとに開催された。出席した専門家は、高エネルギー核データの評価者、理論的研究者、実験者、利用者及びシグマ委員会委員であった。数GeVまでの入射エネルギーにおける高エネルギー核データは、放射性廃棄物処理のためのスポレーション中性子源、加速器の遮蔽設計、医療用放射性同位元素製造、放射線治療、宇宙空間での宇宙飛行士や装置への宇宙線の影響の研究、宇宙物理学などの多岐にわたる分野から必要とされている。第2回専門家会議の後、わが国では評価及び理論的研究の進展及びその結果の集積があり、諸外国での高エネルギー核データ評価活動も盛んになってきた。このような状況を受け、本専門家会議では、高エネルギー核データの評価済ファイルの信頼性検証を行うという視点に立って、高エネルギー核データファイル整備計画、微分及び積分実験、評価の現状及びレビュー手法、処理法と輸送計算法、ベンチマークテスト、海外の動向などが報告・討議された。

東海研究所：〒319-1195　茨城県那珂郡東海村白方白根2-4

Contents

目　　次

1. Project of High Energy Nuclear Data File Production

1.1 Task Force for Integral Test of High Energy Nuclear Data

Yukio OYAMA

Planning Division for Neutron Science, Japan Atomic Energy Research Institute

Tokai-mura, Naka-gun, Ibaraki-ken, 319-11

e-mail: oyama@fnshp.tokai.jaeri.go.jp

According to completion of the JENDL-High Energy file for neutron nuclear cross sections up to 50 MeV, a task force for integral test of high energy nuclear data was organized to discuss a guide line for integral test activities. A status of existing differential and integral experiments and how to perform such a test were discussed in the task force. Here the purpose and outline of the task force is explained with some future problems raised in discussion among the task member.

1. Introduction

In JENDL activities, the working group for evaluation of high energy neutron data has been continued to make nuclear data files for high energy neutron data, JENDL-High Energy files. For such data files, the first data set was compiled up to 50 MeV. The File was requested from IFMIF (International Fusion Materials Irradiation Facility)[1] design team for a standard nuclear data file among the IFMIF international team collaborated under IEA. The IFMIF file also was converted to MCNP library to utilize in the nuclear design. The JENDL-High Energy file will be also extended to up to GeV region for use in high energy accelerator facilities. In this context, JAERI is proposing Neutron Science Project[2] which intends to make high intense and high energy proton accelerator together with an intense spallation neutron source and nuclear transmutation facilities.

As a normal procedure for the evaluated nuclear data files, the JENDL-High Energy file should be tested before using in the design calculation. However, there was very few experiments that can be used for such testing and also no code which uses a library processed directly from the evaluated nuclear data file. These caused a requirement of working group for finding how to solve the problem. Then the Task Force has been organized in the Nuclear Data

Committee.

2. Purpose and Sub-Tasks

The purpose of the present task force was set to the followings.

1) to make it clear how to perform an integral test,
2) to feed back to nuclear evaluation activity from the test method settled ,
3) to consider an integral test from user point of view and application.

To implement these, the following sub-groups were settled.

1) G-1: Differential experimental data
2) G-2: Benchmark Experiment
3) G-3: Data Processing and Neutron Transport Calculation Methods
4) G-4: Method for Data Reviewing
5) G-5: Investigation of the status in the other country

Each group was tried to grasp a status and direction of individual area for a year.

3. New Aspect of Evaluated Nuclear Data for utilization in High Energy Region

Moving from low energy as below 20 MeV to high energy as up to GeV, application codes for particle transport is significantly changed in philosophy of the codes. Most of high energy transport codes do not use the libraries produced from ENDF formatted files. Then this energy shift leads us to the following problems.

1) A method of transport and data library can not be extrapolated from the existing library such as a fusion library made from JENDL-Fusion File below 20 MeV.
2) Integral tests for fusion and shielding neutronics were strongly combined with transport calculation method such as MCNP. Therefore the integral tests were performed by MCNP with ACE-format library converted from ENDF-file..
3) In the high energy particle transport codes such as nuclear cascade codes, a library does not connected directly to ENDF-file and does not required whole set of ENDF-data.
4) Some parameters for application to transport calculation can not be obtained from a file as ENDF-6 format, i.e., the disappearance cross section.

4. Comments from Working Group of High Energy Nuclear Data Library

During discussion in the task force, the recommendation report[3] was provided from the working group of high energy nuclear data library in the Sub-Committee of High Energy Particles in the Reactor Physics Committee. The recommendation included that:

1) Application area can be divided to several hundred MeV and GeV regions for medical use and nuclear energy use, respectively.
2) Problems and issues are pointed out as similar way of the previous section.
3) Types of required data are rather specified to nuclide production and removal cross section for GeV application, while a MCNP type data library is desired for medical use.
4) In conclusion, compromising the best way to provide the evaluated nuclear data, a joint work is necessary between evaluator and code developer.

The above recommendation includes a policy for evaluation of high energy nuclear data files.

5. Concluding Remarks

The Task Force for Integral Test of High Energy Nuclear Data was settled and worked for the last one year. Five sub-working groups were worked to investigate the status of individual area. These results follow the present paper. The goal of the task force has not been finished, because of findings of the problem related to new aspect. However, the next step is expected to start in new activity for high energy data evaluation under recommendations given here.

References

[1]IFMIF CDA Team, "IFMIF, International Fusion Materials Irradiation Facility, Conceptual Design Activity, Final Report," RT/ERG/FUS/96/11, ENEA, Italy (1996)

[2]T. Mukaiyama, et al., "Neutron Science Project at JAERI", Proc. ANS Topical Meeting on Nuclear Application of Accelerator Technology (AccApp'97), Nov. 16-20, Albuquerque, USA (1997)

[3]Working group of high energy nuclear data library, private communication (1998)

2. Differential and Integral Experiments

2.1 Status of Experimental Data for Neutron Induced Reactions

Mamoru BABA
Graduate School of Quantum Science & Energy Engineering
Tohoku University, 980-8579, Sendai Japan
mamoru.baba@qse.toholu.ac.jp

A short review is presented on the status of experimental data for neutron induced reactions above 20 MeV based on the EXFOR data base and journals. Experimental data which were obtained in a systematic manner and/or by plural authors are surveyed and tabulated for the nuclear data evaluation and the benchmark test of the evaluated data.

1.Introduction

This reports reviews the status of experimental data for neutron induced reactions above 20 MeV on the basis of data compilations and papers to support the evaluation and benchmark test of JENDL High Energy File, which is under progress to facilitate the application of large accelerator facilities, i.e., nuclear waste incineration, intense neutron sources and medical application and so on.

In high energy regions, nuclear data evaluation will be mainly based on the theoretical and/or semi-empirical calculations rather than experimental data themselves because the data required are too comprehensive to be measured by experiments, and facilities that enables the neutron experiments above 20 MeV are very limited. Therefore, the main role of experimental data is to validate the models and parameters for the evaluation. From this view point, experimental data that are systematic, i.e., covering a certain number of nuclei, reactions and incident energies, and are studied by plural authors, are highly desirable because they enable the validation of the models and parameters, and also screening of inappropriate data. In addition, it is important for the engineering purposes that the data cover a wide range of energies and angles.

The review is, therefore, mainly focused on the data which were studied in systematic manner or in plural independent experiments. In the following, such systematic data are tabulated irrespective of element because such data are very few in the case of neutron induced reactions. Some figures are also presented to indicate the status of experimental data.

2.Outline of the review

For neutron and proton induced data in 20-1500 MeV region, an extensive review has been reported by A.Koning [Ko93].

In the present review, experimental data for neutron induced reactions were surveyed in the EXFOR system. However, no small number of useful data are not stored in the EXFOR system, while they were reported in literatures and other compilations. Therefore, the survey was extended to Barashenkov compilation [Ba83], journals on nuclear science (Phys. Rev. C, Nucl. Phys., Nucl. Sci. & Eng.,) and proceedings of nuclear data conference (Mito, Jeulich, Gatlinburg, Trieste)..

In the following, data are summarized along with the following classification, according to the experimental method:

1)Total cross section,
2)Neutron scattering and emission cross section,
3)Charged-particle emission cross section ,
4)Activation and isotope-production cross section ,
5)Fission cross section,
6)Gamma-ray production cross section, and
7)Dosimetry, neutron detection cross section.

This classification is slightly different from that in JENDL-HF but convenient to review the experimental data because a)the neutron scattering and emission cross sections are usually measured by similar experimental methods, and b)the gas production cross sections are measured by charged-particle detection. The data for dosimetry and neutron detection are important as the basis for neutronics and nuclear data measurements in the energy region.

As a specific point to the high energy data, neutrons and charged-particles are emitted with strong energy-angle correlation through many reaction channels. Therefore, for realistic estimation of the particle transport and the radiation effects, the energy-angular doubly-differential cross section data are of special importance and should be provided adequately for all major reaction channels energetically possible.

3.Data Status

In the following, typical experimental data which will be useful for the evaluation and the benchmark test are summarized for each quantity, with the EXFOR entry No. or the information to access the data if the data are not stored in EXFOR.

3.1 Total cross section

Total cross section data are important as the basis for neutronic calculations and shielding designs. They are also the basis of nuclear data evaluation because they provide constraints for partial cross sections and the optical model potential. The total cross section can be measured by the

Table 1: Experimental data for the neutron total cross section

Author	En (MeV)	Nuclei / element	Ref.	EXFOR
Larson+	1 – 80	C, O, Al, Si, Ca, Cr, Fe, Ni, Cu, Au, Pb	La80	
Franz +	160 – 575 (22points)	Be, ^{12}C, ^{16}O, Al, V, Mn, Co, Cu, Ag, Ce, Ta, Pb, Bi, ^{238}U	Fr88	22117
Finlay + (LANSCE)	1- 600 (ΔE/E < 1%) ($\Delta\sigma/\sigma$ < 1 %)	Be, C, N, O, ^{19}F, ^{23}Na, ^{27}Al, Si, ^{40}Ca, Cu, ^{90}Zr, ^{93}Nb, Sn, ^{127}I, ^{133}Cs, 181Ta, ^{208}Pb, ^{209}Bi	Fi93	13569
Dietlich+ (LANSCE)		H, ^{6}Li, ^{7}Li, ^{10}B, ^{11}B, B, ^{12}C, ^{13}C, N, O, F, P, S, K, Ti, V, Cr, Mn, (^{54}Fe, ^{56}Fe,) Fe, Co, Ni, Y, Mo, In, (^{182,183,184,186}W), W, Au, Hg, Pb, (Th), ^{238}U	Di97	
Schimmering +	900-2600 (15points)	Be, C, Al, Fe, Ni, Cu, Zn, Ag, Sn, Pb, Bi, U	Sc73	Ref. Table 13569

conventional transmission method with continuous spectrum neutrons. As shown in Table 1, several systematic experimental data have been reported up to GeV or higher. In particular, recent measurements at LANSCE give high precision data up to 600 MeV with the statistical accuracy and the energy resolution around 1 % (Fig.1[Fi93]).[Die97]. They are in good agreement with others (Fig.2[Fi93]), [La80], [Fr88].

3.2 Neutron Scattering cross section

Table 2 summarizes the neutron scattering data. (The H(n,n) reaction is classified in 3.3 charged-particle emission reaction). Neutron scattering and emission data are very few above 25.7 MeV despite of the importance for the transport calculations.

The difficulty of neutron scattering measurements above 30 MeV is in the lack of mono-energetic neutron source. In the region, therefore, the spectra of secondary neutrons can not be measured by the straightforward TOF method, but should be measured with a neutron spectrometer having ray-tracing capability and large angular acceptance. Generally, in addition, the energy

Table 2: Experimental data for neutron scattering above 20 MeV

Institute	En(MeV)	Nuclei / element	Ref.	EXFOR/ Data
Studswick	21.5	Be, ^{14}N, ^{16}O, Mg, ^{24}Mg, ^{27}Al, ^{28}Si, ^{32}S, S, ^{40}Ca, Ca, Cr, ^{52}Cr, Fe, ^{59}Co, ^{58}Ni, ^{89}Y, Ce, ^{206}Pb, ^{209}Bi	O187, O1901 O1902	21123, 21152, 22128, 22048, 22127
Ohio Univ.,	25.7	^{51}V, ^{56}Fe, 65Cu, ^{93}Nb, ^{209}Bi [DDX]	Ma83	Table
	20-26	^{6}Li, ^{7}Li, 10B, C, ^{13}C, N, ^{16}O, ^{18}O, ^{26}Mg, ^{28}Si, ^{32}S, Ca, ^{58}Ni, ^{90,91,92}Zr, ^{93}Nb, ^{208}Pb	Ha88, Fin80 Tay83,Me85 Sa90	21123,21152,13161,13162,12942,
JAERI	21, 28	^{12}C, ^{28}Si, ^{32}S	Ya77, Ya89	21628,21629,22160
Tohoku	35	^{12}C	Ni90	22167
Michigan St. Univ.,	30, 40	C, ^{28}Si, S, Ca, ^{208}Pb	DeV79	12701,12871 12724
CIAE	37	C, Bi	Ta97	
UC Davis	65	C, Si, Ca , Fe, Sn, Pb	Hj94	13510
UC Davis	65	Fe, Sn, Pn [DDX]	Hj95	13510
Oxford	96 136	Li, Be, C, N, Al, Cu, Cd, Pb, U θ = 2-22°	Sa60	21123 21374
UC Davis/ LANL	52.5- 225	^{12}C, ^{40}Ca, ^{208}Pb	Os95	
LANL	3.1-57.5 3.0-200	^{27}Al(n,n`$\gamma_{1.4}$) $^{207,208}$Pb(n,n`γ_{2614})	Pa94 Vo94	13643.002

resolution of the spectrometer is not high enough to separate neutrons due to elastic and inelastic scattering.

For the elastic scattering, nevertheless, several experimental data have been obtained by TOF or spectrometer method by correcting for the inelastic contribution. Fig.3 shows the elastic-scattering data at 65 MeV by UC Davis group using the spectrometer method [Hj95]. New experiments are going on in some laboratories using the ^{7}Li(p,n), T(d,n) quasi-monoenergetic neutron sources [Hj94], [Ta97],[Ol972] and a continuous spallation neutron source [Os95].

For inelastic-scattering and DDX, only a few data are available. Inelastic scattering to discrete levels can be measured only by gamma-ray detection; detailed excitation functions of inelastic-scattering to some levels of Al and Pb were obtained from MeV to 200/400 MeV by the (n,xγ) measurements at LANSCE [Pa94],[Vo94]. For DDX, the data by the UC Davis group at 65 MeV [Hj95] are the only one. The data are shown in Fig.4 in comparison with the (p,p'x) spectra.

Neutron non-elastic (reaction) cross section is also useful for data evaluation and shielding calculation, and several experimental data have been reported [Sc73], [Ze83]. However, these experimental data seem rather uncertain because of various assumptions applied in the data derivation. Therefore, more data are expected for the elastic-scattering and inelastic-scattering.

3.3 Charged particle emission reactions

Table 3 show the summary the data for charged-particle emission reactions.

As for the H(n,p) cross section, many measurements have been done as it is one of the most fundamental quantities in nuclear physics and technology. Based on the experiments and various theoretical analysis, the H(n,p) cross section is known best to several percent even in the intermediate

Table 3: Experimental data for the neutron-induced charged-particle emission cross section

Institute	En(MeV)	Nuclei / Elements	Ref.	EXFOR
UC Davis	25, 40, 65	^{12}C, ^{14}N, ^{16}O [p,d,t, α : DDX] H, ^{4}He, ^{6}Li, ^{7}Li, ^{9}Be, ^{19}F, ^{27}Al, Si, ^{58,60}Ni, ^{90}Zr [(n,p), (n,d) to levels]	Sa83, Sa86 Br91 +	Priv.comm. 12784,12786, 12845,13496
KfK	20.5-48	H	Fi90	22207
LANL	5-50	Be, C, ^{27}Al, Si, ^{56}Fe, ^{59}Co, ^{58,60}Ni, ^{93}Nb, ^{197}Au [p,d,t, α : DDX]	Ha971 Ha972	Priv.comm.
UCL (Louvain)	25-72 ,	H, D, C, O, Al, Si [p,d,t, α : DDX]	Sl95, Sl96 Me97+	Priv.comm. 22303
Tohoku/ JAERI	65, 75	C, Al, Fe [p,d DDX]	Na97	Priv.comm.
Uppsala	97, 162 96	H ^{12}C, ^{54}Fe, ^{56}Fe, Zr, ^{208}Pb	Ol97, Ri97	22223,22277
TRIUMF	198, 280	^{6}Li, ^{12}C, ^{13}C, ^{20}Ne, ^{64}Ni,	JA88	13150
LANL	459	H	No93	13623
LANL	800MeV	H, ^{6}Li, ^{7}Li, Be, ^{27}Al, Cu, ^{64}Ni, [(n,d), Forward angle only]	Ri78	10829

energy region. Recently, however, as shown in Fig.5, Uppsala group reported difference from the accepted values by about 10 % at very backward angles [Ol97],[Ol92]. This problem should be solved urgently because of the importance as the fundamental physics parameter.

For the (n,p) and (n,d) reactions, several systematic experiments have been carried out in the 50-200 MeV region aiming at the physics of the giant resonance and the nuclear structure [Ri78], [Ja88]. In the cases, the data were restricted only to the high energy (low excitation) region and very forward angles, and lacking the low energy part important for the assessment of radiation damage.

Experiments covering a wider energy and angular range were first performed by UC Davis group [Sa83], and recently promoted by UCL [Sl95] (Fig.6), LANL[Ha971], and Tohoku/JAERI [Na97] group using a specially-developed spectrometer with a large dynamic range. For, C, O and Al, data from different groups are now available for inter-comparison. Fig.7 illustrates a comparison of experimental data for the C(n,xp) reaction. The data by two groups are in general agreement but show marked discrepancies in low energy region.

3.4 Activation and isotope-production cross section

Table 4 summarizes the measurements of activation and isotope-production cross sections. Activation cross section data are required for the evaluation of induced activity in accelerator facilities, and for the nuclear data evaluation because they are available over various elements/reactions and energies. For the reason, data have been reported by several groups and new measurements are also planned [Ne97].

The lack of mono-energy neutrons introduces problems also in the activation measurements. Backgrounds due to non mono-energetic neutrons have to be subtracted using the data for low energy

Table 4: Experimental data for the neutron-induced activation and transmutation cross section

Institute	En(MeV)	Nuclei / Elements	Ref.	EXFOR
Tohoku/INS/ TIARA/ RIKEN	30-220 27.5- 38.2	$^{12}C(n,2n)^{11}C$, $^{23}Na(n,2n)^{22}Na$, $^{27}Al(n,2\alpha)^{22}Na$, $^{54}Fe(n,3n)$, (n,t) $^{59}Co(n,2n)^{58}Co$, $^{59}Co(n,4n)56Co$, $^{nat}Cu(n,sp)^{56}Mn$, ^{60}Co, ^{60}Cu, ^{61}Cu, ^{65}Ni $^{209}Bi(n,Nn)$: N = 3-12	Ki98 Na98 Uw94	22335.010
Uppsala/ Hannover	78	C,O, Al, Si, Fe, Co, Ni, Cu, Ag (AMS technique)		
LANL	3-200 23-27 14.7-21	$^{27}Al(n,x\gamma)$Al, Mg, Na, Ne, F production $^{207,208}Pb(n,x\gamma)$Pb, Tl, Hg $^{12}C(n,2n)$, Fe(n,2n)	Pa94 Vo94	13643 13644 11303.002 12936.007
Jeulich	22.5	C(n, t), $^{54}Fe(n,t)$ (n, ^{3}He)		20840
Kurchatova	22- 37.5 17.5-37.5	$^{12}C(n,2n)$, $^{16}O(n,2n)$		40715
LANL Ohio Univ.	23-27 22-26	$^{12}C(n,2n)$		11303

region. Therefore, experimental data should be accumulated from low energy and care should be taken for background subtraction. Consequently, systematic studies are very important to obtain consistent data up to higher energies. T.Nakamura et al. reported many data between 20 MeV and 210 MeV using various facilities. Figs.8 and 9 illustrate the data of $^{12}C(n,2n)$ and $^{209}Bi(n,Nn)$ reaction [Na98], [Ki98]. The latter data are expected to be used as a neutron spectrometer in tens to hundred MeV region.

On the transmutation and isotope-production reaction, (n,xγ) measurement at LANSCE enabled a lot of information to be obtained as a consistent data set over a wide energy range [Pa94], [Vo94].

For C, Al, Fe and Pb, activation and isotope-production data from several groups are available for inter-comparison.

3.5Fission Cross Sections

In Table 5, shown are the experimental data on neutron induced fission cross section.

Fission cross sections data are important not only for the energy production but also for the dosimetry or neutron measurements, and have been measured at various laboratories using continuous spallation neutrons or quasi-monoenergetic neutrons by the $^{7}Li(p,n)$ reaction. The measurement can be done by counting fission fragment yields by an multi-plates ionization chamber. Most measurements were done relative to ^{235}U using a back-to-back fission chambers and their absolute values are determined using the absolute values by LANL using the H(n,p) cross section. Therefore, new absolute measurements are highly expected as well as ratio data up to higher energies. Some measurements are also done on the energy, mass and angular distribution of fission fragments which will be useful to study the mechanism of the nuclear fission.

Table 5 Fission cross section measurements above 20 MeV

Institute	En(MeV)	Nuclei / Elements	Ref.	EXFOR
LANL	0.5-400	^{238}U ^{232}Th, $^{233,234,236}U$, ^{237}Np	Li88	Priv. Comm.
Gatchina/KRI	1 – 200	^{232}Th, $^{235,238}U$, ^{237}Np	Fo97	*1
Uppsala/KRI	70-160	^{208}Pb, ^{209}Bi, ^{238}U ^{232}Th, ^{235}U, ^{238}U,	Ei96	22320
UCL/PTB	34, 46, 61	^{238}U	New97	
IPPE	20.5-21.0	^{238}U		40169
Kuchatova	21.7 - 23.2 22.9 - 23.2	^{197}Au Pt		41037.007 41037.006
ICP	120-380 380	^{209}Bi, ^{235}U, ^{238}U Pb, Tl, ^{197}Au, Pt, W, ^{232}Th		41212
ITEF	1140-7303 2217-8084 3015-3170	^{235}U ^{235}U ^{239}Pu		40156.005 40156.004 40156.006
BRC	22.8 – 28.2	^{235}U, ^{238}U, ^{239}Pu		21685

*1: See the report by Shcherbakov in this proceedings.

In Fig.9, shown is the comparison of fission cross sections between neutron induced fission and proton-induced fission [Co96], which is interesting to see the relation between neutron-induced reactions and proton induced reactions.

3.6 Gamma-ray production cross section

Several experimental data have been reported on the gamma-ray production cross section. Among them, the measurements at LANSCE provided high resolution gamma-ray spectra for MeV to 200 or 400 MeV neutrons using an intense spallation neutron source. The gamma-ray spectrum data brought detailed information on the inelastic-scattering via the discrete levels, isotope-production and transmutation cross sections over a wide range of neutron energy. The inelastic scattering cross section of discrete levels for En>20 MeV can be obtained only by this way because of the limited energy resolution of neutron spectrometers for secondary neutrons.

Therefore, the gamma-ray production data provides not only engineering data for shielding and heating calculations but also very useful information on the reaction and the nuclear structure.

3.7 Dosimetry and neutron detector cross section

In the energy region above 20 MeV, the method of dosimetry and neutron detection should be developed further. For the purpose, activation or isotope-production reactions with a suitable decay scheme and a half-life will be useful as well as the n-p scattering and fission.

New data have been reported on the activation or isotope-production, for example, Bi(n,Nn), Al(b,xn), Pb(n,xn) seem to be good candidates for the purposes. Appropriate reactions should be chosen as the standard reaction for dosimetry and neutron detection, and their data should be updated based on the recent experimental data.

As noted above, the H(n,p) reaction is the best known one while some problems are pointed out. Neutron induced fission will also be useful for flux measurements and dosimetry, because of the simplicity and the stability of fission chambers. For the purpose, fission cross section data above 400 MeV are expected.

4. General comment and Summary

As noted above, experimental data on neutron induced reaction above 20 MeV are very few and not satisfactory in quality. Such a situation will be largely due to the scarcity of appropriate neutron source facilities and motive force for the measurements. In particular, the lack of mono-energy neutrons makes difficult the experiments of neutron scattering, activation and isotope production cross sections. In addition, neutron experiments in the past were mainly motivated by the physics point of view, and restricted only in the region of the physical interest.

In these ten years, nevertheless, new neutron source facilities have been developed and several new measurements have been conducted in this energy region in reply to the growing interest for high energy nuclear data required for application of high energy accelerators. These experimental data overlap to some extent in nuclei, reactions, and the incident energies, and form a fairly good data base to update the evaluation and do benchmark test of the evaluation. Nevertheless, further progress in neutron data measurements is needed because the data are not sufficient yet both in quantity and quality. To promote the experimental activity, installation of appropriate neutron sources, with a high intensity and a short pulse-duration, are essential as remarked by the outstanding achievement and activities at LANSCE spallation source.

Acknowledgement: The author wishes to thank Dr. N.Yamano and S.Tanaka for providing him with very useful information and references. Many thank are also to Mr.Y.Nauchi and T.Nunomiya for their cooperation in the survey of articles.

References

1

[Ko93]A.J.Koning, ECN-C793-005(1993)

[Ba83] B.C.Barashenkov, "Cross Section of Interactions of Particles and Nuclei with Nuclei " JINR, Dubna (1983)

3.1

[La80] D.C.Larson, BNL-NCS-51245 (1980) p.277

[Fra88] J.Franz et al.: Nucl.Phys., A490 667 (1988)

[Fin93] R.W.Finlay et al: Phys. Rev., C47(1) (1993) 237

[Di97] F.S.Dietrich et al.: Proc. Conf. Nuclear Data, 1997 Treieste, to be published,

[Sc73] W.Schimmering et al.: Phys. Rev., C7, 248 (1973)

3.2

[Ol87] N.Olsson et al: Nucl. Phys., 472, 237 (1987),

[Ol901] N.Olsson et al.; ibid., 509, 161 (1990)

[Ol901] N.Olsson et al.: ibid., 513, 205 (1990)

[Ma83] A.Marcinkowski et al.: Nucl.Sci. Eng.,□□・ 83 13 (1983),

[Fin80] R.W.Finlay and J.Rapaport: BNL-NCS-51245 (BNL 1980) p.375

[Tay83] R.C.Taylor, J.Rapaport, R.W.Finlay, G.Randers-Pheson: Nucl. Phys., 401 237 (1983)

[Me85] A.S.Meigooni, R.W.Finlay, J.S. Peteler, J.P.Delaroche: Nucl.Phys., 445 304 (1985)

[Sa90] E.T. Sadowski, H.D.Knox, D.A.Resler, R.O.Lane: Phys. Rev., C42 190 (1990)

[Ha88] L.F.Hansen et al.: Phys. Rev., C38 525 (1988)

[Ya77] Y.Yamanoucti: Nucl. Phys., A283, 23 (1977)

[Ya89] Y.Yamanouti et al.: JAERI-M 89-119

[Ni90] T.Niizeki et al.: Nucl. Instrum. Methods, 287, 455 (1990),

[DeV79] Dissertation, Michigan State Univ., (1979)

[Ta97] H.Tan et al: Proc. Conf. Nuclear Data, 1997 Treieste, to be published,

[Hj94] E.L.Hjort et al.: Phys.Rev., C53(1), (1996) 237

[Hj95] E.L.Hjort et al.: Phys.Rev., C50(1), 275 (1994)

[Os95] J.H.Osborn, JR: Dissertation, Univ. of California, Davis (1995)

[Vo94] H.Vonach et al.: Phys. Rev., C50 (4) 1952 (1994)

[Sa60] G.L.Salman: Nucl Phys., 21, 15 (1960)

[Za80]C.I.Zanelli et al.: BNL-NCS-51245 (BNL 1980) p.313

3.3

[Ol97] N.Olsson et al.: Phys.Rev., C45 (2) R496 (1992), and Proc. Int. Conf. Nuclear Data, 1997 Tre? 垜ieste, to be published

[Sa83] T.S.Sabramanian et al.: Phys.Rev., C28 (2), (1983) 521

[Sa86] T.S.Sabramanian et al.: Phys.Rev., C34 (5), (1986) 1580

[Br91] F.P.Brady et al.: Phys. Rev., C43 2284 (1991)

[Fi90] G.Fink et al.: Nucl. Phys., A518 561 81990)

[Ha971] R.C.Haight: Int. Conf. Nuclear Data, 1997 Treieste, to be published,

[Ha972] R.C.Haight, F.B.Bateman, S.M.Stebenz, M.B.Chadwick, P.G.Young, S.M.Grimes: ibid.,
[Sl95] I.Slypen, V.C.Corcalciuc, J.P.Meulders, M.B.Chadwick: Phys.Rev., C53 (3), 1310 (1996)
[Sl96] I.Slypen, V.C.Corcalciuc, J.P.Meulders: Phys.Rev., C51 (3), 1304 (1995)
[Me97] J.P.Meulders et al.: Proc. Int. Conf. Nuclear Data, 1997 Treieste, to be published
[Na97] Y.Nauchi et al.: ibid.,
[Ri97] Rigbom et al.: Nucl. Phys., A617 31□・ □6 (1997)
[Ja88] K.P.Jackson, A.Celler, W.P.Alford et al., Phys. Lett., B201 25 (1988)
[Ri78] P.J.Riley et al.: Phys. Rev., C17, 1881 (1978)
[Ol972] Olsson, N., et al: Proc. Int. Conf. Nuclear Data, 1997 Treieste, to be published
3.4
[Ki98] E.Kim et al.: Nucl. Sci. Engi., 129 1 (1998)
[Na98] T.Nakamura et al.: J. Atomic Energy Society 40 (1) 15 (1998) (in Japanese)
[Uw94] Y.Uwamino et al.: J. Nucl. Sci.Technol., 31(1) 1 (1994)
[Pa94]H.Hitzenberger, A.Pavlik et al.: Proc. Int. Conf. Nuclear Data, Gatlinburg 1994, p.367
[Vo94]H.Vonach, A.Pavlik et al.: Phys. Rev., C50(4) 1952 (1994)
[Ne97] S.Newmann et al.: Proc. Int.Conf. Nuclear Data, Tieste 1997, to be published.
3.5
[Li88] P.W.Lisowski et al., Proc. Co・ onf.., Nuclear Data, 1988 Mito, p.91
[Fo97]A.V.Fomichev et al.: Proc. Conf., Nuclear Data, Trieste 1997, to be published
[Ei96] Eismont, V.P, et al.: Phys. Rev., C53 (6) 2911 (1996)
[New97]Newhauser, W.D. et al: Proc. Int.Conf., Nuclear Data, 1997 Trieste, to be published
[Co96] H.Conde et al.: Proc. Conf. Accelerator-Driven Transmutation Technology and Application, (1995 Kalamar)
3.6
[Ra88] P.Ramakrishnan, G.Mitchel, G.Gould: Nucl. Sci. Eng., 98 348 (1988)
[Pa94]H.Hitzenberger, A.Pavlik et al.: Proc. Int. Conf. Nuclear Data, Gatlinburg 1994, p.367
[Vo94]H.Vonach et al.: Phys. Rev., C50(4) 1952 (1994)
[Ta94] E.Tanabe , K.Shin, T.Nakamura: J.Nucl. Sci. Technol., 31(11), 1133 (1994)
3.7
[Ki98] E.Kim et al.: Nucl. Sci. Engi., 129 1 (1998)
[Na98] T.Nakamura et al.: J. Atomic Energy Society 40 (1) 15 (1998) (in Japanese)
[Li88] P.W.Lisowski et al., Proc. Conf.., Nuclear Data, 1988 Mito, p.91
[Fo97]A.V.Fomichev et al.: Proc. Conf., Nuclear Data, Trieste 1997, to be published

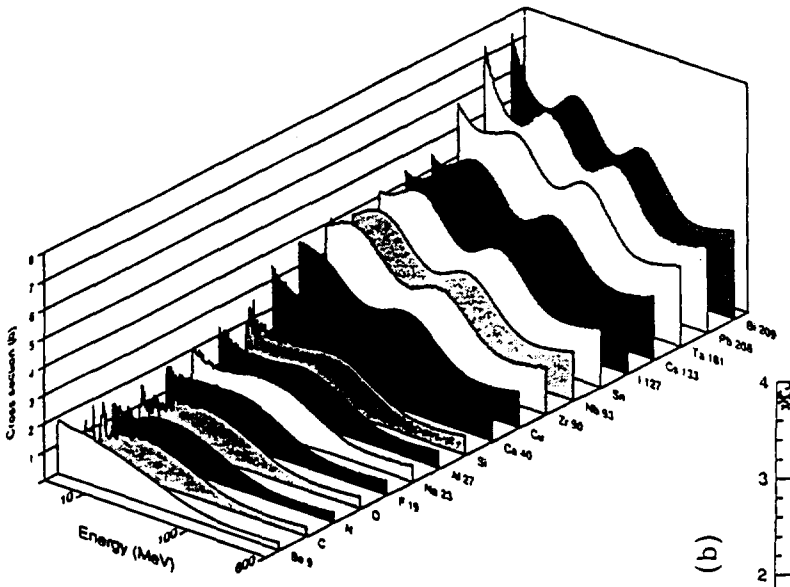

Fig.1: Experimental data of neutron total cross section [Fi93].

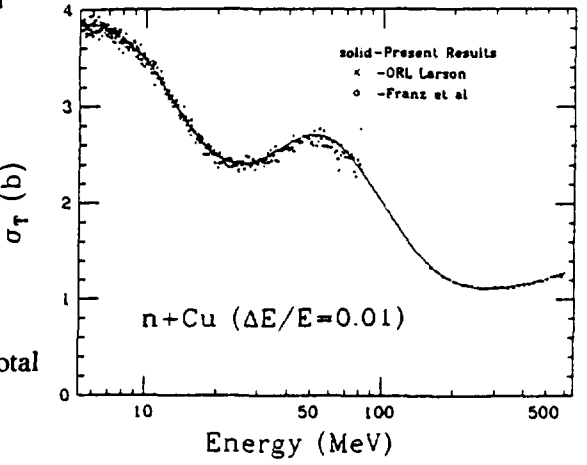

Fig.2: Comparison of neutron total cross section data [Fi93]

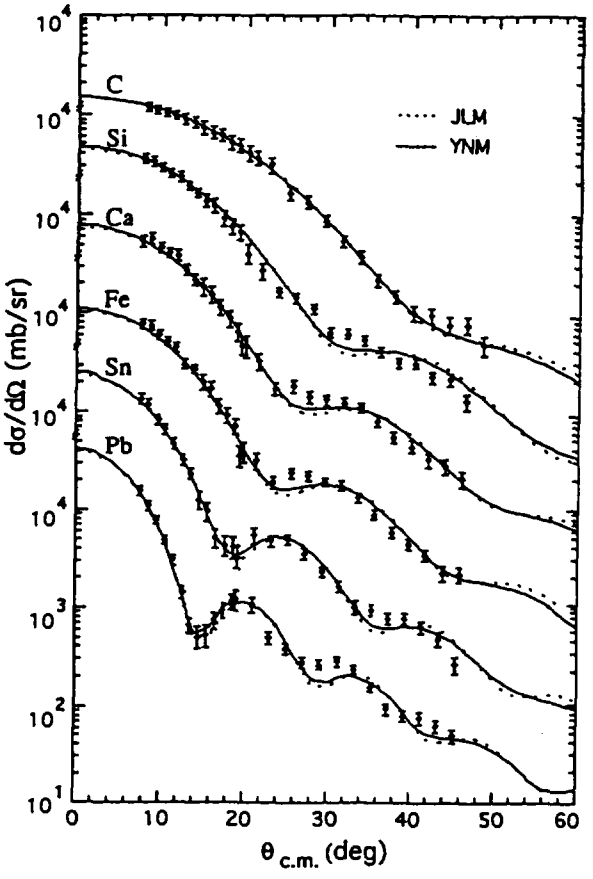

Fig.3: Neutron elastic scattering cross section [Hj94]

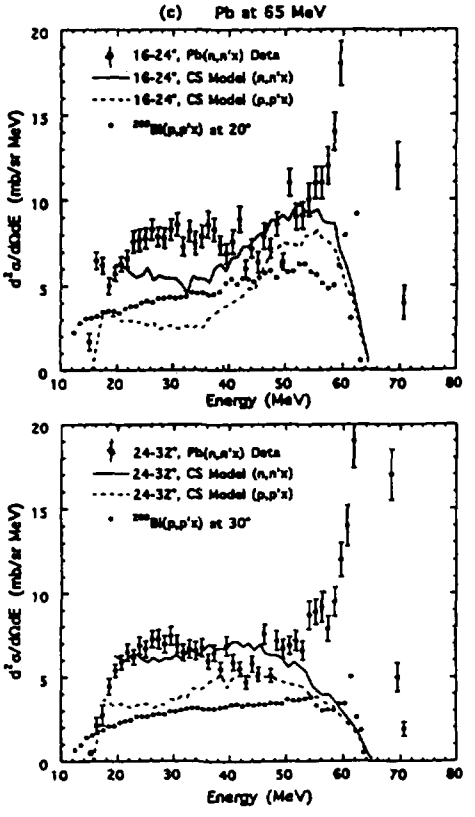

Fig.4: Neutron emission spectra of Pb [Hj95].

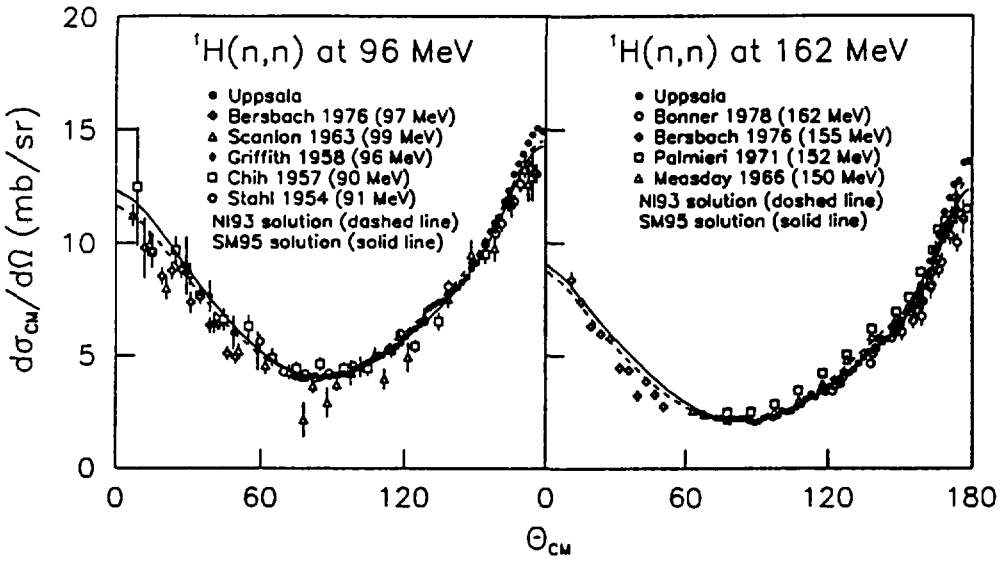

Fig.5: Neutron scattering cross section of hydrogen [Ol97].

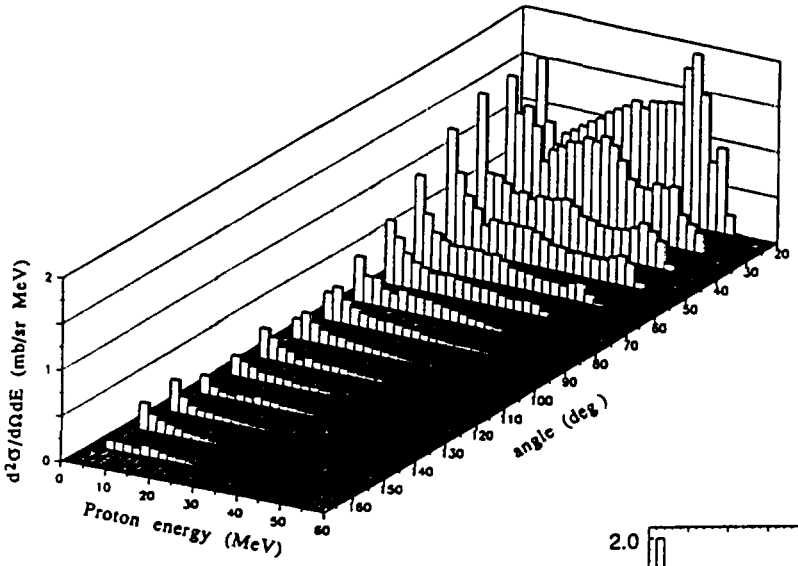

Fig.6: Double-differential ^{12}C(n,xp) cross section [Sl95].

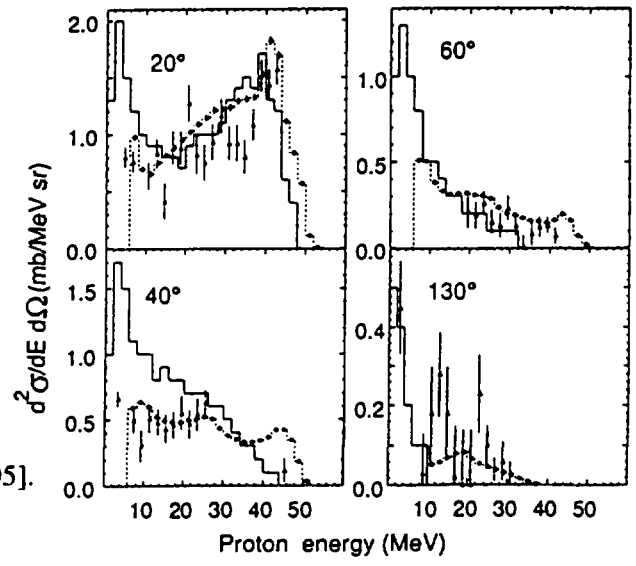

Fig.7: Comparison of ^{12}C(n,xp) spectra [Sl95].
Open dot; experiment by Ref.[Sl95],
Triangle; experiment by Ref.[Sa83],
Histogram; cascade model calculation.

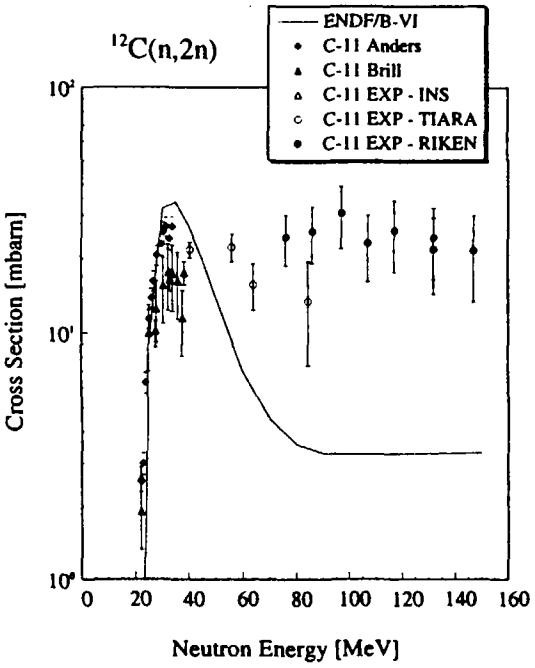

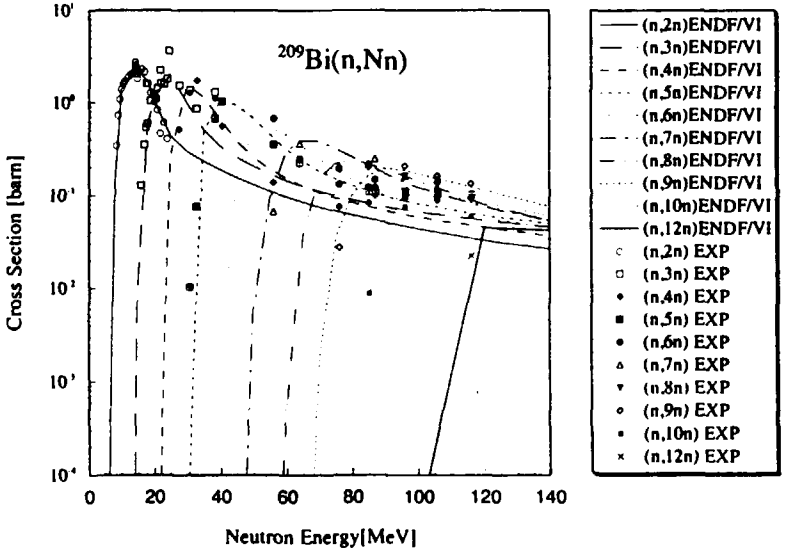

Fig.8:
^{12}C(n,2n) and ^{209}Bi(n,Nn) cross section [Na98].

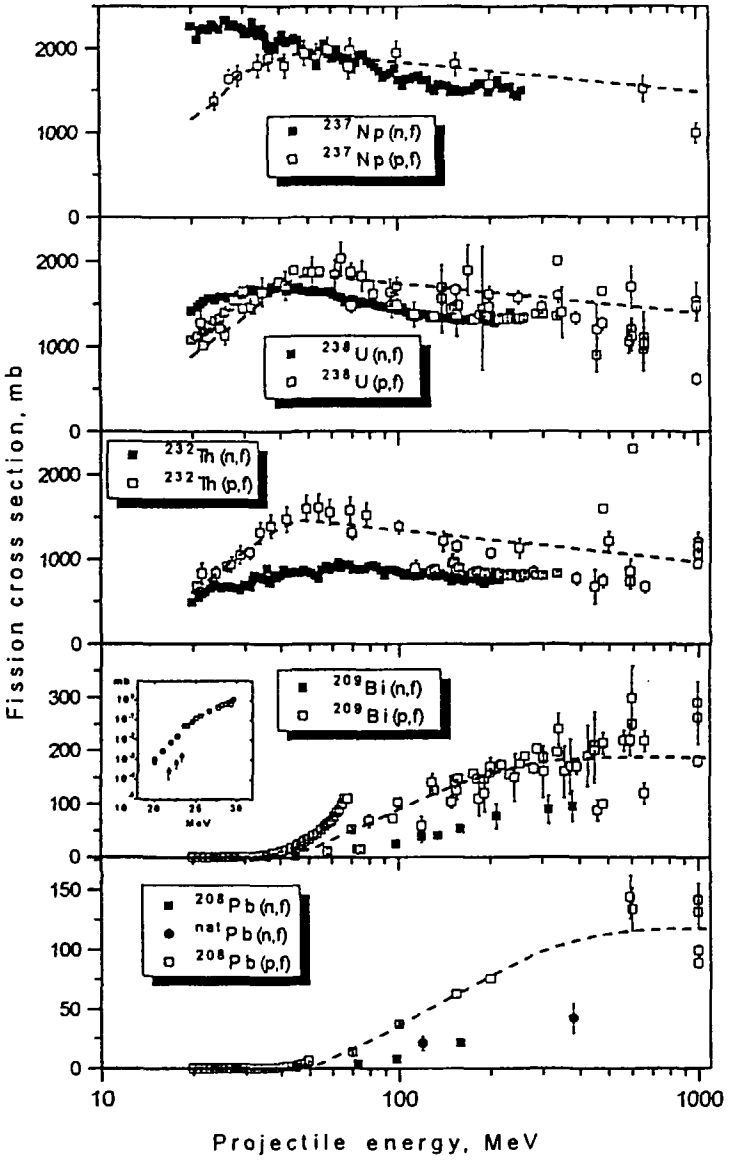

Fig.9: Comparison of (n,f) and (p,f) cross sections [Co96].

2.2 Status of experimental data of proton-induced reactions for intermediate-energy nuclear data evaluation

Yukinobu WATANABE*, Toshihiko KAWANO
Department of Advanced Energy Engineering Science, Kyushu University,
Kasuga, Fukuoka 816-8580, Japan
*e-mail: watanabe@aees.kyushu-u.ac.jp

Naoki YAMANO
Department of Nuclear Design,Sumitomo Atomic Energy Industries, Ltd.
2-10-14 Ryogoku, Sumida-ku, Tokyo 130, Japan

Tokio FUKAHORI
Nuclear Data Center, Japan Atomic Energy Research Institute
Tokai-mura, Naka-gun, Ibaraki-ken 319-1106, Japan

The present status of experimental data of proton-induced reactions is reviewed, with particular attention to total reaction cross section, elastic and inelastic scattering cross section, double-differential particle production cross section, isotope production cross section, and activation cross section.

1. Introduction

In recent years, proton nuclear data are required in various fields related to advanced science and technology using high energy protons beams, such as accelerator-driven transmutation of nuclear waste, radio therapy with high-energy proton beam, and so on. Proton nuclear data evaluation for JENDL High Energy File is now in progress by the High Energy Nuclear Data Working Group organized under the Japanese Nuclear Data Committee [1]. An effort to get the latest information on experimental data is necessary towards the evaluation of intermediate-energy nuclear data.

Previously, Koning[2] reported the status of neutron and proton reaction data in the incident energy range up to 1500 MeV by scanning two databases, Nuclear Structure References (NSR) [3] and EXFOR [4], including references up to the year 1992. The tables given in his report serve to show us the gaps and well-investigated areas of cross section measurements in the energy range. However, the quality of the cross sections of each reaction type, such as total reaction cross section and elastic scattering cross section, was not discussed.

In this work, eleven target nuclides with a high priority for intermediate-energy nuclear data evaluation are chosen and cross section measurements of proton-induced reactions are surveyed in the energy range from the threshold energy up to some tens of GeV. The status of available experimental data is overviewed in accordance with a category of the cross sections proposed in the JENDL High Energy Files.

2. Scope and method of data retrievals

The widely used EXFOR database was employed for retrievals of the currently available experimental data. It contains the numerical data for cross section measurements in addition to the references. We also made use of bibliographic information given in journal publications, reports and conference proceedings in nuclear physics (*i.e.*, Physical Review C, Nuclear Physics A, etc.).

The scope of data retrievals is given in Table I. Either selected target nuclide has a high priority for various proton beam applications. As for iron, the natural isotope was also included.

Table I: Scope of retrieval of available proton reaction data

(1) Target nuclide	^{12}C, ^{14}N, ^{16}O, ^{27}Al, ^{28}Si, ^{56}Fe (^{nat}Fe) ^{58}Ni, ^{90}Zr, ^{184}W, ^{208}Pb, ^{209}Bi
(2) Energy range	Whole energy range included in the EXFOR database
(3) Category of cross section	(A) Total reaction cross section (or total cross section) (B) Elastic scattering cross section (C) Inelastic scattering cross section (D) Double-differential particle production cross section (E) Isotope production cross section and activation cross section

2. Review of experimental data

2.1 Result of EXFOR retrievals

A result of EXFOR retrievals is shown in Table II. The number of data entries in the EXFOR is given. Each column - (p.NON), (p.EL), and (p.INL) - corresponds to total reaction cross section, elastic scattering cross section, and inelastic scattering cross section, respectively. Neutron and charged-particle production cross sections including double-differential cross section (DDX) and activation/isotope production cross sections are assigned in the category (p.NON).The number of the data of DDX type is also given in the brackets in both (p.INL) and (p. NON) columns. An overview of each cross section will be given in the following subsections on the basis of Table II and additional bibliographic information.

Table II: Number of available experimental data compiled in EXFOR. The figure in the brackets stands for the number of DDX data entry.

Target nuclide	Total Entry Number	(p.NON)	(p.EL)	(p.INL)	(p.X)
C-12	362	7	111	157	87 [48]
N-14	26	1	3	5	17 [8]
O-16	333	2	52	236	43 [16]
Al-27	214	6	18	2	188 [72]
Si-28	46	0	10	20	16 [7]
Fe-56	140	3	32	54	51 [10]
Fe-nat	567	2	9	0	556 [20]
Ni-58	296	2	40	99	155 [110]
Zr-90	303	1	49	168 [64]	85 [67]
W-184	2	0	1	1	0
Pb-208	486	3	71	346	66 [56]
Bi-209	69	0	5	1	63 [29]

2.2 Total reaction cross section

As can be seen from Table II, the number of experimental data available in the EXFOR database is very limited. Another data source, Bauhoff's compilation [5], indicates that there are further available numerical data over 58 elements: the total entry number is 712 for the total reaction cross section and 73 for the total cross section. The experimental data for carbon are plotted in Fig.1 as an example. Full circles correspond to the data available in the EXFOR database. Note that the Bauhoff's compilation covers all the data in the EXFOR database for the selected eleven nuclides. Most of the data are rather old because only one reference has been found later than 1980 in the Bauhoff's compilation. The old data have rather large error bars and are not in good agreement with each other. Two groups [6,7] have derived systematics of proton reaction cross sections using the Bauhoff's compilation and such systematics will be useful in future nuclear data evaluation. In addition, it should be noted that a table of numerical data in a TeX format and a list of bibliographies by Barashenkov[8] are available.

2.3 Elastic and inelastic proton scattering cross section

The number of entries of the data categorized as elastic and inelastic scattering cross sections is given in the 4th and 5th columns in Table II. A large number of data are compiled in the EXFOR database, especially, ^{12}C, ^{16}O, ^{90}Zr, and ^{208}Pb. We can find much more experimental data by a survey based on bibliographic information. Some features of these data are summarized below:

- Two or more measurements for the same incident energy and target nucleus are few.
- Since the angular distributions become very forward-peaked with increase in incident energy, the angular region are limited to forward angles at incident energies higher than 200 MeV.
- Most of the data for energies below 200MeV are rather old (before 1980's), depending on the performance of accelerators

- Spin observables (*e.g.*, analyzing powers) can also be found in the EXFOR database. The data of spin observables are necessary to extract the spin-orbit term from the optical model analysis and establish more reliable theoretical models.
- As for the data of elastic scattering, we can choose useful and reliable data from references by surveying the study about intermediate energy optical potentials. For example, the work done by Hama et al.[9,10] and the proceedings of specialist's meeting on nucleon-nucleus optical model up to 200 MeV[11] are useful.

2.4 Double-differential cross section

The data of double-differential cross section (DDX) type are included in the categories (p,INL) and (p,X) in Table II. We have inspected experimental data measured after 1970 using the EXFOR database and additional bibliographic information. Target nuclides except for those in Table I are also included in the inspection. The result is summarized in Tables III with the references. The last column of these tables shows us whether the data set is compiled in the EXFOR database or not. Figure 2 illustrates a distribution of DDX measurements in a two-dimensional plane of incident energy and target mass number: full circles for light-ion emission (p, d,t,He-3, and He-4) and open rectangles for neutron emission. Some features of available DDX data are summarized in the following.

- Measurements of DDX data listed in Table II have mainly been carried out in association with the study of preequilibrium nuclear reactions and the needs for engineering applications.
- As for the data of neutron production, there are several systematic measurements that have been done since 1990's from the points of view of applications. Most of these data are available in the EXFOR database.
- There are several experimental data of charged-particle emission covering the energy range below 200 MeV, *e.g.*, a series of measurements between 100 and 200 MeV at NAC, while those above 200 MeV are very limited. These data have not yet been compiled completely in the EXFOR database.
- At energies above 200 MeV, there are some measurements [12,13,14] done at very small angles in the study of spin-isospin response in nuclear excitation, except for the measurements listed in Table III.

2.5 Isotope production cross section and activation cross section

These data are categorized in the sixth column in Table II. It is found that a large number of experimental data are available in the EXFOR database, except for ^{184}W. Further inspection for six elements (C, O, Al, Si, W, and Pb) was done by one of the authors (N.Y.). The result for C is given in Table IV as an example. The right column shows a result of inspection of each data. The cross section itself is given in the case of one or two data points, and the number of data points or the number of produced elements/nuclides in the case of more than three data points. The symbol "x" means our judgment that the data is not appropriate for nuclear data evaluation. Such a careful and time-consuming work will be needed to select

reliable and useful data for nuclear data evaluation from a huge number of experimental data.

We can also find many literatures about the measurements of isotope production cross sections and activation cross sections. Among them, recent measurements done by Th. Schiekel et al.[15] and M. Gloris et al.[16] provide us useful information on proton-induced nuclide production cross sections in the intermediate energy range from 80 to 1600 MeV.

3. Concluding remarks

We have reviewed the status of the currently available experimental data of proton-induced reactions at intermediate energies on the basis of the EXFOR database and the literatures related to nuclear physics. It was found that quite a number of experimental proton data are now available over the wide range of incident energy and target mass, compared with neutron data.

Some conditions on the experimental data needed in nuclear data evaluation can be summarized in the following: (i) several data for a certain reaction of interest exist and no serious inconsistency is seen among them, and/or (ii) there are the data measured systematically with a wide dynamic range of incident/outgoing energies and angles. Many proton reaction data do not necessarily meet such the conditions at the present stage, because most of them were measured in the experiments dedicated to the study of nuclear physics rather than in application-oriented experiments, except for several measurements for double differential (p,xn) cross sections. In the future, therefore, further experimental efforts will be necessary for reliable proton nuclear data evaluation.

Finally, it should be mentioned that most of the latest measurements are not necessarily available in the EXFOR database and there is a time lag between the publication in journals and conference proceedings and the compilation in the EXFOR database. It is recommended that such inconvenient situation will be improved as soon as possible as a first step towards intermediate-energy nuclear data evaluation.

References

[1] T. Fukahori, presented at this meeting.

[2] A.J. Koning, "Review of High Energy Data and Model Codes for Accelerator-based Transmutation", report ECN-C—93-005 (1993).

[3] C.L. Dunford and T.W. Burrows, "National Nuclear Data Center online nuclear data service", BNL report NNDC/ONL-92/08.

[4] NEA report DBG-006.2, "EXFOR network service" (1989).

[5] W. Bauhoff, Atomic Data and Nuclear Data Tables, **35**, 430 (1986).

[6] L. Sihver, et al., Phys. Rev. C **47**, 1225 (1993).

[7] H.P. Wellisch and D. Axen, Phys. Rev. C **54**, 1329 (1996).

[8] B.C. Barachenkov, "Cross Sections of Interactions of Particle and Nuclei with Nuclei", JINR, Dubna (1993).

[9] S. Hama, et al., Phys. Rev. C **41**, 2737 (1990).

[10] E.D. Cooper, et al., Phys. Rev. C **47**, 297 (1993).

[11] Proceedings of a Specialists Meeting on Nucleon-Nucleus Optical Model Up to 200 MeV, 13-15 Nov., 1996, Bruyères-le-Châtel, France, NEA Nuclear Science Committee (1997).

[12] L. W. Swenson et al., Phys. Rev. C **40**, 246 (1989).

[13] O. Häusser et al., Phys. Rev. C **43**, 230 (1991).

[14] T. Wakasa et al., Phys. Rev. C **55**, 2909 (1997).

[15] M. Gloris et al., Nucl. Instr. & Meth. **B113**, 429 (1996).

[16] Th. Schiekel et al., Nucl. Instr. & Meth. **B114**, 91 (1996).

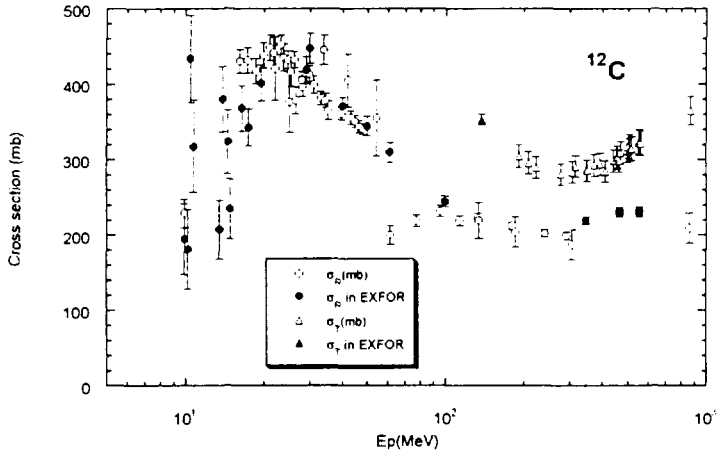

Fig.1 Total reaction cross sections (circles) and total cross sections (triangles) taken from Ref.[5]. The data available in the EXFOR database are given as full symbols.

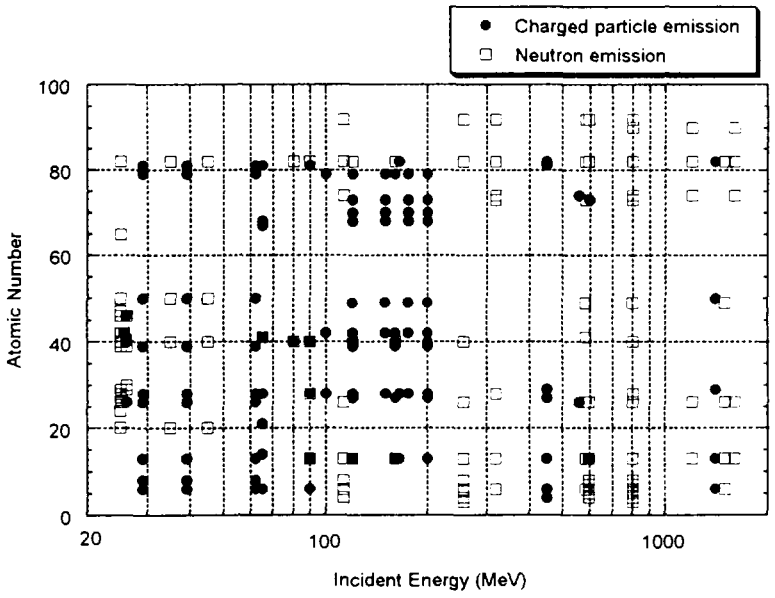

Fig.2 Distribution of the available double-differential cross section data. Full circles and open rectangles represent light-ion emission and neutron emission, respectively.

Table III-1 A list of DDX measurements for incident proton energies of E_p= 20 to 100 MeV

No.	E_{inc} (MeV)	Target nuclei	Emitted particles						Outgoing Energies Range (MeV)	Lab. Angles Range (deg)	Laboratory & remarks	Ref.	EXFOR
			p	d	t	^{3}He	^{4}He	n					
1	25.6, 26	^{98}Mo, ^{106}Pd	○						7-E_{max}	30-150	Kyushu- JAERI	WA95	
2	26	^{54,56}Fe, ^{90}Zr, ^{93}Nb	○						3-E_{max}	20-150	Kyushu- JAERI	WA97	
3	29, 39, 62	^{12}C, ^{16}O, ^{27}Al, ^{54}Fe, ^{56}Fe, ^{60}Ni, ^{89}Y, ^{120}Sn, ^{197}Au, ^{209}Bi	○	○	○	○	○		(a few~10)-E_{max}	12-160	ORNL	BE73	○
4	65	^{12}C, ^{28}Si, ^{45}Sc, ^{58}Ni, ^{93}Nb, ^{165}Ho, ^{166}Er, ^{209}Bi	○	○			○		10-E_{max} for p,d 30-E_{max} for ^{4}He	20-150	RCNP $A_y(E,\theta)$	SA80	○
5	80	^{90}Zr	○						20-E_{max}	24-145	NAC	CO91	○
6	90	^{12}C	○						10-E_{max}	20-75	NAC	FO88	
7	90	^{27}Al, ^{58}Ni, ^{90}Zr, ^{209}Bi	○	○	○	○	○		2.5-E_{max} for p, d, ^{4}He 5.5-E_{max} for t 11.5-E_{max} for ^{3}He	20-140	Maryland	WU79	○
8	100	^{58}Ni	○	○	○	○	○		12.5-E_{max}	15-155	Maryland	WU79	○
9	25	Ag						○	6.5-E_{max}	4-159	?	GR76	
10	26	^{64}Zn, ^{65}Cu, ^{89}Y						○	4-E_{max}	3.5-159	LLNL	SC83	
11	25	^{50,52,53}Cr, ^{54,56,58}Fe, ^{59}Co, ^{60}Ni, ^{63}Cu, ^{89}Y, ^{90,91,92,94}Zr, ^{92,94,95,96,97,98,100}Mo, ^{110}Pd, ^{159}Tb						○	5.4-E_{max}	3.5-159	LLNL	SC84	
12	25.6	^{92,94,95,96,97,98,100}Mo						○	1-E_{max}	3-177	Hamburg	MO86	
13	26.1	^{104,105,106,108,110}Pd						○	3-E_{max}	3-177	Hamburg	HO91	
14	25, 35, 45	^{48}Ca, ^{90}Zr, ^{120}Sn, ^{208}Pb						○	8-E_{max}	5-160	MSU	BL76	
15	65	^{93}Nb						○	15-E_{max}	0-110	RCNP, $A_y(E,\theta)$	SA83	
16	80.5	^{90}Zr, ^{208}Pb						○	20-E_{max}	30-135	IUCF	TR89	○
17	90	^{27}Al ^{58}Ni ^{90}Zr, ^{209}Bi						○	5-E_{max}	20-135	Maryland	KA83	○

注) $A_y(E,\theta)$：偏極分解能測定データ

Table III-2: A list of DDX measurements for incident proton energies above 100 MeV

No.	E_{inc}(MeV)	Target nuclei	Emitted particles						Outgoing energies Range (MeV)	Lab. Angles Range (deg)	Laboratory & remarks	Ref.	EXFOR
			p	d	t	^{3}He	^{4}He	n					
1	100,120,150 175, 200	^{197}Au	○						20-E_{max}	15-120	NAC	CO90	
2	100,120,150 175, 200	^{58}Ni	○						20-E_{max}	15-120	NAC	FO91	○
3	120	^{90}Zr	○						20-E_{max}	24-145	NAC	CO91	○
4	100,120,150 175, 200	^{58}Ni, ^{100}Mo, ^{197}Au	○						20-E_{max}	15-120	NAC	RI92	
5	120, 160, 200	^{89}Y, ^{90}Zr, ^{92,94,96,98,100}Mo	○						20-E_{max}	15-160	NAC	RI94	○
6	120,150,175 , 200	^{115}In, ^{167}Er, ^{173}Yb, ^{181}Ta	○						20-E_{max}	15-160	NAC	RI96	
7	120, 160, 200	^{27}Al, ^{59}Co, ^{197}Au					○		30-E_{max}	10-160	NAC	CO96	
8	120, 160, 200	^{59}Co, ^{197}Au				○			30-E_{max}	10-160	NAC	CO97	
9	165	^{27}Al, ^{58}Ni, ^{60}Ni, ^{208}Pb	○	○			○		?	25-150	?	SE82	
10	200	^{27}Al, ^{197}Au	○	○	○	○	○		?	14-135	KFA	MA84	
11	450	Be, C, Al, Cu, Co, Pb, Bi	○						100-450	0-60	ORNL	WA72	
12	558	Fe, W	○	○					?	10-60	?	BE76	
13	600	^{27}Al, ^{181}Ta	○						?	30-150	?	CO81	
14	1400, 2500, 3000, 4500	C, Al, Cu, Sn, Pb	○						40-170	30-120	KEK, Also, π^-beam	SH83	
15	3000,4000	Al, Pb	○						100-1200	37-90	KEK, Also, π^-beam	EN85	
16	12000	Al, Cu, Ag, Ta	○						7.5-140	90	KEK, π^-emission	SH83	

Table III-3: A list of DDX measurements for incident proton energies above 100 MeV (neutron production)

No.	E_{inc}(MeV)	Target nuclei	Emitted particles						Outgoing energies Range (MeV)	Lab. Angles Range (deg)	Laboratory & remarks	Ref.	EXFOR
			p	d	t	^{3}He	^{4}He	n					
17	120, 160	^{27}Al, ^{90}Zr, ^{208}Pb						○	20-E_{max}	0-145	IUCF	SC90	○
18	256, 800	Li, Al, Zr, Pb						○	20-E_{max}	7.5-150	LANL	ST93	○
19	585	C, Al, Fe, Nb, In, Ta, Pb, U						○	0.9- E_{max}	30-150	PSI	CJ87	○
20	113	Be, C, O, Al, Fe, W, Pb, U						○	0.5-E_{max}	7.5-150	LANL	ME89	○
21	256	Be, C, O, Al, Fe, Pb, U						○	0.5-E_{max}	7.5-150	LANL	ME92	○
22	318, 800	C, Al, Ta, Ni, W, Pb, U						○	?	?	LANL	ME86	
23	597	Be, B, C, N, O, Al, Fe, Pb, U						○	0.5-E_{max}	30-150	LANL	AM93	○
24	800	Be, B, C, N, O, Al, Fe, Cd, W, Pb						○	0.3-E_{max}	30-150	LANL	AM92	○
25	800,1500, 3000	C, Al, Fe, In, Pb						○	1-E_{max}	15-150	Kyushu-KEK	IS97	

References of Table III

[AM92] W.B. Amian, R.C. Byrd, C.A. Goulding, M.M. Meier, G.L. Morgan, C.E. Moss, and D.A. Clark, Nucl. Sci. Eng., **112**, 78 (1992).

[AM93] W.B. Amian, R.C. Byrd, D.A. Clark, C.A. Goulding, M.M. Meier, G.L. Morgan, and C.E. Moss, Nucl. Sci. Eng., **115**, 1 (1993).

[BE73] F.E. Bertrand and R.W. Peelle, Phys. Rev. C **8**, 1045 (1973).

[BE76] S.M. Beck and C.A. Powell, N.A.S.A. technical note, NASA TN D-8119, 1976.

[BL76] M. Blann, R.R. Doering, Aaron Galonsky, D.M. Patterson, and F.E. Serr, Nucl. Phys. **A257**, 15 (1976).

[CJ87] S. Cierjacks, Y. Hino, F. Raupp, L. Buth, D. Filges, P. Cloth, and T.W. Armstrong, Phys. Rev. C **36**, 1976 (1987).

[CO81] K.R. Cordell, S.T. Thornton, L.C. Dennis, R.R. Doering, R.L. Parks, and T.C. Schweizer, Nucl. Phys. **A352**, 485 (1981).

[CO90] A.A. Cowley, S.V. Förtsch, J.J. Lawrie, D.M. Whittal, F.D. Smit, and J.V. Pichler, Z. Phys. **A336**, 189 (1990).

[CO91] A.A. Cowley, A. van Kent, J.J. Lawrie, S.V. Förtsch,, D.M. Whittal, J.V. Pichler, F.D. Smit, W.A. Richter, R. Lindsay, I.J. van Heerden, R. Bonetti, and P.E. Hodgson,
Phys. Rev. C **43**, 678 (1991).

[CO96] A.A. Cowley, G.J. Arendse, J.W. Koen, W.A. Richter, J.A. Stander, G.F. Steyn, P. Demetriou, P.E. Hodgson, and Y. Watanabe, Phys. Rev. C **54**, 778 (1996).

[CO97] A.A. Cowley, G.J. Arendse, G.F. Steyn, J.A. Stander, W.A. Richter, S.S. Dimitrova, P. Demetriou, P.E. Hodgson, Phys. Rev. C **55**, 1843 (1997)

[EN85] H. En'yo, S. Sasaki, T. Nagae, K. Tokushuku, M. Sano, M. Sekimoto, J. Chiba, K. Ichimaru, T. Mori, T. Katsumi, H. Yokota, and R. Chiba, Phys. Lett. **158B**, 681 (1985): PhD Thesis, University of Tokyo (1985).

[FO88] S.V. Förtsch, A.A. Cowley, J.V. Pichler, D.M. Whittal, J.J. Lawrie, J.C. Van Staden, E. Friedland, Nucl. Phys. **A485**, 258 (1988).

[FO91] S.V. Förtsch, A.A. Cowley, J.J. Lawrie, D.M. Whittal, F.D. Smit, and J.V. Pichler, Phys. Rev. C **43**, 691 (1991).

[GR76] S.M. Grimes, J.D. Anderson, and C. Wong, Phys. Rev. C **13**, 2224 (1976).

[HO91] S. Hölbling, R. Caplar, S. Stamer, R. Langkau, and W. Scobel, Z. Phys. **A338**, 11 (1991).

[IS97] K. Ishibashi, H. Takada, T. Nakamoto, N. Shigyo, K. Machata, N. Matsufuji, S. Meigo, S. Chiba, M. Numajiri, Y. Watanabe, and T. Nakamura, J. Nucl. Sci. Technol., **34**, 529 (1997).

[KA83] A. M. Kalend, B.D. Anderson, A.R. Baldwin, R. Madey, J.W. Watson, C.C. Chang, H.D. Holmgren, R. W. Koontz, J.R. Wu, and H. Machner, Phys. Rev. C **28**, 105 (1983).

[MA84] H. Machner, D. Protic, G. Riepe, J.P. Didelez, N. Frascaria, E. Gerlic, E. Hourani, and M. Morlet, Phys. Lett. **138B**, 39 (1984).

[ME86] M.M. Meier, D.B. Holtkamp, G.L. Morgan, H. Robinson, G.J. Russell, E.R. Whitaker, W.B. Amian, and N. Paul, Radiation Effects **96**, 73 (1986).

[ME89] M.M. Meier, D.A. Clark, C.A. Goulding, J.B. McClelland, G.L. Morgan, C.E. Moss, W.B. Amian, Nucl. Sci. Eng., **102**, 310 (1989).

[ME92] M.M. Meier, W.B. Amian, C.A. Goulding, G.L. Morgan, and C.E. Moss, Nucl. Sci. Eng., **110**, 299 (1992).

[MO86] E. Mordhorst, M. Trabandt, A. Kaminsky, H. Krause, and W. Scobel, Phys. Rev. C **34**, 103 (1986).

[RI92] W.A. Richter, A.A. Cowley, R. Lindsay, J.J. Lawrie, S.V. Förtsch, J.V. Pilcher, R. Bonetti, and P.E. Hodgson, Phys. Rev. C **46**, 1030 (1992).

[RI94] W.A. Richter, A.A. Cowley, G.C. Hillhouse, J.A. Stander, J.W. Koen, R. Lindsay, R.E. Julies, J.J. Lawrie, J.V. Pilcher, and P.E. Hodgson, Phys. Rev. C **49**, 1001 (1994).

[RI96] W.A. Richter, S.W. Steyn, A.A. Cowley, J.A. Stander, J.W. Koen, R. Lindsay, G.C. Hillhouse, R.E. Julies, J.J. Lawrie, J.V. Pilcher, and P.E. Hodgson, Phys. Rev. C **54**, 1756 (1996).

[SA80] H. Sakai, K. Hosono, N. Matsuoka, S. Nagamachi, K. Okada, K. Maeda, H. Shimizu, Nucl. Phys. **A344**, 41 (1980).

[SA83] H. Sakai, K. Hatanaka, N. Matsuoka, T. Saito, A. Shimizu, T. Motobayashi, and T. Shibata, Phys. Lett. **133B**, 375 (1983).

[SC83] W. Scobel, L.F. Hansen, B.A. Pohl, C. Wong, and M. Blann, Z. Phys. **A311**, 323 (1983).

[SC84] W. Scobel, M. Blann, T.T. Komoto, M. Trabandt, S.M. Grimes, L.F. Hansen, C. Wong, and B.A. Pohl, Phys. Rev. C **30**, 1480 (1984).

[SC90] W. Scobel, M. Trabandt, M. Blann, B.A. Pohl, B.R. Remington, R.C. Byrd, C.C. Foster, R. Bonetti, C. Chiesa, S.M. Grimes, Phys. Rev. C **41**, 2010 (1990).

[SE82] R.E. Segel, T. Chen, L.L. Rutledge, Jr., J. V. Maher, John Wiggins, P.P. Singh, and P.T. Debevic, Phys. Rev. C **26**, 2424 (1982).

[SH83] T.-A. Shibata, K. Nakai, H. En`yo, S. Sasaki, M. Sekimoto, I. Arai, K. Nakayama, K. Ichimaru, H. Nakamura-Yokota, and R. Chiba, Nucl. Phys. **A408**, 525 (1983).

[ST93] S. Stamer, W. Scobel, B.A. Amian, R.C. Byrd, R.C. Haight, J.L. Ullmann, R.W. Bauer, M. Blann, B.A. Pohl, J. Bisplinghoff, R. Bonetti, Phys. Rev, C **47**, 1647 (1993).

[TR89] M. Trabandt, W. Scobel, M. Blann, B.A. Pohl, R.C. Byrd, C.C. Foster, R. Bonetti, Phys. Rev. C **39**, 452 (1989).

[WA72] J.W. Wachter, W.A. Gibson, and W.R. Burrus, Phys. Rev. C **6**, 1496 (1972).

[WA95] Y. Watanabe, A. Aoto, H. Kashimoto, S. Chiba, T. Fukahori, K. Hasegawa, M. Mizumoto, S. Meigo, M. Sugimoto, Y. Yamanouti, N. Koori, N.B. Chadwick, P.E. Hodgson, Phys. Rev. C **51**, 1891 (1995).

[WA97] Y. Watanabe, S. Yoshioka, M. Harada, K. Sato, Y. Nakao, H. Ijiri, S. Chiba, T. Fukahori, S. Meigo, O. Iwamoto, N. Koori, to be published in Proc. of Int. Conf. On Nuclear Data for Science and Technology, May 19-24, Trieste, Italy: JAERI-Conf 97-005 (1997) p. 301

[WU79] J.R. Wu, C.C. Chang, and H.D. Holmgren, Phys. Rev. C **19**, 698 (1979).

Table IV: Result of EXFOR retrieval of proton-induced isotope production cross sections for carbon

Work no	Z-A	Reaction		Emin (eV)	Emax (eV)	Lab	Yr	comments
50018.002	C-12	(P,2HE3),,SIG	Li-7	5.0000E+07	5.0000E+07	LPI	78	0.4±0.4mb
50018.002	C-12	(P,2P),,SIG	B-11	5.0000E+07	5.0000E+07	LPI	78	47+9/-11mb
50018.002	C-12	(P,D+A),,SIG	Be-7	5.0000E+07	5.0000E+07	LPI	78	8.2±1.7mb
50018.002	C-12	(P,P+D),,SIG	B-10	5.0000E+07	5.0000E+07	LPI	78	37+8/-10mb
50018.002	C-12	(P,P+3-LI-6),,SIG	Li-6	5.0000E+07	5.0000E+07	LPI	78	0.3+0.5/-0.3mb
50018.002	C-12	(P,HE3+A),,SIG	Li-6	5.0000E+07	5.0000E+07	LPI	78	1.2±0.5mb
50018.002	C-12	(P,P+HE3),,SIG	Be-9	5.0000E+07	5.0000E+07	LPI	78	4.5+1.5/-0.3mb
50018.002	C-12	(P,T+HE3),,SIG	Be-7	5.0000E+07	5.0000E+07	LPI	78	0.9±0.5mb
50020.002	C-12	(P,X)2-HE-3,,SIG		6.6000E+08	6.6000E+08	DUB	73	
50020.002	C-12	(P,X)1-H-2,,SIG		6.6000E+08	6.6000E+08	DUB	73	
50020.002	C-12	(P,X)2-HE-4,,SIG		6.6000E+08	6.6000E+08	DUB	73	
50020.002	C-12	(P,X)1-H-3,,SIG		6.6000E+08	6.6000E+08	DUB	73	
50030.002	C-12	(P,X)ELEM/MASS,IND,SIG		6.6000E+08	6.6000E+08	DUB	77	
50030.007	C-12	(P,X)2-HE-3,IND,SIG		6.6000E+08	6.6000E+08	DUB	77	
50030.007	C-12	(P,X)1-H-3,IND,SIG		6.6000E+08	6.6000E+08	DUB	77	
50030.008	C-12	(P,X)1-H-3,IND,SIG		6.6000E+08	6.6000E+08	DUB	77	
50043.002	C-12	(P,XN+4P),IND,SIG,,REL	Li-6>9	1.0000E+09	1.0000E+09	RI	76	
50043.007	C-12	(P,XN+4P),IND,SIG,,RAW		1.0000E+09	1.0000E+09	RI	76	
50050.002	C-12	(P,2P),IND,SIG	B-11	5.0000E+07	5.0000E+07	LPI	79	47±9mb
50050.002	C-12	(P,2P+T+A),IND,SIG	He-4	5.0000E+07	5.0000E+07	LPI	79	10±2mb
50050.002	C-12	(P,D+HE3+A),IND,SIG	He-4	5.0000E+07	5.0000E+07	LPI	79	9.4±3.1mb
50050.002	C-12	(P,P+2D+A),IND,SIG	He-4	5.0000E+07	5.0000E+07	LPI	79	6.7±3.5mb
50050.002	C-12	(P,P+D+A),IND,SIG	Li-6	5.0000E+07	5.0000E+07	LPI	79	7.4±2.9mb
50050.002	C-12	(P,P+HE3),IND,SIG	Be-9	5.0000E+07	5.0000E+07	LPI	79	4.5±1.5mb
50050.002	C-12	(P,P+D),IND,SIG	B-10	5.0000E+07	5.0000E+07	LPI	79	37±8mb
50050.002	C-12	(P,D+A),IND,SIG	Be-7	5.0000E+07	5.0000E+07	LPI	79	8.2±1.7mb
50050.002	C-12	(P,3P+A),IND,SIG	He-6	5.0000E+07	5.0000E+07	LPI	79	1.9±1.9mb
50050.002	C-12	(P,2P+A),IND,SIG	Li-7	5.0000E+07	5.0000E+07	LPI	79	11.8±3.6mb
50050.002	C-12	(P,P+2A),IND,SIG	He-4	5.0000E+07	5.0000E+07	LPI	79	37±2.3mb
50050.003	C-12	(P,2P+D),IND,SIG	Be-9	5.0000E+07	5.0000E+07	LPI	79	1.4±1.2mb
50050.003	C-12	(P,P+3-LI-6),IND,SIG	Li-6	5.0000E+07	5.0000E+07	LPI	79	0.3+0.5/-0.3mb
50050.003	C-12	(P,P+D+HE3),IND,SIG	Li-7	5.0000E+07	5.0000E+07	LPI	79	0.06±0.06mb
50050.003	C-12	(P,HE3+A),IND,SIG	Li-6	5.0000E+07	5.0000E+07	LPI	79	1.2±0.5mb
50050.003	C-12	(P,3P),IND,SIG	Be-10	5.0000E+07	5.0000E+07	LPI	79	1.3±1.3mb
50050.003	C-12	(P,P+D+T),IND,SIG	Be-7	5.0000E+07	5.0000E+07	LPI	79	0.03±0.03mb
50050.003	C-12	(P,P+T+HE3),IND,SIG	Li-6	5.0000E+07	5.0000E+07	LPI	79	0.03±0.03mb
50050.003	C-12	(P,P+D+T+HE3),IND,SIG	He-4	5.0000E+07	5.0000E+07	LPI	79	0.1±0.1mb
50050.003	C-12	(P,2HE3),IND,SIG	Li-7	5.0000E+07	5.0000E+07	LPI	79	0.4±0.4mb
50050.003	C-12	(P,T+HE3),IND,SIG	Be-7	5.0000E+07	5.0000E+07	LPI	79	0.9±0.5mb
50065.002	C-0	(P,X)6-C-11,CUM,SIG,,REL		1.5000E+08	6.6000E+08	DUB	57	
a0518.002	C-12	(P,X)4-BE-7,,SIG		2.4600E+07	9.6300E+07	TUH	93	* 21points
a0518.002	C-12	(P,X)4-BE-10,,SIG		2.4600E+07	9.6300E+07	TUH	93	* 21points
a0519.002	C-12	(P,X)4-BE-7,,SIG		1.6000E+09	1.6000E+09	TUH	93	x
a0530.002	C-12	(P,X)4-BE-7,IND,SIG		2.7870E+07	9.4480E+07	UH	91	* 20points
60022.002	C-12	(P,N+P),UND,SIG,,,EVAL	C-11	5.0000E+07	2.8000E+10	BNL	63	
60022.006	C-12	(P,X)4-BE-7,,SIG,,,EVAL		5.0000E+07	2.8000E+10	BNL	63	
60047.002	C-12	(P,G),,SIG		5.0000E+06	1.1000E+07	ORL	55	
60076.005	C-12	(P,N+P),UND,SIG	C-11	8.5000E+06	1.0400E+08	HRV	52	* 42points
60077.002	C-12	(P,N+P),UND,SIG,,A	C-11	1.5900E+07	3.2000E+07	BRK	52	* 42points
60077.003	C-12	(P,N+P),UND,SIG,,A	C-11	9.3000E+07	3.4000E+08	BRK	52	* 8points
60092.002	C-12	(P,2P),CUM,SIG	B-11	4.1000E+07	2.5000E+10	PAR	77	* 5points
60092.002	C-12	(P,N+2P),CUM/UND,SIG	B-10	4.1000E+07	2.5000E+10	PAR	77	* 5points
60094.003	C-12	(P,N+P),UND,SIG	C-11	5.9100E+08	5.9100E+08	CER	61	
60095.002	C-12	(P,N+P),UND,SIG	C-11	2.0700E+07	5.0500E+07	BNL	63	* 9points
60101.002	C-12	(P,N+P),UND,SIG,,A	C-11	1.7000E+08	3.5000E+08	BRK	56	
60101.009	C-12	(P,N+P),UND,SIG,,A	C-11	3.4000E+08	3.4000E+08	BRK	56	
c0056.002	C-0	(P,X)6-C-11,,SIG		3.8500E+08	3.8500E+08	LVP	68	
c0058.002	C-12	(P,N+P),UND,SIG	C-11	5.0700E+07	1.5860E+08	HRV	66	* 17points
c0059.002	C-0	(P,X)MASS,,SIG		4.5000E+07	1.0000E+08	MRY	76	
c0059.003	C-0	(P,X)ELEM/MASS,,SIG		1.0000E+08	1.0000E+08	MRY	76	

Table IV: Continued

Work no	Z-A	Reaction		Emin (eV)	Emax (eV)	Lab	Yr	comments
c0060.002	C-0	(P,X)6-C-11,,SIG		4.6100E+08	4.6100E+08	CHI	56	
c0060.003	C-0	(P,X)6-C-11,,SIG		4.6100E+08	4.6100E+08	CHI	56	
c0061.011	C-12	(P,2N+P),UND,SIG	C-10	1.5500E+08	1.5500E+08	PAR	63	
c0062.005	C-13	(P,N),,SIG		1.5500E+08	1.5500E+08	PAR	65	
c0062.011	C-12	(P,N+P),UND,SIG	C-11	1.5500E+08	5.7000E+09	PAR	65	
c0070.003	C-13	(P,N),,SIG		3.2391E+06	4.2500E+06	SWR	79	
c0206.002	C-12	(P,N+P),,SIG		2.8800E+08	3.8300E+08	LVP	60	
98207.002	C-12	(P,N+P),,SIG		2.0200E+08	3.4200E+08	LVP	60	
98207.003	C-12	(P,N+P),,SIG		2.0200E+08	3.5200E+08	LVP	60	
98208.012	C-12	(P,3N+3P),,SIG	Be-7	3.5200E+08	3.5200E+08	LVP	60	
98209.002	C-12	(P,N+P),,SIG		5.9100E+08	5.9100E+08	CER	61	
98214.002	C-12	(P,N+P),,SIG		4.2000E+08	2.9500E+09	BNL	54	
c0216.002	C-12	(P,N+P),,SIG		2.0000E+09	3.0000E+09	BNL	58	
c0220.003	C-12	(P,N+P),,SIG	Be-7	5.7000E+09	5.7000E+09	BRK	60	
c0220.004	C-12	(P,N+P+A),,SIG		5.7000E+09	5.7000E+09	BRK	60	
98221.002	C-12	(P,N+P),,SIG		3.0000E+09	6.0000E+09	LRL	60	
98224.008	C-12	(P,X)4-BE-7,,SIG		6.2000E+08	2.9000E+09	BNL	62	
98226.003	C-12	(P,X)4-BE-10,,SIG		2.2000E+08	2.2000E+08	SDC	64	
98226.004	C-12	(P,X)4-BE-10,,SIG		2.2000E+08	2.2000E+08	SDC	64	
98228.002	C-12	(P,X)4-BE-9,,SIG		1.5000E+08	6.0000E+08	CSN	71	3.2±0.4,5.3±0.7mb
98228.003	C-12	(P,X)4-BE-10,,SIG		1.5000E+08	6.0000E+08	CSN	71	1.1±0.1,2.8±0.4mb
c0231.002	C-12	(P,N+P),,SIG		2.8000E+10	2.8000E+10	BNL	62	
98232.002	C-12	(P,X)2-HE-6,,SIG		2.8000E+07	4.4000E+07	MHG	70	
98232.003	C-12	(P,X)3-LI-7,,SIG		2.8000E+07	4.4000E+07	MHG	70	
98232.004	C-12	(P,X)4-BE-8,,SIG		3.2000E+07	4.4000E+07	MHG	70	
98232.005	C-12	(P,X)4-BE-9,,SIG		3.2000E+07	4.4000E+07	MHG	70	
98232.006	C-12	(P,X)4-BE-10,,SIG		2.4600E+07	4.4000E+07	MHG	70	
98232.007	C-12	(P,X)6-C-11,,SIG		2.1700E+07	4.4000E+07	MHG	70	
98233.002	C-12	(P,X)3-LI-6,,SIG		1.5000E+08	6.0000E+08	CSN	72	11.6±1.6,15.5±2.2mb
98233.002	C-12	(P,X)4-BE-7,,SIG		1.5000E+08	6.0000E+08	CSN	72	12.1±1.2,11.0±1.1mb
98233.003	C-12	(P,X)3-LI-7,,SIG		1.5000E+08	6.0000E+08	CSN	72	9.2±1.6,13.6±2.1mb
98234.002	C-12	(P,X)4-BE-7,,SIG		2.4500E+07	1.5500E+08	ORL	67	
98235.002	C-0	(P,X)4-BE-7,,SIG		2.2500E+08	7.3000E+08	USA	60	
98235.003	C-0	(P,X)1-H-3,,SIG		2.2500E+08	7.3000E+08	USA	60	
98235.004	C-0	(P,X)4-BE-7,,SIG		2.2500E+08	7.3000E+08	USA	60	
98235.005	C-0	(P,X)1-H-3,,SIG		2.2500E+08	7.3000E+08	USA	60	
98235.006	C-0	(P,X)4-BE-7,,SIG		2.2500E+08	3.0000E+08	USA	60	
98235.007	C-0	(P,X)1-H-3,,SIG		2.2500E+08	3.0000E+08	USA	60	
98235.008	C-0	(P,X)4-BE-7,,SIG		2.2500E+08	7.3000E+08	USA	60	
98235.009	C-0	(P,X)1-H-3,,SIG		4.0000E+08	4.0000E+08	USA	60	
98236.003	C-0	(P,X)3-LI-9,,SIG		1.0000E+09	2.8000E+09	BNL	65	
98236.068	C-12	(P,4P),,SIG	Li-9	1.0000E+09	2.8000E+09	BNL	65	
98237.003	C-0	(P,X)3-LI-9,,SIG		1.5600E+08	1.5600E+08	PAR	68	
98237.028	C-12	(P,4P),,SIG	Li-9	1.5600E+08	1.5600E+08	PAR	68	
98243.002	C-12	(P,X)2-HE-6,,SIG		1.0000E+09	2.8500E+09	BNL	58	
98247.002	C-12	(P,X)3-LI-7,,SIG		4.4000E+07	5.5000E+08	CSN	65	
98247.003	C-12	(P,X)3-LI-6,,SIG	+(P,X)2-HE-6	4.4000E+07	5.5000E+08	CSN	65	
98247.004	C-12	(P,X)3-LI-7,,SIG	+(P,X)4-BE-7	4.4000E+07	5.5000E+08	CSN	65	
98255.002	C-0	(P,X)4-BE-7,,SIG		1.0000E+09	3.0000E+09	BNL	58	
c0259.003	C-0	(P,X)4-BE-7,,SIG		3.3500E+08	3.3500E+08	LRL	51	
c0261.011	C-0	(P,X)4-BE-7,,SIG		2.8000E+10	2.8000E+10	BNL	62	
c0315.002	C-12	(P,X)6-C-12,PAR,SIG,G		6.0000E+06	2.3000E+07	WAU	81	
c0397.002	C-0	(P,X)6-C-11,,SIG		9.8060E+07	9.8060E+07	MCG	64	
c0408.002	C-12	(18-AR-40,X)ELEM/MASS,,SIG		8.5200E+09	8.5200E+09	BRK	79	
o0044.002	C-12	(P,3N+3P),UND,SIG	Be-7	3.3500E+07	1.4920E+08	PAR	61	* 12points
o0044.024	C-12	(P,X)1-H-3,,SIG		1.5000E+08	1.5000E+08	PAR	61	
o0046.002	C-12	(P,X)1-H-1,,SIG		6.0000E+08	6.0000E+08	CLE	75	
o0046.002	C-12	(P,X)1-H-2,,SIG		6.0000E+08	6.0000E+08	CLE	75	
o0046.002	C-12	(P,X)1-H-3,,SIG		6.0000E+08	6.0000E+08	CLE	75	
o0046.002	C-12	(P,X)2-HE-3,,SIG		6.0000E+08	6.0000E+08	CLE	75	

Table IV: Continued

Work no	Z-A	Reaction		Emin (eV)	Emax (eV)	Lab	Yr	comments
o0046.002	C-12	(P,X)2-HE-4,,SIG		6.0000E+08	6.0000E+08	CLE	75	
o0048.002	C-12	(P,N),PAR,SIG	N-12	2.5800E+07	2.5800E+07	CLU	74	3.45±0.49mb
o0065.002	C-13	(P,2N+P),IND,SIG		1.8200E+07	3.0600E+07	LVN	89	
o0065.003	C-13	(P,N),,SIG		5.2000E+06	3.0600E+07	LVN	89	
o0073.023	C-0	(P,X)4-BE-7,CUM,SIG		1.3000E+08	3.9600E+08	CAR	64	
o0077.027	C-12	(P,3D),UND,SIG		5.0000E+08	2.9000E+09	CAR	68	
o0081.002	C-12	(P,NON),,SIG		3.0000E+07	6.0800E+07	ORL	71	
o0156.027	C-12	(P,PIP+X),SEQ,SIG		5.8500E+08	5.8500E+08	VIL	80	
o0156.027	C-12	(P,PIN+X),SEQ,SIG		5.8500E+08	5.8500E+08	VIL	80	
o0213.003	C-12	(P,TOT),,SIG		2.3100E+08	5.5200E+08	CER	72	
o0213.011	C-0	(P,TOT),,SIG,,,CALC		2.3100E+08	5.5200E+08	CER	72	
o0217.020	C-12	(P,INL),PAR,SIG		1.8200E+08	1.8200E+08	UPP	57	
o0217.021	C-12	(P,INL),PAR,SIG		1.8200E+08	1.8200E+08	UPP	57	
o0247.008	C-12	(P,TOT),,SIG		1.3700E+08	1.3700E+08	HAR	61	
o0247.008	C-12	(P,TOT),,SIG		1.3700E+08	1.3700E+08	HAR	61	
65001.008	C-13	(P,N),,SIG		3.8800E+06	5.2700E+06	ORL	59	
65050.002	C-12	(P,G),,SIG		8.5000E+04	1.3000E+05	LRL	57	
65051.002	C-12	(P,P+N),,SIG	C-11	2.7600E+07	4.1800E+07	CAN	58	* 31points
65051.003	C-12	(P,P+N),,SIG	C-11	1.8000E+07	3.1800E+07	CAN	58	* 36points
65055.002	C-14	(P,N),,SIG	N-14	6.8000E+05	1.4800E+06	ORL	59	

2.3 Spallation Neutron Experiment at SATURNE

Shin-ichiro Meigo
Spallation Neutronics Laboratory, Center for Neutron Science, Japan Atomic Energy Research Institute
Tokai-mura, Naka-gun, Ibaraki-ken 319-1195
e-mail: meigo@linac.tokai.jaeri.go.jp

The double differential cross sections for (p,xn) reactions and the spectra of neutrons produced from the thick target have been measured at SATURNE in SACLAY from 1994 to 1997. The status of the experiment and the preliminary experimental results are presented.

1. Introduction

The new proposals for Accelerator Driven Systems (for example, ref.[1, 2, 3]), that might be used to burn long-lived isotopes or to produce energy, has raised new needs for experiments and data in the domain of spallation. The design of the target-blanket assembly requires a detailed knowledge of the spallation process. In particular, it will be important to know the number of spallation neutrons produced per incident proton and their energy and angular distributions, in order to optimize the target composition and geometry, and also to estimate radiation damage in target and structural materials due to outgoing particles with much higher energy than in conventional reactors.

Simulation codes describing elementary production of particles in spallation reactions, as well as the transport of these particles in thick targets, are available. However, recent intercomparisons of these codes, organized by OECD/NEA [4, 5], have shown them to be of limited reliability, especially above 800 MeV where experimental data are scarce. Two types of measurement are necessary: the generation of fundamental nuclear data to improve the basic nuclear models used in simulation codes; and thick target measurements to validate the transport part of the codes and determine the performance of spallation targets.

A program to measure the double differential cross sections for the production of neutrons induced by protons on various thin and thick targets, has been done at the SATURNE accelerator in Saclay, using two different experimental techniques that allows the detection of neutrons from 1.5 MeV to 1 GeV. This experiment is a collaboration principally between Laboratoire National SATURNE, CEA-DAM Bruyères-le-Châtel, CEA-DSM Saclay and CNRS/IN2P3.

2. Experiment

2.1 Measurements of double differential cross section

The double differential cross section for (p,xn) reactions at 0° has been measured at SATURNE as phase 1 experiment [6, 7] since 1994. After phase 1 the experiment was continued at the another the beam port that made possible to measure the angular differential data 0° to 160°. The schematic view of the experimental setup is shown in Fig. 1. The incident energies of protons are 0.8, 1.2 and 1.6 GeV. For the double differential cross section thin targets of C,

Fe, Zr, Pb and Th are used which are cylindrical shape of 3 cm in diameter. Thickness of those samples is thinner than 8 cm and makes energy deposition less than 2 MeV.

For the low energy part of the neutron spectra (from 1.5 to 400 MeV) NE213 liquid scintillator (16 cm in diameter 10 cm in long) and an NE102 plastic scintillator were used. In order to obtain lower energy part around 1.5 MeV, four small NE213 scintillators (13 cm in diameter 5.6 cm long) were also employed. Time-of-flight is measured between incident protons tagged by a NE102 and NE213 scintillators. The pulses of photo multiplier associated with the NE102 scintillator are used to stop the time-of-flight analysis and to measure the incident proton intensity. The number of incident protons was 5 x 10^6 per an incident pulse of which time duration was 2 ms. The signal of NE213 detector is used to start the time-of-flight measurements and to reject gamma-rays from neutron by pulse shape discrimination. Charged particles are eliminated by a plastic scintillator in anti-coincidence. The obtained energy resolution is still better than 10% for the worse case at 400 MeV.

At high energies, the time-of-flight technique is not adequate to ensure a sufficient energy resolution due to short flight path. Therefore, the neutron is detected using (n,p) scattering on a two liter liquid hydrogen target in the energy range from 200 MeV to the beam energy. The trajectory of recoil proton in magnetic spectrometer was observed by three wire chambers constituted of two (X and Y) planes. A coincidence between two plastic scintillators triggers data acquisition and enables discrimination between charged particles by time-of-flight. An additional magnet in front of the liquid hydrogen allows to reject remaining charged particles which was mainly produced by the (n,p) reactions in the collimator. The two techniques overlap for an energy region between 200 and 400 MeV.

For the case of magnetic spectrometer, the number of incident protons are so large that it is impossible to count each protons. The number of protons was monitored by the two telescopes of three scintillators aiming at a mylar foil placed upstream in the beam. The absolute normalization was made by the activation of carbon slice and aluminum foil. In this normalization $^{12}C(p,^{11}C)$ and $^{27}Al(p,^{7}Be)$ reactions were used.

In order to reduce the neutrons produced by the room-scattering, the target was surrounded by the ordinal concrete with collimator holes 10 cm in diameter. For the estimation of the contribution of the scattering inside the collimator, the additional measurement was carried out by using iron shadow bar that screened only the detector but not shadowed collimator. By the shadow bar experiment, it was found that the contribution in the collimator was less than 2% for 2 MeV neutrons.

2.2 Measurements of spectrum of neutron from thick target

For thick target experiments, only time-of-flight technique was employed to measure produced neutron spectrum. Thick cylindrical Al, Fe and Pb targets were used. Those diameter were 10 and 20 cm and lengths were thicker than the range of the incident protons. By the concrete collimator, neutron detectors could not see the total area of the target. In the experiment the target was shifted to measure axial distribution according to the incident proton direction. The length between the center of the geometry and the incident surface of the target was chosen as 10, 30 and 50 cm.

3. Data reduction and experimental results

For the time-of-flight technique, the determination of detector efficiency is the main problem. The detection efficiency for NE213 was measured and is shown in the Fig. 2. These efficiencies were measured in Bruèyes-le-Châtel, Uppsala university and SATURNE for the energy region between 10 and 20 MeV, region between 20 and 80 MeV and above 100 MeV,

respectively. These results are compared with the calculation results with the code KSU and revised KSU which was changed the cross section for C(n,α) reaction. It is found for region between 20 and 80 MeV the original-KSU gives 20% small than the experiment and that the revised KSU agreed with the experiment. The interpolated values of the experimental efficiency results were used in the data reduction of the neutron production cross section and thick target yield.

The author also measured the detection efficiency of NE213 (16 cm in diameter and 16 cm long) [8] and found that the calculation by the original-KSU gave 20% larger value than experimental data. This tendency conflicts with the experimental result of Uppsala. This discrepancy can not be explained completely. It might be produced by the individual characteristic of detectors.

The preliminary experimental results for the double-differential cross sections are shown in Fig. 3. The present result for Pb(p,xn) reaction are compared with another experimental results in Fig. 3. The present results agree with the data measured at LANL. In the data analysis of KEK results, the calculation code of SCINFUL-R[8] , which gave 30 % smaller detection efficiency than the revised-KSU, was employed to obtain the cross section. The result of KEK, however, agreed with the present results within the experimental error of 20 % which is not shown in Fig. 3.

4. Comparison with the calculation results

Using experimental results, the validation of the calculation code NMTC/JAERI[11] was performed. In the calculation NMTC/JAERI and MCNP[12] was used. NMTC/JAERI calculated the nuclear reactions and the particle transport above 20 MeV. MCNP calculated the neutron transport below 15 MeV using a continuous energy cross section library FSXLIB-J3R2[13] processed from the nuclear data file JENDL-3.2. The level density parameter derived by Baba was used in the statistical decay calculation. Additional calculations were also performed by substituting the in-medium nucleon-nucleon(N-N) cross sections for the free ones in the nuclear reaction calculation part of NMTC. In this calculation, were employed the in-medium N-N cross section parametrized similarly to those of Cugnon[14].

In the thick target experiment, the detector accepted the neutron produced from the partial area of the target because of the concrete collimator. In the calculation, the collimator between two pallarel conical planes was employed to obtain high statistical results. By the comparison of results between this simplified geometry and the exact geometry, it was found the difference of neutron flux between two geometry models was less than 10 %. The calculated neutron spectrum was normalized by the factor between two geometry models.

In Fig. 4., the comparison of neutron spectra produced from the lead target is shown. It is observed that the calculation with the free N-N cross sections are in good agreement with the experiment for the energy below 20 MeV. The calculations with free cross section, however, are about 50 % or more lower than the experiment between 20 and 80 MeV. On the other hand, the calculation with in-medium N-N cross sections shows much better agreement with the experiment. This improvement is ascribed to the fact that the increase of the high energy nucleon emission diminishes the excitation energy of a residual nucleus so that the neutron emission from the evaporation process is suppressed. The calculation with the in-medium N-N cross section successfully reproduces the overall measured neutron spectra in the angular region smaller than 100° although the code give slightly lower neutron yields below 10 MeV. For the backward angles, the energy spectrum above 20 MeV is smaller than the experimental.

The author also measured the neutron spectra produced from the thick lead target [15] in KEK. In this experiment, as well as the present comparison, it was observed that by using

in-medium N-N cross section the calculation improved for higher energy and gave the smaller results for the backward angles.

Some studies showed that the inclusion of the preequilibrium process or the refraction and reflection process improved the backward neutron emission significantly. By the inclusion of those processes, the disagreement of the thick target will be more improved.

5. Summary

The neutron production double-differential-cross section and the spectra of neutron produced from thick target has been measured at SATURNE in Saclay. In the experiment, time-of-flight and magnetic spectrometer techniques were used to measure the spectrum. A good agreement between the results of the two experimental techniques, which overlap in the energy range 200 to 400 MeV. The present differential neutron production cross section agreed with the experimental results obtained at LANL and KEK even the detection efficiency was different. The final experimental results will be published in this year.

The calculation with NMTC/JAERI was compared with the thick target experimental results. By using in-medium nucleon-nucleon cross section the calculation was improved for the outgoing energy above 20 MeV.

Unfortunately, the accelerator of SATURNE has shut down after December of 1997 because of budget cut. In the further planing, the charged particles produce reaction cross section will be measured at COSY in Jülich. In that experiment, the present magnetic spectrometer will be transported to Jülich and will be used as a charged particle spectrometer.

References

[1] Bowman, C.D., *et al.,*: "Nuclear energy generation and waste transmutation using an accelerator-driven intense thermal neutron source", Nucl. Instr. and Meth. **A320**, 336 (1992).

[2] Takizuka, T., Nishida, T., Mizumoto, M. and Yoshida, H.: "Present status of accelerator based transmutation study at JAERI", Proceedings of the 8th Journees Saturne, Saclay May 5-6, 1994.

[3] Rubbia, C., *et al.,*: "Conceptual design of a fast neutron operated high power energy amplifier", *preprint CERN/AT/95-44(ET)* (1995).

[4] Blann, M., Gruppelaar, H., Nagel, P. and Rodens, J.: "International Code Comparison for Intermediate Energy Nuclear Data", *OECD/NEA* (1994).

[5] Filges, D., Nagel, P. and Neff, R. D. : "OECD thick target benchmark for lead and tungsten", *Report NSC/DOC(95) 2* (1995).

[6] Borne, F., *et al.*: "Spallation neutron spectra measurements part I: Time-of-flight technique", *Nucl. Instr. and Meth.*, **A385**, 339 (1997).

[7] Martinez, E., *et al.*: "Spallation neutron spectra measurements part II: Proton recoil spectrometer", *Nucl. Instr. and Meth.*, **A385**, 345 (1997).

[8] Meigo, S.: "Measurements of the response function and the detection efficiency of an NE213 scintillator for neutrons between 20 and 65 MeV", *Nucl. Instr. and Meth.*, **A401**, 365 (1997).

[9] , Amian, W. B., *et al.*: "Differntial neutron production cross section for 800-MeV protons", *Nucl. Sci. Eng.*, **112**, 78 (1992).

[10] Ishibashi, K.,*et al.*: "Measurement of Neutron-Production Double-Differential Cross Sections for Nuclear Spallation Reaction Induced by 0.8, 1.5 and 3.0 GeV Protons" *J. Nucl. Sci. Technol.*, **34**, 529 (1997).

[11] Nakahara, Y., Tsutsui, T.: *JAERI-M, 82-198*, (1982).

[12] Briesmeister, J.F., *et al.*: *LA-12625*, (1993).

[13] Kosako, K., *et al.*: *JAERI-DATA/Code*, 94-020 (1994).

[14] Cugnon, J.: Phys. Rev. C, **22**, 1885 (1980).

[15] Meigo, S., *et al.*: "Measurements of Spallation Neutron from a Thick Lead Target Bombarded with 0.5 and 1.5 GeV protons", *Proc. ICANS-XIII and ESS-PM4*, Villigen, Switzerland, Vol. II, 442 (1995).

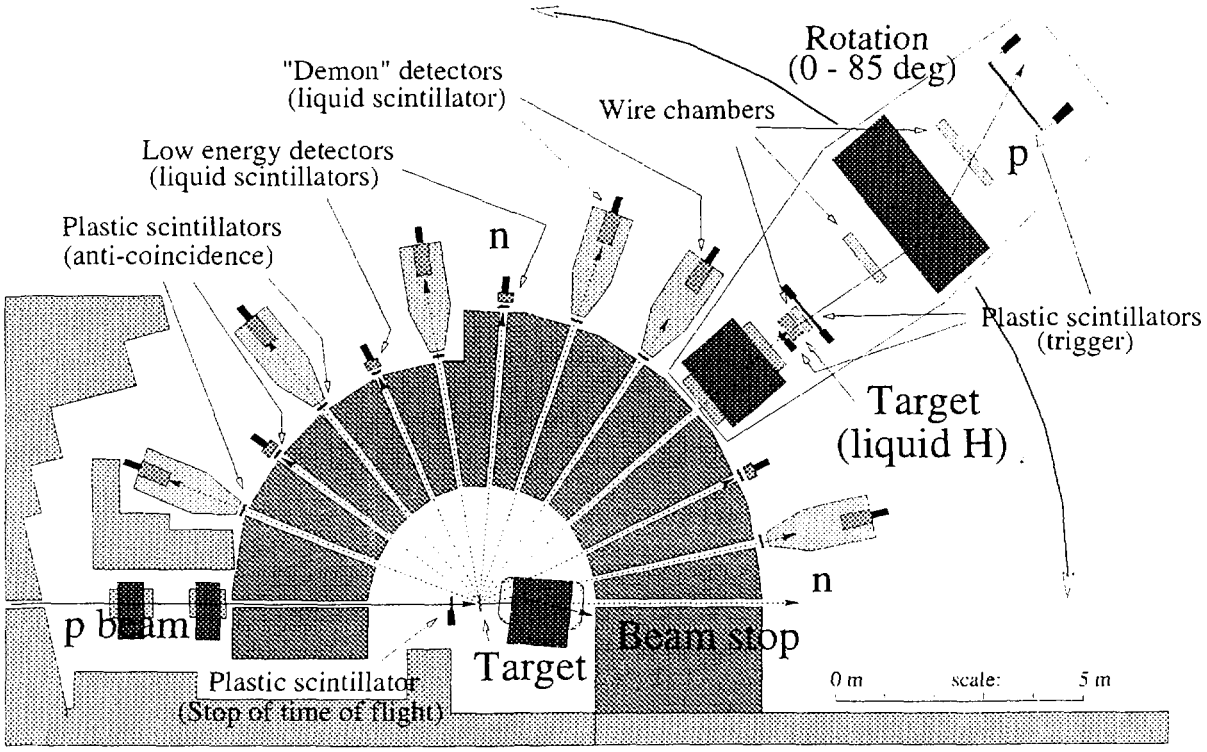

LNS, poste "Transmutation" Phase 2.

Figure 1: Experimental setup for the measurement of the angular distribution of neutrons: from 1.5 to 400 MeV) by time-of-flight, and above 200 MeV with a magnetic spectrometer.

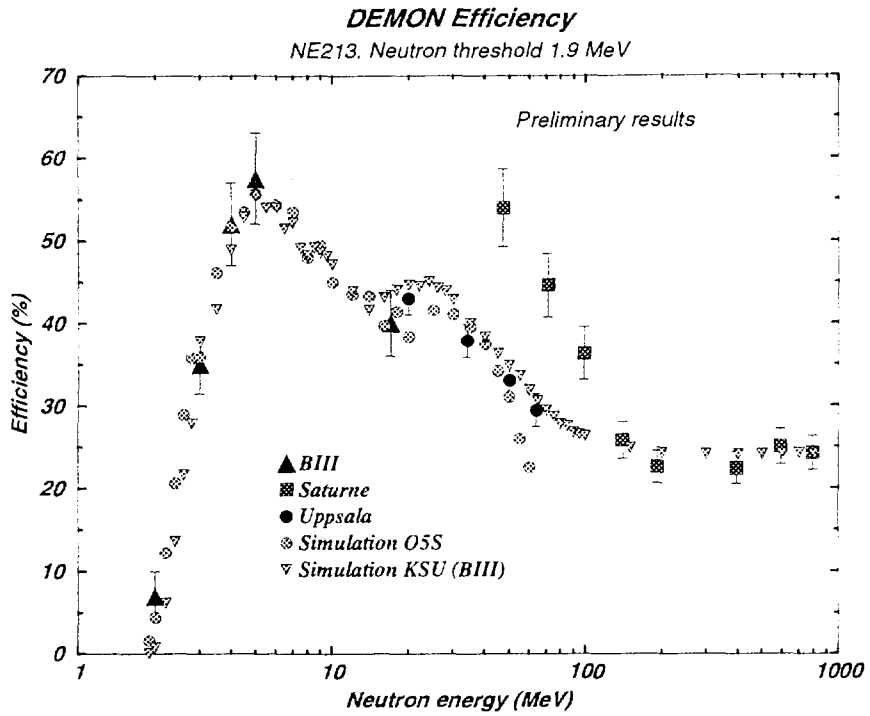

Figure 2: Neutron detection efficiency for the NE213 detector (16 cm in diameter and 10 long).

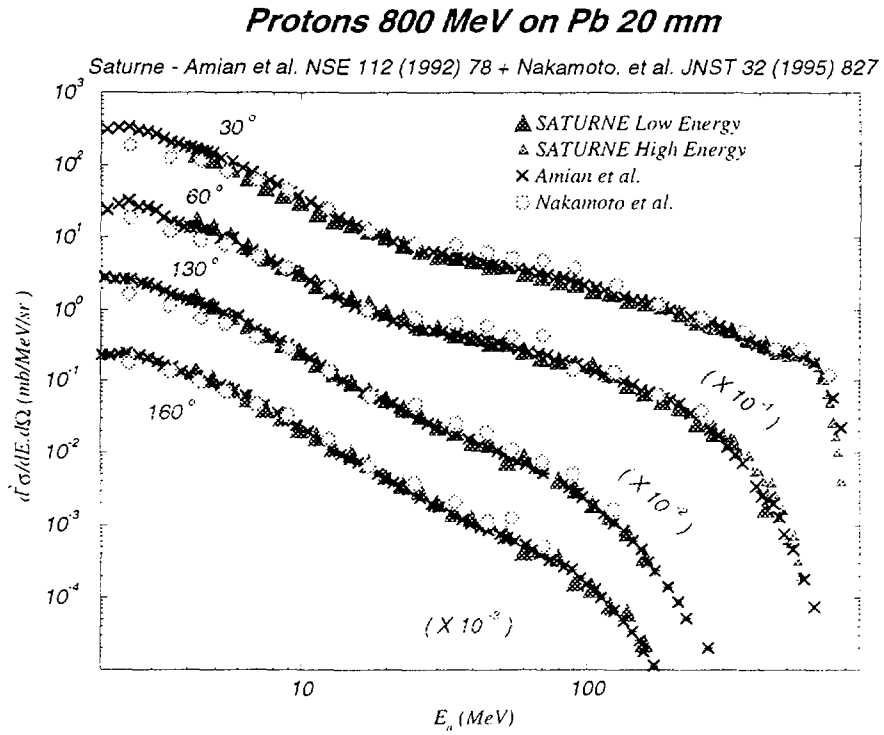

Figure 3: Present experimental result of Pb(p,xn) cross section for 0.8 GeV protons. Cross and circle marks stands for the experimental results at LANL[9] and KEK[10], respectively.

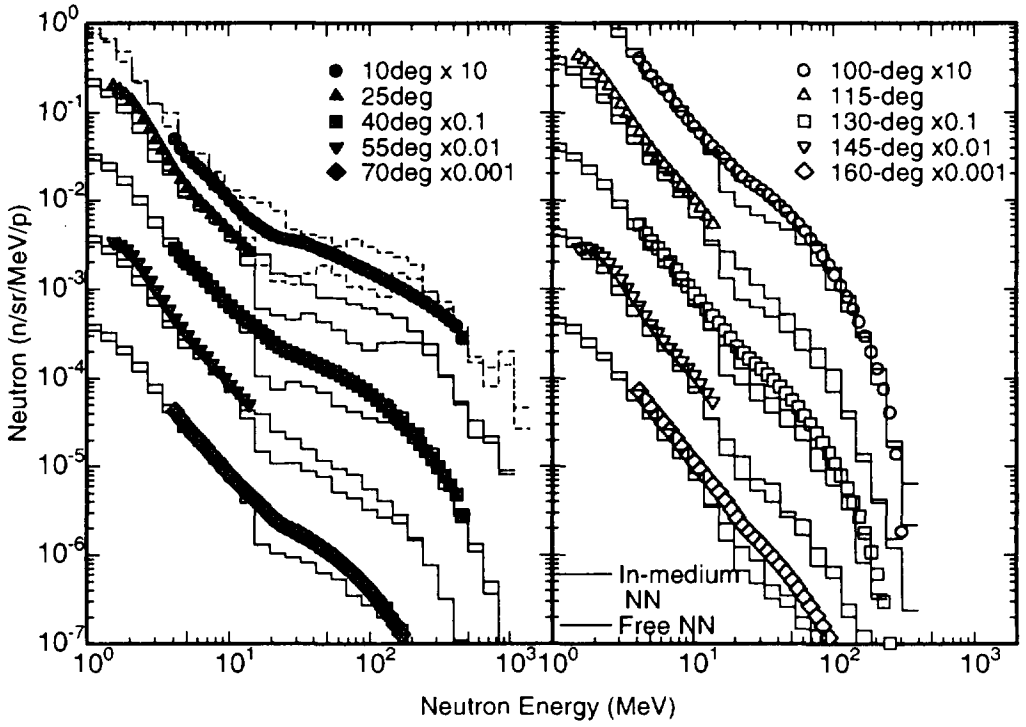

Figure 4: Spectrum of neutron produced from a thick lead target (20 cm in diameter and 65 cm long) bombarded with 1.2 GeV protons. The calculation was performed by NMTC/JAERI and MCNP with in-medium and free nucleon-nucleon (N-N) cross section.

3. Status of Evaluation and Reviewing Methods

3.1 Status of JENDL High Energy File --- Evaluation Method, Tools, Specification, Release Procedure, etc. ---

Tokio Fukahori
Nuclear Data Center, Japan Atomic Energy Research Institute
Tokai-mura, Naka-gun, Ibaraki-ken, 319-1195 Japan
fukahori@cracker.tokai.jaeri.go.jp

The ENDF-6 format file should be kept as a standard distribution file and it is not difficult to convert into some other form for code's libraries. From this point of view, status of JENDL High Energy File is introduced in this report as well as evaluation strategy, recommended specification, stored nuclides and quantities, a format structure, evaluation methods and tools, and release plan.

1. Introduction

It is important for producing JENDL High Energy File (JENDL-HE) to make clear and revise physical quantities required by uses and supplying procedure of high energy nuclear data at the right moment. As a basic strategy, the method and procedure of nuclear data supply;

1) Producing ENDF format file
2) Processing the file by certain codes (NJOY, etc.)
3) Making libraries for utility codes like MCNP, Group Constants, etc.

will not be changed. Since

1) a ENDF-6 format file has universal validity for global distribution,
2) it must be useful to store isotope production cross sections for activation and dosimetry usage, and
3) it must be used to store double differential particle production cross sections (DDX) for conventional transport calculation,

the ENDF-6 format file should be kept as a standard distribution file and it is not difficult to convert into some other form for code's libraries.

From above point of view, status of JENDL High Energy File is introduced in this report as well as evaluation strategy, recommended specification, stored nuclides and quantities, a format structure, evaluation methods and tools, and release plan.

2. Stored Nuclides and Priorities

Stored nuclides and evaluation status of the neutron file up to 50 MeV for IFMIF are shown in Table 1. At this moment, evaluation has been done for 40 nuclides and remained for 23 nuclides for this neutron file. For the evaluated 40 nuclides, results are being compiled into ENDF-6 format. Natural element will be constructed from each stable isotope and kept consistency as data for the isotope is evaluated. Especially for the important natural elements like iron, connection at 20 MeV to JENDL Fusion File or JENDL-3.2 should be carefully considered results and experiences from their benchmark test, since natural data for the element like iron were evaluated for just the natural element independent for isotopes.

The 122 isotopes (1^{st} priority: 42 isotopes, 2^{nd} priority: 40, 3^{rd} priority: 40) indicated in Table 2 will be stored in JENDL High Energy File up to 3 GeV. It is necessary to consider about the priority more. For instance, the priority for the nuclides, which have some benchmark experiments, should be higher. The priority for nuclides needed for the projects for JAERI Center for Neutron Science (accelerator, transmutation, etc.), Japan Hadron Facility (JHF) and so on will be discussed furthers.

3. Physical Quantities and Format

ENDF-6 Format is adopted, since this format is widely used and many processing codes adopting it. The relation of physical quantities and MF/MT numbers in ENDF-6 format is explained in Table 4, where MF numbers of 1, 2, 3, 4, 5, 6, ... mean comments and some data for fission reaction, resonance parameters, cross sections, angular distributions, energy spectra, double differential cross sections (DDX), ... respectively.

Combining method on file format structure with JENDL Fusion File or JENDL-3.2 is considered as following:

1) File structure of the file below 20 MeV is converted to same as JENDL High Energy File.
2) For elastic and inelastic scattering reactions to discrete levels, file structure below 20 MeV is adopted to higher energy.
3) In the case of adopting JENDL-3.2 and no γ production data in it, γ production data evaluated for higher energy are used.

The NEANSC/WPEC/SG13 recommendation for format structure of high energy files will be consistently adopted. The two slightly different format structures exist as JAERI-BNL and LANL recommendations. Recommendation of NEANSC/WPEC/SG13 is fully adopted by LANL File. Deference between JAERI-BNL and LANL recommendations is basically that particle production DDX is stored in MT=201-207 instead of MT=5. It is not a big problem, since both structures are easy to be converted. The merit of JAERI-BNL recommendation is extrapolation possibility to store meson production DDX. Considering release of MCNPX

code for transport calculation, for which NJOY code can process the library, the preprocessor for NJOY should be prepared to convert LANL format structure fully adopted to new version of NJOY.

4. Evaluation Strategy

In this section, overview of required accuracy for individual physical quantities is considered. Considering quantities are:

1) Particle Production DDX → Transport Calculation
2) Isotope Production Cross Section → Dosimetry and Activation

Options for transport calculations and needs of nuclear data in the intermediate energy region are summarized as following three categories.

1) Cascade Codes (Higher Energy: > 150～250 MeV) + Transport Codes (MCNP, ANISN, DORT, DOT, etc.) → DDX needed up to 150～250 MeV (LANL Method)
2) Transport Codes only → DDX needed in all the energy region
3) Empirical and/or Semi-empirical Codes → DDX needed in all the energy region

As an example of LANL case, MCNPX code is used up to 150 MeV by using existing nuclear data library and LAHET code is adopted above the energy and for the nuclides without library. In this case, transport cross section (DDX) library up to 150 MeV with good accuracy is required. Considering accelerators for radiation therapy, the changing energy (Ex) is about 250 MeV. Except determination of Ex value, the transport cross section should be prepared only below energy of Ex.

Isotope production cross section is needed in all the energy region as a nuclear data file, since cascade code is not suitable to calculate with short CPU time, enough energy points and accuracy. It is important to determine the changing energy (Ex).

5. Recommended Specification of JENDL High Energy File

The recommended specification of JENDL High Energy File according above discussion is introduced in this section. This recommendation is a general specification for guideline of producing the file and further discussion is necessary. The recommended specification is following:

1) Upper Energy of JENDL High Energy File: 3 GeV (for JHF Storage Ring)
2) Isotope Production Cross Section: Preequilibrium-Statistical Model Codes [ALICE-F (< 3 GeV), FKK-GNASH (< 250 MeV), SINCROS-II (< 50 MeV)]
3) Particle Production DDX: Preequilibrium-Statistical Model Codes (< 250 MeV), QMD and /or Cascade Codes (150, 250, 350, 500, 700, 1000, 1500, 2000, 3000 MeV)

4) For light mass nuclides: SCINFUL/DDX, EXFON, etc.

6. Release Procedure

The release scheme follows similar as JENDL General Purpose File as well as discussing with High Energy Nuclear Data Evaluation WG and JENDL Compilation Group. The current release plan is summarized in Table 3. The evaluated files will be released every year from 1999 following the priority list (Table 2). It may be revised due to status and needs changing.

File review and benchmark test will be done. Detailed discussion for file review and benchmark test are reported in this proceeding. The revised data according to the review and test will be included into the next release.

7. Summary

Reviewed and recommended were status, stored nuclides, evaluation status, physical quantities, format, evaluation strategy and methods, and release procedure. In the intermediate energy region, there is not enough experimental data for both of differential and integral measurements. The role of data review and benchmark testing is much more important than that below 20 MeV. The strategy and specification for evaluation of JENDL High Energy File were considered in this situation. It is still necessary to discuss for details between evaluators and users of high energy nuclear data. Author is waiting your suggestions and comments.

Table 1 Neutron File up to 50 MeV for IFMIF

Compiling (40 nuclides)	H-1(< 1 GeV), C-12(< 80 MeV), Na-23, Mg-24,25,26, Al-27, Si-28,29,30, K-39, Ca-40,42,43,44,46,48, Ti-46,47,48,49,50, V-51, Cr-50,52,53,54, Mn-55, Fe-54,56,57,58, Ni-58,60,61,62,64, Cu-63,65, Y-89
Evaluating (23 nuclides)	Li-6,7, Be-9, B-10,11, N-14, O-16, K-41, V-50, Co-59, Mo-92,94,95,96,97,98,100, W-180,182,183,184,186, Au-197

Table 2 Neutron & Proton File up to 3 GeV (Total: 122 nuclides)

1st priority (42 nuclides)	H-1, C-12, N-14, O-16, Na-23, Al-27, Cr-50,52,53,54, Fe-54,56,57,58, Ni-58,60,61,62,64, Cu-63,65, Ta-181, W-180,182,183,184,186, Au-197, Hg-196,198,199,200,201,202,204, Pb-204,206,207,208, Bi-209, U-235,238
2nd priority (40 nuclides)	Mg-24,25,26, Si-28,29,30, K-39,41, Ca-40,42,43,44,46,48, Ti-46,47,48,49,50, V-51, Mn-55, Co-59, Zr-90,91,92,94,96, Nb-93, Mo-92,94,95,96,97,98,100, Pu-238,239,240,241,242
3rd priority (40 nuclides)	Li-6,7, Be-9, B-10,11, C-13, F-19, Cl-35,37, Ar-35,38,40, V-50, Zn-64,66,67,68,70, Ga-69,71, Ge-70,72,73,74,76, As-75, Y-89, Th-232, U-233,234,236, Np-237, Am-241,242,242m,243, Cm-243,244,245,246

Table 3 Release Plan of JENDL High Energy File

Files	Release
Neutron File for IFMIF (< 50 MeV, 25 elements, 63 isotopes)	1998.10
1st Priority Nuclides (< 3 GeV, 15 elements, 39 isotopes)	1999.3
2nd Priority Nuclides (< 3 GeV, 8 elements, 23 isotopes)	2000.3
3rd Priority Nuclides (< 3 GeV, 23 elements, 54 isotopes)	2001.3

*: Revised nuclides according to file reviews and benchmark tests will be included in next release.

Table 4 Physical quantities stored in JENDL High Energy File and related MF/MT numbers

MT	MF	Reactions	Comments
1	2,3	Total	Only for neutron
2	2,3,4(6)	Elastic	Only for nuclear scattering
3	3	Non-elastic (Total reaction)	Sum. Of MT=4,5,18,102
4	3	Inelastic	Sum. Of MT=51-90
5	3,6	Isotope production	In the case including PKA spectra, LAW=7 is adopted. Otherwise LAW=0.
18	1,2,3,6	Fission	+ FP yield and neutron data (prompt, delayed, spectrum)
51-90	3,4(6, LAW=2), 12,14,15	Discrete inelastic	Basically only below 20 MeV In above case, σ =0.
102	2,3,12,14,15	Capture	Basically only below 20 MeV
201	3,6	Neutron production	No discrete levels*1 and no fission
202	3,6	Photon production	No discrete + capture level*2 Constructed from MF=13/MT=3 or inverse way (< 20 MeV)
203	3,6	Proton production	*3
204	3,6	Deuteron production	*3
205	3,6	Triton production	*3
206	3,6	He-3 production	*3
207	3,6	Alpha production	*3
208	3,6	π^- production	If necessary. *3
209	3,6	π^0 production	If necessary. *3
210	3,6	π^+ production	If necessary. *3
211	3,6	K^- production	If necessary. *3
212	3,6	K^0 production	If necessary. *3
213	3,6	K^+ production	If necessary. *3

*1: Elastic and discrete inelastic scattering reactions are not included in this MT section.

*2: No inelastic and capture gamma ray is included in this MT section.

*3: LAW=1 (Legendre Coeff. or Kalbach-Mann Sys.) or LAW=7 (Table).

3.2 Strategy on Review Method for JENDL High Energy File

Naoki Yamano

Department of Nuclear Design, Sumitomo Atomic Energy Industries, Ltd.

2-10-14 Ryogoku, Sumida-ku, Tokyo 130-0026

e-mail: yamano@sae.co.jp

Status on review method and problems for a High Energy File of Japanese Evaluated Nuclear Data Library (JENDL-HE File) has been described. Measurements on differential and integral data relevant to the review work for the JENDL-HE File have been examined from a viewpoint of data quality and applicability. In order to achieve the work effectively, strategy on development of standard review method has been discussed as well as necessity of tools to be used in the review scheme.

1. Introduction

Recent trend of nuclear data is focusing on intermediate and high energy applications such as medical diagnostics and therapy, transmutation of nuclear waste, irradiation test of materials for fusion reactor, nondestructive analysis and *in-situ* measurement related to increasing radiation utilization facilities with high-energy accelerators. The Japanese Nuclear Data Committee (JNDC) determined to promote a project on evaluation of JENDL High Energy File (JENDL-HE File) [1], and the Phase-I evaluation up to 50 MeV has being proceeded for 31 elements and 81 nuclei in a High Energy Nuclear Data Evaluation Working Group. In the current JENDL-HE project, a similar framework adopted in the JENDL evaluation activity for JENDL-3.3 is applied to review and validation for JENDL-HE File. In the evaluation for JENDL-3.3, two working groups are in charge of evaluation and three groups take the review and validation work. The same review scheme adopted in the JENDL evaluation is also expected to JENDL-HE Phase-I because the highest energy of nuclear data is 50 MeV. However, Phase-II evaluation of JENDL-HE File is planning to extend energy range above 1 GeV, so that the same methodology adopted in the JENDL evaluation technology cannot apply to the higher energy region.

In the present study, problems in the current review method for the JENDL-HE File will be described in Chap. 2 through brief examination of differential and integral measurements relating to nuclear data evaluation for JENDL-HE. Necessity of various tools will be shown in Chap. 3 to be used in the review work. In Chap. 4, We will discuss strategy on development of standard review scheme for the JENDL-HE File.

2. Status of Current Review Method

A schematic flow of evaluation for the JENDL-HE File is shown in Fig. 1. The review process consists of logical and physical check of data. The logical check includes examinations of file format definition, consistency between data and sum rules of these numerical values. Most of these items are automatically checked by using some checker programs. However, the physical check should be done by comparing with experimental data. For the JENDL-HE File, review work is required to check the following cross sections:

(1) total cross section (total reaction cross section for incident protons),
(2) elastic cross section,
(3) inelastic cross section from discrete levels,
(4) energy-angle double differential cross section (DDX) for (n,Xn), (n,Xp), (p,Xp) and (p,Xn) reactions,
(5) gamma-ray production cross section for (n,Xγ) and (p,Xγ) reactions,
(6) gas production cross section for (n,Xp), (n,Xd), (n,Xt), (n,Xh), (n,Xα), (p,Xn), (p,Xd), (p,Xt), (p,Xh) and (p,Xα) reactions,
(7) isotope production cross section.

For the quantity and quality of experimental data described above, capsule review work has been performed by a Task Force on Integral Evaluation for JENDL-HE File (JHEFIE) in JNDC. In the Task Force, available sources in Exchange Format Data Base (EXFOR), progress reports and proceedings were searched and examined on applicability to the review work of the JENDL-HE File. Data quality and the availability for differential and integral measurements will be shown by other presentations in this meeting. Measurements of neutron induced reactions above 20 MeV are accumulating during the last 10 years and the domestic results of isotope production cross sections are summarized in Table 1. [2] However, the status is insufficient to check data accuracy and consistency from a viewpoint of Quality Assurance Program for the JENDL-HE File.

In the circumstances, we propose the review work of the JENDL-HE File should be made not only comparison with cross-section measurements but also using available sources relevant to nuclear data. We can use some existing compilations, systematics and integral data to estimate data accuracy for target applications. In order to discuss the proposition, we made comparison of isotope production cross sections between The Los Alamos 150 MeV library (LANL/HE-1) [3] and ACSELA library [4]. The LANL/HE-1 is an evaluated nuclear data file for incident neutrons and protons up to 150 MeV produced by Los Alamos National Laboratory. The LANL/HE-1 contains complete nuclear data for 15 elements, 33 nuclei in the ENDF-6 format. The ACSELA library is a compilation of isotope production cross sections adopted in an IRAC code system [5] developed by Japan Atomic Energy Research Institute (JAERI). Isotope production cross sections in the ACSELA library consist of 57 elements, 136 nuclei and data were mainly compiled with ALICE-F [6] calculation for 9 projectiles of neutron, proton, deuteron, alpha, ^{12}C, ^{14}N, ^{16}O, ^{20}Ne and ^{40}Ar.

Energy range for incident neutron, proton, deuteron and alpha is up to 150 MeV, and the other projectiles are considered up to 500 MeV. Comparisons of isotope production cross sections for incident neutrons between LANL/HE-1 and ACSELA with measurements are shown in Figs. 2.1~2.6. Figures 3.1~3.6 indicate these for incident protons. We tried scoring the results of comparison with measurement between LANL/HE-1 and ACSELA. The score is shown in Table 2 where symbols and the criteria of scoring were decided as described in Table 3. In the case of $^{57}Fe(p,n)^{57}Co$ reaction in which many measurements are available to trace cross-section curve, LANL/HE-1 shows good agreement with experiment. However, the other case in which a few measured data are only available, LANL/HE-1 and ACSELA showed similar trend for cross-section profile and the same data quality was concluded.

In the JENDL evaluation, integral test of nuclear data with various benchmarks is a powerful test suite and gives essential information for validation of nuclear data accuracy. In the medium energy region, integral data such as shielding benchmark and measurement of thick target yields have being obtained especially in domestic activities. The analysis for these integral data is not easy to perform because cross-section processing from nuclear data and the transport method are not well established in the energy region. However, we should make use of integral data because these have information for verification of target applications through complicated process of multiple reaction sequences in matter. Methodology of the integral test with shielding benchmarks established in the JENDL evaluation [7] can be applied in the medium energy range.

3. Tools for Review Work

In the JENDL evaluation, various tools were developed and used in the review work. For the JENDL-HE project, the similar tools such as CHESTOR [8], SPLINT [9] and File-Checker [10] were prepared in order to utilize evaluation and the review works. However, experimental data acquisition system directly from EXFOR Data Base is not installed in Nuclear Data Center (NDC) of JAERI. In 1998, the NDC will become a mirror site of EXFOR Data Base, so that the excellent data retrieval and plotting system including DDX and ELEMENT/MASS presentations should be developed. Editing utility such as CRECTJ [11] adopted in the JENDL evaluation is also needed to treat full ENDF-6 format capability. In addition to these tools, a benchmark test suite should be prepared to derive thick/medium-range target yields from the JENDL-HE File.

4. Strategy on Development of Standard Review Scheme

From the review on current status of the JENDL-HE project, we will discuss the strategy on development of review scheme for the JENDL-HE File. The difference of review work between JENDL-HE and JENDL is that the review of JENDL-HE includes not only comparison of differential cross sections but also examination of integral data because the differential data measurement is insufficient to satisfy quality assurance, so that available sources relating to nuclear data should be used to supply information absent in

differential data. In order to develop the standard review scheme, tools described in the previous chapter are urgently required, and efforts to establish effective scheme will be needed including consideration of existing compilations and systematics treatment. For integral data, data acquisition and selection works for measurements of thick/medium-range target yields and simple transmission experiments are required in order to make benchmarks. Numerical data processing scheme should also be prepared from the JENDL-HE File to transport codes with group-wise and point-wise cross sections, and cascade-simulation codes.

5. Concluding Remarks

Status on the JENDL-HE project has been reviewed and the problems in the review method were described. In order to discuss quantity and quality of differential data measurements, domestic activities on cross section measurement were summarized and comparison of isotope production cross sections between the Los Alamos 150 MeV library and the ACSELA compilation was performed. Tools urgently required in the review work for the JENDL-HE File were presented and a proposal has been concluded that the integral data should be considered in the review scheme as well as examination of differential cross-section data. Strategy on development of standard review scheme for the JENDL-HE project was discussed and the direction to establish effective review scheme has been described.

References

[1] Fukahori, T., Chiba, S., Kishida, N., et al.: "Status of JENDL Intermediate Energy Nuclear Data Files," Proc. of Int. Conf. on Nuclear Data for Science and Technology, Trieste, May 19-24, 1997. (to be published)

[2] Fukahori, T., et al.: J. Atomic Energy Society of Japan, **40**[1], pp. 3-28 (1998). (in Japanese)

[3] Chadwick, M.B., Young, P.G., MacFarlane, R.E.: private communication (1997).

[4] Tanaka, S., Yamano, N., Hata, K., et al.: "Development of IRAC code system to calculate induced radioactivity produced by ions and neutrons," Proc. of 8th Int. Conf. on Radiation Shielding, Arlington, April 24-28, 1994, Vol. 2, pp. 965-971, American Nuclear Society Inc. (1994).

[5] Tanaka, S., Fukuda, M., Nishimura, K., et al.: JAERI-Data/Code 97-019 (1997). (in Japanese)

[6] Fukahori, T.: "ALICE-F Calculation of Nuclear Data up to 1 GeV," Proc. of the Specialists' Meeting on High Energy Nuclear Data, Tokai, October 3-4, 1991, JAERI-M 92-039, pp. 114-122 (1992).

[7] Yamano, N.: Annals of Nuclear Energy, **24**[13], pp. 1085-1094 (1997).

[8] Fukahori, T.: private communication (1995).

[9] Narita, T., Nakagawa, T., Kanemori, Y., et al.: JAERI-M 5769 (1974). (in Japanese)

[10] Fukahori, T.: private communication (1995).

[11] Nakagawa, T.: private communication (1984).

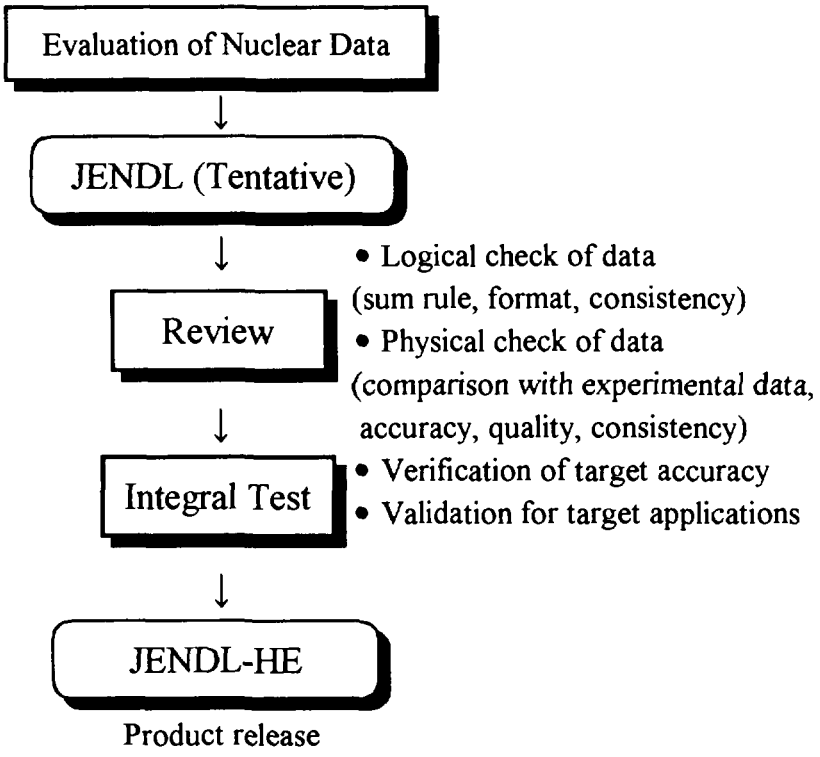

Fig. 1 Schematic flow of JENDL-HE File evaluation

Table 1 Recent domestic measurements of isotope production cross sections*

^{23}Na(n,2n)^{22}Na:	13～39MeV	^{197}Au(n,2n)^{196}Au:	8～39MeV
^{27}Al(n,2n)^{26}Al:	12～38MeV	^{nat}Mg(n,xnp)^{42}Na:	5～39MeV
^{27}Al(n,α)^{24}Na:	5～39MeV	^{nat}Si(n,xnp)^{28}Al:	5～39MeV
^{51}V(n,α)^{48}Sc:	7～39MeV	^{nat}Si(n,xn2p)^{27}Mg:	10～39MeV
^{51}V(n,p)^{51}Ti:	5～39MeV	^{nat}Si(n,xnp)^{29}Al:	7～39MeV
^{50}Cr(n,3n)^{48}Cr:	10～39MeV	^{nat}Ca(n,xnp)^{42}K:	5～39MeV
^{50}Cr(n,2n)^{49}Cr:	10～39MeV	^{nat}Ca(n,xnp)^{43}K:	5～39MeV
^{55}Mn(n,pα)^{51}Ti:	22～39MeV	^{nat}V(n,xn2p)^{46}Sc:	18～39MeV
^{55}Mn(n,4n)^{52}Mn:	34～39MeV	^{nat}V(n,xn2p)^{47}Sc:	7～39MeV
^{55}Mn(n,2n)^{54}Mn:	11～39MeV	^{nat}Cr(n,xnp)^{52}V:	5～39MeV
^{63}Mn(n,3n)^{61}Cu:	21～39MeV	^{nat}Cr(n,xnp)^{53}V:	5～39MeV
^{63}Mn(n,2n)^{65}Cu:	11～39MeV	^{nat}Cu(n,xn2p)^{62m}Co:	7～39MeV
^{65}Mn(n,p)^{65}Ni:	4～39MeV	^{nat}Zn(n,xn2p)^{65}Ni:	7～39MeV
^{64}Zn(n,t)^{62}Cu:	10～39MeV	^{nat}Zn(n,xnp)^{64}Cu:	1～39MeV
^{64}Zn(n,3n)^{62}Zn:	24～39MeV	^{nat}Zn(n,xnp)^{66}Cu:	5～39MeV
^{64}Zn(n,2n)^{63}Zn:	13～39MeV	^{nat}Zn(n,xnp)^{68m}Cu:	5～39MeV
^{197}Au(n,4n)^{194}Au:	10～39MeV	^{197}Au(n,2n)^{196m}Au:	10～39MeV
^{12}C(n,2n)^{11}C:	20～150MeV	^{47}Ti(n,np)$^{46m+g}$Se:	13～39MeV
^{30}Si(n,np)^{29}Al:	17～39MeV	^{52}Cr(n,2n)^{51}Cr:	10～39MeV
^{48}Ti(n,np)^{47}Sc:	10～39MeV	^{59}Co(n,3n)^{57}Co:	10～85MeV
^{59}Co(n,2n)$^{58m+g}$Co:	10～85MeV	^{58}Ni(n,2n)^{57}Ni:	10～39MeV
^{59}Co(n,4n)^{56}Co:	30～80MeV	^{55}Mn(n,2n)^{54}Mn:	11～39MeV
^{25}Mg(n,np)^{24}Na:	13～39MeV	^{54}Fe(n,2n)^{53}Fe:	15～39MeV

Table 1 Recent domestic measurements of isotope production cross sections* (continued)

^{55}Mn(n,pα)^{51}Ti:	20～39MeV	^{54}Fe(n,3n)^{52}Fe:	27～39MeV
^{54}Fe(n,t)^{52}Mn:	27～39MeV	^{nat}Cu(n,xnp)^{65}Ni:	50～120MeV
^{63}Cu(n,3n)^{61}Cu:	10～39MeV	^{nat}Cu(n,xn)^{60}Cu:	40～85MeV
^{nat}Cu(n,xn)^{61}Cu:	40～120MeV	^{nat}Cu(n,xnp)^{56}Mn:	50～120MeV
^{nat}Cu(n,xnp)^{58}Co:	40～120MeV	^{64}Zn(n,2n)^{63}Zn:	10～39MeV
^{209}Bi(n,3n)^{207}Bi:	15～39MeV	^{64}Zn(n,3n)^{62}Zn:	10～39MeV
^{209}Bi(n,4n)^{206}Bi:	25～150MeV	^{209}Bi(n,6n)^{204}Bi:	40～150MeV
^{209}Bi(n,5n)^{205}Bi:	30～120MeV	^{209}Bi(n,8n)^{202}Bi:	65～150MeV
^{209}Bi(n,7n)^{203}Bi:	50～150MeV	^{209}Bi(n,10n)^{200}Bi:	85～150MeV
^{209}Bi(n,9n)^{201}Bi:	70～150MeV	^{209}Bi(n,12n)^{198}Bi:	115～150MeV
^{209}Bi(n,11n)^{199}Bi:	105～150MeV	^{197}Au(n,2n)$^{196m+g}$Au:	10～32MeV
^{45}Sc(n,3n)^{43}Sc:	10～32MeV	^{50}Cr(n,x)^{48}V:	10～32MeV
^{45}Sc(n,2n)^{44m}Sc:	10～32MeV	^{50}Cr(n,x)^{49}V:	10～32MeV
^{45}Sc(n,2n)^{44g}Sc:	10～32MeV	^{48}Ti(n,x)$^{46m+g}$Sc:	10～32MeV
^{45}Sc(n,p)^{45}Ca:	10～32MeV	^{48}Ti(n,p)^{48}Sc:	10～32MeV
^{45}Sc(n,α)^{42}K:	10～32MeV	^{59}Co(n,p)^{59}Fe:	10～32MeV
^{58}Ni(n,x)^{56}Co:	10～32MeV	^{59}Co(n,α)^{56}Mn:	10～32MeV
^{58}Ni(n,x)^{57}Co:	10～32MeV	^{58}Ni(n,p)$^{58m+g}$Co:	10～32MeV
^{63}Cu(n,3n)^{61}Cu:	10～32MeV	^{65}Cu(n,2n)^{64}Cu:	10～32MeV
^{64}Zn(n,p)^{64}Cu:	10～32MeV	^{66}Zn(n,2n)^{65}Zn:	10～32MeV
^{66}Zn(n,p)^{66}Cu:	10～32MeV	^{66}Zn(n,x)^{64}Cu:	10～32MeV
^{85}Rb(n,3n)^{83}Rb:	10～32MeV	^{85}Rb(n,2n)^{84m}Rb:	10～32MeV
^{85}Rb(n,2n)^{84g}Rb:	10～32MeV	^{85}Rb(n,p)^{85m}Kr:	10～32MeV
^{85}Rb(n,α)^{82}Br:	10～32MeV	^{87}Rb(n,2n)^{86}Rb:	10～32MeV
^{87}Rb(n,x)^{85m}Kr:	10～32MeV	^{87}Rb(n,p)^{87}Kr:	10～32MeV
^{87}Rb(n,α)^{84}Br:	10～32MeV	^{89}Y(n,3n)^{87m}Y:	10～32MeV
^{89}Y(n,2n)^{88}Y:	10～32MeV	^{90}Zr(n,3n)^{88}Zr:	10～32MeV
^{90}Zr(n,2n)^{89m}Zr:	10～32MeV	^{90}Zr(n,2n)^{89g}Zr:	10～32MeV
^{90}Zr(n,x)^{88}Y:	10～32MeV	^{90}Zr(n,p)^{90m}Y:	10～32MeV
^{90}Zr(n,p)^{90g}Y:	10～32MeV	^{93}Nb(n,2n)^{92m}Nb:	10～32MeV
^{103}Rh(n,3n)^{101m}Rh:	10～32MeV	^{103}Rh(n,3n)^{101g}Rh:	10～32MeV
^{103}Rh(n,2n)^{102m}Rh:	10～32MeV	^{103}Rh(n,2n)^{102g}Rh:	10～32MeV
^{103}Rh(n,p)^{103}Ru:	10～32MeV	^{169}Tm(n,3n)^{167}Tm:	10～32MeV
^{169}Tm(n,2n)^{168}Tm:	10～32MeV	^{191}Ir(n,3n)^{189}Ir:	10～32MeV
^{191}Ir(n,2n)^{190m1}Ir:	10～32MeV	^{191}Ir(n,2n)^{190m2}Ir:	10～32MeV
^{191}Ir(n,2n)^{190g}Ir:	10～32MeV	^{191}Ir(n,p)^{191m}Os:	10～32MeV
^{191}Ir(n,p)^{191g}Os:	10～32MeV	^{191}Ir(n,α)^{188m}Re:	10～32MeV
^{191}Ir(n,α)^{188g}Re:	10～32MeV	^{193}Ir(n,2n)^{192m}Ir:	10～32MeV
^{193}Ir(n,p)^{191m}Os:	10～32MeV	^{193}Ir(n,p)^{191g}Os:	10～32MeV
^{193}Ir(n,α)^{190g}Re:	10～32MeV	^{197}Au(n,3n)^{195}Au:	10～32MeV

* Fukahori, T., et al.: J. Atomic Energy Society of Japan, **40**[1], pp. 3-28 (1998).
Measurements were performed at the following facilities:

- p-Li Neutron Source at TANDEM (JAERI-Tokai): 10～32MeV
- p-Li Neutron Source at CYRIC (Tohoku-Univ.): 20～40MeV
- p-Be, p-Li Neutron Source at INS (Tokyo-Univ.): 20, 25, 30, 35, 40MeV
- p-Li Neutron Source at TIARA (JAERI-Takasaki): 45, 50, 55, 60, 65, 70, 80, 90MeV
- p-Li Neutron Source at RIKEN: 90, 100, 110, 120, 135, 150MeV

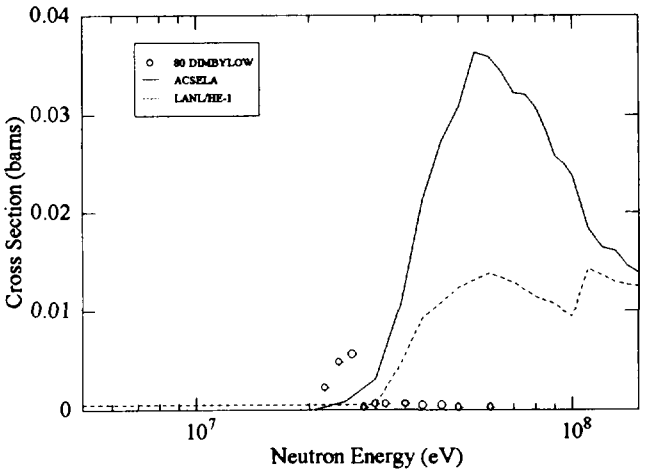

Fig. 2.1 ^{12}C (n,t) ^{10}B Production Cross Section

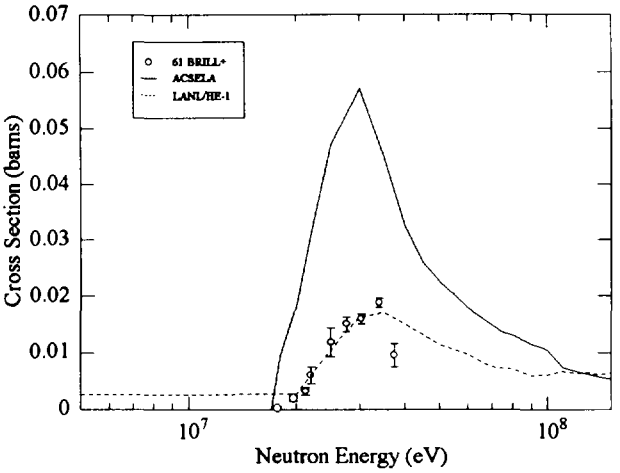

Fig. 2.2 ^{16}O (n,2n) ^{15}O Production Cross Section

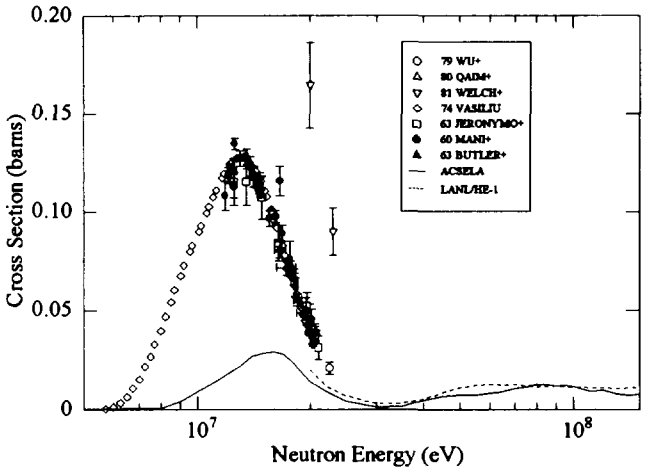

Fig. 2.3 ^{27}Al (n, α) ^{24}Na Production Cross Section

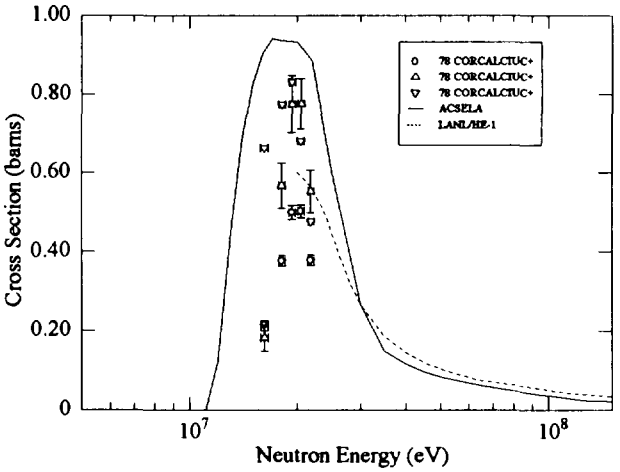

Fig. 2.4 ^{56}Fe (n,2n) ^{55}Fe Production Cross Section

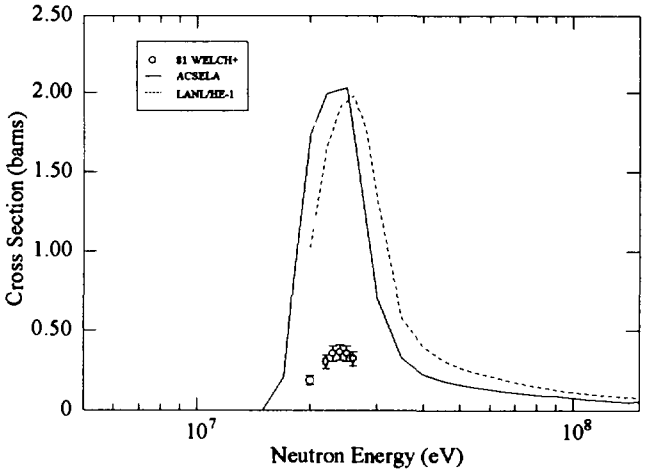

Fig. 2.5 ^{206}Pb (n,3n) ^{204}Pb Production Cross Section

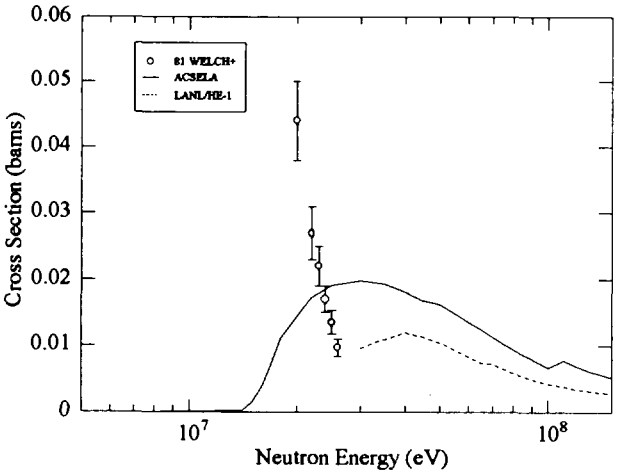

Fig. 2.6 ^{208}Pb (n,p) ^{208}Tl Production Cross Section

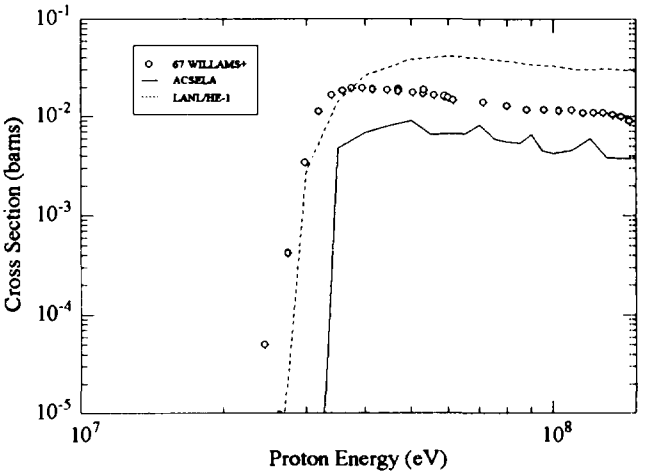

Fig. 3.1 ^{12}C (p,x) ^{7}Be Production Cross Section

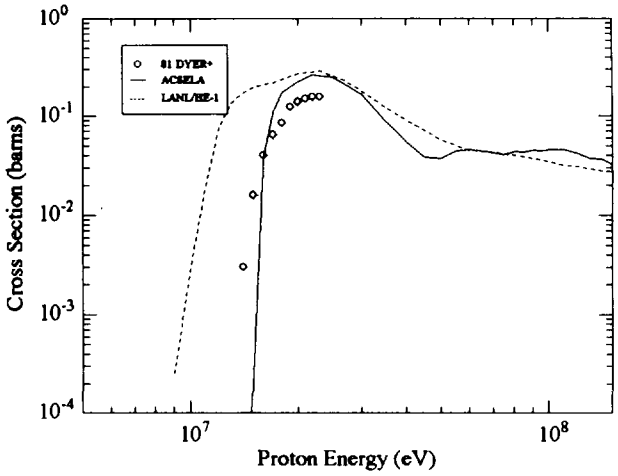

Fig. 3.2 ^{16}O (p,x) ^{12}C Production Cross Section

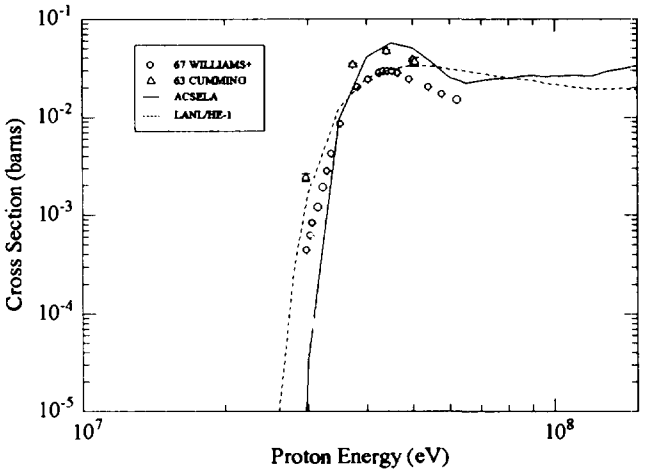

Fig. 3.3 ^{27}Al (p,x) ^{22}Na Production Cross Section

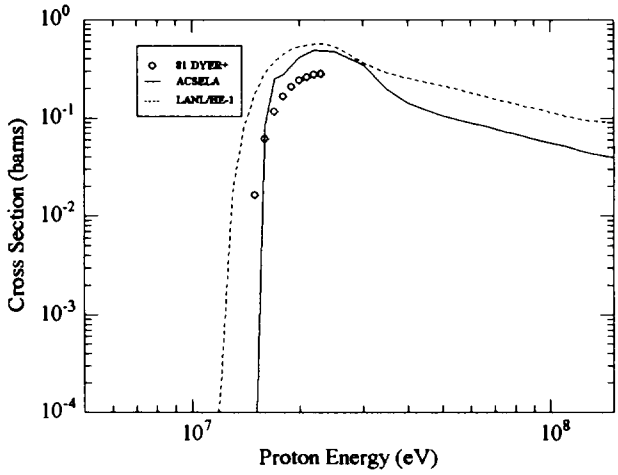

Fig. 3.4 ^{56}Fe (p,x) ^{55}Fe Production Cross Section

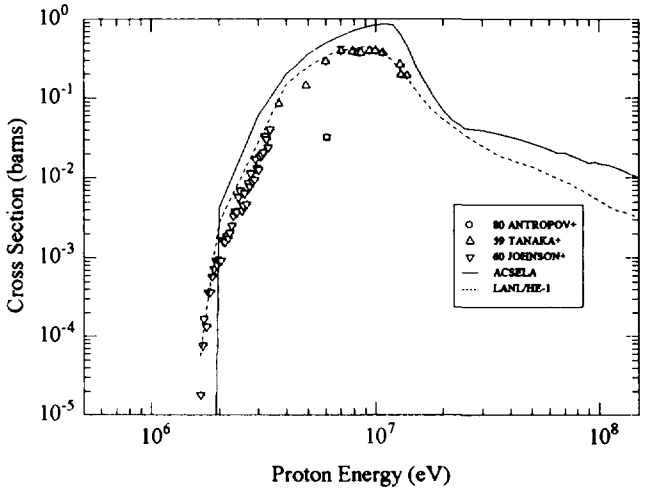

Fig. 3.5 ^{57}Fe (p,n) ^{57}Co Production Cross Section

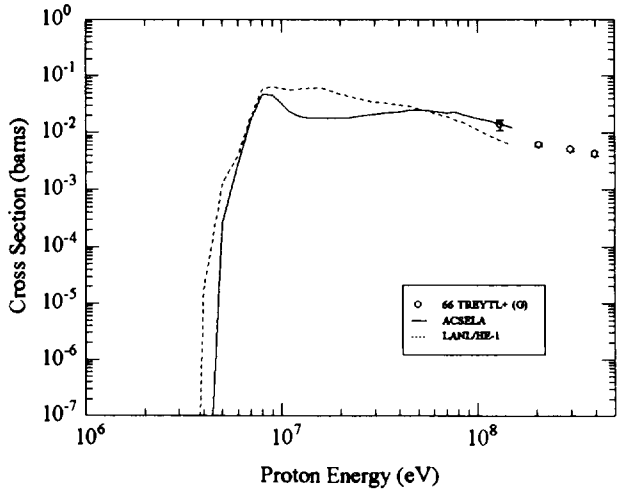

Fig. 3.6 ^{186}W (p,n) ^{186}Re Production Cross Section

Table 2 Comparison of isotope production cross section between LANL/HE-1 and ACSELA

incident protons			incident neutrons		
target	product	score	target	product	score
C12	He6	?	C12	C11	? A
C12	Li6	? ○	C12	Be9	★★
C12	Li7	?	C12	B10	?
C12	Be7	★	C12	B12	? A
C12	Be9	?	C12	B11	?
C12	B10	★ ○	C12	He4	?
C12	C11	★★ ○			
O16	C12	? S	O16	O15	★★★A
			O16	C13	★ ○
			O16	N14	?
Al27	F18	★	Al27	Al26	★ A
Al27	Na22	★★ ○	Al27	Na24	○
Al27	Na24	★	Al27	Mg25	?
Al27	Si27	★★ ○	Al27	Na25	? ○
			Al27	Mg27	? ○
			Si28	Mg25	?
			Si28	Al28	★ ○
Si29	Al28	?			
Si30	Mg28	?			
Si30	Al29	?			
Fe56	Fe55	★ ○	Fe56	Fe55	★★ A
Fe56	Co55	★★ ○	Fe56	Mn56	★★ ○
Fe56	Co56	★★			
Fe57	Co57	★★★○			
Fe58	Co58	-----			
			W184	Ta182	?
			W186	Hf183	?
W186	Hf184	-----	W186	Hf184	?
W186	Ta185	? A	W186	Ta185	?
W186	Re186	★★ ○	W186	Ta186	★★
			Pb206	Pb204	? ○
			Pb208	Tl208	?
			Pb208	Tl207	?

Table 3 Criteria of scoring and symbols

★★★	good agreement with experimental data
★★	close to experimental data
★	similar to experimental data
○	the same trend between LANL/HE-1 and ACSELA
A	good agreement between LANL/HE-1 and ACSELA in the energy range above 100MeV
S	the same trend between LANL/HE-1 and ACSELA in the energy range above 100MeV
?	unknown (few experimental data)
-----	data not given in LANL/HE-1 but include ACSELA

4. Processing and Transport Calculation Method

4.1 Transport Code and Nuclear Data in Intermediate Energy Region

A. Hasegawa[1], *F.Maekawa*[2], *K. Ueki*[3],
K.Kosako[4], *N.Odano*[1], *Y.Oyama*[5]

1) Department of Nuclear Energy System, Japan Atomic Energy Research Institute
2) Department of Material Science, Japan Atomic Energy Research Institute
3) Ship Research Institute
4) Sumitomo Atomic Energy Industry
5) Center for Neutron Science, Japan Atomic Energy Research Institute

Report on the
"Problems in the Processing of Intermediate Energy Nuclear Data File and Transport Codes"
in the Task Force on JENDL High Energy File Integral Evaluation (JHEFIE)

abstract

We briefly reviewed the problems of intermediate energy nuclear data file and transport codes in connection with processing of the data. This is a summary of our group in the task force on JENDL High Energy File Integral Evaluation (JHEFIE). In this article we stress the necessity of the production of intermediate evaluated nuclear data file up to 3 GeV for the application of accelerator driven transmutation(ADT) system. And also we state the necessity of having our own transport code system to calculate the radiation fields using these evaluated files from the strategic points of view to keep our development of the ADT technology completely free from other conditions outside of our own such as imported codes and data with poor maintenance or unknown accuracy.

1. Current User Profile of Intermediate Nuclear Energy Data

Main points stated here are presented in OYAMA Report ,"Present Status and Propositions for the Intermediate Energy Nuclear Data Library", which is issued by the Research Committee of Reactor Physics of JAERI, at 5 March, 1998.[1] In that report potential users and their characteristic features (· Required Physical Quantities, · Required Materials , · Required Accuracy, · Used Method (Typical)) for the intermediate nuclear data files are summarized very compact as shown in the followings.

1). Accelerator Driven Hybrid Nuclear Energy Production System

For this application, proton and neutron data up to 1.5GeV are requested from JAERI's project of the center for neutron science. In the case for muon catalyzed fusion being planned in RIKEN, upper

limit is extended to 3GeV.

・ Required Physical Quantities:

Transport calculation (particle fields calculation) for neutron, proton, gamma-ray and charged particles are required to get the estimation of the amount of product nuclides, induced radio-activity, material damage and nuclear transmutation rate. In some cases for the fundamental plant design, nuclear - thermal coupled calculation is required. To identify the radiation field of the intermediate energy range dosimetry data are inevitable.

・ Required Materials:

Structural Material, minor actinides, nuclear fuel, coolant material (for example, water, liquid metal, molten salt) are required.

・ Required Accuracy:

Target accuracy for the estimation of nuclear transmutation, induced radio activity and criticality are 10% , 20-30% and 1% respectively.

・ Method (Typical methods currently adopted):

i) Nuclear Transmutation System

Target + Criticality Calculation

➔ ATRAS[2] (NMTC+MCNP, NMTC+TWODANT)

Burn-up Calculation ➔ BURNER

Nuclear Heating Calculation ➔ NMTC[3]

ii) Design of Neutron Source

Cold Neutron Source

➔ NMTC + MCNP[4] LCS [5](LAHET[6] + MCNP)

➔ HERMES [7](HETC-KFA+MORSE-CG+EGS4+NDEM)

FLUKA[8]

MCNPX[9] (MCNP (150MeV) + HETC[10] embedded)

2). Accelerator Facility Shielding Design

For the JHF project, proton data up to 50GeV are required. For other application such as JAERI OMEGA project, neutron and proton data up to 1.5GeV are required.

・ Required Quantities:

proton, neutron Source Term Evaluation

Bulk shields: Intermediate Energy Neutron Transport Calculation (Deep Penetration)

Streaming (Maze)

Sky shine (Large Scale Calculation 100m – several Km)

Exposure Evaluation

Induced Radioactivity (Induced Activation)

- Required Material:

  Concrete, iron, tungsten, earth, copper, stainless steel etc.

- Required Accuracy:

  Exposure 50%

  Induced Activity 50%

- Method (Typical):

  i) Bulk Shield

  Simple Formulae → Moyer Model

  Monte Carlo Calculation → MARS[11], FLUKA

  Deterministic Calculation → DORT[12]/HIRO86[13] < 400 MeV

  Point Kernel Method → PKN[14] < 400 MeV

  ii) Streaming

  Monte-Carlo Calculation MCNP, MVP[15],....

  Deterministic DOT, DORT

  Semi Empirical Recipe Tesch Formulae

  iii) Sky Shine

  Deterministic DOT, SHINE-II

  Semi Empirical Recipe Nakamura Formilae, Stevenson-Thomas Formulae

  iV) Induced Radioactivity

  NMTC , HETC

3). Medical Applications

For the irradiation and production of radio isotope, proton data up to 250 MeV are required.

- Required Quantities:

  Source Term Evaluation: proton transport calculation

  Produce Radio Isotopes: nuclear transmutation by proton

  Shielding of Secondary neutrons produced by primary proton reaction

- Material:

  Shielding Materials, phantom(model of human kind)

- Required Accuracy:

  Exposure: 5%

  Contribution from neutron will be ignored.

4). IFMIF project

For IFMIF (International Fusion Material Irradiation Facility) project, neutron data up to 50 MeV are requested.

2. Overview of Transport Method for the Calculation of Radiation Field

Overview of the current calculation paradigm used in the estimation of the radiation fields is shown in Fig. -1.

1. Deterministic Method

- Differential Transport Method

  Sn→ ANISN DOT DORT TORT Pn → PN
- Integral Transport Method PALLAS BERMUDA
- Analytic Approximation ANCAS Point Kernel
- Semi Empirical Recipes Moyer

2. Stochastic Method

- Monte Carlo Simulation

  up to 20 MeV: point model: MVP MCNP

  group model: VIM TART97

  intermediate energy: HETC LAHET MCNPX FLUKA GEANT

3. Adjusted Library

- Generate some special libraries only applicable some specific problems

  ex. HILO86

Fig.1 Calculation Paradigm for the Transport Code Currently Used (Neutrons)

For neutron calculations, deterministic methods are fundamental tools for shielding design of the nuclear facilities such as reactors, fuel processing plant, accelerators, and recently including space craft for the outer-space applications. In this method, the Sn codes are most frequently used. Many codes having general purpose applicability have been developed. But there are some drawbacks for these codes, they are poor treatment for the scattering anisotropy and the ray effects in the scattering source calculation. Former point is resolved introducing double differential type treatment instead of Legedle expansion.

Analytical Solutions has following advantages compared with other methods. It is intuitive because it is developed by the clear understanding of physics of radiation transport, and it can give particle spectra as well as attenuation data, within the reasonable computation time independent with shield thickness. On the other hands, following disadvantages are inevitable, i.e., it needs adequate cross-section database for accurate results and severe approximations and low geometry approximations (usually one-dimentional) are inevitable.

Recently computer simulation techniques become common tools in shielding design. It has the special advantage because it represents mathematical equivalent of doing a measurement on a mock-up. The methodology is well developed in low energy (< 20 MeV) region and high energy (>1000MeV) region. Recent advances in 'universal' codes which cover all energy range will be a powerful tool for the high energy application users.

Computer Simulation has many advantages. It enables effectively to deal with complicated geometry in three dimensions easily. And also it yields detailed data on the particles such as fluences, energy deposition, etc. For disadvantages, it needs extensive database for interaction and particle production cross sections. For realistic deep penetration problems severe weighting should be used. And generally I/O routines are not very user friendly.

Phenomenological models use some physical insight to justify general form and fixed parameters to which should be prepared by fitting to the results of measurements . Usually it applicable only the region where attenuation is exponential (i.e. not where cascade is still building up).

As to the proton transport in the intermediate proton energies (50 - 1000 MeV), calculation is very difficult because significant variation in cross-sections is foreseen but we have sparse experimental data, and hadronic cascade is not yet in equilibrium in this range.

In the high primary proton energies (> 1 GeV), phenomenological model is fully developed only for lateral shield(Moyer model). In this model a single effective attenuation length is usually used. Angular dependence is approximated by an exponential and dose equivalent is assumed proportional to high energy particle fluence.

For protons as well as for neutrons, the method is still developing stage. The development is continuing to enjoying the recent advancements of the software technology in the transport calculations.

3. Recommendation for Method Development

Nuclear data and radiation transport codes are needed to calculate radiation fields and to design shields. New Codes are always expected to break the status of the technology.

Two codes are newly found in the survey adding to the commonly used codes in Japan. They are MCNPX[9] and TART97[16]. Those two codes are in the category of stochastic methods. The former is a point Monte Carlo code with the extension of the charged particle treatments and high energy libraries and the latter is a group model Monte Calro code with new features represented as enabling multi processing, no upper limit for the input data limitation and long run random number generator. Due to the group model, the latter code is benefited for calculation speed compared with point energy model. Due to the same reason, it has also special advantages for the treatment of self-shielding effect especially for the unresolved resonance regions by using the multi-band parameters compared with other point Monte Carlo code, in which self-shielding effects are not properly treated. We already

started to implement and utilize these new codes to check the code performance and their abilities.

From the discussions of availability of codes, following two points are recommended further.

Availability of source code: Availability of source code is not foreseen for FLUKA or MCNPX. Usage of these code should be rather cautious because there is a danger. That is, data update / version update are completely depends on the host agency, i.e., where the original code comes from. When we encountered logical errors in such cases, we have nothing to do about that. Usually bug is inevitable for the software, especially for the latest or newly developed ones. We stress here importance of transparency of the source code to users. In the software, the most important part is the logic. The code logic should be opened to users because there are no error free programs.

Reference code for common usage in the intermediate energy region: Do we need our own code ? Should we develop our own code system? Majority of the answer to these questions is yes. That is, many people want to maximize the usage of our specific code or to adopt the code in their own specific purposes. We must have our own code system. But also we have negative answer. That is rather minority. They say that if the maintenance (version up/upgrade) for the imported code will be continuously made in future, we do not need our own code.

What criteria should be required as the reference code? For Licensing use, V&V (verification and validation) should be thoroughly made, enabling quality assurance through benchmark test by the available integral experiments. Code comparison should be made for the typical examples between the candidate code and the proven code which have already gained reputation in the fields. Data base (especially nuclear data) improvements are inevitable according to the feedback information from code and data experiences. All related design tools including nuclear design, thermal hydraulics design as well as structural design are totally coupled/coordinated under this concept.

4. Recommendation for Evaluated Data File Development

For the current data & methods, following points are claimed from users:

1) Poor calculation accuracy for produced nuclides

2) Poor cross section accuracy in the energy range less than several hundreds MeV

3) Poor accuracy for 2ndary gamma-ray production cross-section

4) Poor accuracy for pion or muon cross-section

5) Poor cross-section data accuracy for light elements nuclides

Based on these feedback information as well as the requests for data stated in section 1, we stress here to improve the quality of the data on the following points in the evaluation stage, nuclide production cross section, high accuracy for induced activities and nuclides production cross sections, selection of proper dosimetry nuclides for the Dosimetry file, especially the last item is highly requested from design team of ADT.

We are now developing our own evaluated nuclear data file in the intermediate energy range. For

JENDL High Energy File, we develop it in the two step method. For phase-1. neutron files up to 50MeV is developing and for phase-2 neutron and proton data up to 2 GeV will be produced after the first step. Other than JENDL, ENDF/B-VI High Energy File (up to 1 GeV only a few nuclides). ENDL (up to 250MeV, mainly tissue-resident, structural material) and LANL files exist.

Special remarks of neutron cross section in intermediate energy range (20-100MeV) is stated here. In this energy range, cross sections are very difficult to describe with simple theories. For the sophisticated evaluations, we need many physics of nuclear reaction mechanism like compound nuclear formation with statistical decay, direct process and pre-compound process. Nuclear reaction models in this energy range must cover all of these processes and competition between them.

There had been two approaches for the estimation of the cross sections in this energy range. One is an extension of nuclear model code used in the intra-nuclear cascade code by the inclusion of pre-equilibrium and direct processes. For example, a system code composed from LAHET (LANL) and MCNP (<20MeV) codes, for the calculation between 20MeV to 100 MeV intra-nuclear cascade and pre-compound code are used, and above 100 MeV original HETC is used, and less than 20MeV MCNP is employed. Original HETC (ORNL) code is a successor of O5R. Original O5R code is used up to 15MeV and above intra-nuclear cascade code is used in the HETC. As to HERMES (KFA. Julich) the same strategy is taken for the code design for the intra-nuclear cascade code. HETC is the ancestor.

The other approach is the extension of evaluated nuclear cross section data base. In this approach, data base update is usually performed based on the feed back information from the measured cross-section data and integral information from application users. In this case continuous data base update is possible. Evaluated data base provide the most accurate representation of the cross section. Feedback by benchmark test is easily made by this approach. Thus all feedback information is reflected and thus improved results are shared by all of the users of this evaluated files. This point is very important compared with the method using intra-nuclear cascade code, where only the user of the same intra-nuclear cascade code can be benefited, not expand any more.. Now you can see there is a big point for the producing of evaluated nuclear data files compared with using the intra-nuclear cascade code. Every improved data base updated in the common files will be shared all of the users of this data base. By this method, transport calculation is made quite faster than the previous method because there is no need for the cross section calculations.

5. Summary

We briefly reviewed the problems of intermediate energy nuclear data file and transport codes in connection with processing of the data. We stress the necessity of the production of intermediate evaluated nuclear data file up to 3 GeV for the application of accelerator driven transmutation(ADT) system. And also we state the necessity of having our own transport code system to calculate the

radiation fields using thus developed evaluated files from the strategic points of view to keep our development of the ADT technology completely free from other conditions outside of our own.

References

1) Y. OYAMA et al: "Present Status and Propositions for the Intermediate Energy Nuclear Data Library", Report for Research Committee of Reactor Physics of JAERI (1998) (in Japanese).

2) Sasa T., Nishida T., Takizuka T., et.al.:"Development ATRAS(Accelerator-based Transmutation Reactor Analysis System)", JAERI-Review 96-012, pp197 (1996).

3) Coleman W.A. and Armstrong T.W.: "NMTC Monte Carlo Nucleon Meson Transport Code System," ORNL-4606, ORNL (1970)

4) Briesmeister J.F. (Ed.) : "MCNP - A General Monte Carlo N-Particle Transport Code, Version 4A," LA-12625 (1993).

5,6) Prael R, and Lichtenstein H.: "User Guide to LCS: The LAHET Code System", LA-UR-89-3014, LANL (1989).

7) P.Cloth et al. : Julich Report KFA/Jul-2203 (1988).

8) Fasso A., Ferrari A., Ranft J., at al.: "FLUKA 92 ", Proc. Of the Workshop on "Simulating Accelerator Radiation Environments", Santa Fe, Jan. 11-15, 1993.

9) Hughes H.G., Adams K.J., Chadwick M.B. et.al.:"MCNPX - The LAHET/MCNP Code Merger," LA-UR-97-1638 (1997).

10) Armstrong T.W., Chandler K.C.: "HETC Monte Carlo High Energy Nucleon Meson Transport Code," ORNL-4744, ORNL (1972).

11) Mokov, V.N. : "The MARS code system user's guide", version 13(95), FERMILAB-FN-628, (1995).

12) W.A. Rhoades and R.L. Childs: "An Updated Version of the DOT 4 One-and Two-Dimensional Neutron/Photon Transport Code", ORNL-5851 (April 1982).

13) R.G. Alsmiller, Jr., J.M. Barnes and J.D. Drischler:"Neutron Photon Multigroup Cross Sections for Neutron Energies Less Than or Equal to 400 MeV (Revision 1). ORNL/TM-9801 (Feb. 1986). & Kotegawa H. et al.:"Neutron Photon multigroup cross-sections for neutron energies up to 400 Mev: HILO86R-Revision of HIRO86 Library, JAERI-M 93-020 (1993).

14) Kotegawa H. et al.: "PKN-H: A point kernel Shielding calculation Code for For Fast Neutron Source Up to 400 MeV", JAERI-Data/Code 95-004 (1995).

15) Mori T. and Nakagawa M.: "MVP/GMVP: General Purpose Monte Carlo Codes for Neutron and Photon Transport Calculations based on Continuous Energy and Multigroup Methods." JAERI-Data/Code 94-007 (1994).

16) Cullen D.E. : "TART97 A Coupled Neutron-Photon 3-D, Combinatorial Geometry Monte Carlo Transport Code," UCRL-ID-126455, Rev.1, LLNL (1997).

4.2 Present Status of Processing Method

Kazuaki KOSAKO
Sumitomo Atomic Energy Industries, Ltd.
2-10-14 Ryogoku, Sumida-ku, Tokyo 130-0026
e-mail: kosako@sae.co.jp

Present status of processing method for a high-energy nuclear data file was examined. The NJOY94 code is the only one available to the processing. In Japan, present processing used NJOY94 is orienting toward the production of traditional cross section library, because a high-energy transport code using a high-energy cross section library is indistinct.

1. Introduction

For some spallation accelerator projects, activity for producing the evaluated high-energy nuclear data file (HEF) started at USA, Europe and Japan. Evaluation of JENDL High-Energy File (JENDL/HE)[1] is started at JAERI in Japan. A nuclear data file is converted to a cross section library available for a transport code. A nuclear data processing code makes the conversion. The traditional processing procedure will be unchanged in the area of high-energy over 20 MeV. The processing and evaluation for HEF depend on the leading activity at LANL in USA.

2. Particle

In area of fission and fusion reactors, neutron and photon are primary particles for targeting on transport calculation. In area of high-energy, transport calculation for various particles is necessary and the energy ranges by particles are as follows: neutron and photon are all energy, proton is over 1 MeV, charged particles, pion and muon over about 150 MeV, and other meson over about 3 GeV (if necessary, electron is over 1 keV). Neutron is also the dominant particle in this area, and photon is important in shielding. Selection of target particles for HEF depend on the upper energy of HEF and the contribution to neutron and photon production. There is no general nuclear data processing code for particles except neutron and photon. If those particles are needed, processing code must be improved. For transport calculation, each particle has cross section and energy-angle distributions of total, scattering and particle production in HEF.

3. High-Energy File Format

Neutron HEF consists of cross sections, angular distributions and energy-angle distributions of partial reactions as same as ENDF/B-VI[2]. But cross sections of the high-energy part over 20 MeV is constituted of total, elastic, and particle production (MT=201 to 207) or nuclide production (MT=5). The angular distributions are given to only elastic and the energy-angle distributions are done to particle or nuclide production. MT is reaction types of the ENDF-6 format[3].

There are two types of HEF formats by storage method of production cross sections of various particles generated from reactions with incident particle. One is JAERI-BNL format[1] for storing as particle production data (MT=201 to 207), and it is accepted to the format of JENDL/HE. Another is LANL format[4,5] for storing as nuclide production data (MT=5), and it is used to the format of LANL 150 MeV nuclear data library[5]. The JAERI-BNL format has expansibility up to meson, but it needs that the definition of MT=201 in the ENDF-6 format changes total neutron production into inelastic neutron production (and MT=202 excludes radioactive capture). In principle, these HEF formats are possible to mutually convert between them.

Another problem in neutron HEF evaluation is consistency with the verified nuclear data file under 20 MeV. The parts under 20 MeV of JENDL/HE and LANL libraries are brought them from JENDL-3.2[6] and ENDF/B-VI, respectively. Therefore, the discontinuous data often occurs at the connected energy (20 MeV), because evaluation concepts between energy regions over and under 20 MeV differ. Since verification of data 16 to 20 MeV is insufficient, the evaluation around the connected energy is very difficult.

4. Target Transport Code

Traditional transport codes as DORT[7] and MCNP[8] have the specific format of cross section library. However, available high-energy transport codes don't have that library and produce necessary cross section data within the code as NMTC/JAERI97[9]. If the transport code don't need the external cross section library, the processing of nuclear data is unnecessary. If the code is modified for using a new external library, the processing is needed. Therefore, the nuclear data processing code is used for the modified high-energy and traditional transport codes. To be processing, a target (or standard) transport code in high-energy area must be selected to fix the necessity of library. In Japan, the target code has not determined yet. Therefore, present processing is orienting toward the production of traditional cross section library as using to MCNP and DORT/TORT[7].

Advantage in using a new external library is that more precise calculation is possible, but disadvantage is that the definition of library format and the modification of code need additionally. Advantage of traditional library is that additional modification don't need, but

disadvantage is that particles except neutron and photon can't treat.

5. Processing Code and Method

The nuclear data processing code produces the cross section library for the transport code from the evaluated nuclear data file. Processing of HEF is possible, but traditional codes must be modified and expanded. The requirement to the processing code for HEF are as follows: (1) acceptance of the ENDF-6 and HEF formats, (2) exclusion of maximum energy limit as 20 MeV, (3) process of particle (MT=201 to 207) or nuclide (MT=5) production data, (4) production of the library with applicable format for transport code, (5) acceptance of data by various particles.

As the released processing code for HEF, the NJOY94 code[10] is the only one at present. Plans of other processing codes are unknown and aren't expected too much, because there is no strong request. The updated version of NJOY94 goes on expanding at LANL to process the new LANL 150 MeV nuclear data library. The version is available for neutron and proton incident library with LANL format. Processing of photonuclear data is planning as next stage, but other particles are unknown. The version produces the cross section libraries for MCNP, MCNPX[11] and multigroup type. The release will become on and after next year. In Japan, the NJOY94/JHE code process JENDL/HE (under 50 MeV, phase-I) with JAERI-BNL format for neutron and produce a library for MCNP. The JHELIB library for MCNP was produced by NJOY94/JHE at 300 K and it includes 36 nuclides. Na-23 and Mn-55 in JENDL/HE aren't included in it, because the evaluated data has self-inconsistency. Also, a multigroup and MCNP libraries were produced by NJOY94 from the LANL 150 MeV library and ENDF/B-VI high-energy file and the test calculations used them are trying.

The phase-I version of JENDL/HE for the IFMIF project generally consists of the partial reaction cross sections under 20 MeV and the particle production cross sections over 20 MeV. The multiplicity of neutron production cross sections (MT=201) is always 1.0. Thus, the correct reaction cross sections can't calculate, and the production cross sections can't directly use to the library. To be process, the following assumption and thinking were introduced into NJOY94/JHE over 20 MeV: (a) absorption reactions ignore, (b) main reactions are elastic (MT=2) and nonelastic (MT=3) scattering, (c) neutron is generated by nonelastic reaction (that is, nonelastic cross sections is seen as neutron production one) and the neutron multiplicity is the one divided neutron production cross sections by nonelastic cross sections. (d) gamma-ray production data (MT=202) relates to above nonelastic reaction over 20 MeV. (e) energy-angle distributions are used neutron production ones (MT=201). Fig. 1 shows main cross sections over 10 MeV of Fe-56 (JENDL/HE) and the neutron multiplicity over 20 MeV. The multiplicity with the blacked reverse triangle is roughly proportional to neutron production cross sections, because nonelastic cross sections is roughly flat. There are two

problems in the processing of JENDL/HE. One is the treatment of gamma-ray production data (GPD; MT=202) given under 20 MeV for half nuclides, because of no GPD in evaluation under 20 MeV. The GPD by capture reaction is given until 100 keV. Thus, the energy range from 100 keV to 20 MeV lacks GPD by the assumption of (d). MT=202 under 20 MeV must be changed to other representation as nonelastic. Another is the treatment of fission and capture over 20 MeV, if any. In this case, total cross section is summation of elastic, fission, capture and tentative nonelastic (subtracted fission and capture from nonelastic).

Future problems in processing are as follows.

(i) Target transport code using an external library based on HEF over a few 100 MeV is indistinct.

(ii) The processing code depends completely on the NJOY code. The release of new NJOY version is unknown. Improvement work of NJOY94/JHE has to continue because of the correspondence to JENDL/HE, if the entire conversion from JAERI-BNL to LANL format isn't supported.

(iii) If a multigroup cross section library produced from HEF is widely used, the adjustment of library is necessary to correct the effect by particles except neutron and photon.

References

1) Fukahori T. and Chiba S.: Proc. Second Specialists' Meeting on High Energy Nuclear Data, Tokai, Jan. 26-27, 1995, JAERI-Conf 95-016, p46 (1995).
2) Rose P.F. (ed.): "ENDF-201 ENDF/B-VI Summary Documentation," BNL-NCS-17541 (1991).
3) Rose P.F. and Dunford C.L. (ed.): "ENDF-102 Data Formats and Procedures for the Evaluated Nuclear Data File ENDF-6," BNL-NCS-44945 (1990).
4) Koning A.J. and Hogenbirk A.: "High Energy Nuclear Data Files from ENDF-6 to NJOY to MCNP," NEA/NSC/DOC(97)8 (1997).
5) Young P.G. and Chadwick M.B.: Proc. Int. Conf. on Nuclear Data for Science and Technology, Trieste, May 19-24, 1997.
6) Nakagawa T., et al.:"Japanease Evaluated Nuclear Data Library Version 3 Revision-2: JENDL-3.2," J. Nuc. Sci. Technol., 32[12] 1259 (1995).
7) Rhoades W.A. and Childs R.L.: "An Updated Version of the DOT 4 One- and Two-Dimensional Neutron/Photon Transport Code," ORNL-5851 (1982). Rhoades W.A. and Simpson D.B.: "The TORT Three-Dimensional Discrete Ordinates Neutron/Photon Transport Code (TORT Version 3)," ORNL/TM-13221 (1996).
8) Briesmeister J.F. (ed.): "MCNP - A General Monte Carlo N-Particle Transport Code, Version 4B," LA-12625-M (1997).
9) Takada H., et al.: "An Upgraded Version of the Nucleon Meson Transport Code:

NMTC/JAERI97," JAERI-Data/Code 98-005 (1998).
10) MacFarlane R.E.: "The NJOY Nuclear Data Processing System, Version 91," LA-12740-M (1994).
11) Little R.C., et al.: Proc. Int. Conf. on Nuclear Data for Science and Technology, Trieste, May 19-24, 1997.

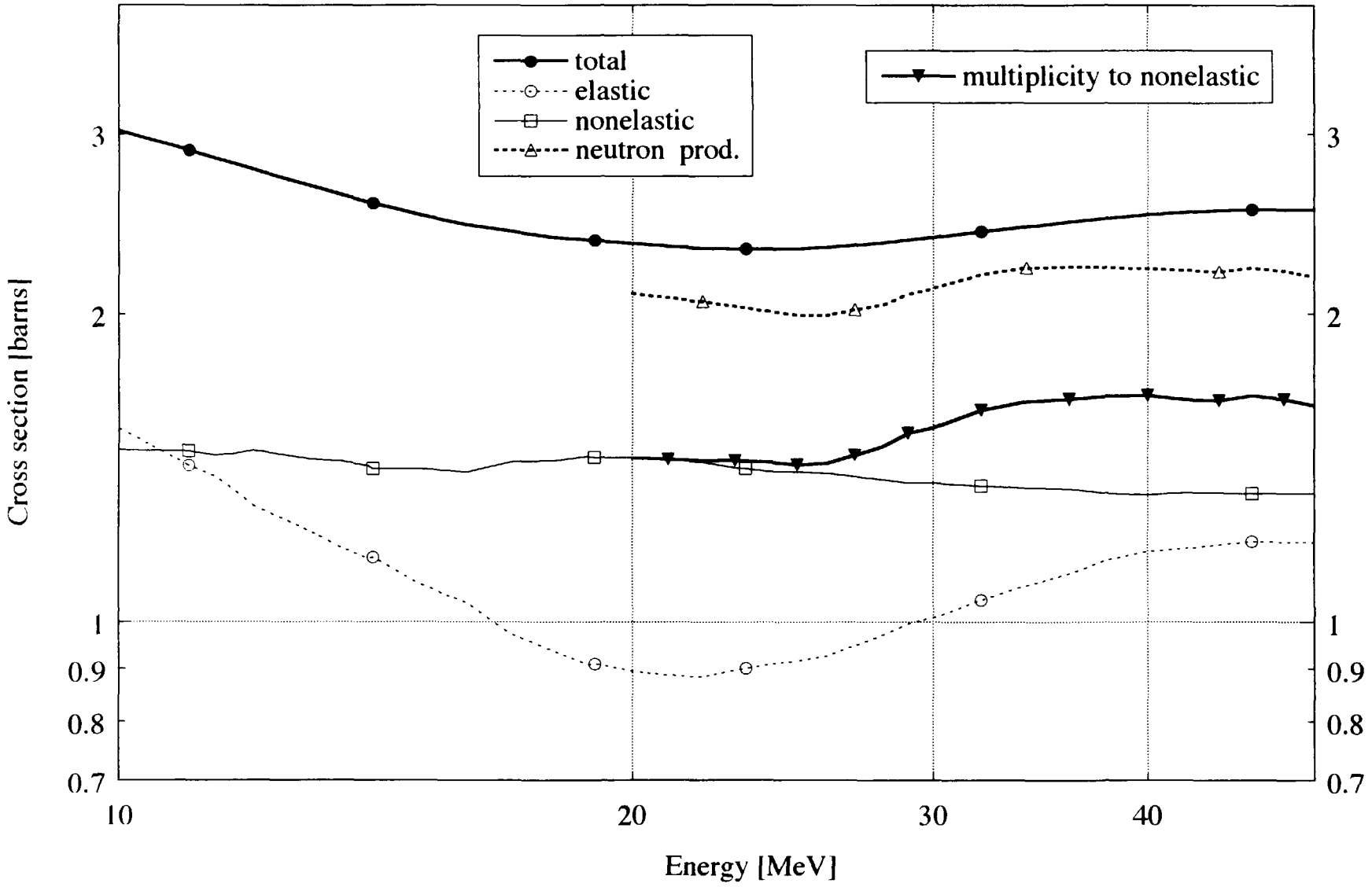

Fig. 1 Cross sections and neutron multiplicity of Fe-56 (JENDL High-Energy File)

5. Benchmark Tests

5.1 Review of Recent Benchmark Experiments on Integral Test for High Energy Nuclear Data Evaluation

Hiroshi NAKASHIMA, Susumu TANAKA, Chikara KONNO, Tokio FUKAHORI and Katsumi HAYASHI*

Japan Atomic Energy Research Institute
Tokai-mura, Naka-gun, Ibaraki 319-1195 Japan
e-mail: nakasima@shield4.tokai.jaeri.go.jp
**Hitachi Engineering Company*
Saiwai-cho, 3-2-1, Hitachi, Ibaraki 317, Japan

A survey work of recent benchmark experiments on an integral test for high energy nuclear data evaluation was carried out as one of the work of the Task Force on JENDL High Energy File Integral Evaluation (JHEFIE). In this paper the results are compiled and the status of recent benchmark experiments is described.

1. Introduction

Recently high energy accelerators are widely used in a variety of purposes such as medical and industry application fields, and projects using high intensity and high- and medium-energy accelerators are promoted in various countries for basic and applied sciences. For the design of the accelerator and target facilities high energy particle transport Monte Carlo codes are mainly utilized, and discrete ordinates codes are also applied with nuclear data set for the shielding design.

At the Japanese nuclear data committee (JNDC), evaluation work of nuclear data up to 50 MeV will be finished in 1998 and the data will be open to the public as the first version of JENDL High Energy File (JENDL/HE) in near future. As the second step of JENDL/HE, the energy region is expected to be extended up to a few GeV for the high energy accelerator facility designs.

It is important to survey the present status of the benchmark experiments suitable for the integral test, because the experimental data are essential to estimate the accuracy of JENDL/HE. Therefore, a survey work of recent benchmark experiments on integral test for high energy nuclear data was carried out as one of the work of the Task Force on JENDL High Energy File Integral Evaluation (JHEFIE).

2. Status of survey works

Many of reports were reviewed in two reports [1, 2] as annotated references, and some benchmark experiments were summarized by the Accelerator Shielding Working Group in the Research Committee on Radiation Behavior in the Atomic Energy Society of Japan[3]. Succeedingly the work, some benchmark experiments were summarized and compiled by the Shielding Working Group of the Research Committee on Reactor Physics of Japan Atomic Energy Research Institute for preparing benchmark problems for the meeting on "Shielding Aspects of Accelerators, Targets and Irradiation Facilities" jointly organized by the OECD/NEA and RSICC(USA).[4, 5] The problems were analyzed by various codes to estimate the accuracy of the shielding code and the related data and reported at the meetings.[6, 7, 8] Simultaneously, five benchmark experiments are compiled and maintained as an electric media: SINBAD by RSICC[9]. A surveyed result was presented by Hayashi et al. at the meeting, and thick target neutron yield (TTY) are summarized as shown in Fig. 1.[10]

In the previous work the collection was done in order to estimate the accuracy of the shielding code and the related data, so all the experiment are not accurate enough to discuss nuclear data in

detail. Therefore, the experiment suitable for the nuclear data integral test were selected again from the collection of this work and the previous surveyed results[4, 5, 10].

3. Survey work

3.1 Selection criteria

The selection criteria in this survey work is the followings.

(1) The energy of the incident particles is restricted from 20 MeV up to a few GeV, because the energy range of JENDL/HE is expected to be up to a few GeV.

(2) TTY should be included in the collection, because TTY is observed as a combination of microscopic nuclear reaction and macroscopic particle transport and is suitable for the integral test.

(3) The literature including databases since 1993 should be covered. The literature before 1993 were already surveyed as described above.

3.2 Literature Coverage

The papers referenced are from the following journals, proceedings, reports and databases since 1993.

A. Journals
- (1) IEEE Trans. Nucl. Phys.,
- (2) Int. J. Appl. Radiat. Isotopes,
- (3) Health Phys.,
- (4) Med. Phys.,
- (5) Nucl. Instrum. Methods -A, B,
- (6) Nucl. Phys. A,
- (7) Nucl. Sci. Eng.,
- (8) Particle Accelerators,
- (9) Phys. Med. Biol.,
- (10) Phys. Rev. C,
- (11) Radiat. Prot. Dosimetry,

B. Proceedings
- (12) Proc. ICANS Mtg.,
- (13) Proc. ICRS8 Mtg.,
- (14) Proc. SARE Mtg.,
- (15) Proc. SATIF Mtg.,

C. Reports
- (16) Reports published by Institutes,

D. Databases
- (17) IAEA data base,
- (18) EXFOR,
- (19) SINBAD

4. Surveyed results

Table 1 compiles the references surveyed in this work. Each entry block lists the full title of the paper, authors' names, and the literature source followed by information on the accelerator (facility), type and energy of the projectile, composition and thickness of the target, experimental method, and measured quantities. Calculation methods applied for the experiment are also listed in the entry blocks.

From the surveyed results and the collection in the previous work[1-10], the following experiments were selected as benchmark problems suitable for the integral test. These experiments are categorized in three fields: spectrum measurements up to and above about 250 MeV, and reaction rate distribution measurements with activation methods. Spectrum measurements are the most

suitable for the integral test of nuclear data. On the other hand, the reaction rate measurements is effective to know particle behavior inside the experimental assembly, although the data have ambiguities of reaction cross sections of activation foils used in the experiment. The spectrum measurements are separated at the energy of about 250 MeV, because the accuracy of the nuclear data evaluation related to the transport cross section is expected to be higher in the energy region up to about 250 MeV. The reasons are followings.

(1) The nuclear data up to 150 MeV are evaluated in the Los Alamos library.[8]

(2) Some medical facilities are planed to be constructed and the particle energy used in these facilities are about 250 MeV. For the shielding design, discrete ordinates and Monte Carlo codes used in the energy range up to 20 MeV for reactor shielding designs are being planed to be used, because the contribution of the charged particles generated by the secondary neutrons would not seriously affect to the calculated results in the case that only neutron transport is calculated.

5. Status of benchmark experiments

5.1 Transmission experiments

Figures 2, 3 and 4 show the set up of A.2, A.3 and A.5 experiments listed in Table 2. In these figures the change of transmission experimental setups is presented from A.2 to A.5 experiments. A white neutron source, which was generated from the carbon target contacted on the experimental assembly, was used in A.2 experiments. In the experiment, intensity of neutron above 20 MeV is not so high, compared with that below 20 MeV, and background neutron restricts the thickness of the assembly. A.3 experiment used white but collimated neutron, and in the experiment the energy range increased up to about 50 MeV. By using monoenergetic neutron source generated by ^{7}Li(p, n) reaction, A.4 experiment clarified neutron behavior above 20 MeV. Finally A.5 experiments were carried out in good geometry with monoenergetic neutron source. The final experimental configuration made possible to estimate the accuracy of not only neutron total cross sections but also the angular distributions of neutron elastic scattering in the energy region up to about 70 MeV.

The neutron transmission experiments are limited in the energy region up to 70 MeV, as shown in Table 2. The reason is that there are no suitable monoenergetic neutron field and detector for the spectrum measurement above about 120 MeV. As for the neutron source, ^{7}Li(p, n) reaction is usually used as an monoenergetic neutron source, because of its large neutron yield. The ratio of the peak component to the continuum region in the source neutron spectrum, however, decreases with increasing the incident proton energy. Although in the transmission experiment the collimated neutron beam is preferable to reduce the background neutron scattered in the experimental room, thickness of the shielding wall for separating the neutron source and the experimental assembly is required to be increased with increasing the neutron energy. Concerning to the detector used behind an experimental assembly, an unfolding technique with an organic scintillation counter is usually used to obtain the neutron spectrum. To apply this technique for the experiment, the detector is required to fully stop the proton scattered by the neutrons to be measured. This results a need of big scintillator that causes the position ambiguity. This means other methods such an activation method with an unfolding technique should be used for the spectrum measurement, although neutron source of high intensity is required to apply the method for the measurement and the accuracy of the reaction cross section used for the measurement should be high.

5.2 Thick target neutron yield measurements

Many TTY measurements were carried out in the energy range above 100 MeV as shown in Fig. 1. As the spectrum measurement, time-of-flight technique is applicable in the TTY measurements. In the measurement the correction for the mean emission time of neutron from the target can be ignored, because the target is small, compared to the experimental assembly used in the transmission experiment.

The data are suitable to estimate the accuracy of high energy particle transport codes, because TTY composes of the transmission of incident particles, angular distribution of neutron production,

and neutron transport in the target. In order to apply the integral test of nuclear data, however, a code to convert to TTY from neutron production and transport cross sections should be made.

TTY is effective to compensate the missing region of the neutron production double-differential data, although TTY has difficulty to discuss the accuracy of nuclear data directly as described above. Actually the experimental set up for the TTY measurement is simple, compared to that of the cross section measurement, because the TTY measurement does not need a beam dump which traps the transmitted protons through the thin target, that generates background neutrons in the cross section measurement.

For practical purposes of shielding designs, the systematics of TTY is useful, because TTY is used as a source term of neutron transport calculation using discrete ordinates and Monte Carlo codes. Especially the systematics up to 250 MeV is important for the design of medical accelerator facilities. The systematics above this energy is also meaningful for the thick shield surrounding the intense neutron target irradiated by protons up to a few GeV. Actually pion reaction cross section is not so high in this energy region and neutrons up to a few hundreds MeV, which generated by the high energy neutron transmitted in the thick shield, are dominant deep inside the thick shield, therefore the neutron transport codes with neutron nuclear data library are applicable for the design.

5.3 Reaction rate distribution measurements

The reaction rate distribution measurements are effective to estimate the neutron flux and the energy deposition inside and on the surface of the target assembly. The applicability of the reaction rate distribution measurement to the integral test strongly depends on the accuracy of reaction cross sections of nucleus in activation foils used in the measurements. Because the measured reaction rates are the results of integration over the neutron and proton energies, the excitation functions of reaction cross sections should be exactly known to estimate the accuracy of the calculated results and the related cross sections: reaction and transport cross sections. The detail evaluation for reaction cross sections is highly required in the energy region above 20 MeV. The requirement comes from the filed of health physics as well, because some reaction cross sections are used for dosimetry.

It is proposed to measure the integrated reaction cross sections over the energy region covered by white neutron source in the energy region above 20 MeV. The reason is as follows. It is difficult to establish a monoenergetic neutron field above 20 MeV, and only quasi-monoenergetic neutron source is available to the measurement in the energy region. In energy region above 210 MeV there is no existing quasi-monoenergetic neutron field in the world. Therefore the white neutron filed having the well-known neutron spectrum is also effective to estimate the accuracy of the reaction cross sections.

6. Proposal for future work

1) Collection of numerical data

Because most of the experiments surveyed in this work are published in journals and proceedings, not all the numerical data is available. For the integral test of JENDL/HE, it is dispensable to collect the numerical data. However, the target materials to be estimated should be clarified and limited, because a lot of work is necessary for the collection and compilation.

2) Database

EXFOR is not effective to this work, even for TTY unfortunately, because EXFOR is tailored for the survey of nuclear data. On the other hand, databases for integral experiments: SINBAD, are maintained by RSICC as an electric media. It seems to be the easiest way and effective to resister the experimental data to SINBAD rather than to compile original new database.

3) Proposal of new experiments

Neutron transmission measurement in the energy region from 70 MeV to a few GeV would

be required, because some important parameters for shielding designs, such a neutron attenuation length, are still the question under discussion. The parameter is not directly related to this work, but the data is beneficial to the integral test.

Integral tests of neutron reaction cross sections by using white neutron sources would be also required, although most of neutron reaction cross sections can be tested by the measurement of proton reaction cross sections in the energy region above 100 MeV except for threshold energy region.

References

[1] T. Nakamura, et al.: "Annotated References on Neutron and Photon Production from Thick Targets Bombarded by Charged Particles", Atomic Data and Nuclear Data Tables, 32, 471-501 (1985).
[2] H. Hirayama, et al.: "Annotated References of Shielding Experiment and Calculation of High Energy Particles", KEK report 90-18 (1990).
[3] H. Hirayama, et al.: "Accelerator Shielding Benchmark Problems", KEK report 92-17 (1993).
[4] H. Nakashima, et al.: "Benchmark Problems for Intermediate and High Energy Accelerator Shielding", JAERI-Data/Code 94-012 (1994).
[5] Y. Nakane et al.: "Neutron Transmission Benchmark Problems for Iron and Concrete Shields in Low, Intermediate and High Energy Proton Accelerator Facilities", JAERI-Data/Code 96-029 (1996).
[6] K. Hayashi, et al.: "Accelerator Shielding Benchmark Analysis and Future Items to be solved", OECD Documents SATIF-1 Shielding Aspects of Accelerators, Targets and Irradiation Facilities, p.135 (1994).
[7] H. Nakashima, et al.: "Accelerator Shielding Benchmark Experiment Analyses", OECD Documents SATIF-2 Shielding Aspects of Accelerators, Targets and Irradiation Facilities, p.115 (1995).
[8] Y. Nakane, et al.: "Intercomparison of Neutron Transmission Benchmark Analyses for Iron and Concrete Shields in Low, Intermediate and High Energy Proton Accelerator Facilities", OECD Documents SATIF-3 Shielding Aspects of Accelerators, Targets and Irradiation Facilities, p.151 (1997).
[9] H. T. Hunter, et al.: "SINBAD-A Shielding Integral Benchmark Archive and Database for PC's", Proc. on 8th International Conference on Radiation Shielding, p.795, Arlington, USA, 24-28 April, 1994 (1994).
[10] K. Hayashi, et al.: "Survey of Thick Target Neutron Yield Data and Accelerator Shielding Experiments", OECD Documents SATIF-2 Shielding Aspects of Accelerators, Targets and Irradiation Facilities, p.41 (1995).
[11] P. G. Young, et al.: "Neutron- and Proton-Induced Nuclear Data Libraries to 150 MeV for Accelerator-Driven Applications", Proc. Int. Conf. Nucl. Data Sci. Tech., Trieste, Italy, 19-24 May, 1997, to be published (1998).
[12] M. M. Meier, et al.: Nucl. Sci. Eng., 102, 310 (1989).
[13] M. M. Meier, et al.: ibid., 104, 339 (1990).
[14] M. M. Meier, et al.: ibid., 110, 299 (1992).
[15] K. Shin, et al.: ibid., 71, 294 (1979).
[16] Y. Uwamino, et al.: ibid., 80, 360 (1982).
[17] K. Shin,et al.: ibid., 109, 380 (1991).
[18] Y. Arakita, et al.: Nucl. Instrum. Methods., 164, 255 (1979).
[19] S. Ban, et al.: ibid., 184, 409 (1981).

Table 1 References on experiments suitable for the integral test

DANIEL_92
"Neutron Production in Lead Target by High-Energy Light-Mass Heavy Ions"
A. V. Daniel, et al.
JINR-1-92-174 (1992)

1) Accelerator:	synchrophasotron , JINR
2) Projectile:	p(2.0, 2.55 GeV)
3) Target(thickness):	Be, Al, Cu, Cd, Pb
4) Shielding Material:	
5) Geometry:	Cylinder
6) Experimental Method:	TOF
7) Calculation:	SITHA
8) Measured Quantities:	Neutron Spectra

ISHIKAWA_94
"Neutron Penetration Through Iron and Concrete Shields with the Use of 22.0- and 32.5-MeV Quasi-Monoenergetic Sources"
T. Ishikawa, Y. Miyama and T. Nakamura
Nucl. Sci. Eng., 116, 278-290(1994)

1) Accelerator:	Cyclotron
2) Projectile:	p(25, 35 MeV)
3) Target(thickness):	Li(2 mm)
4) Shielding Material:	Iron(~40 cm), Concrete(~100 cm)
5) Geometry:	Slab
6) Experimental Method:	NE213, Bonner Ball, PRPC
7) Calculation:	MORSE-CG
8) Measured Quantities:	Neutron Spectra

MEIGO_95
"Measurements of Spallation Neutrons from a Thick Lead Target Bombarded with 0.5 and 1.5 GeV Protons"
S. Meigo, et. al.
Proc. of ICANS-XIII, 442-453 (1995)

1) Accelerator:	12 GeV synchrotron, KEK
2) Projectile:	p(0.5, 1.5 GeV)
3) Target(thickness):	Pb(15x15x20 cm)
4) Shielding Material:	
5) Geometry:	Rectangular
6) Experimental Method:	TOF
7) Calculation:	NMTC/JAERI+MCNP-4A
8) Measured Quantities:	Neutron Spectra

NAKAO_96
"Transmission Through Shields of Quasi-Monoenergetic Neutrons Generated by 43- and 68-MeV Protons - I : Concrete Shielding Experiment and Calculation for Practical Application"
N. Nakao, et. al.
Nucl. Sci. Eng., 124, 228-242(1996)

1) Accelerator:	AVF Cyclotron at TIARA, JAERI
2) Projectile:	p(43, 68 MeV)
3) Target(thickness):	Li(3.6, 5.2 mm)
4) Shielding Material:	Concrete(25~200cm)
5) Geometry:	Slab
6) Experimental Method:	BC501A, Bonner Ball
7) Calculation:	MORSE-CG, DOT3.5, HETC-KFA2
8) Measured Quantities:	Neutron Spectra

NAKASHIMA_96
"Transmission Through Shields of Quasi-Monoenergetic Neutrons Generated by 43- and 68-MeV Protons - II : Iron Shielding Experiment and Analysis for Investigating Calculational Method and Cross Section Data"
H. Nakashima, et. al.
Nucl. Sci. Eng., 124, 228-242(1996)

1) Accelerator:	AVF Cyclotron at TIARA, JAERI
2) Projectile:	p(43, 68 MeV)
3) Target(thickness):	Li(3.6, 5.2 mm)
4) Shielding Material:	Fe(10~130 cm)
5) Geometry:	Slab
6) Experimental Method:	BC501A, Bonner Ball
7) Calculation:	MORSE-CG, DOT3.5, HETC-KFA2
8) Measured Quantities:	Neutron Spectra

NAKAO_97
"Measurements and Calculations of Neutron Energy Spectra behind Polyethylene Shields Bombarded by 40- and 65-MeV Quasi-Monoenergetic Neutron Source"
N. Nakao, et. al.
J. Nucl. Sci. Technol., 34(4), 348-359 (1997)

1) Accelerator:	AVF Cyclotron at TIARA, JAERI
2) Projectile:	p(43, 68 MeV)
3) Target(thickness):	Li(3.6, 5.2 mm)
4) Shielding Material:	Polyethylene (30.5~183cm)
5) Geometry:	Slab
6) Experimental Method:	BC501A, Bonner Ball
7) Calculation:	MORSE-CG
8) Measured Quantities:	Neutron Spectra

TAKADA_97A
"Reaction Rate Distribution Measurement and Analysis for 0.895 and 1.21 GeV Proton Bombardment on Thick Tungsten Target"
H. Takada, et. al.
Proc. SARE3, 255-263 (1997)

1) Accelerator:	Institute of High Energy Physics, Russia
2) Projectile:	p(0.895, 1.21 GeV)
3) Target(thickness):	W(20x60 cm)
4) Shielding Material:	
5) Geometry:	Cylinder
6) Experimental Method:	Activation method
7) Calculation:	NMTC/JAERI, LAHET, HERMES
8) Measured Quantities:	Reaction Rate Distribution

TAKADA_97B
"Measurement of Reaction Rate Distributions in a Lead Assembly Bombarded with 500 MeV Protons"
H. Takada, et. al.
Proc. SARE3, 284-292 (1997)

1) Accelerator:	Booster synchrotron, KEK
2) Projectile:	p(500 MeV)
3) Target(thickness):	Pb(60x100 cm)
4) Shielding Material:	
5) Geometry:	Cylinder
6) Experimental Method:	Activation method
7) Calculation:	NMTC/JAERI
8) Measured Quantities:	Reaction Rate Distribution

Table 2 List of the experiments suitable for the integral test

A. Spectrum measurements up to about 250 MeV
- A.1 TTY measurement by proton of 113 and 256 MeV (LANL) [12, 13, 14]
- A.2 Transmission experiment of neutrons from carbon bombarded by 52-MeV-proton (INS) [15, 16]
- A.3 Transmission experiment of neutrons from copper bombarded by 65-MeV-proton (Osaka Univ./ Kyoto Univ.) [17]
- A.4 Transmission experiment of neutrons from ^{7}Li bombarded by 22- and 32.5-MeV-protons (CYRIC) [ISHIKAWA_94 in Table 1]
- A.5 Transmission experiment of neutrons from ^{7}Li bombarded by 43- and 68-MeV-protons (JAERI/Tohoku Univ.) [NAKAO_96, NAKASHIMA_96 and NAKAO_97 in Table 1]

B. Spectrum measurement above about 250 MeV
- B.1 TTY measurement by proton of 0.5 and 1.5 GeV (KEK/JAERI) [MEIGO_95 in Table 1]
- B.2 TTY measurement by proton of 2 and 2.55 GeV (JINR) [DANIEL_92 in Table 1]
- B.3 TTY measurement by proton of 0.8, 1.2 and 1.6 GeV (Saclay/JAERI) [unpublished]

C. Reaction rate distribution measurement with activation method
- C.1 Iron beam dump experiment by proton of 500 MeV (KEK) [18, 19]
- C.2 Tungsten beam dump experiment by proton of 0.9 and 1.2 GeV (ITEP/JAERI) [TAKADA_97A in Table 1]
- C.3 Lead beam dump experiment by proton of 500 MeV (KEK/JAERI) [TAKADA_97B in Table 1]

Fig.1-1 (p,xn) thick target yield data [10]

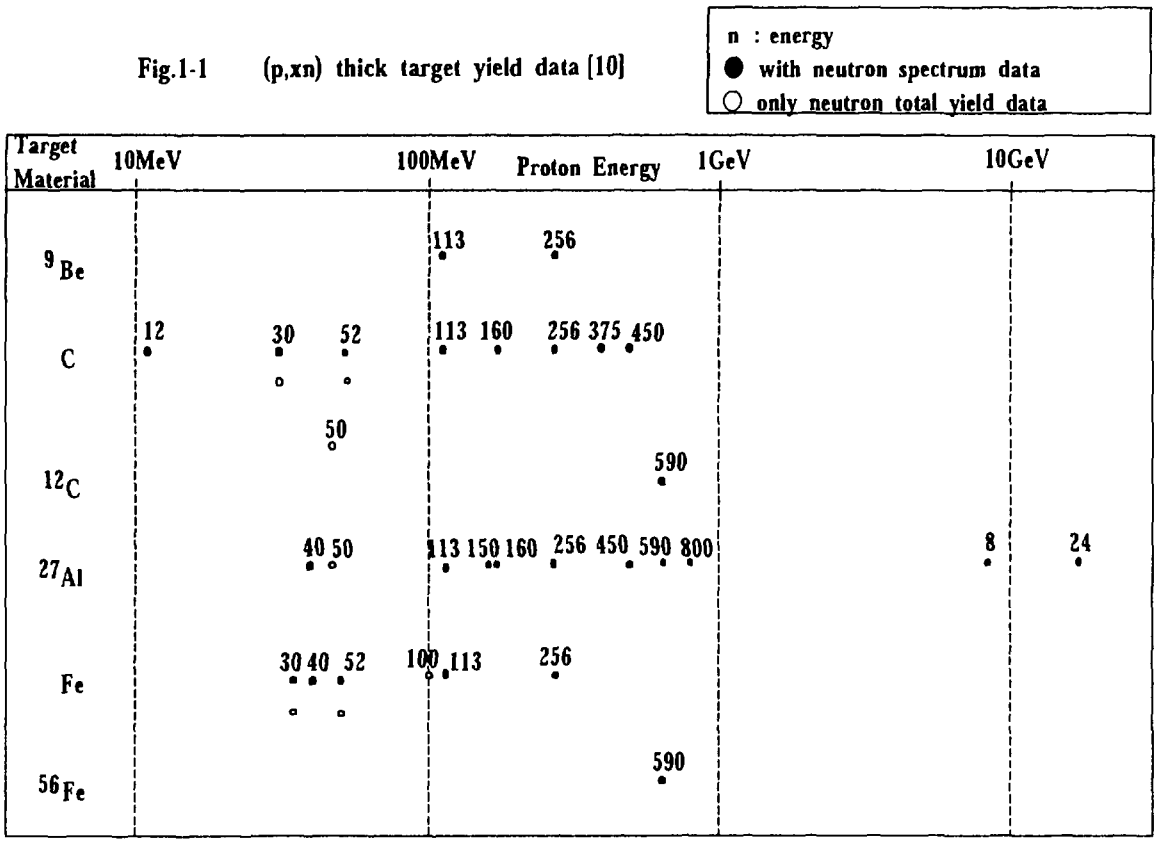

Fig.1-2 (p,xn) thick target yield data [10]

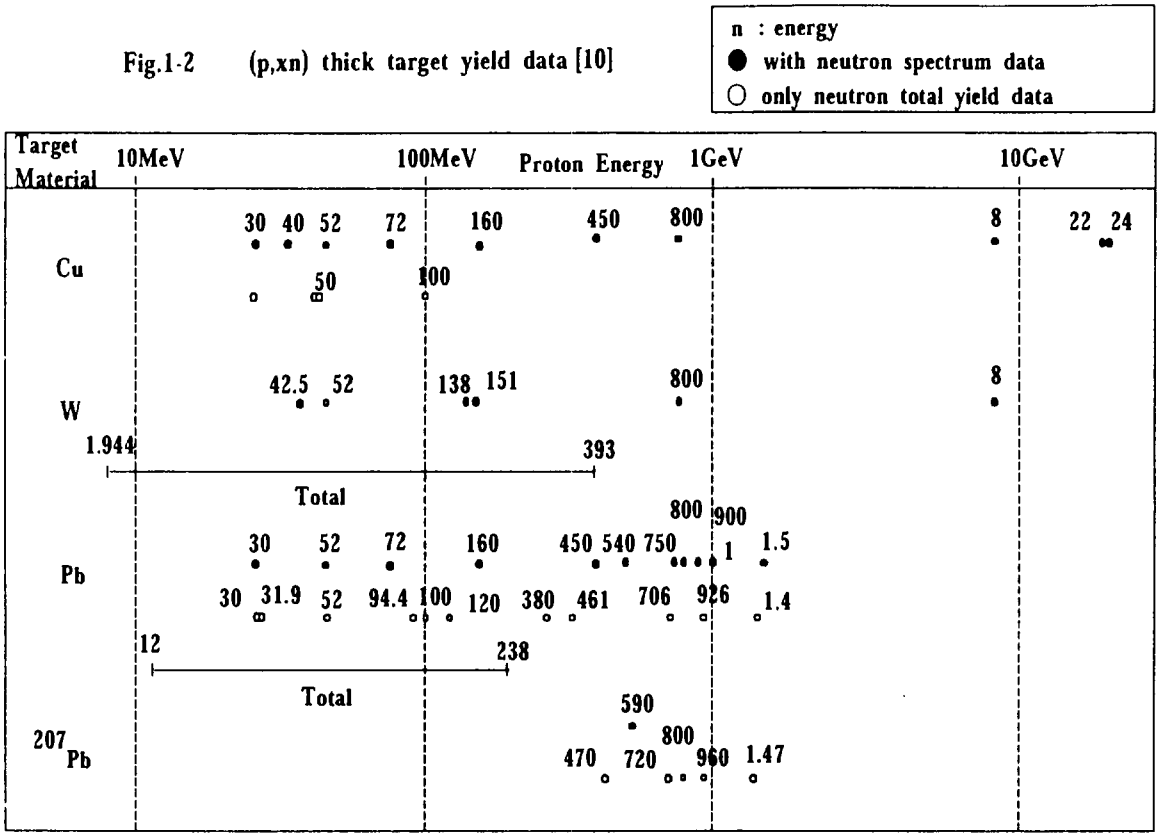

Fig.1-3 (p,xn) thick target yield data [10]

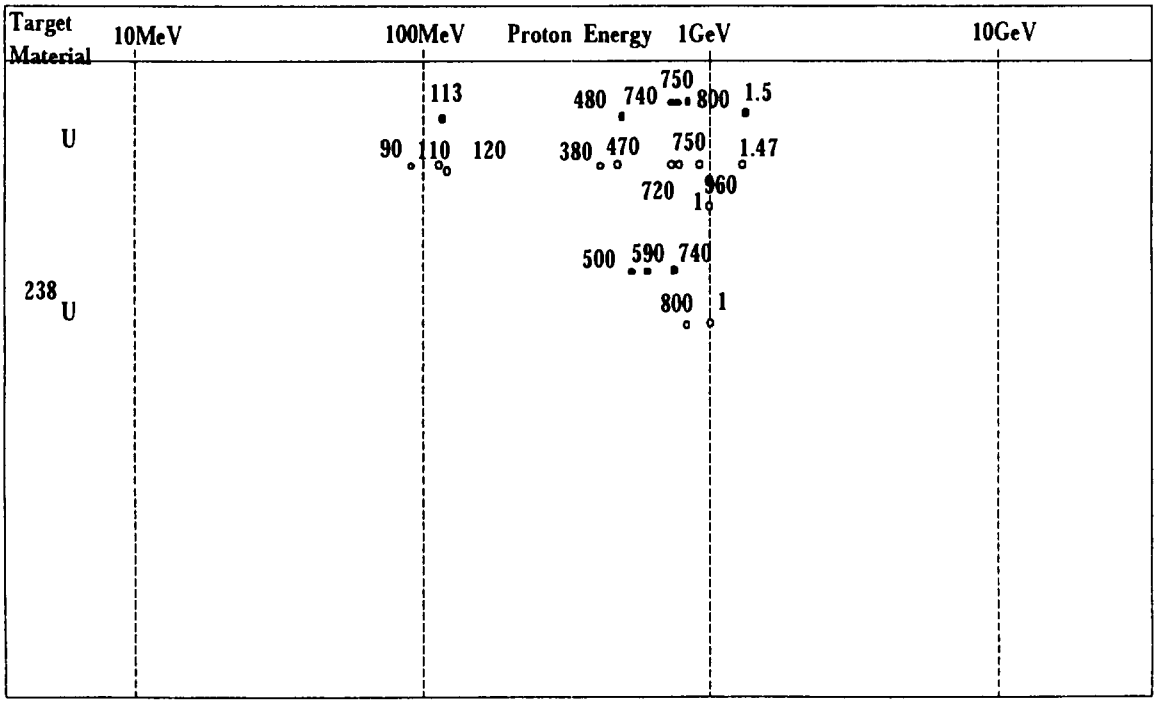

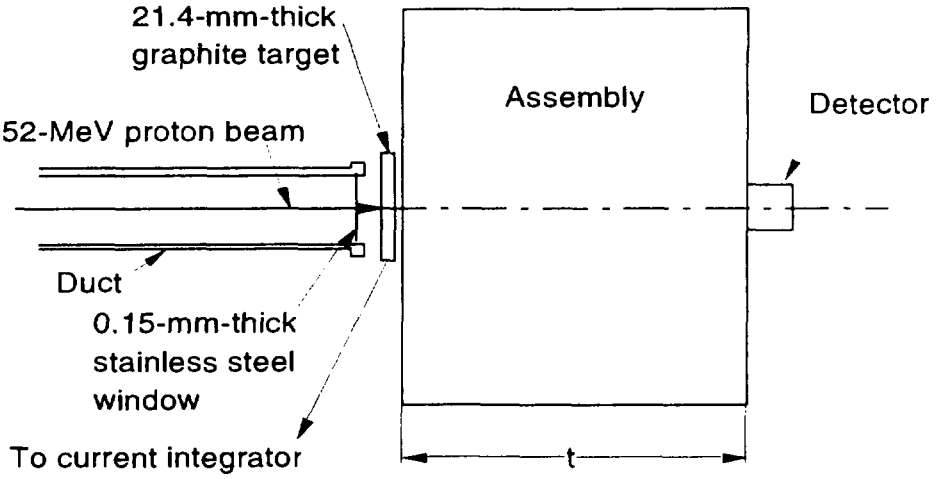

Fig. 2 Setup for the A.2 experiments [15, 16]

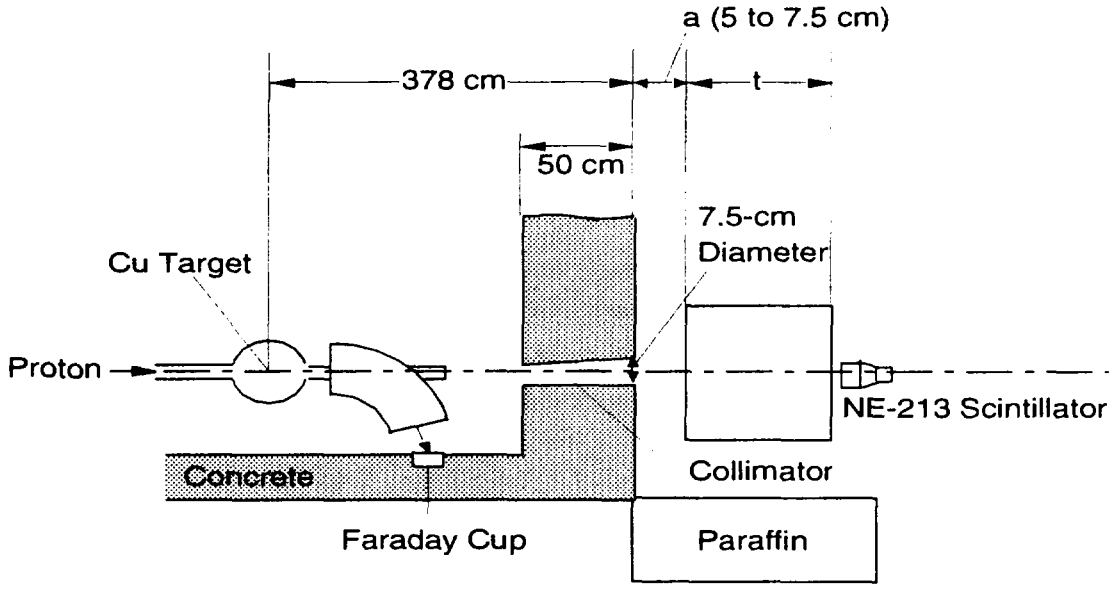

Fig. 3 Setup for the A.3 experiment[17]

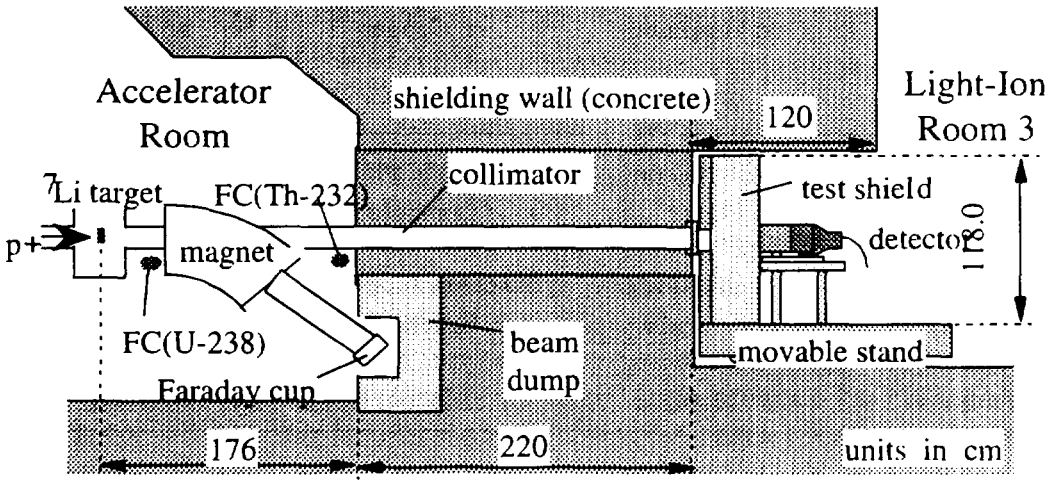

Fig. 4 Setup for the A.5 experiments[NAKAO_96, NAKASHIMA_96, NAKAO_97 in Table 1]

5.2 Benchmark Test with MCNP Code

Fujio MAEKAWA and Masayuki WADA
High Energy Neutron Laboratory, Japan Atomic Energy Research Institute
Tokai-mura, Naka-gun, Ibaraki-ken 319-1195 JAPAN
e-mail: fujio@fnshp.tokai.jaeri.go.jp

Benchmark test of JENDL High Energy File has started with the MCNP code. Some problems of cross section data were pointed out. Selection of cross section data below 20 MeV was discussed.

1. Introduction

Evaluation activities of JENDL High Energy (JENDL-HE) File are now in progress, and expected to be completed by the end of 1998 for the phase-I up to 50 MeV. To clarify problems and demonstrate validity of the cross section data in JENDL-HE File, we have started benchmark tests of JENDL-HE File for neutron transport cross section data up to 50 MeV with the MCNP code [1] by analyzing benchmark experiments. Table 1 summarizes the benchmark experiments [2-8] employed for the tests. The calculated results with JENDL-HE File were compared to the experimental data as well as results of other cross section libraries.

Table 1 Benchmark experiments employed for the tests.

Facility / Institute	INS / Tokyo Univ.	RCNP / Osaka Univ.	TIARA / JAERI
Neutron Source	52-MeV Proton on Graphite	65-MeV Proton on Copper	43- & 68-MeV Proton on Lithium
Source Spectrum	White	White	Quasi-Mono-Energetic
Material	C, Fe, Concrete, Water	C, Fe, Pb, Concrete	Fe, Concrete, Polyethylene
Measured Quantity	Neutron & Photon Spectrum	Neutron & Photon Spectrum	Neutron Spectrum, Fission Rate
References	[2, 3]	[4, 5]	[5-8]

2. Transport Calculation Code and Cross Section Library

Results by four combinations of a transport code and a cross section library shown in Table 2 were compared with the experimental data. In this work, neutron transport calculations by the MCNP-4B code with two cross section libraries, JENDL-HE File and 100XS, were performed. For JENDL-HE File, the ACE format cross section library [9] produced by the NJOY -94.66 code was used. The 100XS library [10], which is included in the MCNP-4B code package, contains neutron transport cross section data up to 100 MeV for nine elements based on nuclear data evaluated at LANL in about 1989. The MCNP with ENDF/B-VI High Energy File and the MORSE with HILO86 calculations for the INS and RCNP experiments were conducted as a part of "Accelerator Shielding Benchmark Experiment Analyses" in 1995. [11] Results of the MORSE with HILO86 calculations for the TIARA experiments have been described in the references [5-7].

Table 2 Four combinations of a transport code and a cross section library for the benchmark tests.

Transport Code	Cross Section Library	References
MCNP-4B	JENDL-HE File	This Work
MCNP-4B	100XS [10]	This Work
MCNP-4A	ENDF/B-VI High Energy File	[11]
MORSE	HILO86 (Multi-group)	[5-7, 11]

Since evaluation of JENDL-HE File was in progress, cross section data have not been given for all the candidate elements. Table 3 shows status of the evaluation at the time of transport calculation, i.e., the winter of 1998. Solid and open circles indicates whether the transport cross sections are available or not, respectively, at that time for the four libraries. The HILO86 multi-group library contains all the cross sections needed for calculations of the six materials used in the experiments, i.e., carbon, iron, lead, polyethylene, water and concrete. Calculations for five and three materials are possible with 100XS and ENDF/B-VI High Energy File, respectively. Although transport cross section data for 12 elements have been prepared for JENDL-HE File, needed cross section data are given only for iron experiments. To test other cross section data in JENDL-HE File, calculations of concrete were also conducted by using cross section data of JENDL-HE File as many as possible. Cross sections of Mg, Al, Si, K, Ca and Fe in JENDL-HE File were used for the concrete calculations with supplying cross sections of H and O from 100XS.

All the calculations start with source neutrons produced by the proton bombardment on the target materials. Neutron transport is simulated by the Monte Carlo method with utilizing

evaluated cross sections. Hadron cascade is not considered in the calculations. Neutron production by secondary charged particles is not treated in the calculations, however, this effect can be considered as negligibly small in the energy region of interest at most 68-MeV.

Table 3 List of available cross section data for the four neutron transport cross section libraries. Solid and open circles indicates whether the transport cross sections are available or not, respectively.

	HILO86	ENDF/B-VI High Energy	100XS	JENDL-HE File
H	●		●#	○
Li				○
Be			●	○
B	●			○
C	●	●	●	○
N	●			○
O	●		●	○
Na	●			○
Mg	●			●
Al	●		●	●
Si	●		●	●
S	●			
K	●			●
Ca	●		●	●
Ti				●
V				●
Cr	●			●
Mn				○
Fe	●	● (^{56}Fe)	●	●
Ni	●			●
Cu				●
Y				●
Nb				○
Mo				○
W	●		●	○
Pb	●	● (^{208}Pb)		○
Bi		●		○
U			● (^{238}U)	○
others*				○

Cross section data of hydrogen-1 up to 100 MeV are available in the cross section library for ordinary ENDF/B-VI (not High Energy File).

* F, Cl, Ar, Co, Zn, Ga, Ge, As, Zr, Ta, Au, Hg, Th, Np, Pu, Am and Cm

3. Results of Benchmark Tests

3.1 Iron

Figure 3.1 shows neutron spectra on the beam axis for the TIARA iron shield experiment for several thicknesses calculated with JENDL-HE File and 100XS compared with the measured data. Figure 3.2 shows similar neutron spectra on and off beam axis of the iron shield of 40 cm in thickness. Calculated to experimental (C/E) ratios for peak (35~45 MeV) and tail (10~35 MeV) neutron fluxes are derived from the spectra, and compared in Figs. 3.3 and 3.4.

On the beam axis, with increase of shield thickness, JENDL-HE gives smaller neutron fluxes (C/E~ 1/4 at 100 cm), while 100XS predicts the neutron flux larger (C/E ~ 3 at 100 cm). This trend can be explained by the difference of cross sections between the two libraries, as shown in Fig. 3.5. In the energy range of 20 ~ 50 MeV, either total cross sections are almost the same each other while elastic scattering cross section of JENDL-HE is considerably smaller than that of 100XS. When the elastic scattering cross section is given larger, scattered neutrons going to forward direction are enhanced resulting in higher neutron fluxes behind thick shields.

Comparisons of neutron fluxes between on and off the beam axis are useful to examine angular distribution of secondary neutrons. Although neutron fluxes calculated with 100XS are systematically larger than the measured data, the overestimation does not depend on the offset distance. On the other hand, neutron fluxes calculated by JENDL-HE, especially peak fluxes, are predicted smaller with increase of the offset distance. This result suggests for the JENDL-HE evaluation that the probability of secondary neutrons going to forward direction by the elastic scattering reactions should be decreased.

3.2 Concrete

Neutron spectra and C/E ratios for the TIARA concrete shield experiment are shown in Figs. 3.6 ~ 3.9, as similar to the iron experiment. As a whole, agreements between the calculations to the experiment are better than those for the iron case. All the C/E ratios by JENDL-HE are in the range of 0.9 ~ 1.5 for the shield thicknesses up to 150 cm and for both the fluxes on and off the beam axis.

4. Cross Section Data Below 20 MeV

In principle, the existing JENDL data such as JENDL Fusion File and JENDL-3.2 are merged to JENDL-HE File as the low energy part below 20 MeV. A large amount of benchmark experiments for fusion and fission reactors are still valuable for validating the low energy part of JENDL-HE File. As an example, benchmark calculations for the FNS iron benchmark experiment [12, 13] for fusion were performed.

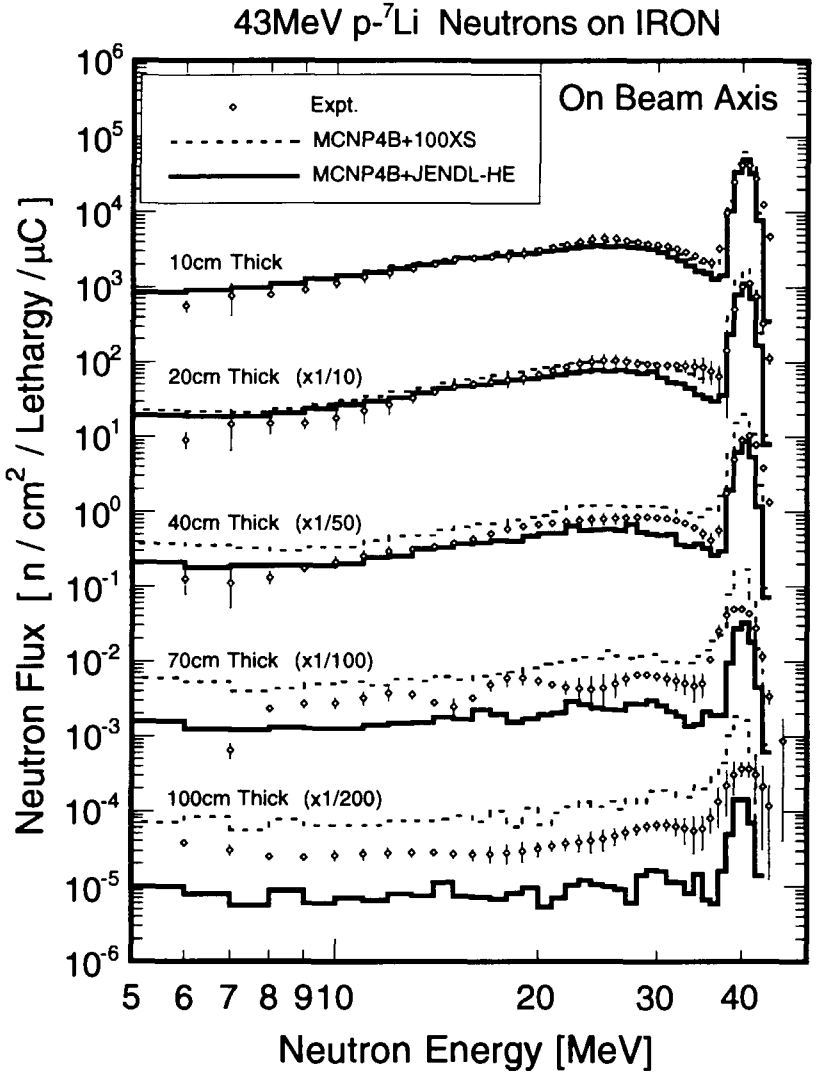

Fig. 3.1 Comparison of measuerd and calculated neutron spectra on the beam axis for the TIARA iron shield experiment.

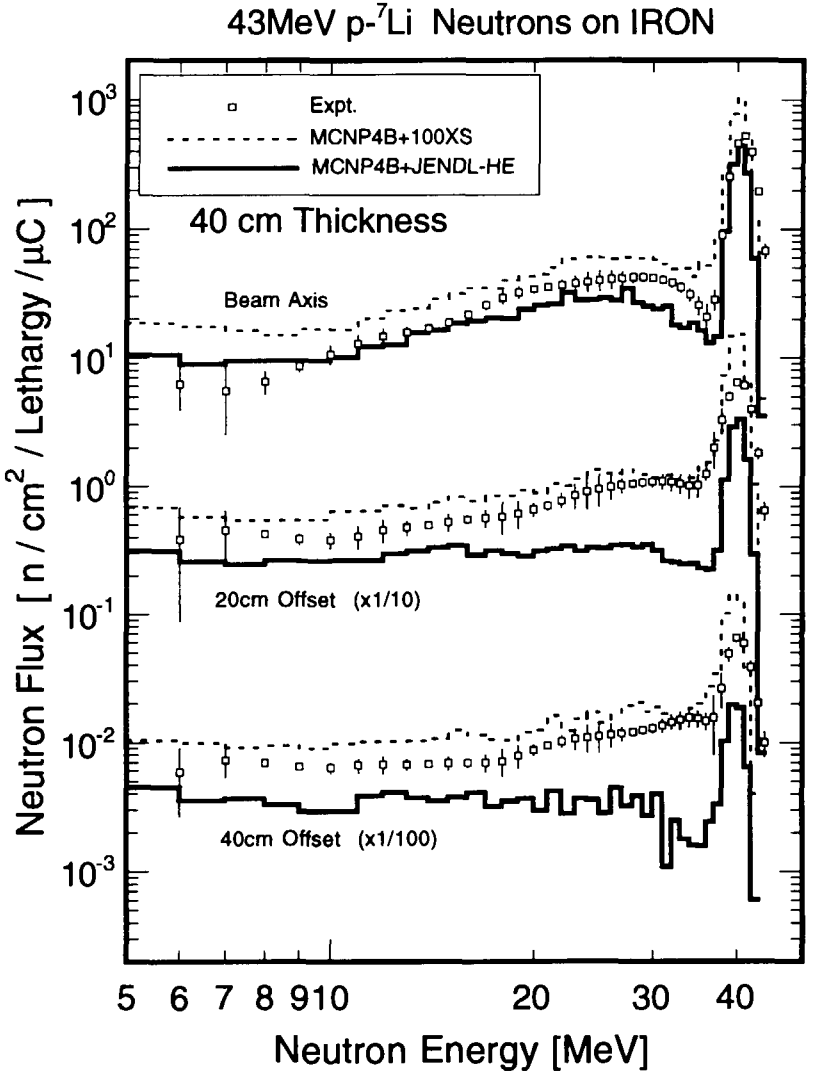

Fig. 3.2 Comparison of measuerd and calculated neutron spectra on and off the beam axis for the TIARA iron shield experiment.

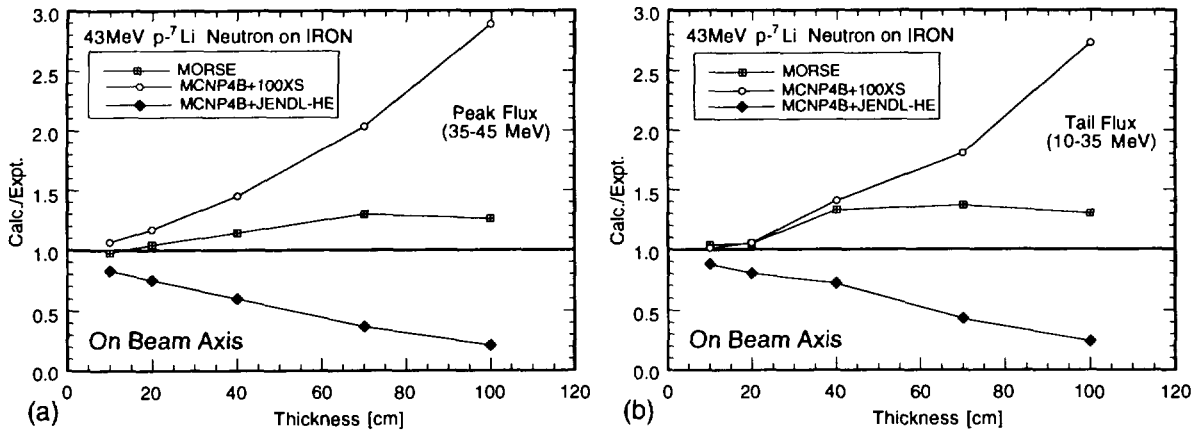

Fig. 3.3 Calculated to experimental ratios of (a) peak (35~45 MeV) and (b) tail (10~35 MeV) neutron fluxes on the beam axis for the TIARA iron shield experiment.

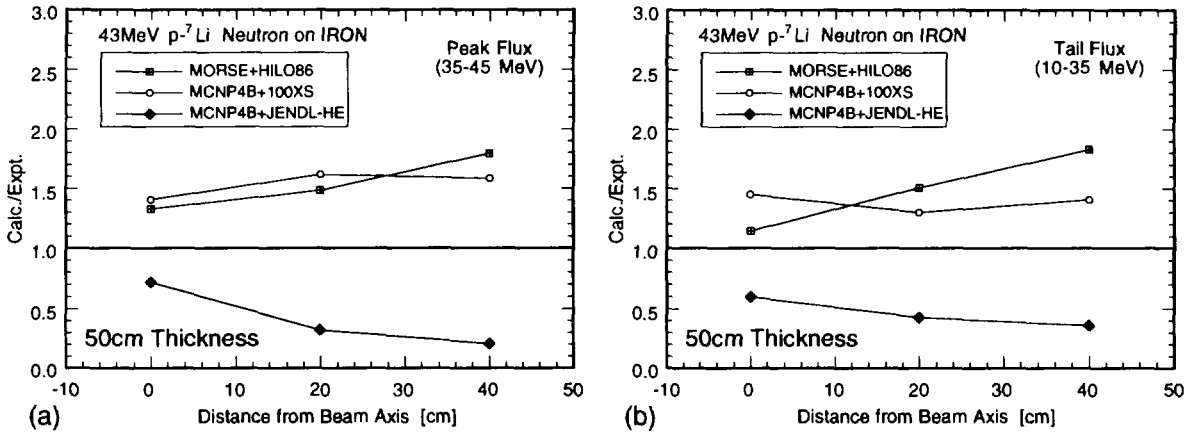

Fig. 3.4 Calculated to experimental ratios of (a) peak (35~45 MeV) and (b) tail (10~35 MeV) neutron fluxes on and off the beam axis for the TIARA iron shield experiment.

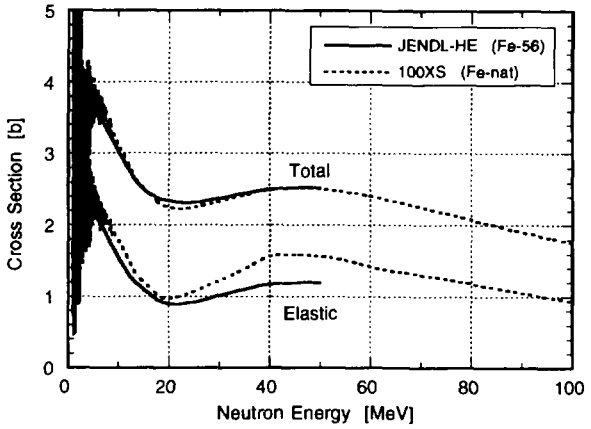

Fig. 3.5 Total and elastic scattering cross sections of iron in JENDL-HE File (Fe-56) and the 100XS library (Fe-nat).

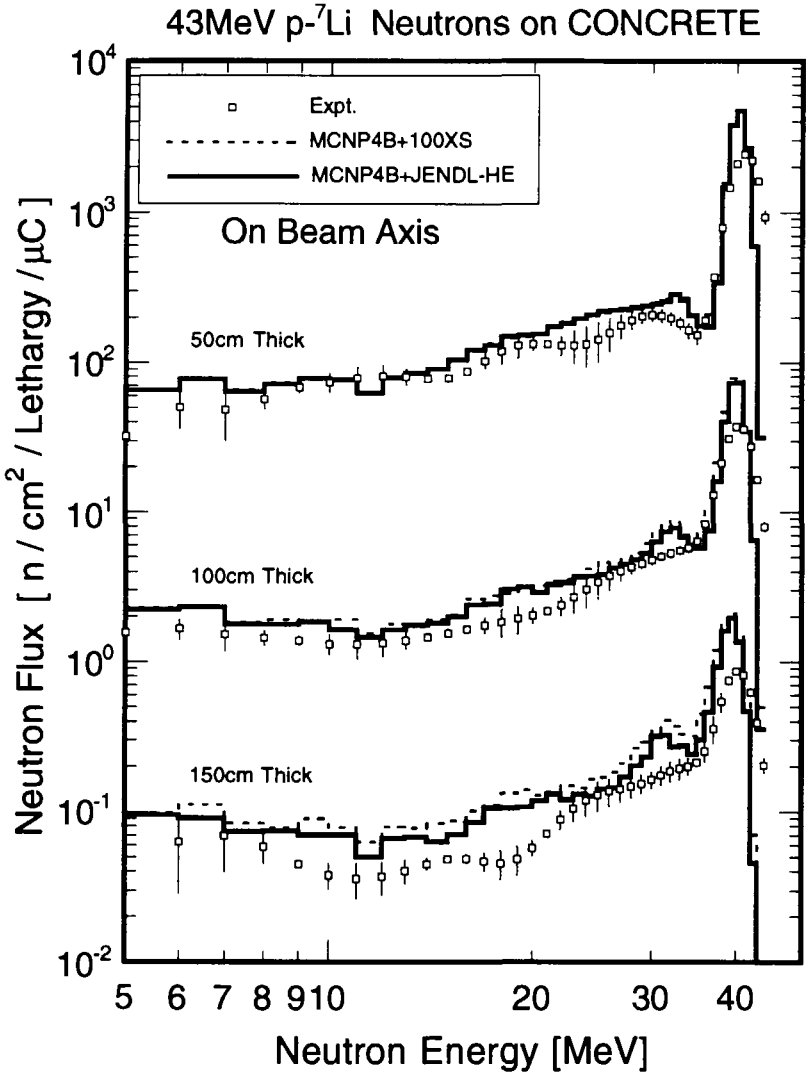

Fig. 3.6 Comparison of measuerd and calculated neutron spectra on the beam axis for the TIARA concrete shield experiment.

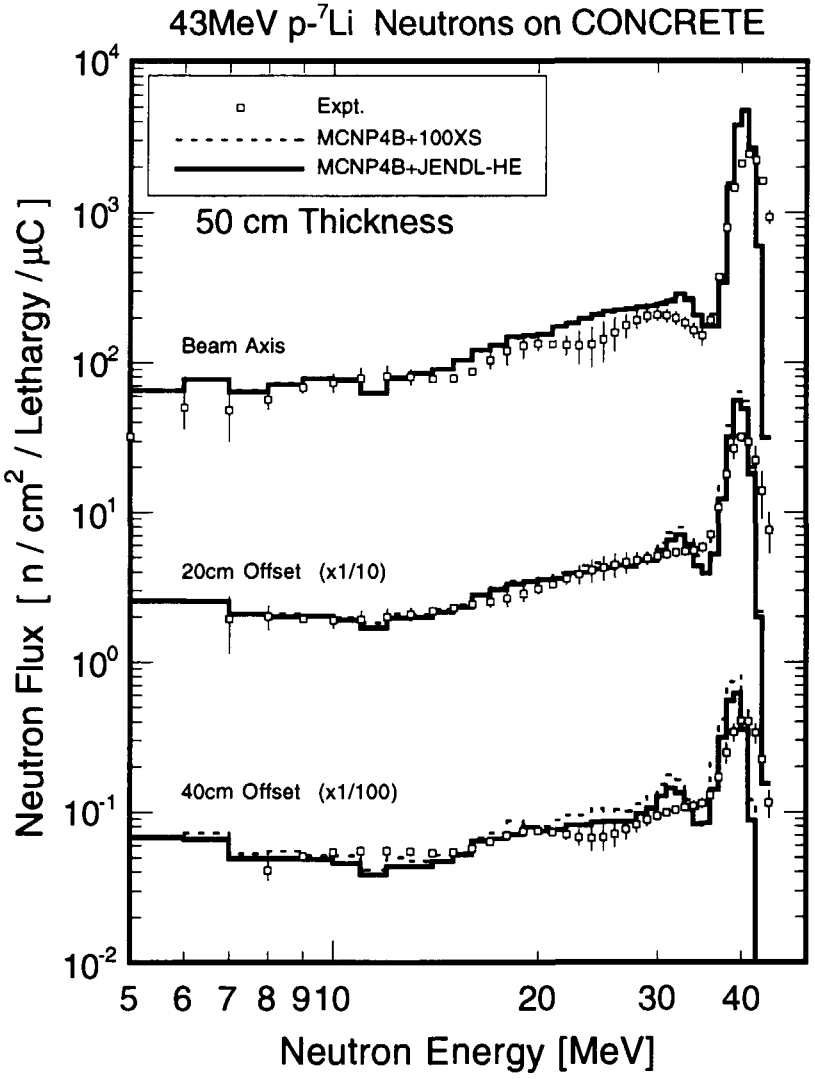

Fig. 3.7 Comparison of measuerd and calculated neutron spectra on and off the beam axis for the TIARA concrete shield experiment.

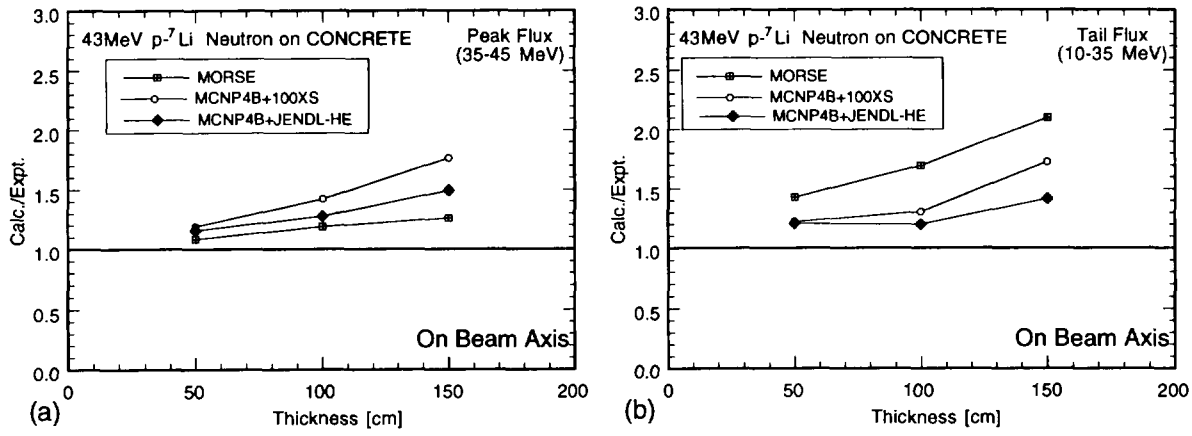

Fig. 3.8 Calculated to experimental ratios of (a) peak (35~45 MeV) and (b) tail (10~35 MeV) neutron fluxes on the beam axis for the TIARA concrete shield experiment.

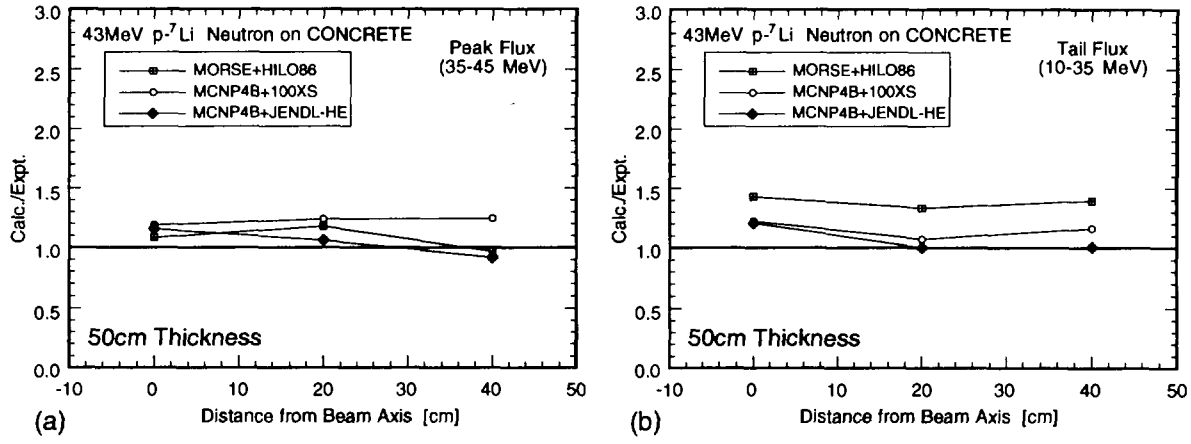

Fig. 3.9 Calculated to experimental ratios of (a) peak (35~45 MeV) and (b) tail (10~35 MeV) neutron fluxes on and off the beam axis for the TIARA iron shield experiment.

Figure 4.1 shows calculated neutron spectra by JENDL-HE File and 100XS compared with the measured data. Both calculations, especially JENDL-HE, do not predict appropriately the measured spectrum. In JENDL Fusion File and JENDL-3.2, cross section of iron is provided for four iron isotopes as well as elemental iron which is a mixture of four isotopes in natural abundance. The elemental iron data have been refined by a number of benchmark tests because use of the elemental iron data has been recommended. Contrary, the isotopic data have not been examined well. The history is represented clearly in Fig. 4.2 that is a comparison of calculated neutron spectra with the elemental and isotopic iron data of JENDL Fusion File. The spectrum with the elemental data agrees almost perfectly with the measured data while large discrepancies between the calculated spectrum with the isotopic data and the measured data are found.

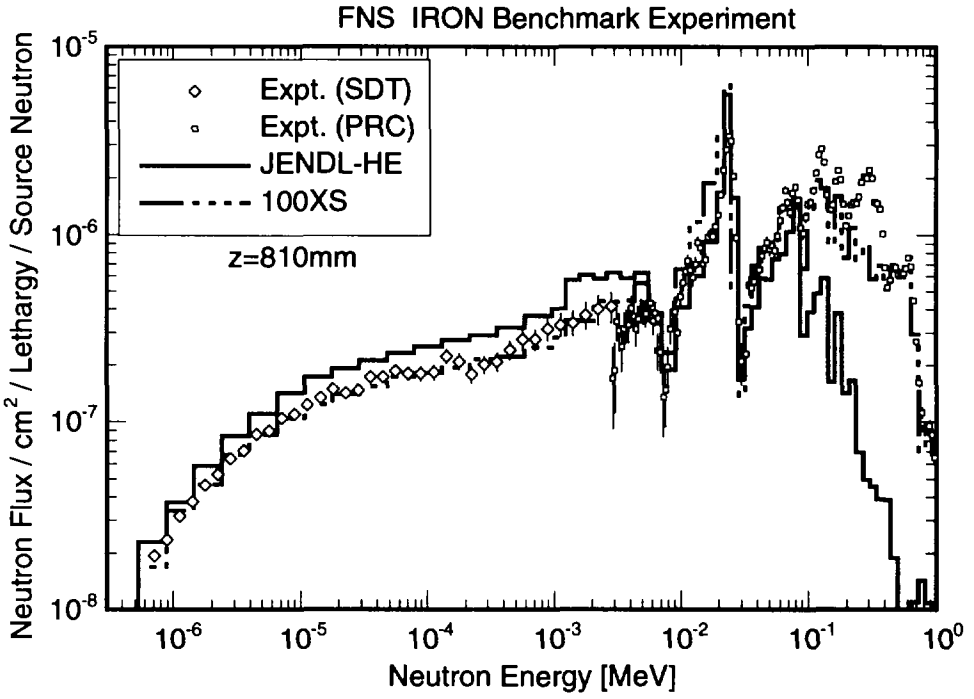

Fig. 4.1 Comparison of measured and calculated (JENDL-HE File & 100XS) neutron spectra for the FNS iron benchmark experiment.

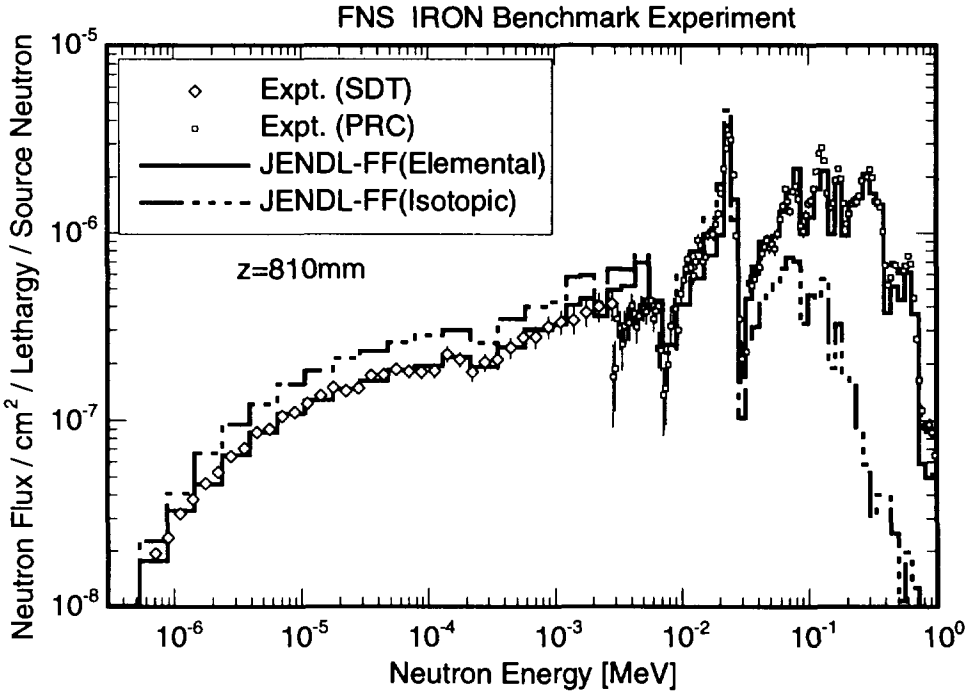

Fig. 4.2 Comparison of measured and calculated (elemental and isotopic evaluation of JENDL Fusion File) neutron spectra for the FNS iron benchmark experiment.

For elements for which both elemental and isotopic cross section data are provided in JENDL Fusion File and JENDL-3.2, one can select the data from the two to be merged to JENDL-HE File as the low energy part below 20 MeV. This iron benchmark test suggests that well-validated elemental data should be merged to JENDL-HE File rather than the isotopic data which have not been tested well so far.

5. Concluding Remarks

Benchmark test of JENDL High Energy File has started with the MCNP code. Some problems of cross section data were pointed out. Selection of cross section data below 20 MeV was discussed.

Acknowledgments

The authors are grateful to Drs. H. Nakashima, T. Fukahori, S. Chiba and K. Kosako for their help to conduct the benchmark tests.

References

[1] Briesmeister J. F. (Ed.): "MCNP™ - A General Monte Carlo N-Particle Transport Code, Version 4B", LA-12625-M, Los Alamos National Laboratory (1997).

[2] Uwamino Y., et al: Nucl. Sci. Eng., 80, 360 (1982).

[3] Nakashima H., et al.: "Benchmark Problems for Intermediate and High Energy Accelerator Shielding", JAERI-Data/Code 94-012 (1994).

[4] Shin K., et al.: Nucl. Sci. Eng., 109, 380 (1991).

[5] Nakao N., et al: Nucl. Sci. Eng., 124, 228 (1996).

[6] Nakashima H., et al.: Nucl. Sci. Eng., 124, 243 (1996).

[7] Nakao N., et al: Nucl. Sci. Eng., 134, 348 (1997).

[8] Nakane Y., et al: "Neutron Transmission Benchmark Problems for Iron and Concrete Shields in Low, Intermediate and High Energy Proton Accelerator Facilities", JAERI-Data/Code 96-029 (1996).

[9] Kosako K.: Private communication (1998).

[10] Little R. C.: "Summary Documentation for the 100XS Neutron Cross Section Library (Release 1.0), LA-UR-96-24, Los Alamos National Laboratory (1995).

[11] Nakashima H., et al.: "Accelerator Shielding Benchmark Experiment Analyses", Proc. Specialists' Meeting on Shielding Aspects of Accelerators, Targets and Irradiation Facilities, Geneva, Switzerland, Oct. 12-13 (1995).

[12] Konno C., et al.: Fusion Eng. Des., 18, 297 (1991).

[13] Maekawa F. and Oyama Y.: Nucl. Sci. Eng., 125, 205 (1997).

6. International Trend

6.1 Los Alamos Activities on High-Energy Nuclear Data Evaluation

Satoshi Chiba
Research Group for Hadron Science, Japan Atomic Energy Research Institute
Tokai-mura, Naka-gun, Ibaraki-ken 319-11
e-mail : chiba@cracker.tokai.jaeri.go.jp

Status and evaluation method of Los Alamos High Energy Nuclear Data File is reviewed.

1. Introduction

Evaluation for neutron- and proton-induced nuclear cross section libraries up to 150 MeV is in progress at Los Alamos National Laboratory. The details of the evaluation method, status and implementation in MCNPX will be described in a forthcoming paper[1], so only a brief explanation on the evaluation method and status will be given in this report.

2. Overview and status

The Los Alamos library consists of general purpose (transport) library and activation library. In general, the transport library is evaluated with GNASH code, while the activation library is being prepared with HMS (Hybrid Monte-Carlo) Alice code[2] although there are many common features in the evaluation of these libraries. The HMS Alice is a monte-carlo version of Alice, which is capable of treating the multi-particle pre-equlibrium emission to any steps, a feature not implemented in the original version of Alice. In this report, I will concentrate on a short description of evaluation of general purpose library using the GNASH code. As of April 1998, evaluation has been finished for the elements of H, C, N, O, al, Si, P, Ca, Cr, Fe, Ni, Cu, Nb, W and Pb including most of the stable isotopes. A similar evaluation is on-going for Mercury isotopes where the lower energy part, i.e., for energy below 20 MeV, is taken from the recent JAERI evaluation[3] for the neutron library.

3. Evaluation method

The GNASH code in use at Los Alamos was integrated by A.J. Koning in a code system "QUICKGNASH" with a number of pre- and post-processing programs. Figure 1 shows a simplified flow of QUICKGNASH code system. Firstly, a program "pregnash" is executed to produce input data for ECIS96 and GNASH (version gn8cp3). The, ECIS96 generates the elastic scattering angular distributions, transmission coefficients for n, p, d, t and α particles (^{3}He emission is usually ignored in Los Alamos evaluation) and direct inelastic scattering cross sections which are then formatted by "postecis" program for use in GNASH. Then GNASH code is executed. If some modifications are needed, the input data for GNASH, transmission coefficients or the input data for "pregnash" are modified. Finally, "gscan" code formats the output of GNASH to ENDF format, and PKA spectra are generated.

Typical results of Los Alamos Evaluation and GNASH calculations are given in Figs. 2, 3 and 4.

References
[1] M.B. Chadwick et al, to be submitted to Nucl. Sci. Eng.
[2] M. Blann, Phys. Rev. C54, 1341(1996).
[3] K. Shibata et al, J. Nucl. Sci. Technol. 34, 1171(1997).

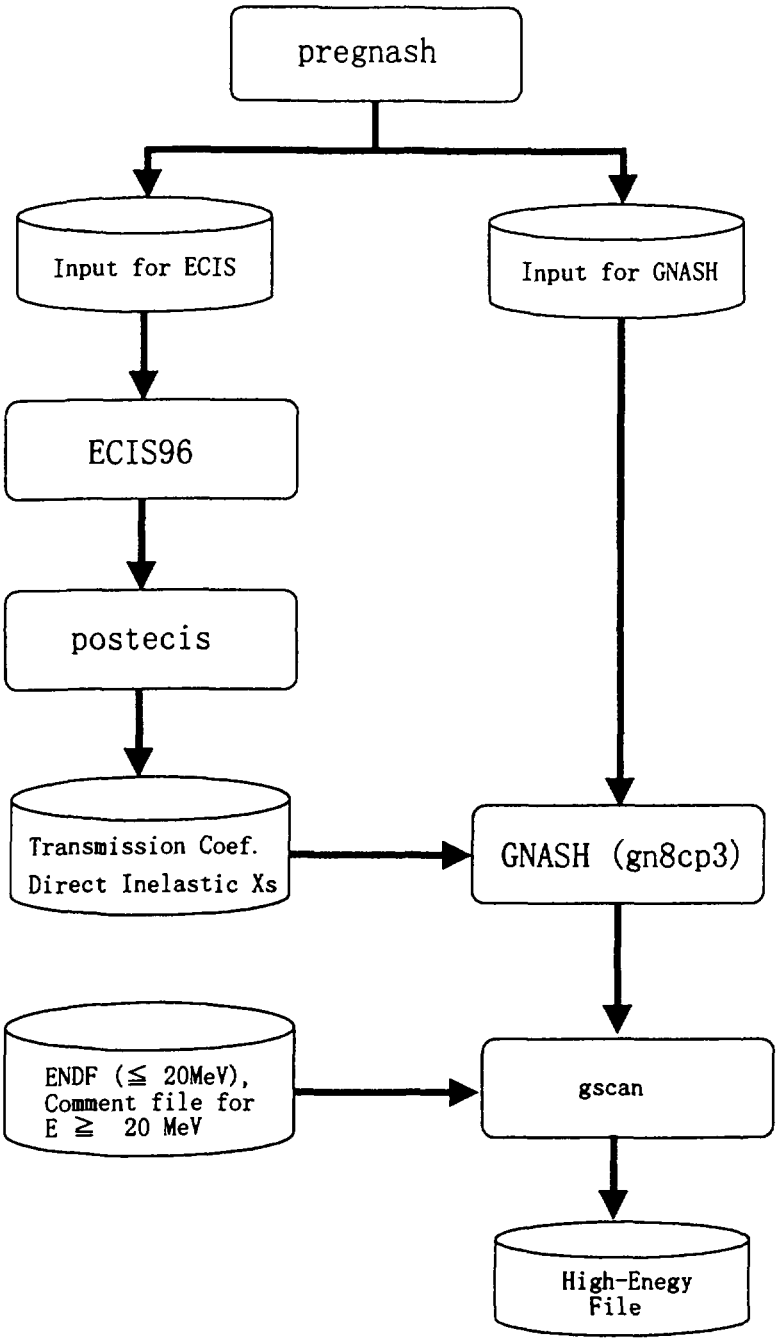

Fig. 1 Simplified flow of QUICKGNASH

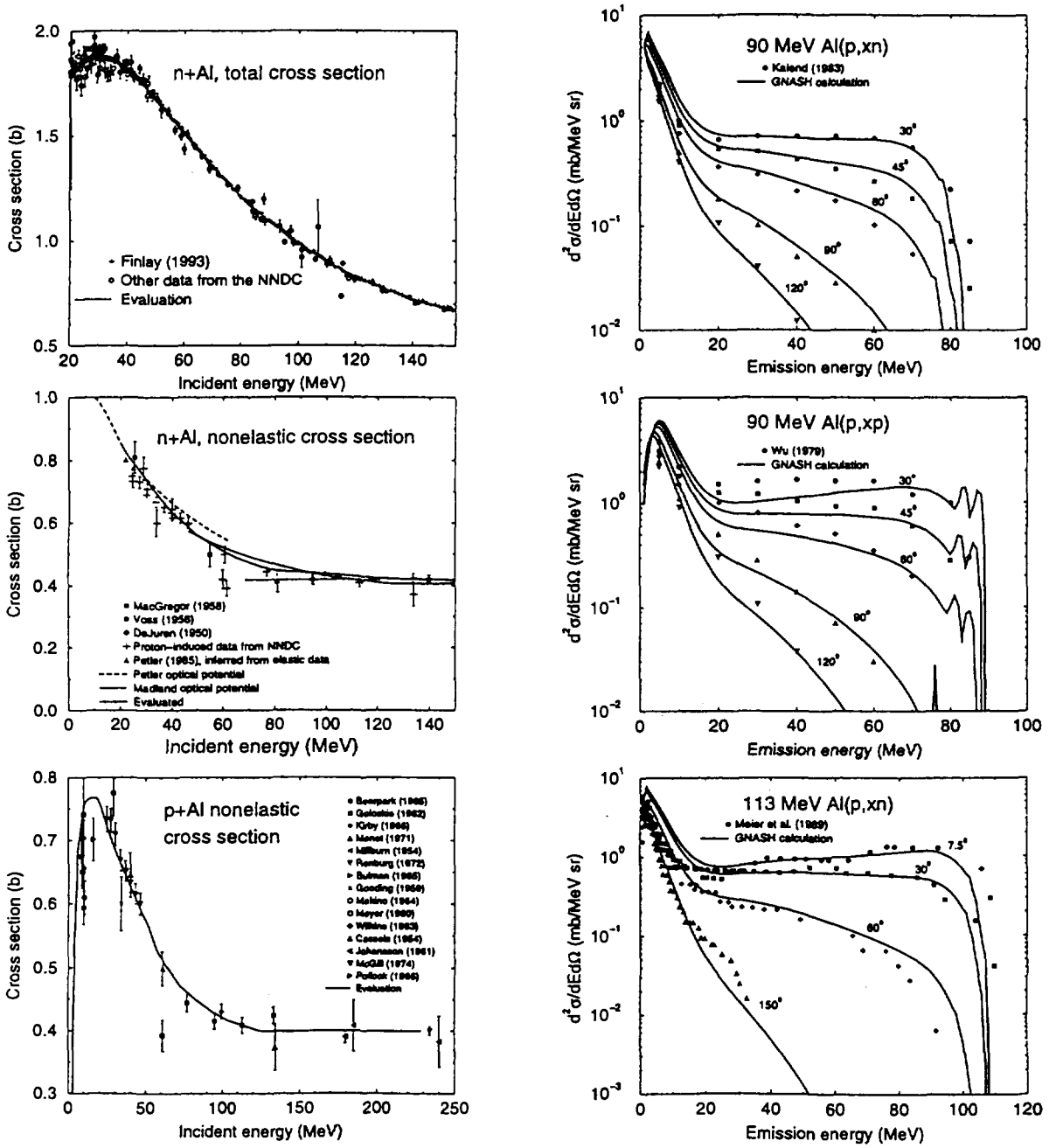

Fig. 2 Los Alamos Evaluation for Al

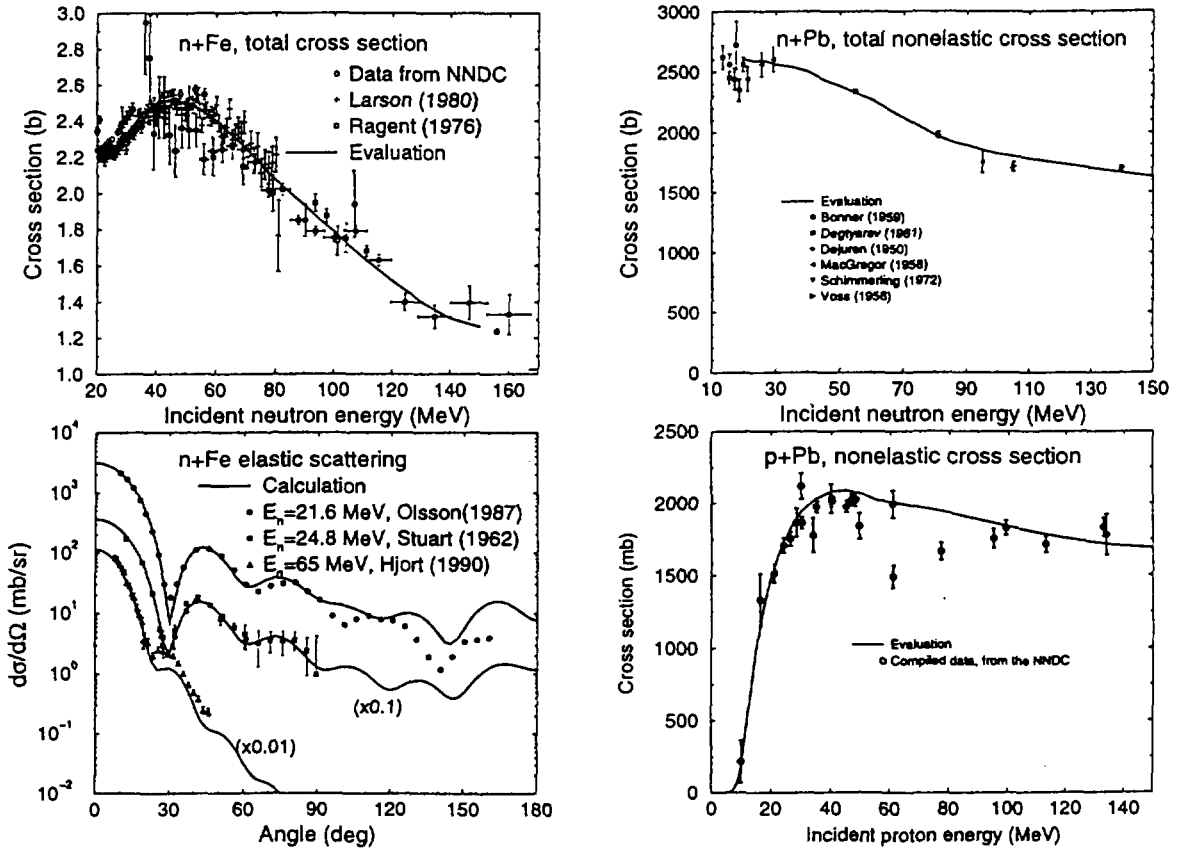

Fig. 3 Los Alamos Evaluation for Fe (left) and Pb (right)

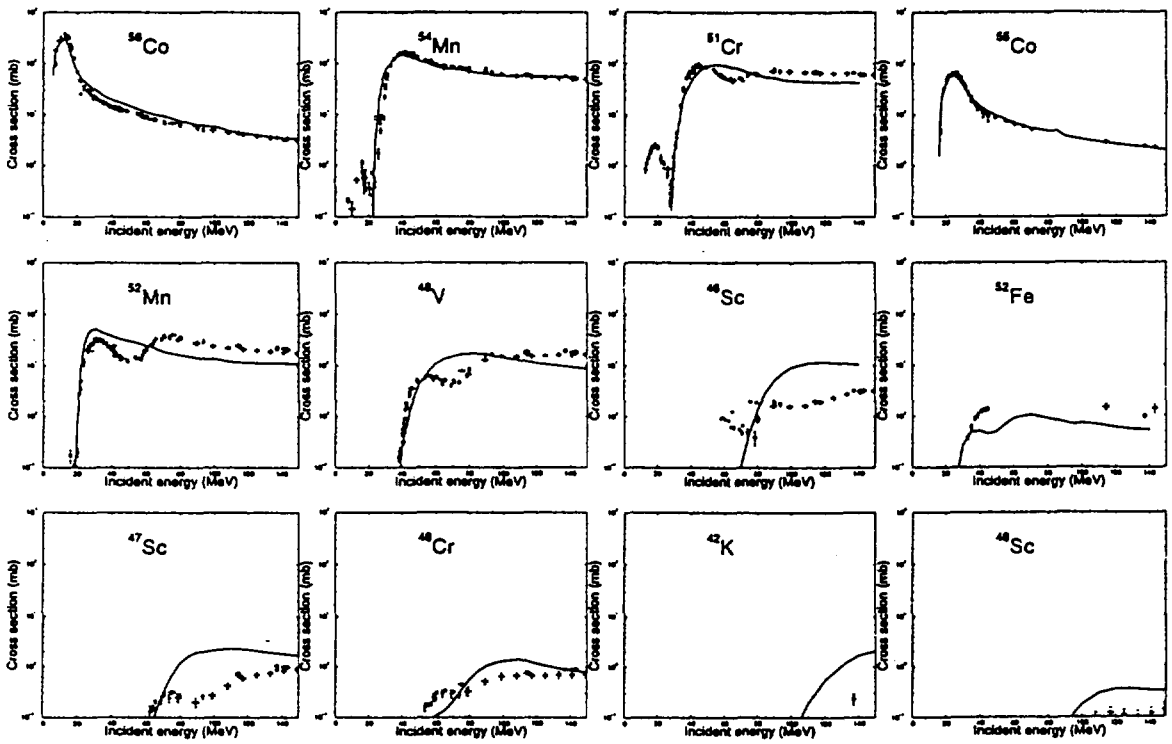

Fig. 4 Isotope Production Cross Sections from Fe + p Reactions

6.2 Nuclear Design Aspect of the Korean High Intensity Proton Accelerator Project

Jonghwa Chang, Tae-Yung Song
Korea Atomic Energy Research Institute
P. O. Box 105, Yusong, Taejon, Korea, 305-600

A plan to construct a high current proton accelerator has been proposed by KAERI. We are presenting the required nuclear design to support the project as well as a brief overview of the proposed proton accelerator. The target and core design is highlighted to show feasibility of incineration of minor actinides from the spent fuel of light water reactors. Radiation shielding and activation anaylses are also important for the design and the license of the accelerator.

1. Introduction

KAERI is developing a high current proton accelerator, named KOMAC, for the application of nuclear transmutation using a subcritical reactor. The final goal of the project is to construct and operate a proton accelerator of 1 GeV with 20 mA and a test reactor of 1 GWth to verify transmutation capability. As shown in Fig. 1, the acceleration devices are starting from an injector at 50 keV, an RFQ up to 3 MeV, two CCDTL up to 100 MeV, a super-conducting linac (SL) up to 260 MeV and another SL up to 1 GeV. Intermediate goal is to finish the first CCDTL for extracting the proton beam of 20 MeV with 20 mA until the beginning of next century[1].

A feasibility study is undergoing for the subcritical reactor of 1,000 MW_{th} which is to incinerate the toxic minor actinides in the spent fuels from the commercial light water reactors.

For the successful design of the KOMAC project, a nuclear design is required for the following fields:

- Target and core design,
- Radiation Shielding, and
- Activation of accelerator components.

2. Target design

The target converts the 1 GeV proton beam into the neutrons through the spallation reaction. The core incinerates the toxic nuclides into less toxic nuclides. To enhance the incineration rate, the core contains fissile materials as the neutron multiplicator. The effective multiplication constant will be limited to 0.97 for generic safety of the reactor.

The design code for target and core is the LCS package which was developed at Los Alamos[2]. LAHET computes intra nuclear cascade using Bertini's INC model and computes Monte Carlo spatial transport problems for protons, pions, muons, deuterons, tritons, photons as well as neutrons. For neutron transport of energy less than 20 MeV, MCNP4 handles the problem using a surface source file generated during LAHET run.

A liquid lead-bithmus mixture is considered as the first candidate of target material. The liquid target may have a beam window problem and it is difficult to anticipate the degree of damage under the high temperature and radiation environment. Therefore, tungsten is selected as the second option for the target. The range of 1 GeV proton beam incident on the lead-bithmus target is 603 gm/cm^2 (or 57 cm). The proton trajectory is almost linear and the energy decrease is also linear along the range. The secondary particles by 1 GeV proton beam are mostly neutrons, and protons, alphas, deuterons etc. are also emitted as displayed in Table 1. Figure 2 shows the production and leakage of neutron for lead and tungsten with a varying diameter of target cylinder. The neutron production is similar for both materials. However the neutron leakages are very different for a solid target. For the tungsten target, a relatively large absorption cross section is the cause of the rapid decrease of leaking neutrons.

To achieve a high incineration rate of minor actinides, the spectra of neutron must be hard and the rate of neutrons produced be high. This concept introduces the metallic coolant and fuel whether it is solid or liquid. The design of the target is related to the hardness of neutron spectrum. Figure 3 shows the average energy of produced and leaked neutrons. The energy of spallation neutron is about 7.1 MeV for 1 GeV proton beam. However that of leaking neutron outside the target ranges from 6 to 2 MeV, which is largely dependent of the target volume and material.

The estimation of residual spallation product is studied using LAHET code for the case of tungsten target. Figure 4 displays the atomic number of the spallation product. Medium Z number nuclides are produced more from the fission induced by the higher energy proton.

3. Radiation Shielding

Shielding of an accelerator during operation and against accident is an important aspect is securing a construction and operation license from the government. It is necessary to estimate the radiation dose during operation at the outside of shield of the beam dump, the transmission line, and the target. During a radiation accident, proper designation of the restricted area must also be analysed.

The KOMAC will use different buildings for different energy ranges. So, it needs to optimize shielding requirements for different proton energy beams. The upper energies may be 100 MeV, 260 MeV, and 1 GeV.

Proton loses energy continuously with the interaction of electron clouds around atom[3]. The loss of energy is almost linear in traveling path. For low energy proton beam, this path is just a few millimeters, so the thick target yield may be more important than energy dependent cross section. However for proton beams of 1 GeV order, the range is 60 cm to 160 cm. For this situation, we need the energy dependent proton interaction cross section to know space dependency of the secondary particle.

Among the secondary particles, neutrons will contribute significantly. Ref. 4 reported the thick target neutron yield for 52 MeV proton beam which is important for low energy proton shielding.

For the shielding calculations, we need the source term and attenuation term. The source term mainly consists of neutron production due to proton bombardment. The attenuation term is the neutron cross-sections for the high energy transport calculation. According to Ref. 5, the calculated source term is 5 - 0.5 times different from measurement and the attenuation

length is 1.5 times larger for 230 MeV protons, which results in about 25 times overestimation in dose. Recently reported calculation results using LAHET are much better, however there are still discrepancies[6]. The other calculations around 50 MeV give positive results when the code is used with DLC119/HILO86 library[7, 8].

The measured neutron production cross section data for Be, B, C, N, O, Al, Fe, Cd, W, Pb, and ^{238}U, are found for proton energy of 113 - 800 MeV[9]. It reports agreement with the calculations for heavy nuclides.

During the construction and operation, the proton beam dump is also an important source of radiation and heating. Carbon block is a popular candidate as the dump material. The energy deposition in the carbon block is needed for the cooling of the dump. Ref. 10 reports that the energy deposition inside carbon and structure is predictable within the error of 20 % with LCS.

4. Activation

Activation of the accelerator components shall be considered on the aspect of the maintenance of the system as well as the material damage. The accelerating channels are made of 5 cm- thick copper tube for proton energy of up to 100 MeV, 3 to 5 mm thickness high purity superconducting niobium cavity up to 1 GeV. The supporting structure material is stainless steel.

The loss of the proton beam is less than 1 nA/meter and it will hit the wall nearly parallel to the beam direction. So, the tube will be activated primarily by a few tens MeV proton, however the secondary neutron contribution is also important in the energy range. The helium production is an important mechanism for radiation damage, too.

The coolant surrounding the tube will be also activated and will be contaminated by the fragments from the tube or cavity. In Ref. 11, the activated gamma-emitting nuclides in the coolant of a 590 MeV proton accelerator are detected as ^{7}Be, ^{60}Co, ^{65}Zn, ^{54}Mn, ^{122}Sb, and ^{124}Sb. Among them, ^{7}Be is the spallation product of ^{16}O and the other isotopes are originated from the neutron capture.

5. Conclusion

We have presented an overview of the KOMAC project and requirements of nuclear design. This project has been barely started. The important things besides the construction of the proton accelerator are to show the quantitative feasibility of the minor actinide incineration and to perform a nuclear design to hold the intense proton beam up to 100 MeV.

References

[1] C.K. Park et al., "The KOMAC Project; Accelerator and Transmutation Project in Korea," The First Asian Particle Accelerator Conference (APAC98), KEK, Tsukuba, Japan, March 23-27, 1998.

[2] R. E. Prael and H. Lichtenstein, "Users Guide to LCS: The LAHET Code System," LA-UR-89-3014, LANL (1989)

[3] J.F.Ziegler et al., "The Stopping and Range of Ions in Solids," Pergamon Press (1985).

[4] K. Shin et al, "Thick-Target Neutron Yield for Charged Particles," Nuc. Sci. and Eng. 120, 40 (1995)

[5] J.V.Siebers et al, "Shielding Measurements for 230- MeV Protons," Nuc. Sci. Eng. 115, 13 (1993)

[6] J.V. Siebers et al, "Shielding Calculations for 230- MeV Protons Using the LAHET Code System," Nuc. Sci. Eng. 122, 258 (1996)

[7] N. Nakao et al., "Transmission Through Shields of Quasi- Monoenergetic Neutrons Generated by 43- and 68- MeV Protons - I: Concrete Shielding Experiment and Calculation for Practical Application," Nuc. Sci. Eng. 124, 228 (1996)

[8] R. G. Alsmiller, Jr. et al, "Neutron Photon Multigroup Cross Sections for Neutron Energies up to 400 MeV (Revision 1)," ORNL/TM-9801, ORNL (1986)

[9] W.B. Amian et al, "Differential Neutron Production Cross Sections for 800 MeV Protons," Nucl. Sci. Eng. 112, 78 (1992)

[10] C. A. Beard and V. I. Belyakov-Bodin, "Comparison of Energy Deposition Calculations by the LAHET Code System with Experimental Results," Nucl. Sci. and Eng. 119, 87 (1995)

[11] C. Degueldre et al., "Behavior and Removal of Radionuclides Generated in the Cooling Water of a Proton Accelerator," Nucl. Sci. Eng. 120, 65 (1995)

Table 1. Secondary particles produced by an 1 GeV proton incident upon lead target

Particle / Energy(MeV)	n	p	α	d	^{3}H	π	^{3}He
0 - 1	5.2	-	-	-	-	-	-
1 - 10	17.3	1.26	0.02	0.51	0.31	0.01	0.00
10 - 100	3.9	2.01	1.17	0.29	0.21	0.25	0.04
100 - 1000	0.9	0.79	-	-	-	0.10	-
Total	27.3	4.06	1.19	0.80	0.52	0.37	0.04

Table 2. Range of proton beam (gr/cm2)

Materal	density (gr/cc)	Proton Energy		
		100 MeV	250 MeV	1 GeV
Water	1.00	7.60	37.4	322
Carbon	2.25	8.54	41.9	360
Concrete	2.34	9.15	44.7	381
Stainless Steel	8.00	11.1	53.7	449
Copper	8.92	11.7	56.1	467
Niobium	8.57	12.5	59.7	494
Tunsten	19.35	15.2	72.4	584
Pb+Bi liquid	10.60	15.9	74.4	603

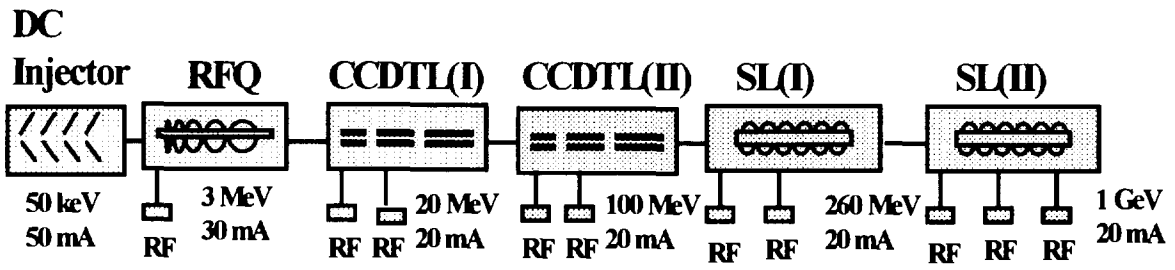

Figure 1. Diagram of KOMAC

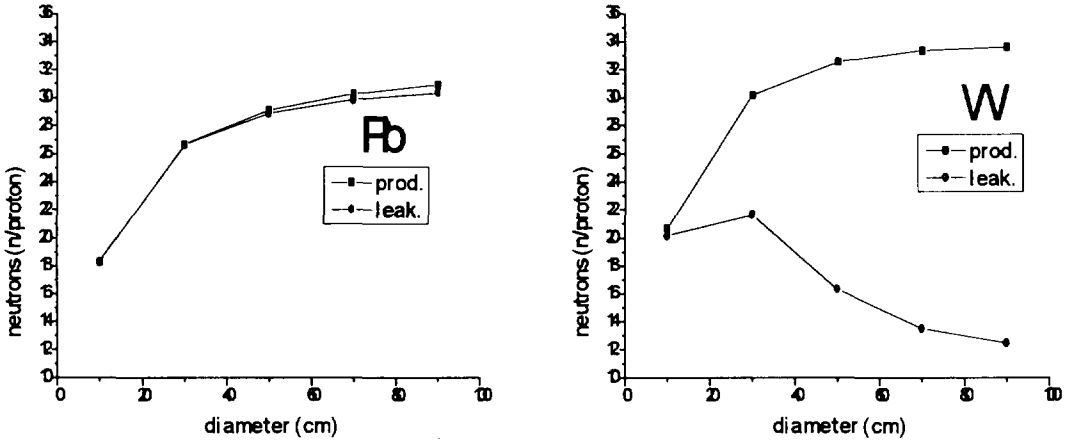

Figure 2. Neutron(<100MeV) production and leakage as a function of target diameter (beam energy=1 GeV, height=50 cm)

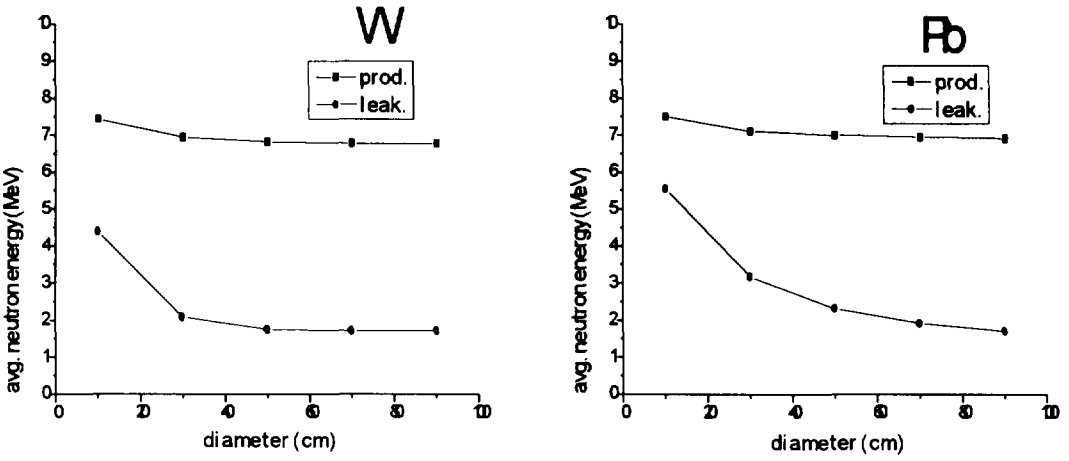

Figure 3. Average neutron(<100MeV) energy as a function of target diameter (beam energy=1 GeV, height=50 cm)

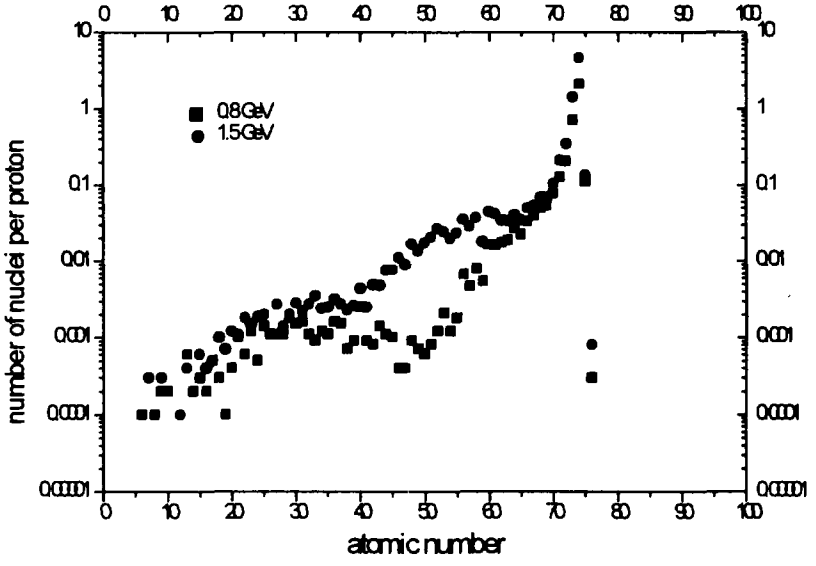

Figure 4. The distribution of the number of nuclei produced by activation as a function of atomic number for proton beam energies of 0.8 GeV and 1.5 GeV.

6.3 Inter-comparison of High Energy Files [Neutron-Induced, from 20 to 150 MeV]

LEE Young-Ouk* FUKAHORI Tokio
Nuclear Data Center, JAERI
* Permanent Address: Nuclear Data Evaluation Lab., KAERI

Recent new applications using accelerator-driven system require well-tested nuclear data when modeling the interaction of neutrons above 20 MeV. This work is aimed to review evaluation methods applied in currently available neutron high energy files above 20 to 150 MeV, to inter-compare their evaluated cross sections on some important isotopes, and to analyze resulting discrepancies. Through out these, integrities and consistencies of the high energy files are checked, applicability of physics models and evaluation methodologies are assessed, and some directions are derived to improve and expand current JENDL High Energy File.

I. Introduction

Nuclear data on conventional thermal and fast reactors mainly consist of neutron induced cross sections in energy below 20 MeV. Recent new applications such as radiation transport simulations of cancer radiotherapy and the accelerator-driven transmutation of waste require well-tested nuclear data of neutrons above 20 MeV.

To provide a link between nuclear reaction physics and applied analysis, there are two approaches. One is to perform the calculation of both microscopic nuclear reactions using intra-nuclear cascade (INC) model and macroscopic transport processes by one computer code such as LCS, LAHET and HERMES. However, the underlying physical assumptions of the INC model are not well satisfied below 100 MeV. The other is to use nuclear model calculations, benchmark them with available experimental data and store the data into evaluated data files, using the ENDF-6 format. After processing, the data libraries can serve as input for deterministic or Monte Carlo nuclear reaction codes. Above 150 MeV, however, pion production becomes important and the present ENDF-6 format is not so practical to cover such reactions that both methods are regarded as complementary approaches for the transportation analyses. Currently some evaluation works are in progress to build up high energy libraries for neutron and proton above 20 MeV.

This work is aimed to review evaluation methods applied in currently available neutron high energy files above 20 to 150 MeV, to inter-compare their evaluated cross sections on some important isotopes, and to analyze resulting discrepancies. Through out these we could check integrities and consistencies of the files, applicability of physics models and evaluation methodologies adopted, and derived some directions to improve and expand current JENDL High Energy File.

II. Status of High-Energy Libraries

Brief status and contents of currently available high-energy libraries are summarized in Table 1. Still most of these libraries are considered to be in evolving stage, i. e. receiving feedbacks and being updated.

JENDL-HE: The JENDL High Energy File [1] includes nuclear data for proton- and neutron-induced reactions. The evaluation work is separated into two phases. The energy range of the phase-I is up to 50 MeV, mainly for the International Fusion Material Irradiation Facility(IFMIF). The energy range for the phase-II is up to 2 GeV mainly for a project of Center for Neutron Science of JAERI. Below 20 MeV, the data of JENDL Fusion File or JENDL-3.2 are adopted basically.

LANL-HE: LANL-HE cross section libraries [2] have evaluated cross sections for important materials to energies in the 150-250 MeV range for use in accelerator applications. A new version of the Monte Carlo code MCNP is being developed to utilize these new data libraries. The current contents include the cross sections to 150 MeV for incident neutrons and protons on various isotopes of H, C, N, O, Al, Si, Ca, Fe, W, and Pb.

ECN-HE: ECN High Energy File [3] contains 150 MeV neutron and proton transport data files for FE-54, 56, 58, Ni-58, 60. The high-energy part of the data files consists of results from model calculations, which are benchmarked against the available experimental data. These high-energy data are created with a code system built around the nuclear reaction codes ECIS96 and GNASH.

BNL (ENDF/B-VI HE) As a special purpose file of ENDF/B-VI.4, ENDF/B-VI HE [4] contains neutron and proton-induced cross sections for C-12 (2 GeV), Fe-56, Pb-208 and Bi-209 up to 1 GeV.

FZK (Forschungszentrum Kalsruhe): FZK released neutron induced high energy files [5] for Fe-56 Cr-52, V-51 to 50 MeV mainly for IFMIF purpose.

WIND and MENDL-2(IPPE): The Waste Incineration Nuclear Data library [6] (WIND) contains evaluated data for 576 neutron induced fission and threshold reactions for isotopes of U, Np and Pu, and one file containing data for 32 proton induced reactions for U-238, in the energy range up to 100 MeV. The Medium Energy Nuclear Data Library [7] (MENDL) is a neutron reaction data library for nuclear activation and transmutation at intermediate energies. This library contains, for 505 stable and unstable target nuclides, production cross-sections for the formation of radioactive product nuclides for incident neutrons with energies up to 100 MeV.

III. Procedure of Inter-comparison

Selection of Libraries: Among seven libraries listed in Table 1, five evaluated high energy libraries were selected such as JENDL High Energy File of JAERI, ENDF/B-VI High Energy File of BNL, High Energy File of LANL, JEFF-3.0 High Energy File from ECN and IFMIF neutron file from FZK. These libraries have standard ENDF-6 format which enables us directly compare their evaluated cross sections each other without relying on benchmarking calculation with transport analysis.

Materials and Cross Sections: As for isotopes, following three nuclides were selected: carbon which is important in dosimetry and radiation therapy, aluminium and iron in shielding and structural material for accelerator-driven system and fusion. As for the cross section, total, elastic, non-elastic, some of isotope production cross sections and neutron emission DDX were compared each other against available experimental data.

Experimental Data: Basically, EXFOR data bank [8] of NEA were surveyed in the energy range of 20 - 150 MeV for above mentioned three material. Additional data from other works were also taken into account in some cases.

Conversion of Evaluated Data: Data processing mainly consist of conversion and interpolation of each quantities stored in different formats in the libraries to match with the format of measured data.

IV. Review of Evaluation procedure

Carbon: JENDL adopted microscopic folding model [9] (JLM theory) to calculate the optical model potential (OMP) and used Distorted Wave Born Approximation (DWBA), for inelastic cross sections to the discrete level (direct reaction). For the decaying process, SCINFUL Monte Carlo simulation code [10] were used with the branching ratios for different nuclear reaction pathways inputted, based on optimizations to measured data. In the Monte-Carlo simulation, three-body simultaneous break-up process and two-body sequential decay processes were taken into account in multi-body break-up reactions.

In LANL, a modified coupled-channel optical model was used for OMP and direct reaction calculation, applying Meigooni potential [11] for neutrons, Lane model isospin transformation from neutron potential for proton, and Madland method [12] for deutrons and alphas. Pre-equilibrium particle emission was obtained from FKK theory [13] and Kalbach systematics [14], and pre-equilibrium gammy-ray emission through the Giant Resonance was modeled using a semiclassical exciton model. Equilibrium emission for particles and gamma rays were calculated with Hauser-Feshbach theory [15], conserving angular momentum and parity. To optimize the model calculations, wide range of up-to-date experimental measurements were adopted.

In BNL, Wood-Saxson potential and systematics[16] were used to evaluate total, elastic and non-elastic cross sections for the energy below 30 MeV. For the angular distribution of elastic scattering cross sections, diffraction model was used. Equilibrium and pre-equilibrium emission were evaluated with evaporation [17] and exciton model using ALICE-P code [18]. Above 30 MeV up to 10 GeV, INC code (LAHET) was used along with systematics.

Aluminium: JENDL used SINCROS-II code system [19] which consists of ELIESE-GNASH and DWUCK4. It has modified Walter-Gauss potential [20] for neutron, Perey potential [21] for proton, modified Lemos potential for alpha [22], Lohr-Haeverli potential [23] for deutron and Becchetti-Greenless [24] potential. Direct reactions, pre-equilibrium emission and equilibrium emission were calculated with DWBA, exciton model and evaporation model respectively. The parameters for these models were searched and optimized in such a way to better produce experimental data.

In LANL, optical potential of Petler[25] for neutrons up to 60 MeV, and above this energy the Madland global potential [12] was used. For deutrons, the potential of Perey [21] was used at all energies, and for tritons the Becchetti-Greenlees potential [24] was adopted. the potential of Arthur and Young [22] was used for alpha particles at all energies. DWBA calculations were performed for direct reactions using the DWUCK code [26]. Pre-equilibrium particle emission was obtained from exciton model [27] and Kalbach systematics [14] and independently validated with FKK theory [13] calculation.

Iron: In JENDL, the same evaluation method was applied as described for Aluminum.

LANL used the neutron optical model potential of Arthur et al. [22] up to 26 MeV. Between 26 and 52 MeV, the imaginary volume component of Arthur's potential was modified to better account for non-elastic cross section measurements, and above 52 MeV potential of Madland [12] was used. For protons, the Beccetti-Greenlees potential [24] was utilized below

28 MeV, and the Madland potential [12] was used at higher energies. The global spherical potential of Perey [21] was utilized for deutrons, and the potential of Beccetti-Greenlees [24] was adopted for tritons. The alpha potential of Lemos as adapted by Arthur and Young [22] was used for alpha particles. Direct reaction cross sections to discrete states were calculated with DWBA using the ECIS95 code [28]. Pre-equilibrium particle emission was obtained from exciton model and Kalbach systematics, and validated by FKK theory. Equilibrium emission was calculated with Hauser-Feshbach theory in which angular momentum and parity are conserved. To optimize the model calculations, wide range of up-to-date experimental measurements were adopted.

In BNL, Wood-Saxson potential and systematics were used to evaluate total, elastic and non-elasic cross sections for the energy up to 1 GeV with the experimental data and systematics. The angular distributions of elastic scattering cross sections were obtained from diffraction model modified for relativistic effects and empirical fits to high energy data. Equilibrium and pre-equilibrium emissions were evaluated with evaporation and exciton model using ALICE-P code with adjusting parameters up to 1 GeV.

ECN used Koning-Delaroche potential [29] for neutron and proton, Lohr-Haeberli [23] for deutrons, Becchetti and Greenlees [22] for triton and Macfadden-Satchler [30] for alphas. Direct reactions were calculated with DWBA using ECIS-96 code. Pre-equilibrium cross sections were calculated with the exciton model of Kalbach [27]. For continuum angular distributions, Kalbach's systematics was used for all outgoing particles. Multiple pre-equilibrium emission was taken into account. Equilibrium emissions were calculated with evaporation mode and Gamma-ray transmission coefficients were calculated using the Kopecky-Uhl model [31]. FZK used coupled-channel method based on the Arthur-Young's potential and DWBA with modifications to achieve agreement with available measurement data. Pre-equilibrium and equilibrium emissions were calculated by GDH (Geometrically Dependent Hybrid Exciton) model [32] and evaporation model respectively, using ECIS and ALICE codes. Pre-equilibrium complex particle emission spectra were calculated in the framework of coalescence pick-up model [33].

Above evaluation methods adopted by each library are summarized in Table 2.

V. Results of Inter-comparison

Carbon: In Fig. 1 the evaluated total, non-elastic and elastic cross sections from JENDL, BNL and LANL are shown with various measurements. JENDL and LANL give good agreements with the data in total, elastic and non-elastic cross sections, while non-elastic cross sections of BNL overestimate the data.

In Fig. 2 the evaluated angular distributions of elastic cross sections of JENDL, LANL and BNL at the energy 22, 28.5 and 96 MeV of incident neutron with measurement data. The angular distributions of JENDL and LANL give excellent agreement with data while BNL distributions which were obtained from diffraction model do not describe the data well. The differences at the forward angle among evaluated angular distributions are directly related to the elastic and non-elastic cross sections as seen in Fig. 1.

In Fig. 3 the evaluated (n,2n) cross sections from JENDL, LANL and BNL were compared with five sets of measurements. Although there are discrepancies between measured data above 30 MeV, JENDL gives relatively better agreement than LANL and BNL. Above 60 MeV, the data are not described well by all three evaluated files.

Fig. 4 compares the evaluated (n,xn) emission spectra at 40 MeV from JENDL, LANL and BNL with (p,xp) data, because of no measurement data of (n,xn) emission spectra. It would be expected that C-12(p,xp) and C-12(n,xn) spectra should be similar, particularly for the higher emission energies where Coulomb effects are negligible. LANL and JENDL give good agreement with the data in the entire energy region while JENDL lies slightly below the data at the higher emission energies. BNL shows significant underestimation from intermediate energies where pre-equilibrium are dominant.

Aluminium: In Fig. 5 the evaluated total cross sections from JENDL and LANL libraries are shown with various measurements. LANL cross sections give overall agreement with most of experimental data while JENDL whose energy range is up to 50 MeV, starts to deviate and gives larger values than LANL and the experimental data from the energy of 35 MeV.

Also in Fig. 5 the evaluated elastic and non-elastic cross sections of Al-27 from JENDL up to 50 MeV and LANL up to 150 MeV are compared each other with two energy points of experimental data. It is evident that non-elastic cross sections of JENDL overestimate the data which LANL describes well.

In Fig. 6 the evaluated angular distributions of elastic cross sections at the energy 21.6, 26 MeV from JENDL and LANL, and 96, 136 MeV from LANL, with measurement data. The angular distributions of both two evaluated cross sections give overall agreement with data. However the magnitudes of the distributions of JENDL underestimate the data of 21.6 and 26 MeV due to underestimated elastic cross sections as shown in Fig. 5.

Fig. 7 compares the inclusive cross sections giving residual isotopes of Ne-21,22 Na-23 and Mg-24 against Los Alamos data. Both do not give excessive mismatch with the data except Mg-24 production case where JENDL significantly overestimates the data.

Fig. 8 simply shows the evaluated (n,xn) emission spectra at 40 MeV from MF6 sections of JENDL and LANL without any measurement data. The larger values at lower energies of JENDL spectra could be explained by the overestimation of non-elastic cross sections as pointed in Fig. 5. It is also noted that MF6 of JENDL does not contain inelastic discrete scattering contributions.

Iron: In Fig. 9 the evaluated total cross sections of Fe-nat from JENDL, FZK (< 50 MeV) LANL, BNL and ECN (< 150 MeV) are shown with various measurements. The cross sections from four libraries except FZK show show overall agreement with measurements while FZK does not agree well with measurements and with other evaluated cross sections. At the energy range between 20 - 40 MeV, JENDL and BNL have slight larger values than LANL and ECN which describe better the Lawrence Livermore and Los Alamos data. Fig. 9 also shows that non-elastic cross sections of LANL, BNL and ECN agree well with experimental data while JENDL and FZK overestimate the data, giving smaller elastic cross sections than other three as the case of Aluminium.

In Fig. 10 the evaluated angular distributions of elastic cross sections at the energy 21, 24.8, 26 and 65 MeV from the five libraries with data. The angular distributions of ECN and LANL give excellent agreement with data while the those of JENDL and FZK describe overall shapes of data. However the distributions of BNL does not describe the data well as in the case of Carbon.

Fig. 11 compares the evaluated triton emission and three neutron emission cross sections

from JENDL and LANL with Tohoku university data. As for the triton emission reaction, both of evaluated cross sections significantly underestimate the data. For the three neutron emission cross section, JENDL cross sections values are closer to the measurements.

Fig. 12 compares double-differential and angle-integrated spectra of 25.7 MeV ^{56}Fe(n,xn) reaction against Ohio university measurements, and double-differential and angle-integrated spectra of 65 MeV Fe-nat(n,xn) reaction against UC Davis measurements by processing of MF6 sections from five libraries. Among the evaluated spectra from the five libraries, BNL and FZK do not show inelastic discrete contribution since MF6 sections of these two libraries do not include it. Four of the evaluated spectra give overall agreements with measurements except BNL which significantly underestimates pre-equilibrium contribution at the intermediate energies especially at very forward and backward angles. LANL and ECN give excellent agreements over all three incident energies and all angles with three measurements except in very forward angle at 65 MeV with UC Davis data. At the equilibrium emission region where no measured data exists, JENDL and FZK have larger cross sections than BNL and ECN. These larger parts are considered to be shifted up when optimizing pre-equilibrium part with overestimated non-elastic cross sections.

Fig. 13 compares the angle integrated emission spectra among different decaying models, JENDL without multiple pre-equilibrium (MPE) and LANL/FZK with MPE. As seen in this figure, models with multiple pre-equilibrium correction better describe the spectra of 15 - 20 MeV region.

VI. Summary of Inter-Comparison

Based on the results, this inter-comparison work is summarized as follows:

- In the case of total, non-elastic and elastic cross sections, both microscopic optical model adopted in Carbon of JENDL and phenomenological optical model adopted in Aluminium and Iron of LANL and ECN, together with the sophisticate parameter optimization give overall agreement with the data.
- As for isotope production, some minor channels are not well described yet by current nuclear models. But this doesn't seem to deteriorate the overall consistencies of evaluated files for the actual applications.
- In DDX of Neutron Emission of Carbon, both stringent physics models consisting of FKK and Hauser Feshbach theories, adopted in LANL, and branching ratio adjustment with Monte Carlo simulator used in JENDL give good agreement with the data.
- As for DDX of Aluminium and Iron, models of exciton and Hauser Feshbach corrected with multiple pre-equilibrium, applied in LANL and ECN give better agreement than the models without MPE applied in JENDL and BNL.

VII. Guide to improving and expanding JENDL-HE

To improve and expand current JENDL high energy file, some directions are derived as:

- For Carbon, introduce physics model in decaying process to expand evaluation up to higher energy,
- For Aluminium and Iron, choose more sophisticate optical model, and optimize its parameters with recent data to improve consistency in elastic, non-elastic and emission cross sections,
- To better describe DDXs of Aluminium, Iron, adopt Feshbach-Kerman-Koonin model which explicitly describes MSD and MSC reactions.

As for the structure of library,

- Fully utilize MF6 section to produce self-consistent KERMA factor,
- Remove discontinuity at 20 MeV which is caused by merging JENDL HE and JENDL 3.2.

References

[1] T. Fukahori and S. Chiba, "Status of Nuclear Data Evaluation for JENDL High Energy File", The 2nd Specialists' Meeting on High Energy Nuclear Data, Tokai, Japan, Jan. 26-27 (1995)

[2] M.B. Chadwick, P.G. Young, and R.E. MacFarlane, "The Los Alamos 150 MeV Library", private communication (1997)

[3] A.J. Koning and O. Bersillon, "Neutron and Proton Datafiles up to 150 MeV", private communication (1997)

[4] S. Pearlstein, "ENDF/HE-VI", BNL-NCS-42434 (1990)

[5] Yu. A. Korovin et. al., private communication (1996)

[6] A.Yu. Konobeyev et. al., , "WIND nuclear data library for transactinides at energies up to 100 MeV", report INDC(CCP)-384.

[7] Yu.N. Shubin et al.,"Neutron reaction data library for nuclear activation and transmutation at intermediate energies", IAEA-NDS-136 (1995)

[8] EXFOR http://www.nea.fr/html/dbdata/nds_experimental.htm

[9] J.P. Jeukenne et al., Phys. Rev., **16**, 80 (1977)

[10] M. Harada, et al., Proc. 1995 Nuclear Data Symp., JAERI-M 96-008, p260 (1996)

[11] Meigooni Potential: A.S. Meigooni et al., Nucl. Phys. **A445**, 305 (1985)

[12] D.G. Madland, "Proceedings of a Specialists's Meeting on Preequilibrium Reactions", Semmering, Austria, 10-12 Feb. 1988, NEANDC-245, p.103 (1988)

[13] H. Feshbach, A. Kerman, S. Koonin, Ann. Phys. (NY) **125**, 429 (1980)

[14] C. Kalbach, "Systematics of Continuum Angular Distributions: Extensions to Higher Energies," Phys. Rev. **C37**, 2350 (1988)

[15] W. Hauser and H. Feshbach, Phys. Rev., **87**, 366 (1952)

[16] S. Pearlstein, Nucl. Sci. Eng., **49**, 162 (1972)

[17] V. F. Weisskopf, Phys. Rev., **52**, 295 (1937)

[18] S. Pearlstein, J. Astrophys., **346**, 1049 (1989)

[19] N.Yamamuro, "A Nuclear Cross Section Calculation System with Simplified Input-Format" ,JAERI-M-96-006 (1990)

[20] R.L. Walter and P.P. Gauss, "A Global Optical Potential Model for Neutron Scattering for A>53 and 10 MeV < E < 80 MeV", Proc. Int. Conf. Nuclear Data for basic and Applied Science, Santa Fe, New Mexico, p.1079 (1985)

[21] F.G. Perey, Phys. Rev., **131**, 745 (1963)

[22] E.D. Arthur and P.G. Young, "Evaluated Neutron-Induced Cross Sections for Fe-54,56 to 40 MeV", LA-8626-MS (1980)

[23] J.M. Lohr and W. Haeberli, Nucl. Phys., **A232**, 381 (1974)

[24] F.D. Becchetti, Jr. and G.W. Greenlees, "Polarization Phenomena in Nuclear Reactions", The University of Wisconsin Press, p.682 (1971)

[25] J. S. Petler, M. S. Islam, and R. W. Finlay, "Microscopic Optical Model Analysis of Nucleon Scattering from Light Nuclei," Phys. Rev. **C32**, 673 (1985)

[26] P. D. Kunz, "DWUCK4 - A Distorted Wave Born Approximation Program", University of

Colorado (1974)
[27] C. Kalbach, "PRECO-D2: Program for Calculating Preequilibrium and Direct Reaction Double Differential Cross Sections," LANL report LA-10248-MS (1985)
[28] J. Raynal, "Notes on ECIS94," CEA informal report, Saclay (1995)
[29] A.J. Koning and J.-P. Delaroche, unpublished
[30] L. Macfadden and G.R. Satchler, Nuc. Phys., **84**, 177 (1966)
[31] J. Kopecky and M. Uhl, "Test of gamma-ray strength functions in nuclear reaction model calculations", Phys. Rev., **C42**, 1941 (1990)
[32] M. Blann and H.K. Vonach, Phys. Rev., **C28**, 1475 (1983)
[33] A. Iwamoto and K.Harada, Phys. Rev., **C26**, 1527 (1982)

Table 1. Status and Contents of High Energy Files

	Purpose	E_{max}	Isotopes
JENDL HE	IFMIF (Phase-I)	n: 50 MeV	H, C, Na, Mg, Al, Si, K, Ca, Ti, V, Cr, Mn, Fe, Ni, Cu, Y, Zr, Mo, W
	Accelerator-driven (Phase-II)	n,p: 1 GeV	H, Pb, Bi
LANL HE	Radiotherapy, Accelerator-driven	n,p: 150 MeV	C, N, O, Al, Ca, Fe, Si, W, Pb
BNL HE	Space Application Accelerator-driven	n,p: 1 GeV	C(10 GeV), Fe, Pb, Bi
ECN HE	Accelerator-driven	n,p: 150 MeV	Fe, Ni
FZK HE	IFMIF	n: 50 MeV	Cr, Fe, V
WIND	Transmutation	n,p: 100 MeV	**n**: U, Np, Pu **p**: U
MENDL-2	Transmutation	n: 100 MeV	505 isotopes

Table 2. Evaluation Methods adopted in High Energy Files (neutron-induced)

	Release	E_{max}(MeV)	Optical Model (neutron)	Decaying Process
JENDL	**C** 96	80	**C**: JLM model	**C**: Adjust Branching Ratios
	Al 98	50	**Al,Fe**:Walter-Gauss fit	**Al,Fe**: Exciton + HF theory
	Fe 98	50		
LANL	**C** 97	150	**C**: Meigooni	**C**: FKK + HF theory
	Al 96	150	**Al**: Petler + Madland	**Al,Fe**:Exciton+MPE+HF theory
	Fe 96	150	**Fe**: Arthur + Madland	(FKK for validation)
BNL	**C** 92	10000	Wood-Saxson fit	**C**: GDH+Evaporation+ INC
	Fe 88	1000		**Fe**: GDH + Evaporation
ECN	**Fe** 97	150	Koning+Deraroche	Exciton + MPE + HF theory
FZK	**Fe** 97	50	Wood-Saxson fit	GDH + MPE + Evaporation (Coalescence pickup)

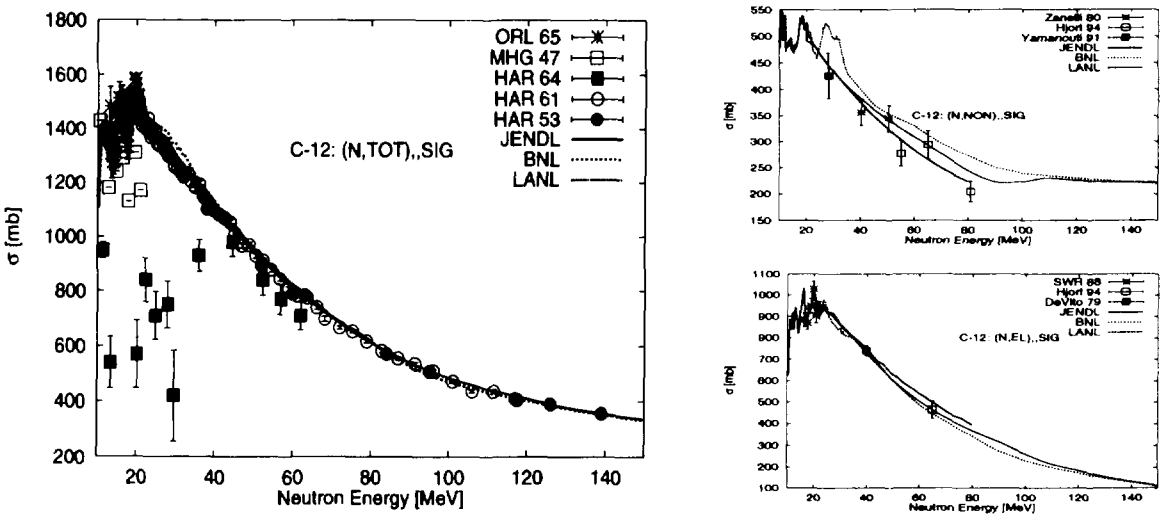

Fig. 1 Carbon : Total, Non-elastic and Elastic Cross Sections

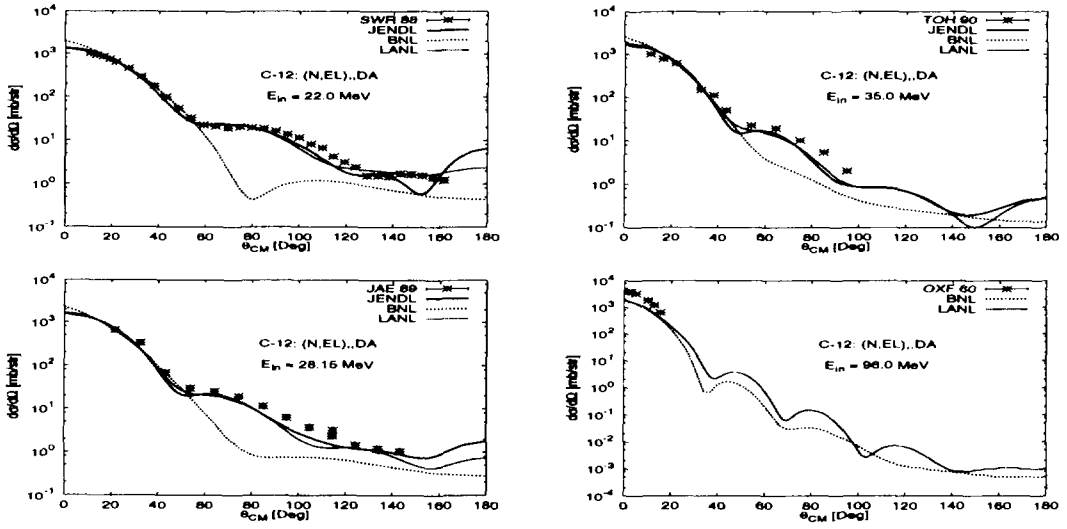

Fig. 2 Carbon : Elastic Angular Distributions

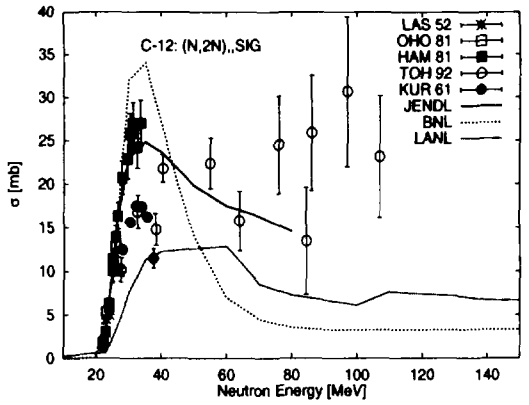

Fig. 3 Carbon: Isotope Production Cross Section : from (n,2n) reaction

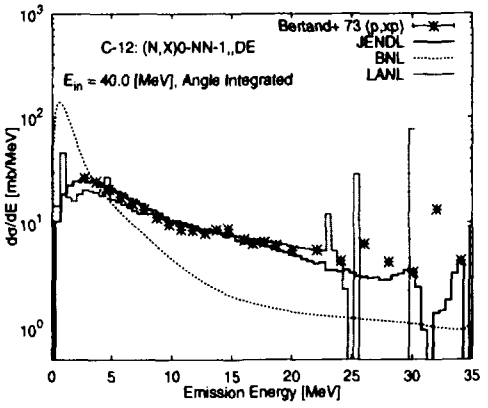

Fig. 4 Carbon: Neutron Emission Spectra

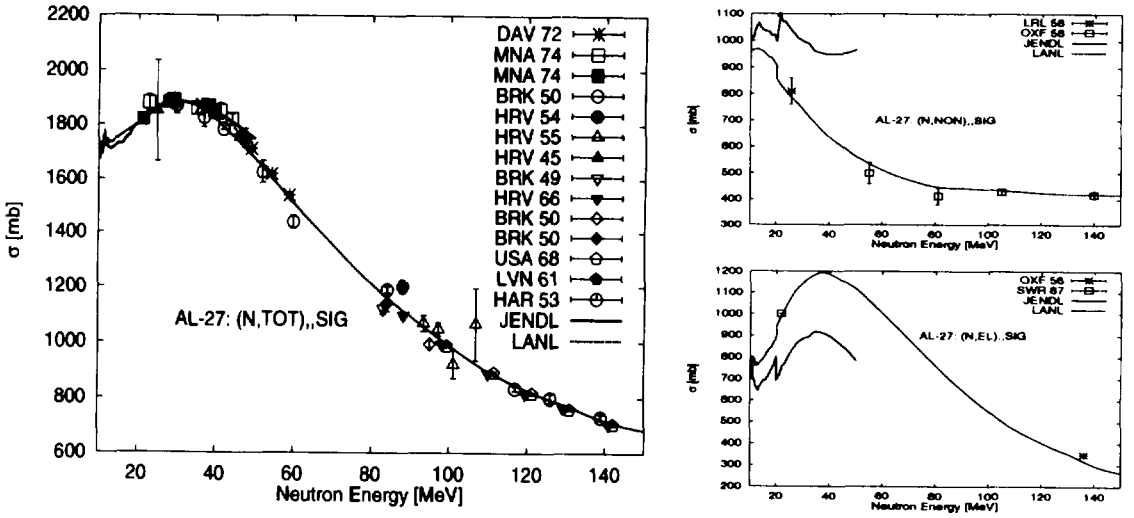

Fig. 5 Aluminium : Total, Non-elastic and Elastic Cross Sections

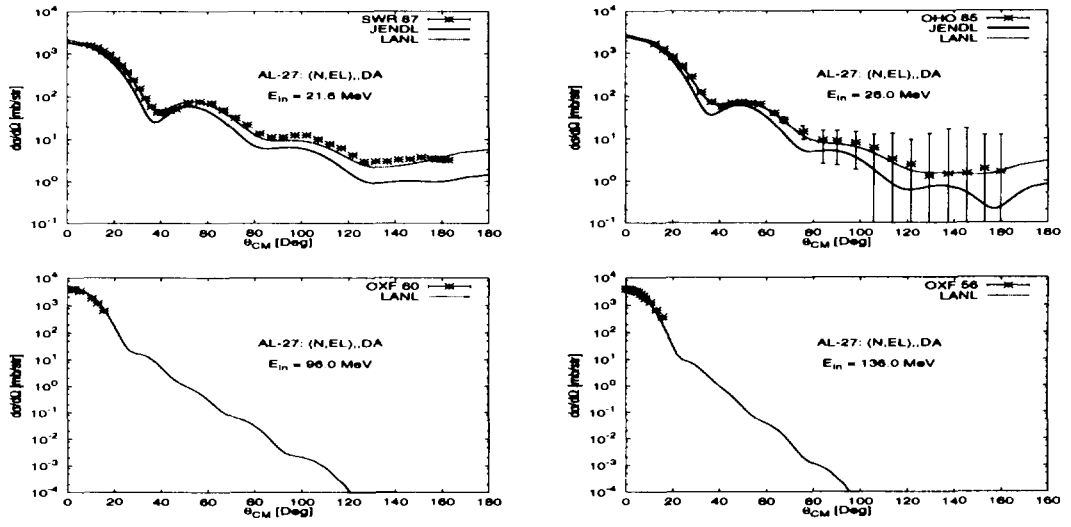

Fig. 6 Aluminium : Elastic Angular Distributions

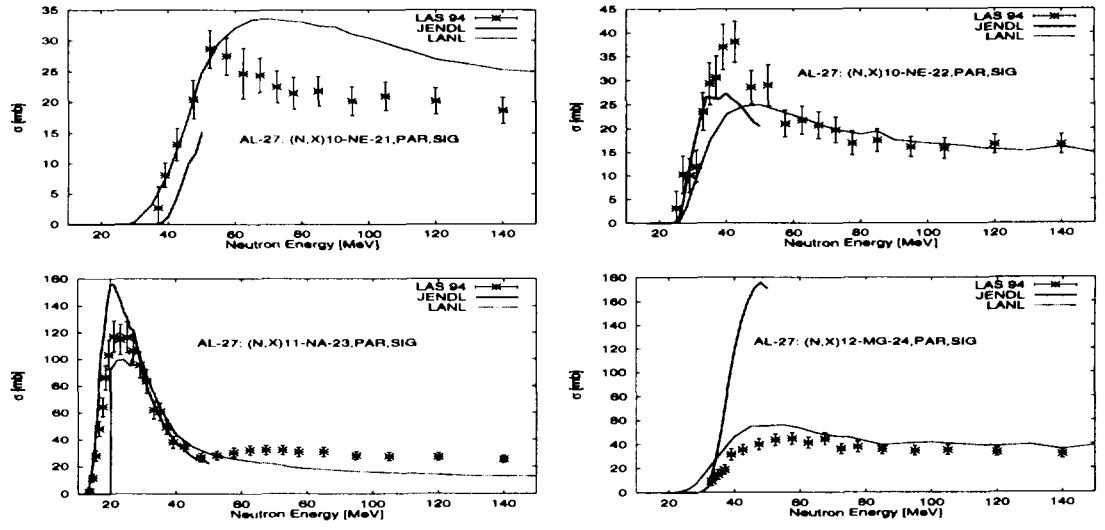

Fig. 7 Aluminium : Isotope Production Cross Sections

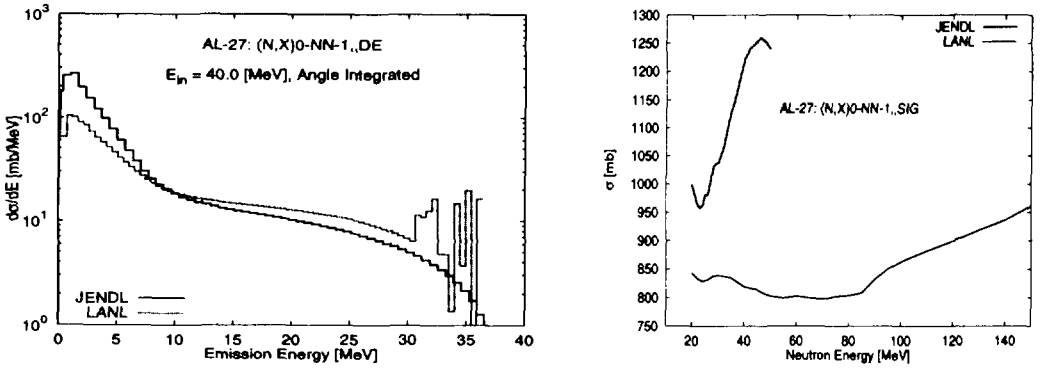

Fig. 8 ALuminium : Neutron Emission Spectra

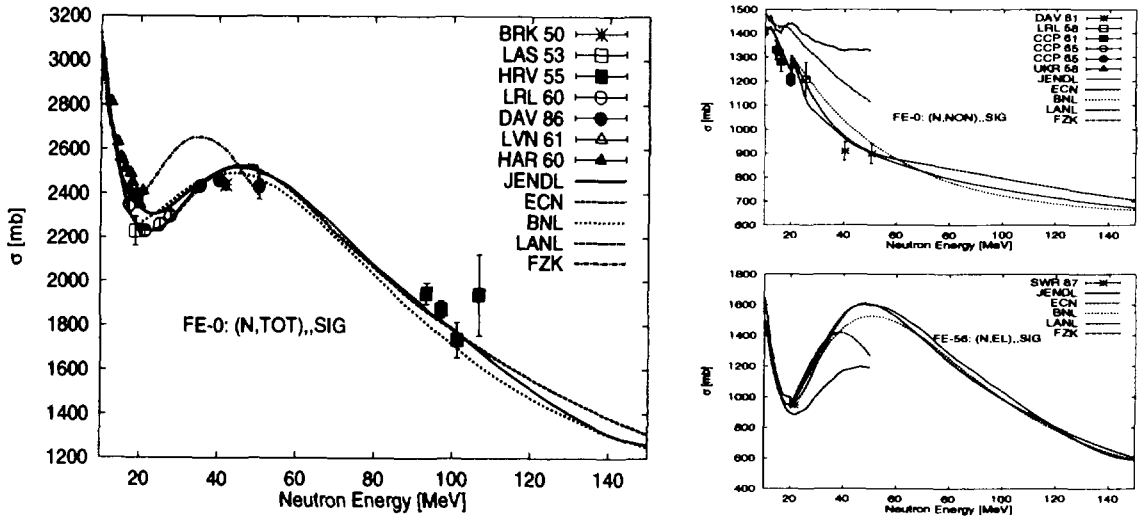

Fig. 9 Iron : Total, Non-elastic and Elastic Cross Sections

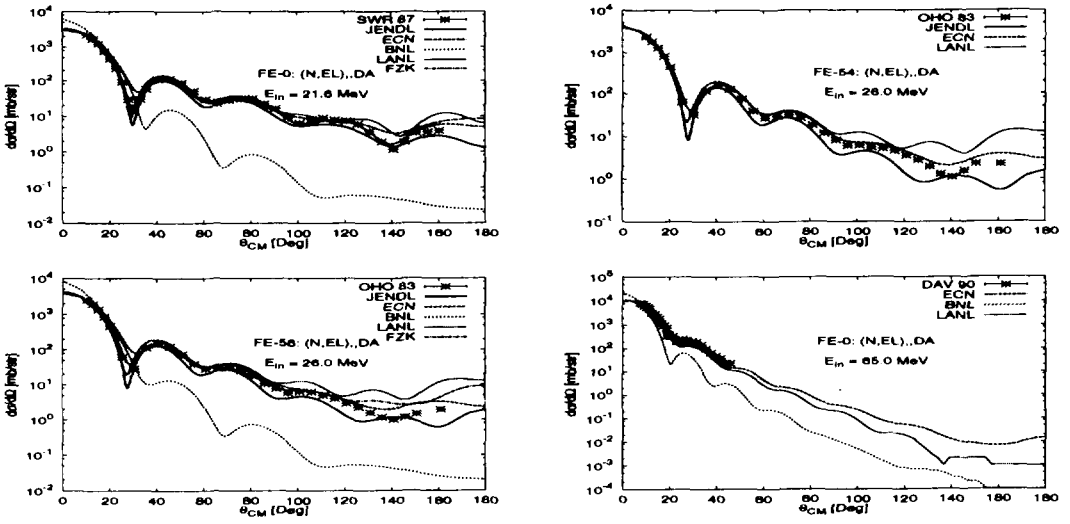

Fig.10 Iron : Elastic Angular Distributions

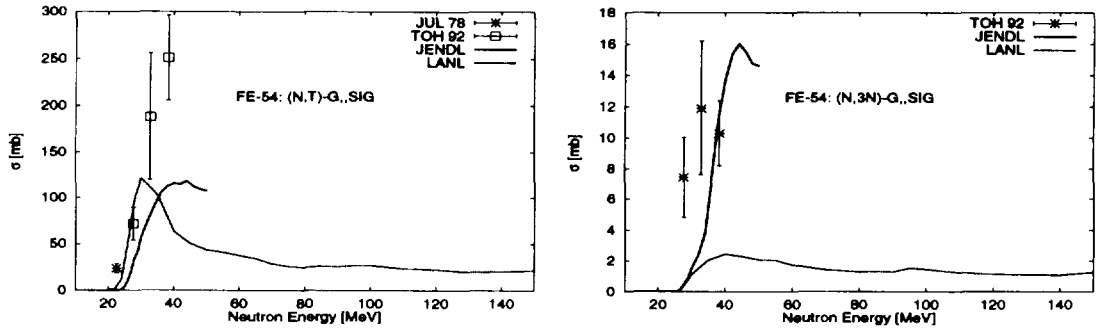

Fig.11 Iron : Isotope Production Cross Sections

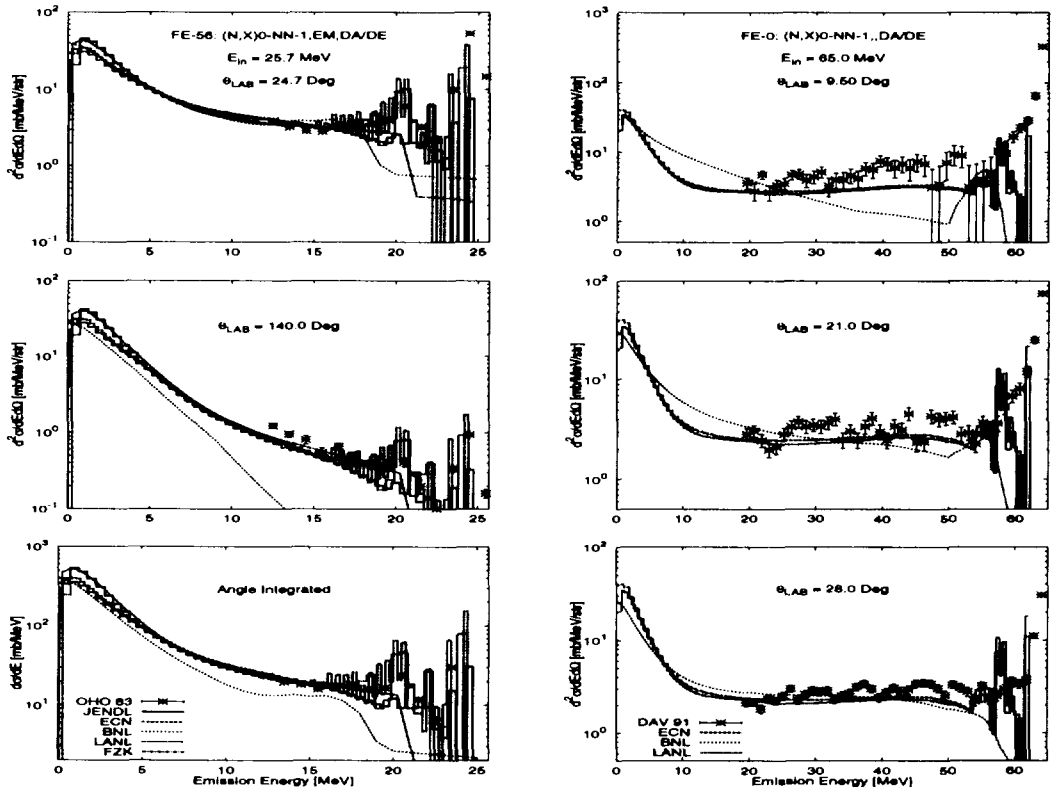

Fig.12 Iron: Neutron Emission DDX

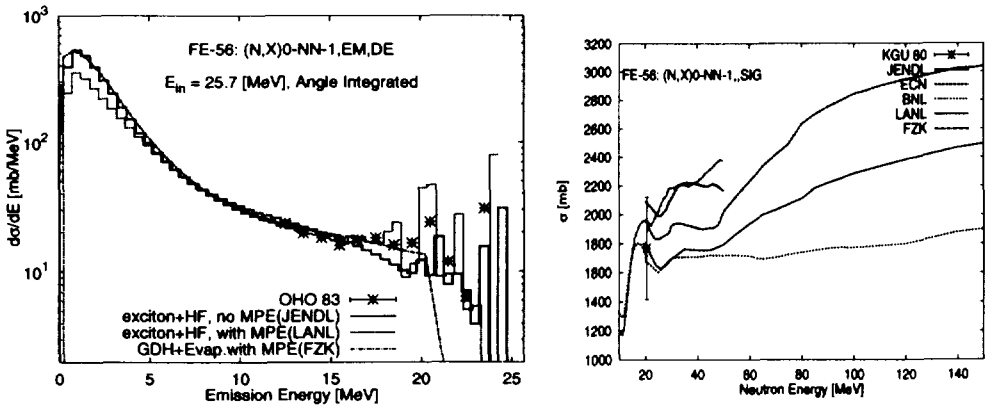

Fig 13 Iron: Neutron Emission DDX and Total Neutron Production Cross Section

6.4 Measurement of neutron-induced fission cross-sections of Th232, U238, U233 and Np237relative to U235 from 1 MeV to 200 MeV

Oleg A. SHCHERBAKOV[1)], Alexander V. FOMICHEV[2)], Andrei Yu. DONETS[2)], Alexander B. LAPTEV[1)], Oleg I. OSETROV[2)], Guennadii A. PETROV[1)]

[1)] *Petersburg Nuclear Physics Institute, 188350, Gatchina, Leningrad district, Russia*
e-mail:scherba@hep486.pnpi.spb.ru
[2)] *V.G. Khlopin Radium Institute, 2-nd Murinski Ave. 28, 194021, St. Petersburg, Russia*

The measurements of neutron-induced cross-section ratios for Th232, U238,U233 and Np237 relative to U235 have been carried out in the energy range from 1 MeV up to 200 MeV using the neutron time-of-flight spectrometer GNEIS based on 1 GeV proton synchrocyclotron. Below 20 MeV, the results of present measurements are roughly in agreement with evaluated data though there are some discrepances to be resolved.

1. Introduction

There is a long standing need in information about fission of heavy nuclei induced by the particles at intermediate energies. Regular experimental studies of fission in this energy region has begun comparatively recently, mainly due to the increased capabilities of modern neutron sources and experimental techniques. Among new applications, the most important are accelerator-driven transmutation of waste reactor materials and energy production, peaceful use of weapon plutonium, accelerator and spaceship shielding, radiation therapy, etc. The solution of these tasks leads to increased requirements on accuracy and reliability of relevant nuclear data which are not fulfilled so far.

At present, the measurements of neutron-induced fission cross-sections for some long-lived actinides in the energy range above 20 MeV with continuous spectrum neutrons are performed only at the WNR/LAMPF facility in Los Alamos [1,2] and the GNEIS facility in Gatchina [3]. Analysis of the experimental data available in the energy range 20-200 MeV, as well as experience in producing evaluated fission cross-sections below 20 MeV, shows that there is a need in new independent measurements aimed to improve fission cross-section data base in the energy range above 20 MeV.

2. Experimental procedure

Fission cross-section ratios for Th232, U238, U233 and Np237 relative to U235 have been measured using the neutron time-of-flight spectrometer GNEIS [4]. This facility is based on the 1 GeV proton synchrocyclotron of PNPI (Gatchina), Fig.1. The water-cooled lead target situated inside the vacuum chamber of the accelerator is used as a pulsed spallation neutron source with average intensity $3 \cdot 10^{14}$ n/s, a burst duration 10 ns and a repetition rate up to 50 Hz. The measurements were performed using a 50-m flight path and neutron beam

contained in an evacuated flight tube. A system of few iron, brass and lead collimators gives the beam diameter of 18 cm at the fission chamber location.

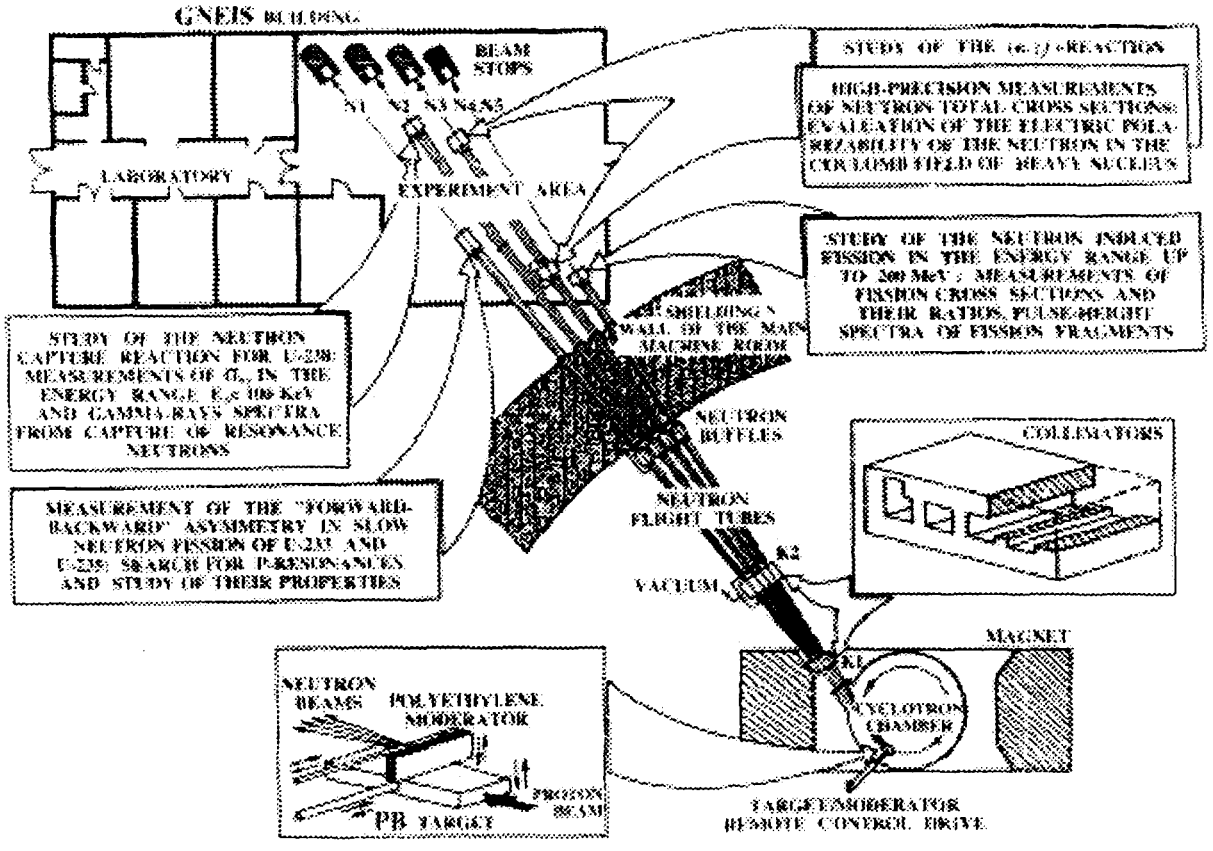

Fig. 1. General layout of the Gatchina neutron time-of-flight spectrometer GNEIS.

The fission reaction rate was measured using a fast parallel plate ionization chamber with electrode spacing 7 mm and filled with methane working gas. The fission chamber held multiplate foils of oxide fission material 200 $\mu g/cm^2$ thick and 18 cm in diameter deposited onto 0.015cm thick aluminum backings. An additional Cf252 deposit was enclosed in the chamber to match the gains of electronics. The distances between the neutron production target and every fission foil were determined using C^{12} neutron transmission resonances. For every isotope under investigation, the time-of-flight and pulse height spectra were accumulated.

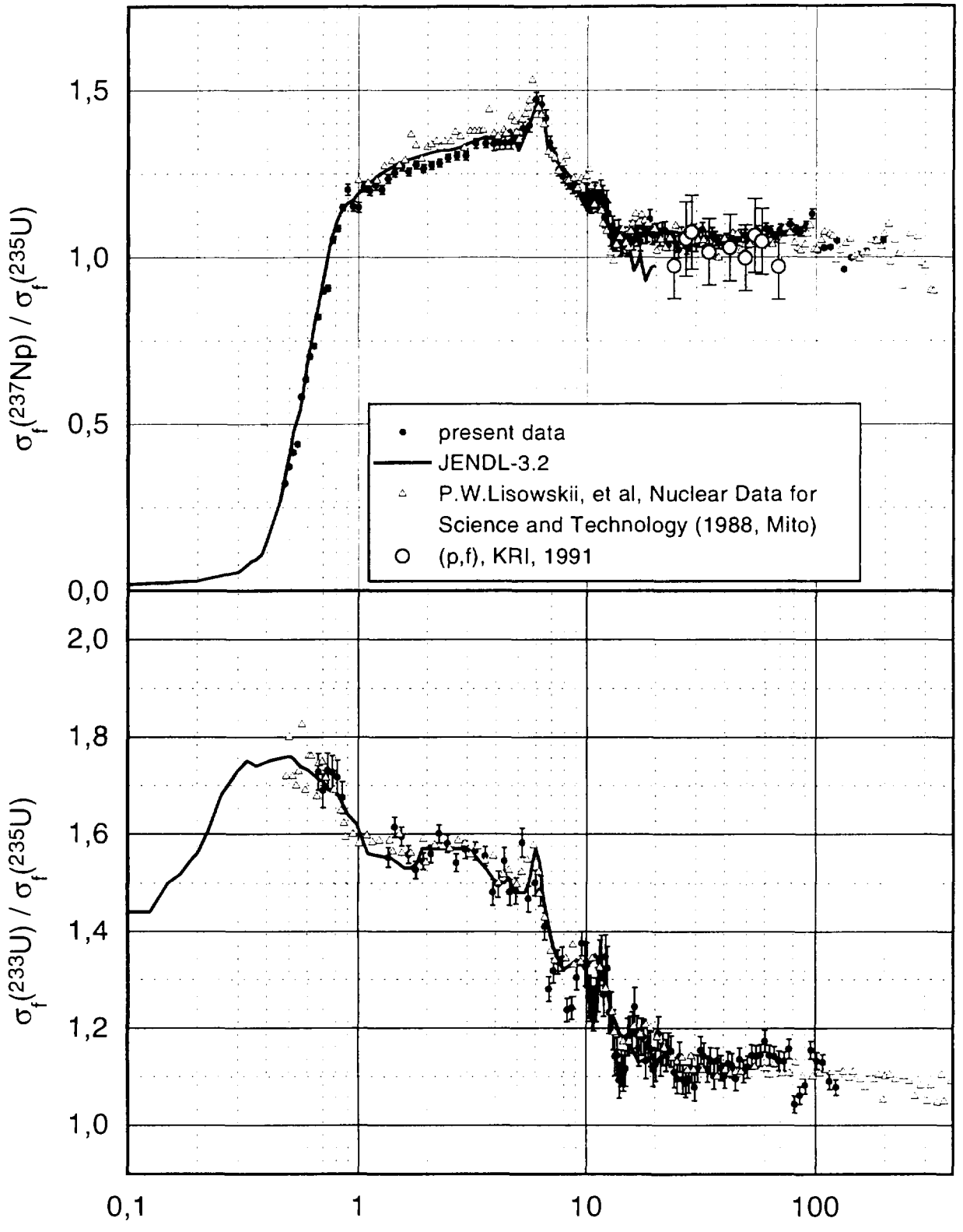

Fig.2. Relative neutron and proton-induced fission cross-section of ^{237}Np and ^{233}U in the energy range below 400 MeV

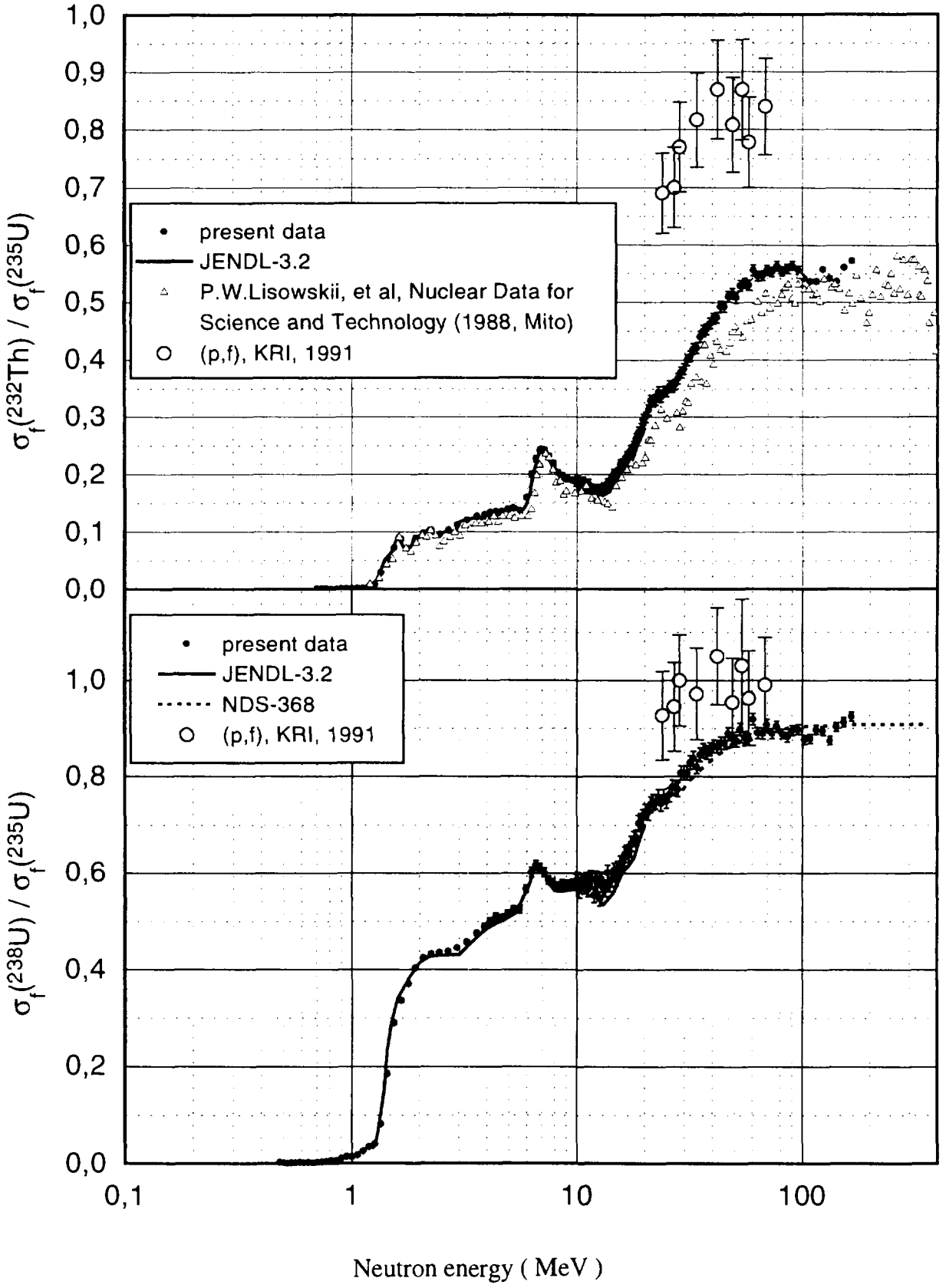

Fig.3. Relative neutron and proton-induced fission cross-section of ^{232}Th and ^{238}U in the energy range below 400 MeV

3. Results and Conclusions

Preliminary results of present measurements are shown in Fig.2,3 for Np237, U233, Th232 and U238, respectively. The error bars represent the statistical errors only (one standard deviation). The solid lines show JENDL-3.2 ratios in the energy range below 20 MeV. Also shown are the data of measurements carried out at the WNR/LAMPF facility in Los-Alamos by P.W. Lisowski et al [1,2].

In general, the comparison of our data with similar results of other authors shows that in the overlapping energy regions (below 20 MeV) our data are roughly in agreement with evaluated data based mainly on the results obtained using electron linacs. There are some discrepances (especially large for Th232) between our and other data which should be resolved. Also, the comparison shows that proton [5] and neutron data are inconsistent, that stimulates elaboration of theoretical model for consistent description of neutron and proton fission cross-sections in the energy range from 20 MeV to 200 MeV.

The measurements described above are planned to be continued and extended to Pu239 and some non-fissile nuclei (W, Pb and Bi) in the course of the ISTC Project 609-97. This work was also supported in part by the Russian Foundation for Basic Research (Grant 96-02-18012).

References

[1] P.W. Lisowski, J.L. Ullmann, S.J. Balestrini, A.D. Carlson, O.A. Wasson, N.W.Hill, Proc. of Int. Conf. on Nuclear Data for Science and Technology, Mito, Japan, May 30-June 3, 1988, p.97.

[2] P.W. Lisowski, A. Gavron, W.E. Parker, S.J. Balestrini, A.D. Carlson, O.A. Wasson, N.W. Hill, Proc. of Int. Conf. on Nuclear Data for Science and Technology, Julich, Germany, May 13-17, 1991. Ed. S.M. Qaim, Springer-Verlag, 1992, p.732.

[3] A.V. Fomichev, I.V. Tuboltseva, A.Yu. Donets, A.B. Laptev, O.A. Shcherbakov, G.A. Petrov, Proc. of Int. Conf. on Nuclear Data for Science and Technology, Julich, Germany, May 13-17, 1991. Ed. S.M. Qaim, Springer-Verlag, 1992, p.734.

[4] N.K. Abrosimov, G.Z. Borukhovich, A.B. Laptev, V.V. Marchenkov, G.A. Petrov, O.A. Shcherbakov, Yu.V. Tuboltsev and V.I. Yurchenko, Nucl. Instr. Meth., A242, 1985, p.121.

[5] A.N. Smirnov, I.Yu. Gorshkov, A.V. Prokofyev, V.P. Eismont, Proc. of Int. Conf on Nucl. Data for Science and Techn., Julich, Germany, May 13-17, 1991, p.751.

6.5 NEUTRON-INDUCED FISSION CROSS SECTIONS OF URANIUMS UP TO 40 MeV

V.M. Maslov*
Radiation Physics & Chemistry Problems Institute, 220109,
Minsk-Sosny, Belarus
e-mail: maslov@sosny.bas-net.by
A. Hasegawa
Nuclear Data Center, Japan Atomic Energy Research Institute,
Tokai-mura, Naka-gun, Ibaraki-ken 319-11
e-mail: hasegawa@cracker.tokai.jaeri.go.jp

Abstract

Statistical theory of nuclear reactions, well-proved below 20 MeV, is applied for ^{235}U and ^{238}U fission data analysis up to ~40 MeV. It is shown that measured data could be reproduced. Chance structure of measured fission cross section is provided, it's validity is supported by description of data for competing (n,xn)-reactions. Role of fissility of target nucleus is addressed. It seems that gap in incident neutron energy interval of 20 MeV - 50 MeV, below which evaluation approaches are well-developed, and above which simplified statistical approaches are valid, could be covered.

1 Introduction

Statistical theory of nuclear reactions, which consistently reproduce fission and (n,xn) reaction data below 20 MeV[1], is applied for ^{238}U and ^{235}U neutron-induced fission data analysis up to 40 MeV incident neutron energy. Calculations with LAHET code system[2] largely overestimate ^{239}Pu/^{235}U neutron-induced fission ratio below 40-50 MeV incident neutron energy. In case of non-fissile target ^{238}U, fission cross sections ratio of ^{238}U/^{235}U is underestimated in the same energy range. For still lower fissility target nuclide ^{232}Th, the consistency of measured and calculated ratios of ^{232}Th/^{235}U is rather poor over the incident neutron energy region of 15-400 MeV. As regards ^{235}U fission cross section itself, it is largely underestimated below 100 MeV in calculations with LAHET, quoted by Lisowski et al.[3]. The discrepancies might be due to usage of Bertini Intranuclear Cascade Model, while it is known that at low energies statistical model codes with preequilibrium emission included, are more justified [4]. A significant difference as compared with STAPRE[5] calculations may arise also due to inconsistent modelling of fission/neutron competition at the evaporation stage of the interaction. Preequilibrium emission, which was not included into LAHET[2] at the time being, also may contribute to the mentioned discrepancies with measured data. .

Previously we have developed a statistical model description of neutron-induced reactions for ^{238}U and ^{235}U up to 20 MeV incident neutron energies. The problem we face at higher

energies is as follows. Do we need any new physics' assumptions at higher incident neutron energies and if not, then up to which energies. Actually we are talking about possible hindrance of fission motion or fission probability and enhanced neutron emission[6]. Note, that only pre-saddle neutron emission might be of any consequence for fission probability. Due to emissive nature of fission process of heavy actinides these effects are not very important at a later stages of emissive cascades. In this respect only non-emissive fission or first-chance fission might be important. However, the contribution of first-chance fission to total fission cross section is decreasing with incident neutron energy due to strong preequilibrium emission of first neutron. Consequently, relevant fission dynamics effects would not be much pronounced in neutron-induced fission of actinides.

It will be demonstrated that measured data trend could be reproduced. Chance structure of measured fission cross section would be provided, validity of observed fission cross section partitioning being supported by description of data for competing (n,xn)-reactions. Role of the fissility of target nucleus is emphasized. It seems that "gap" in incident neutron energies of 20MeV - 50 MeV, above which might be applied statistical approach of ALICE[7] code or LAHET code system at still higher energies is valid, could be covered.

2 THE STATISTICAL MODEL

Hauser-Feshbach statistical model code STAPRE[5] was used for fission data analysis after some modifications. For calculations to be accomplished, the following procedure should be pursued. First, level density parameters are defined, using neutron resonance spacing $\langle D_{obs} \rangle$ estimates for ^{232}U, ^{233}U, ^{234}U, ^{235}U, ^{236}U, ^{237}U and ^{238}U target nuclides. Constant temperature level density parameters T_o, E_o, U_c are defined by fitting cumulative number of low-lying levels. Then fission cross sections ^{232}U, ^{233}U, ^{234}U, ^{235}U, ^{236}U, ^{237}U and ^{238}U target nuclides should be calculated up to emissive fission threshold to extract fission barrier parameters. After that total, reaction and direct excitation cross sections of ground state band levels up to 40 MeV are calculated, meanwhile, neutron transmission coefficients $T_l(E)$ for the code STAPRE are obtained. At last, cross sections up to 40 MeV are calculated. Basically that is just extension of traditional statistical approach up to 40 MeV.

2.1 Optical model

A coupled channels optical model is adopted for calculation of the reaction cross section of target nuclide ^{238}U. The direct excitation of ground state rotational band levels 0^+-2^+-4^+-6^+ was estimated within rigid rotator model using the following optical potential parameters:

$$V_R = 46.29 - 0.3E, MeV, r_R = 1.26\ fm, a_R = 0.63\ fm$$

$$W_D = \begin{cases} 2.92 + 0.4E, MeV, & E \leq 10 MeV. r_D = 1.26\ fm, a_D = 0.52\ fm \\ 6.92\ MeV, & E > 10\ MeV \\ 6.92 - 0.046(E - 20), MeV & E > 20\ MeV \end{cases}$$

$$V_{SO} = 6.2\ MeV, r_{SO} = 1.12\ fm, a_{SO} = 0.47\ fm.$$

This potential parameters were obtained from the analysis of neutron total cross section data, angular distribution data up to 20 MeV incident neutron energy and neutron strength functions [8]. Figure 1 shows the description of total cross section data up to 40 MeV. Figure 2 shows the comparison of reaction cross sections, calculated with different coupled channels optical potentials. In the optical potential, proposed by Young [9] there is a relatively small volume absorption term. It influences total cross section data fit, but changes drastically the reaction cross section shape above ~10 MeV. We argue that adding volume absorption term one faces severe problems with consistent description of fission and (n,xn) reaction cross section data just above 10 MeV incident neutron energy. To follow the fission data trend above 20 MeV, we should introduce instead additional decrease of imaginary potential term W_D.

Due to high fission threshold in case of ^{238}U+n interaction at $E_n \leq 5$ MeV, the main contribution to inelastic scattering comes from the compound processes. For ground state band levels the direct and compound components became comparable above 1.5-2 MeV. The direct excitation cross section of ground state rotational band levels 0^+-2^+-4^+-6^+ changes very smoothly above 20 MeV, decreasing from ~0.3 b to ~0.25 b at 40 MeV. Another direct component is due to excitation of octupole and quadrupole band levels. To calculate the direct excitation cross sections for γ-vibration ($K^\pi = 2^+$) as well as octupole ($K^\pi = 0^-$) band levels one needs a soft rotator model [10]. In a soft rotator model, e.g. deformed non-axial, soft to quadrupole vibrations rotor, collective states structure up to 3 MeV excitation energy was described [10].As regards γ-vibration and octupole band levels, the direct component contribution never exceeds ~20 mbarns above 10 MeV[8]. So we ignored the direct excitation of levels other than ground state band levels above 20 MeV.

2.2 Fission Channel

We proceed within double-humped fission barrier model. The detailed description of the statistical model involved is given elsewhere[1, 11]. Analyzing neutron-induced fission data in a double humped fission barrier model, fission process can be viewed as a two-step process, i.e. a successive crossing over the inner hump A and over the outer hump B. Hence, the transmission coefficient of the fission channel $T_f^{J\pi}(U)$ can be represented as

$$T_f^{J\pi}(U) = \frac{T_{fA}^{J\pi}(U) T_{fB}^{J\pi}(U)}{(T_{fA}^{J\pi}(U) + T_{fB}^{J\pi}(U))}. \tag{1}$$

The transmission coefficient $T_{fi}^{J\pi}(U)$ is defined by the level density $\rho_{fi}(\varepsilon, J, \pi)$ of the fissioning nucleus at the inner and outer humps (i = A,B, respectively):

$$T_{fi}^{J\pi}(U) = \sum_{K=-J}^{J} T_{fi}^{JK\pi}(U) + \int_0^U \frac{\rho_{fi}(\epsilon, J, \pi) d\varepsilon}{(1 + \exp(2\pi(E_{fi} + \epsilon - U)/\hbar\omega_i))}, \tag{2}$$

where the first term denotes the contribution of low-lying collective states and the second term that from the continuum levels at the saddle deformations, ε is the intrinsic excitation energy of fissioning nucleus. The total level density $\rho_{fi}(\epsilon, J, \pi)$ as well as collective states

spectra of the fissioning nucleus is determined by the order of symmetry of nuclear saddle deformation.

Inner and outer fission barrier heights and curvatures as well as level densities at both saddles are the model parameters. They are defined by fitting fission cross section data at incident neutron energies below emissive fission threshold. Fission barrier height values and saddle order of symmetry are strongly interdependent. The order of symmetry of nuclear shape at saddles was defined by Howard & Möller[12] within shell correction method (SCM) calculation. We adopt the saddle point asymmetries from SCM calculations. These saddle asymmetries depend on Z and N of the fissioning nucleus. According to shell correction method (SCM) calculations of Howard and Möller [12] the inner barrier was assumed axially symmetric in case of U compound systems with $A \leq 236$ and asymmetric for $A > 236$. This helps to interpret the non-threshold fission cross section behavior of ^{232}U(n,f)[13] assuming a lowered height of axially symmetric inner hump of ^{233}U, as anticipated by Howard & Möller[12] with SCM calculations. Outer barrier for uranium nuclei is assumed mass-asymmetric.

2.3 Level Density

The total nuclear level density is represented as the factorized contribution of quasiparticle and collective states. The collective contribution of the level density of deformed nuclei at saddles and ground state deformations is defined by the deformation order of symmetry. Once again, we adopt the saddle point asymmetries from SCM calculations by Howard & Möller[12], while ground state deformations are assumed to be quadrupole.

Level densities were calculated with a phenomenological model by Ignatyuk et al. [14], which takes into account the shell, pairing and collective effects in a consistent way

$$\rho(U, J, \pi) = K_{rot}(U, J) K_{vib}(U) \rho_{qp}(U, J, \pi), \tag{3}$$

where $\rho_{qp}(U, J, \pi)$ is the quasiparticle level density and $K_{rot}(U, J)$ and $K_{vib}(U)$ are factors of rotational and vibrational enhancement of the level density. The relation (3) holds in an adiabatic approximation, when collective and intrinsic excitation contributions to the total level density $\rho(U, J, \pi)$ factorize. The quasiparticle level density $\rho_{qp}(U, J, \pi)$ is defined as follows

$$\rho_{qp}(U, J, \pi) = \frac{(2J+1)\omega_{qp}(U)}{4\sqrt{2\pi}\sigma_{\perp}^2 \sigma_{\parallel}} \exp\left(-\frac{J(J+1)}{2\sigma_{\perp}^2}\right). \tag{4}$$

Fission and (n,xn) reaction cross section description near thresholds needs a modification of level density Eq.(3) at low excitation energies. The modelling of total level density at low excitation energies in a constant temperature approximation

$$\rho(U) = K_{rot}(U) K_{vib}(U) \frac{\omega_{qp}(U)}{\sqrt{2\pi}\sigma} = T^{-1} \exp((U - U_o)/T) \tag{5}$$

looks like a simple renormalization of quasi-particle state density $\omega_{qp}(U)$. Here, $\sigma^2 = F_{\parallel} t$ is the spin distribution parameter, t is thermodynamic temperature, $F_{\parallel} = 6/\pi^2 < m^2 >$

$(1 - 2/3\varepsilon)$, where $< m^2 >$ is the average value of the squared projection of the angular momentum of the single-particle states, and ε is quadrupole deformation parameter. Further modification of the level density is related to few-quasiparticle effects which are due to pairing correlations. They are essential for state density calculation at low intrinsic excitation energies either for equilibrium and saddle deformations and influence fission cross section description below ~3 MeV incident neutron energy. The outcome of this level density model sophistication is rather precise description of fission cross section below emissive fission threshold. In case of ^{238}U(n,f) reaction a "cusp" around 2-4 MeV is reproduced[15].

For deformed axially symmetric nucleus

$$K_{rot}(U) = \sigma_{\perp}^2 = F_{\perp} t \tag{6}$$

where $\sigma_{\perp}^2$ is the spin cutoff parameter, $F_{\perp}$ is the nuclear momentum of inertia (perpendicular to the symmetry axis), which equals the rigid-body value at high excitation energies, where the pairing correlations are destroyed, experimental value at zero temperature and is interpolated in between, using the pairing model.

For triaxially asymmetric nuclides the rotational enhancement factor is

$$K_{rot}(U) = 2\sqrt{2\pi}\sigma_{\perp}^2\sigma \ . \tag{7}$$

The closed-form expressions for thermodynamic temperature and other relevant equations which one needs to calculate $\rho(U, J, \pi)$ are provided by Ignatyuk et al. model [14]. We assume no washing out of collective density enhancement, since extension of calculations above emissive fission threshold does not imply that.

The main parameter of the level density a was obtained by fitting the neutron resonance spacing. The neutron resonance spacings $< D_{obs} >$ for $^{232-238}$U were obtained using a method, which takes into account the correlation of weak resonance missing and resonance missing due to poor experimental resolution [16].

The shell correction dependence of $a-$parameter is defined using the following equation [14]:

$$a(U) = \begin{cases} \tilde{a}(1+ \delta W f(U - E_{cond})/(U - E_{cond})), & U > U_{cr} = 0.47 a_{cr}\Delta^2 - m\Delta \\ a(U_{cr}) = a_{cr} & U \leq U_{cr} = 0.47 a_{cr}\Delta^2 - m\Delta, \end{cases} \tag{8}$$

here $m = 0,1,2$ for even-even, odd-A and odd-odd nuclei, respectively; $f(x) = 1 - exp(-\gamma x)$, is the dimensionless function, defining the shell effects dumping; condensation energy $E_{cond} = 0.152 a_{cr}\Delta^2$, where Δ is the correlation function, $\tilde{a}$ is the asymptotic a-parameter value at high excitation energies. We assume that $\tilde{a}$-values for equilibrium and saddle deformations are equal. That means, that a_f/a_n ratio of fissioning and residual nuclei is solely dependent upon respective shell correction values of δW.

The parameters of the level density model for inner and outer saddles and equilibrium deformations are as follows: shell correction δW, pairing correlation functions Δ and Δ_f, at equilibrium deformations $\Delta = 12/\sqrt{A}$, quadrupole deformation ε and momentum of inertia at zero temperature $F_o/\hbar^2$ are given in Table 1. For ground state deformations the shell corrections were calculated as $\delta W = M^{exp} - M^{MS}$, where M^{MS} denotes liquid drop mass

(LDM), calculated with Myers-Swiatecki parameters [17], and M^{exp} is the experimental nuclear mass.

Table 1

Level density parameters of fissioning nucleus and residual nucleus

Parameter	inner saddle	outer saddle	neutron channel
δW, MeV	2.5*	0.6	LDM
Δ, MeV	$\Delta_o + \delta^{**}$	$\Delta_o + \delta^{*}$	Δ_o
ε	0.6	0.8	0.24
$F_0/\hbar^2$, MeV^{-1}	100	200	73

**) for axially asymmetric deformations, 1.5 MeV for axially symmetric deformations;
*)$\delta = \Delta_f - \Delta$ value is defined by fitting fission cross section in the "plateau" region.

3 Cross sections above emissive fission threshold

At higher incident neutron energies when fission reaction of A, A-1, ... compound nuclei, where A is the mass number of target nucleus, is possible after emission of 1,2, ...x neutrons, the observed fission cross section is a superposition of x-chance fission contributions. These contributions are weighted with a probability of 1,2, ...x neutron emission before fission. The fission cross section of (A+1) compound nucleus is called first-chance fission. For fixed statistical model parameters of residual nuclei A, $A-1$...fissioning in (n,nf), $(n,2nf)$ ... reactions, the behavior of the first-chance fission cross section σ_{f1} should make it possible to reproduce the measured fission cross section σ_f. A consistent description of a most complete set of measured data on the (n,f), $(n,2n)$ and $(n,3n)$ reaction cross sections for the ^{238}U target nuclide up to 22 MeV enables one to consider the estimates of σ_{f1} and of the fission probability of the initial compound nuclei ^{239}U as fairly realistic.

Fission cross section of ^{238}U, shown on the Fig.3 demonstrates a step-like structure, relevant to contribution of (n,xnf) reactions to total fission cross sections for x=1,2,3,4. At higher energies this kind of structure appears to be smeared out, contribution of (n,5nf) reaction being relatively small. However, observed fission cross section remains lower than reaction cross section by ~15%. That means neutron emission competition is strong enough even at that high incident neutron energies.

Fission cross section of ^{235}U, shown on the Fig.4 demonstrates a step-like structure, relevant to contribution of (n,xnf) reactions to total fission cross sections only for x = 1,2,3. In other words, with increasing fissility of target nucleus the smearing of step-like structure occurs at lower incident neutron energies. At 40 MeV incident neutron energy fission cross section of ^{235}U almost approaches reaction cross section value, estimated mainly with ^{238}U scattering data.

3.1 Pre-equilibrium contribution of secondary neutron spectra

The hard component of neutron scattering spectra and high energy tail of $^{238}U(n,2n)$ reaction cross section are interpreted as being due to the pre-equilibrium evaporation of neutrons. This feature is parameterized within a conventional exciton model, used in STAPRE code. By fitting the spectra for $E_n = 6-14.7\ MeV$ we get the main parameter of the exciton model, that is the matrix element $M^2 = 10/A^3$, at $E_n \geq 20$ MeV we assume $M^2 = 250/(EA^3)$. Note that, when calculating the exciton state density, the odd-even back-shift is introduced: $\hat{U} = U - \Delta(2 - n)$. The charge conservation and transition rates renormalization were also employed. With all that in mind and in the STAPRE code a pre-equilibrium emission fraction $q(E)$ leading to depletion of compound nucleus states population is obtained, which approaches ~0.95 at $E_n = 40$ MeV. Largely by diminishing the odd-even dependence of $q(E)$ we can fit the ^{235}U fission data with the same M^2 value. These reasonable model fits give rather strong grounds to consider the estimate of contribution of first neutron pre-equilibrium emission $q(E)$ as fairly realistic. They were used also for interpreting the experimental evidence of preequilibrium neutron emission prior to fission, induced by 14.7 MeV neutrons[18].

3.2 Shell effects in first chance fission cross section

The behavior of the first-chance fission cross section σ_{f1} is obviously related with the energy dependence of the first-chance fission probability of the $A+1$ nucleus P_{f1}:

$$\sigma_{f1} = \sigma_c(1 - q(E))P_{f1}. \tag{9}$$

Once the $q(E)$ value is fixed, the first-chance fission probability P_{f1} of the ^{239}U compound nuclide depends only on the level density parameters of fissioning and residual nuclei. That is the ratio of shell correction values $\delta W_{fA(B)}$ and δW_n. The results of different theoretical calculations of the shell corrections as well as of the fission barriers vary by $1 \sim 2\ MeV$. The same is true for the experimental shell corrections, which are calculated with a smooth component of potential energy chosen according to the liquid-drop or droplet model. However the isotopic changes of $\delta W_{fA(B)}$ and δW_n [19] are such that P_{f1} as a function of the difference $(\delta W_{fA(B)} - \delta W_n)$ is virtually independent on the choice of smooth component of potential energy. In addition, existing calculations of the shell corrections do not allow for the influence of the asymmetric deformations on the smooth component of potential energy. Therefore we shall consider the adopted $\delta W_{fA(B)}$ estimates (see Table 1) to be effective, provided that δW_n are obtained with the liquid drop model. The trend of the first-chance fission cross section σ_{f1}shown in Figs. 3,4 could be treated as a manifestation of the shell effects in first-chance fission probability. So it can be stated safely that we have got effective estimates of σ_{f1} which corresponds to best fit of $(n,2n)$, $(n,3n)$ and $(n,3n)$ reaction cross sections.

3.3 (n,xn) reaction cross sections

Estimates of (n,n'), (n,2n), (n,3n), (n,4n) and (n,5n) reaction cross sections for ^{238}U are presented on Fig.5. Note, that for x $\leq$ 3 calculated curves fit available measured data pretty

well[20]. Measured data are indicated only for (n,4n) reaction to demonstrate reasonable trend of calculated curve. The same is the case for ^{235}U target nuclide for (n,2n) and (n,3n) reaction cross sections. The discrepancy occurs in case of (n,4n) reaction. To fit data by Veeser[21] for ^{235}U one should change drastically level density parameters of residual nuclide ^{232}U, which seems unjustified. The important point is that (n,xn) reaction cross sections exhibit a decreasing trend of respective peak values at x > 1 either for ^{238}U and ^{235}U.

3.4 Proton-induced fission

It might be assumed that proton-induced fission is not much different from that of neutron-induced fission at projectile energies of 40 MeV. However above emissive fission threshold relative contribution of non-emissive fission to total fission cross section should be taken into account. Figure 7 shows first chance fission contribution to the observed fission cross section. Description of charge exchange reaction ^{238}U(p,n) and ^{238}U(n,3n)^{236s}Np cross sections[22] might be considered as validation of the consistency of the statistical approach employed. We can compare the contributions of first chance fission to the measured fission cross section of compound nuclide ^{239}Np for proton- and neutron-induced fission. Fission barriers of Np nuclei were obtained by fitting ^{237}Np(n,f) data up to 20 MeV incident neutron energy. Figure 8 shows that in case of proton-induced fission contribution of non-emissive fission to total fission cross section is higher than in case of neutron-induced fission. Specifically, above (n,2nf) reaction threshold difference amounts to 50%. That means that at the same excitation energies the ratios of symmetric to asymmetric fission yields Y_S/Y_A would be rather different. That should be obviously taken into account when using proton-induced fission yields for "extracting" neutron-induced fission yields. First chance fission contribution for ^{238}U(n,f) reaction is not much different from that of ^{237}Np(n,f) reaction. That means it is more sensitive to entrance channel, than fission probabilities of involved nuclei.

4 Conclusions

The statistical Hauser-Feshbach model calculation of neutron-induced reaction for ^{238}U and ^{235}U target nuclides show the fair description of available data base on fission and neutron emission cross sections. The rigid rotator coupled channel model gives fair description of total cross section data up to 30 MeV incident neutron energy.

The transparent statistical model approach gives fair description of the measured data base. It seems that the potential of the statistical theory to provide estimates of actinide fission cross sections up to 40 MeV incident neutron energy is far from exhausted. It seems also, that evaporation/fission mechanism is valid in this excitation energy range. That means that we can apply current approach for other actinide target nuclei at incident neutron energies up to 40 MeV.

*) JAERI' visiting scientist, research was partly supported by International Atomic Energy Agency under the Contract 9837/RO.

References

[1] Maslov V.M., Kikuchi Y., JAERI-Research 96-030, 1996

[2] Prael R.E. Proc. Int. Symp. Nuclear Data Evaluation Methodology, Brookhaven,USA, October 12-16, 1992, p.525. World Scientific, 1993.

[3] Lisowski P.W., Gavron A., Parker W.E. et al. Proc. Specialists' Meeting on Neutron Cross Section Standards for the Energy Region above 20 MeV, Uppsala, Sweden, May 21-23, 1991, p. 177, OECD, Paris, 1991.

[4] Fukahori T., Chiba S., Proc. Second Specialists' Meeting on High Energy Nuclear Data, JAERI, Tokai, Japan, January 26-27,1995, p.46, JAERI-Conf, 95-016, 1995.

[5] Uhl M., Strohmaier B., IRK-76/01, IRK, Vienna (1976).

[6] Hilscher D. and Rossner H. Ann. Phys. Fr., 17, 471 (1992).

[7] Blann M. et al., UCRL-JC-109052 (1992).

[8] Porodzinskij Yu.V., Private communication.

[9] Young P.G., INDC(NDS)-335, p.109 (1994).

[10] Porodzinskij Yu.V., Sukhovitskij E.Sh, Yadernaya Fyzika, 59, 247 (1996).

[11] Ignatjuk A.V., Maslov V.M., In: [2] p.440.

[12] Howard W.M., Möller P. Atomic Data and Nuclear Data Tables,25, 219 (1980).

[13] Maslov V.M., Kikuchi Y. Nucl. Sci. Eng. 124, 492 (1996).

[14] Ignatjuk A.V., Istekov K.K., Smirenkin G.N. Sov. J. Nucl. Phys. 29, 450 (1979).

[15] Maslov V.M. Int.Conf. Nucl. Data for Sci. and Techn., Trieste, Italy, May 19-23, 1997.

[16] Porodzinskij Yu.V., Sukhovitskij E.Sh., Maslov V.M. , Ibid.

[17] Myers W.O., Swiatecky W.J., Ark. Fyzik, 36, 243 (1967).

[18] Boykov G.S., Dmitriev V.D., Kudyaev G.A., Maslov V.M., et al., Ann. Nucl. Energy, 10, 585 (1994).

[19] Bjornholm S., Lynn J.E. Rev. Mod. Phys., 52, 725 (1980).

[20] Maslov V.M. et al., to be published.

[21] Veeser L.R., Arthur E.D., Neutron Physics and Nuclear Data, OECD, Harwell, 1054 (1978).

[22] Maslov V.M. At. Energy, 69, 252 (1990).

^{238}U TOTAL CROSS SECTION

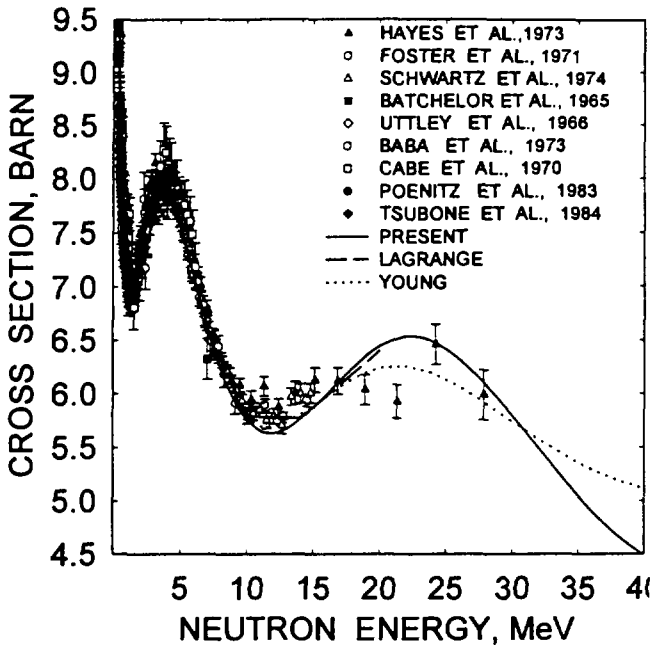

FIG. 1

^{238}U: REACTION CROSS SECTION

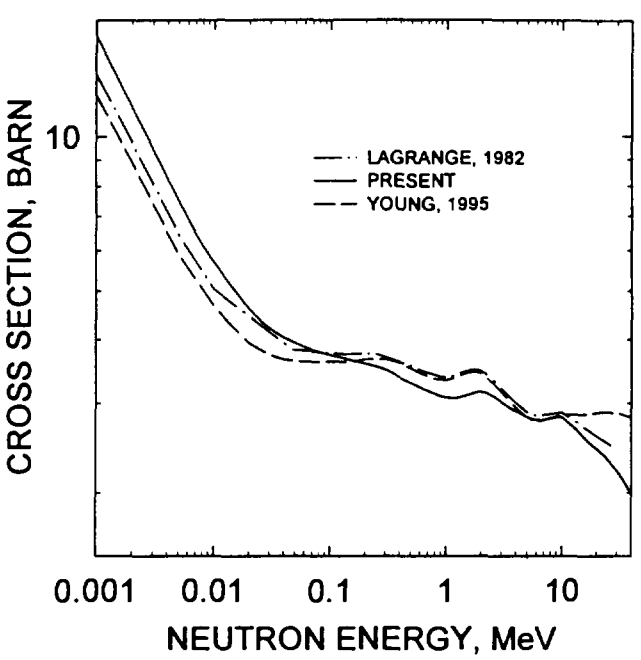

FIG. 2

^{238}U FISSION CROSS SECTION

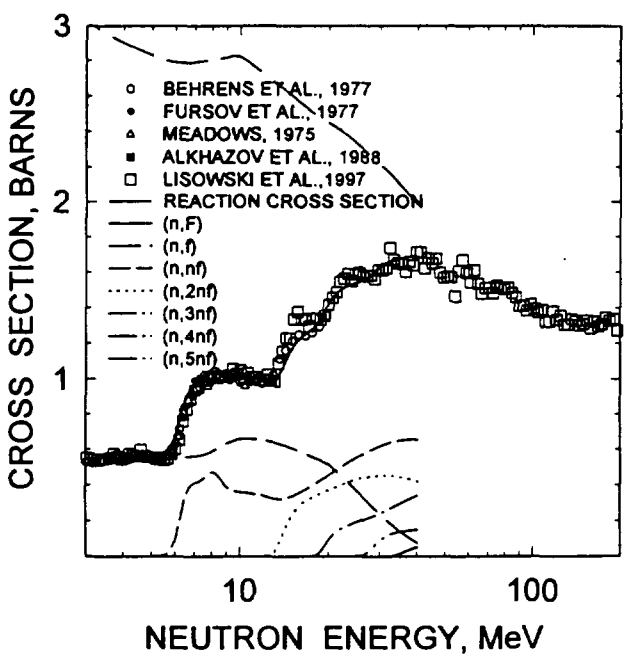

FIG. 3

^{235}U FISSION CROSS SECTION

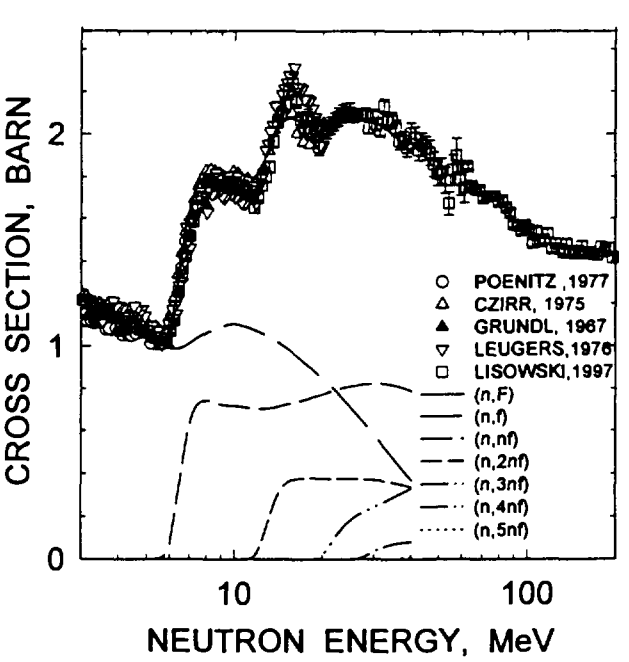

FIG. 4

^{238}U(n,xn) CROSS SECTION

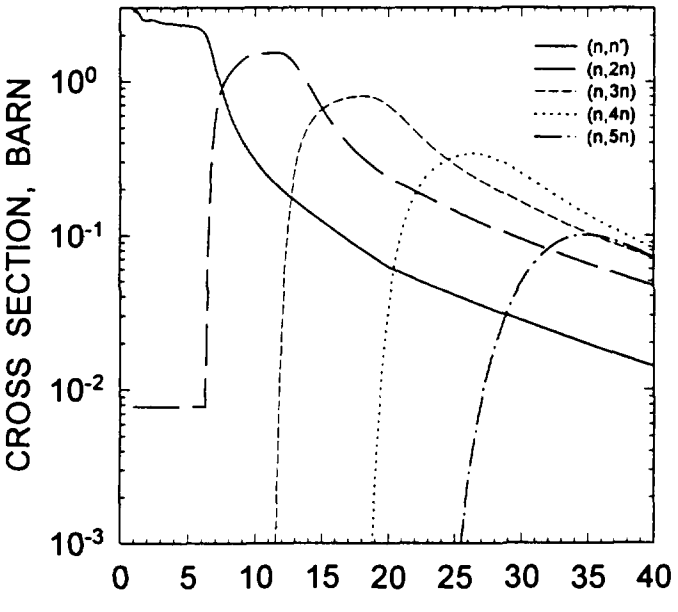

FIG. 5

^{235}U(n,xn) CROSS SECTION

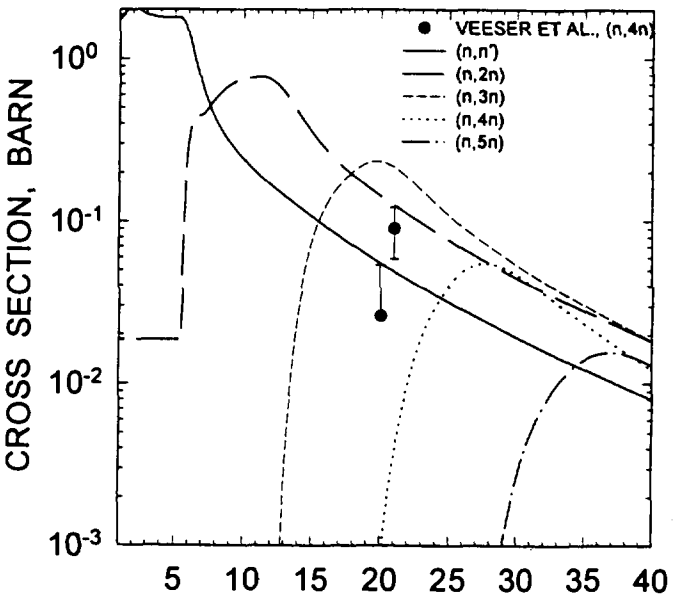

FIG. 6

^{238}U(p,f) CROSS SECTION

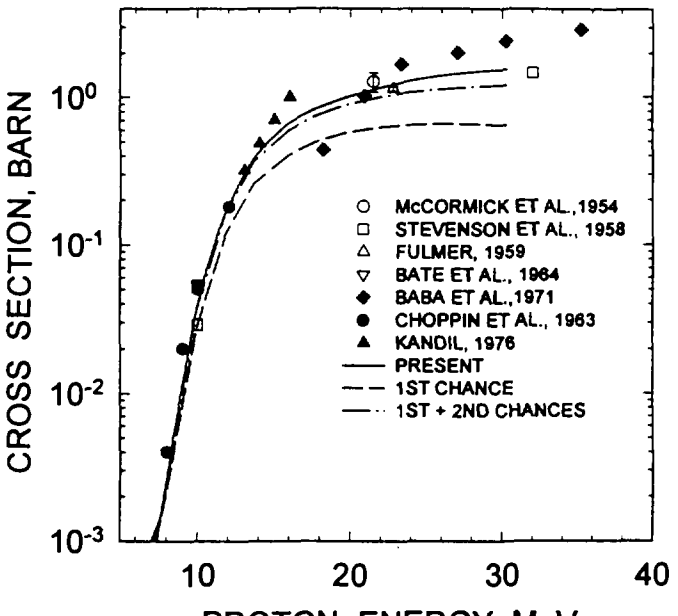

FIG. 7

FIRSTCHANCE FISSION CONTRIBUTION

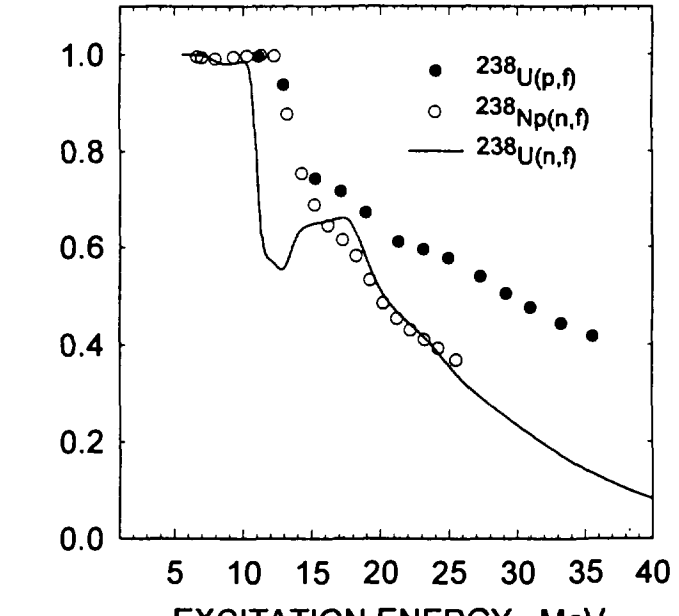

FIG. 8

6.6 Experimental and Computer Simulation Study of Radionuclide Yields in the ADT Materials Irradiated with Intermediate Energy Protons

Yu. E. TITARENKO, O. V. SHVEDOV, V. F. BATYAEV, E. I. KARPIKHIN, V. M. ZHIVUN, A. B. KOLDOBSKY, M. M. IGUMNOV, I. S. SKLOKIN, R. D. MULAMBETOV, A.N. SOSNIN
Institute for Theoretical and Experimental Physics
B.Cheremushkinskaya 25, 117259 Moscow, Russia
e-mail: titaren@vitep5.itep.ru

H. YASUDA, H. TAKADA, S. CHIBA, Y. KASUGAI
Japan Atomic Energy Research Institute, Tokai-mura, Naka-gun, Ibaraki-ken 319-11

S. G. MASHNIK, R. E. PRAEL, M. B. CHADWICK
Los Alamos National Laboratory, Los Alamos, NM 87545, USA

T. A. GABRIEL
Oak Ridge National Laboratory, Oak Ridge, TN 37831, USA

M. BLANN
7210E Calabria ct, San Diego, CA 92122, USA

The results of measurements and computer simulations of the yields of residual product nuclei in ^{209}Bi, ^{208,207,206,nat}Pb, ^{65,63}Cu, ^{59}Co thin targets irradiated by 0.13, 1.2 and 1.5 GeV protons are presented. The yields were measured by direct high-precision γ-spectrometry. The process was monitored by the ^{27}Al(p,x)^{24}Na reaction. 801 cross sections are presented and used in comparisons between the reaction yields obtained experimentally and simulated by the HETC, GNASH, LAHET, INUCL, CEM95, CASCADE, NUCLEUS, YIELDX, QMD and ALICE codes.

1. Introduction

The work is aimed at experimental determining and computer-aided simulating the independent and cumulative yields of residual product nuclei in thin targets made of the target materials and structure materials of the subcritical Accelerator-Driven Technology (ADT) plants [1, 2, 3, 4].

The values of the yields of residual product nuclei produced in thin targets irradiated by medium- and high-energy protons are extensively used in the fundamental and applied scientific researches.

Knowledge of the yield values is necessary when optimizing the accelerator isotope production, designing and operating the high-current accelerators and neutron source targets, in interpreting the cosmic ray nuclear reaction-induced yields of residual product nuclei in meteorites, and for the purposes of astrophysical and medical studies, for space flight researchers. The respective research results are becoming increasingly important in the feasibility analysis of subcritical plant designs, first of all in view of information about the applicability scope of various high-energy nucleon-meson codes used to simulate high-energy interactions in the target and constructional materials, thus permitting the radiation technology parameters of the plants to be calculated more and more reliably.

The present-day accuracy requirements of predicting the yields (both experimental and

computer-simulated) of product nuclei are estimated to be about 10-20% [5, 6]. Therefore, the computational technique accuracy has to be studied to verify and develop further the actual codes.

The predictive power of the computational methods and of the respective computer simulation codes can be estimated by making comparisons with the still scanty present-day experimental data [7, 8]. The actual predictive power of the well-known computational methods is much worse than required 10-20%. Therefore, the predictive power of the codes has to be improved.

The accuracy requirements may be met by step-by-step improvements in the computer simulation of intranuclear processes, as well as by extending the experimental database, in particular the data on the nuclide yields in thin targets irradiated by up-to 2 GeV protons. A comprehensive comparison between the codes and the experimental data is expected to help determine the ranges of energies and mass numbers described most adequately by the codes.

In applications, it is more convenient that the reaction product yields from materials of natural isotopic composition should be used. In verifying the codes, however, the experimental product yields from irradiated high-enriched monoisotopic materials should better be used. The main reason for this is that the particular given reaction products may be formed in many-isotope compositions via different channels, thus camouflaging the simulation errors.

That is why this work is an experimental and computer-simulation study of radioactive nuclide production in the basic accelerator structure materials, i.e., copper isotopes and cobalt, and in main materials of target facilities – lead isotopes and bismuth.

Preliminary results of our measuring the yields of residual nuclei in ^{63}Cu, ^{65}Cu, $^{206-208}$Pb, and ^{209}Bi targets irradiated by 1.5 GeV and 130 MeV protons and in ^{59}Co target irradiated by 1.2 GeV protons, as well as the results of analyzing the measurement results with the HETC, INUCL, and CEM95 codes, are published in [9].

2. Experimental Techniques

The irradiations and measurements were made at ITEP with two independent external proton beams, namely, the high (800-2600MeV) and low (80-200MeV) energy beams.

The following irradiations were made:

- ^{209}Bi, ^{208}Pb, ^{207}Pb, ^{206}Pb, and ^{63}Cu, ^{65}Cu were irradiated with 0.13 and 1.5 GeV protons;
- ^{nat}Pb was irradiated with 1.5 GeV protons;
- ^{59}Co samples[1] were irradiated with 0.13, and 1.2 GeV protons;
- two pairs of ^{63}Cu, ^{65}Cu were irradiated with 1.2 GeV protons being measured at ITEP and JAERI independently.

The irradiation details and the preliminary results of measuring the produced nuclides can be found in our previous works [9, 10]. The techniques and results of measuring γ-ray spectra, processing γ-ray spectra, determining external proton beam energies, measuring geometry parameters of external proton beam shapes, determining neutron background, as well as the method for determination of radioactive nuclide yields are described in detail in [13].

The monitor reaction cross sections used are presented in Table 1.

[1]The chemical composition of the used Co samples was following: Co - 99.3%; Ni - below 0.3%; Fe - below 0.2%; others (Mn, Cu, C, etc.) - below 0.2%.

Table 1: The $^{27}Al(p,x)^{24}Na$ reaction cross sections used in this work

Proton Energy (GeV)	σ (mb)	Refs.
0.13	11.6 ± 0.8	[11]
1.2	10.8 ± 0.8	[7]
1.5	11.9 ± 0.9	[10]

3. Experimental Yields

Table 2 presents the results obtained in $^{63,65}Cu$ irradiated with 1.2 GeV protons at ITEP (89 cross sections) and at JAERI (46 cross sections measured with VHTRC detector and 24 cross sections measured with FNS detector; the total number of different nuclides measured with the two detectors is 50) of all type yields produced in ^{63}Cu and ^{65}Cu irradiated by 1.2 GeV protons at ITEP. 62 cross sections obtained at JAERI coincide with the ITEP cross sections within one experimental error. The remaining 8 cross sections coincide within a doubled experimental error.

Table 3 presents experimental results for independent and cumulative yields of the metastable and ground states from $^{63,65}Cu$ irradiated with 0.13 and 1.5 GeV protons and ^{59}Co irradiated with 0.13 and 1.2 GeV protons.

Table 4 presents the experimental cumulative yields of the ground states of the reaction products for ^{209}Bi and $^{206,107,208,nat}Pb$ irradiated with 0.13 and 1.5 GeV protons, and Table 5 shows the remaining experimental yields of the reaction products.

4. Computer Simulation of measured products

The products of the studied reactions were simulated by eleven different codes, namely,

- the CEM95 Cascade-Exciton Model code [14],
- the CASCADE cascade – evaporation – fission transport code [15],
- the INUCL cascade – preequilibrium – evaporation – fission code [16],
- the HETC cascade – evaporation transport code [17],
- the LAHET cascade – evaporation – fission transport code [18],
- the GNASH code based on the Hauser-Feshbach and preequilibrium approach [19],
- the ALICE code with HMS precompound approach [20],
- the Quantum Molecular Dynamics (QMD) code [21],
- the NUCLEUS cascade – evaporation – fission code [22],
- the semi-phenomenological YIELDX code [23],
- the semi-phenomenological formulae of Foshina et al. [24].

A detailed description of the models used by the CEM95, CASCADE, INUCL, HETC, LAHET, ALICE and GNASH codes may be found in our previous work [10], in Refs. [14]–[20] and the references therein. The QMD, NUCLEUS, and YIELDX, formulae by Foshina et al. are briefly described in [13] and may be found in Refs. [21]-[24].

In the present work, the comparisons of measured data with the calculations are made using two parameters. The first parameter is numbers of "coincidences". A coincidence is defined to be a comparison event, with the simulation-experiment difference not exceeding a factor of 2 ($N_{C_{2.0}}$: $0.5 < \sigma_{cal,i}/\sigma_{exp,i} < 2.0$), and a factor of 1.3 ($N_{C_{1.3}}$: $0.769 < \sigma_{cal,i}/\sigma_{exp,i} < 1.3$). The parameter is presented as a ratio of coincidence numbers ($N_{C_{1.3}}, N_{C_{2.0}}$) to the number of all comparison events (N_S). The number of the coincidences within a factor of 1.3 ($N_{C_{1.3}}$) is

Table 2: Experimental yields of the reaction product metastable and ground states for ^{63,65}Cu at E_p = 1.2 GeV measured at ITEP and JAERI

Product	Half time	Yield	^{63}Cu			^{65}Cu		
			ITEP	JAERI		ITEP	JAERI	
			GC-2518	VHTRC	FNS	GC-2518	VHTRC	FNS
^{65}Zn	244.26d	ind	–	–	–	1.49 ± 0.12	–	–
^{62}Zn	9.26h	ind	0.36 ± 0.04	0.38 ± 0.12	–	0.16 ± 0.02	0.28 ± 0.07	–
^{64}Cu	12.7h	ind	–	–	–	49.1 ± 4.0	–	–
^{61}Cu	3.333h	cum	15.0 ± 2.0	–	–	5.0 ± 0.7	–	–
^{60}Cu	23.7m	cum	1.51 ± 0.14	–	–	0.92 ± 0.10	–	–
^{57}Ni	35.60h	cum	1.01 ± 0.08	1.01 ± 0.11	–	0.31 ± 0.03	0.32 ± 0.04	–
^{62m}Co	13.91m	ind	–	–	–	0.51 ± 0.06	–	–
^{60}Co	5.2714d	m+g	7.7 ± 1.3	–	8.0 ± 0.9	15.0 ± 1.1	–	14.3 ± 1.6
^{58}Co	70.916d	m+g	29.9 ± 2.3	26.2 ± 2.9	25.6 ± 2.9	24.8 ± 1.9	21.8 ± 2.4	21.4 ± 2.4
^{58}Co	70.916d	ind	9.6 ± 3.7	–	–	3.2 ± 2.0	–	–
^{58m}Co	9.15h	ind	20.4 ± 3.9	–	–	21.7 ± 2.6	–	–
^{57}Co	271.79d	cum	30.1 ± 2.3	23.9 ± 2.7	24.7 ± 2.8	19.4 ± 1.5	15.3 ± 1.7	15.8 ± 1.8
^{57}Co	271.79d	ind	27.6 ± 2.3	–	–	17.9 ± 1.4	–	–
^{56}Co	77.27d	cum	8.5 ± 0.8	8.4 ± 1.0	8.4 ± 0.9	4.3 ± 0.4	4.4 ± 0.5	4.4 ± 0.5
^{55}Co	17.53h	cum	1.69 ± 0.16	1.54 ± 0.19	–	0.57 ± 0.06	0.73 ± 0.09	–
^{59}Fe	44.503d	cum	0.64 ± 0.06	0.73 ± 0.11	0.81 ± 0.10	3.9 ± 0.3	3.8 ± 0.4	3.6 ± 0.4
^{53}Fe	8.51m	cum	0.56 ± 0.06	–	–	0.28 ± 0.03	–	–
^{52}Fe	8.275h	cum	0.19 ± 0.02	0.19 ± 0.04	–	0.07 ± 0.01	0.10 ± 0.02	–
^{56}Mn	2.5785h	cum	2.31 ± 0.25	–	–	5.9 ± 0.5	–	–
^{54}Mn	312.12d	ind	20.4 ± 1.6	18.3 ± 2.1	17.6 ± 2.0	21.6 ± 1.6	19.1 ± 2.1	18.9 ± 2.1
^{52}Mn	5.591d	cum	9.1 ± 0.7	8.7 ± 1.0	8.3 ± 1.0	6.4 ± 0.8	6.1 ± 0.7	5.6 ± 0.7
^{52m}Mn	21.1m	cum	1.53 ± 0.18	–	–	0.96 ± 0.11	–	–
^{51}Cr	27.704d	cum	29.2 ± 2.3	26.4 ± 3.0	24.4 ± 2.7	20.8 ± 1.7	21.5 ± 2.4	20.3 ± 2.3
^{49}Cr	42.3m	cum	2.44 ± 0.28	–	–	1.45 ± 0.15	–	–
^{48}Cr	21.56h	cum	0.56 ± 0.05	0.52 ± 0.06	–	0.25 ± 0.03	0.25 ± 0.03	–
^{48}V	15.9735d	cum	13.7 ± 1.2	13.0 ± 1.5	12.4 ± 1.4	10.0 ± 0.9	9.5 ± 1.1	9.1 ± 1.0
^{48}Sc	43.67h	ind	0.47 ± 0.05	0.51 ± 0.15	–	1.11 ± 0.09	1.11 ± 0.16	–
^{47}Sc	3.3492d	cum	3.2 ± 0.3	3.1 ± 0.4	–	5.0 ± 0.4	4.8 ± 0.5	–
^{47}Sc	3.3492d	ind	3.1 ± 0.2	–	–	4.8 ± 0.4	–	–
^{46}Sc	83.810d	m+g	7.6 ± 0.6	7.1 ± 0.8	6.8 ± 0.8	9.1 ± 0.7	8.4 ± 0.9	8.3 ± 0.9
^{44m}Sc	58.6h	ind	7.9 ± 0.6	6.8 ± 0.8	–	5.9 ± 0.7	5.5 ± 0.6	–
^{44}Sc	3.927h	m+g	13.2 ± 2.8	–	–	10.4 ± 2.2	–	–
^{44}Sc	3.927h	ind	6.7 ± 1.4	–	–	5.1 ± 1.1	–	–
^{43}Sc	3.891h	cum	6 ± 0.5	–	–	3.8 ± 0.4	–	–
^{47}Ca	4.536d	cum	0.07 ± 0.01	0.09 ± 0.03	–	0.22 ± 0.03	0.13 ± 0.02	–
^{43}K	22.3h	cum	1.18 ± 0.10	1.17 ± 0.13	–	1.89 ± 0.15	1.82 ± 0.21	–
^{42}K	12.360h	ind	3.4 ± 0.3	3.4 ± 0.4	–	4.3 ± 0.3	3.9 ± 0.4	–
^{41}Ar	109.34m	cum	0.57 ± 0.04	–	–	0.94 ± 0.07	–	–
^{39}Cl	55.6m	cum	0.31 ± 0.03	–	–	0.41 ± 0.03	–	–
^{38}Cl	37.24m	m+g	0.75 ± 0.08	–	–	1.07 ± 0.10	–	–
^{34m}Cl	32.00m	cum	0.35 ± 0.06	–	–	0.18 ± 0.02	–	–
^{29}Al	6.56m	cum	0.20 ± 0.02	–	–	0.26 ± 0.03	–	–
^{28}Mg	20.91h	cum	0.12 ± 0.01	0.15 ± 0.04	–	0.18 ± 0.02	0.22 ± 0.04	–
^{24}Na	14.959h	cum	1.55 ± 0.12	1.42 ± 0.16	–	1.55 ± 0.12	1.67 ± 0.19	–
^{22}Na	2.6088y	cum	1.21 ± 0.16	–	1.13 ± 0.20	0.86 ± 0.08	–	0.83 ± 0.12
^{7}Be	53.29d	ind	4.5 ± 0.4	4.5 ± 0.6	4.8 ± 0.6	4.1 ± 0.5	4.2 ± 0.5	3.8 ± 0.5

Table 3: Experimental yields [mb] of the reaction products for ^{65,63}Cu at Ep = 1.5 GeV and 0.13 GeV, and for ^{59}Co at Ep= 1.2 GeV and 0.13 GeV

			E_p=1.5GeV		E_p=1.2GeV	E_p=0.13GeV		
Nuclide	Half life	Yield	^{65}Cu	^{63}Cu	^{59}Co	^{65}Cu	^{63}Cu	^{59}Co
^{65}Zn	244.26d	ind	2.9 ± 0.3	–	–	–	–	–
^{63}Zn	38.47m	ind	–	–	–	6.9 ± 0.7	–	–
^{62}Zn	9.26h	ind	0.19 ± 0.03	0.49 ± 0.05	–	2.9 ± 0.4	5.1 ± 0.6	–
^{64}Cu	12.700h	ind	58.1 ± 6.6	–	–	130 ± 12	–	–
^{61}Cu	3.333h	cum	5.3 ± 0.7	16.0 ± 1.6	–	29.2 ± 4.8	46.5 ± 4.8	–
^{60}Co	5.2714y	m+g	14.3 ± 2.0	6.1 ± 1.1	–	–	–	–
^{60}Cu	23.7m	cum	1.10 ± 0.12	2.6 ± 0.3	–	3.6 ± 0.4	9.2 ± 0.8	–
^{59}Fe	44.503d	cum	4.8 ± 0.4	0.55 ± 0.10	–	–	–	–
^{58}Co	70.916d	m+g	29.1 ± 3.2	33.2 ± 2.8	54.5 ± 4.2	52.6 ± 5.6	71.3 ± 7.8	124.5 ± 9.3
^{58}Co	70.916d	ind	0.53 ± 0.33	8.3 ± 2.3	21.4 ± 4.0	–	–	30.9 ± 10.7
^{57}Co	271.79d	ind	23.5 ± 2.1	28.6 ± 2.3	32.4 ± 3.1	–	82.9 ± 13.4	110.6 ± 11.7
^{57}Ni	35.60h	cum	0.27 ± 0.02	0.90 ± 0.07	–	–	2.4 ± 0.2	–
^{57}Ni	35.60h	ind	–	–	0.28 ± 0.03	–	–	2.4 ± 0.2
^{57}Co	271.79d	cum	23.8 ± 2.1	29.5 ± 2.3	32.7 ± 2.6	41.2 ± 3.4	85.3 ± 10.1	111.5 ± 8.8
^{56}Mn	2.5785h	cum	5.9 ± 0.5	2.4 ± 0.2	6.7 ± 0.6	3.0 ± 0.4	1.31 ± 0.17	4.8 ± 0.5
^{56}Co	77.27d	cum	3.6 ± 0.4	7.0 ± 0.6	6.4 ± 0.8	–	16.7 ± 4.5	29.2 ± 2.1
^{55}Co	17.53h	cum	0.49 ± 0.04	1.31 ± 0.12	0.84 ± 0.12	–	1.7 ± 0.2	4.5 ± 0.4
^{54}Mn	312.12d	ind	25.8 ± 2.1	19.6 ± 2.4	27.0 ± 2.1	–	–	42.1 ± 3.2
^{53}Fe	8.51m	cum	–	–	2.0 ± 0.4	–	–	1.05 ± 0.13
^{52}Mn	5.591d	cum	4.8 ± 0.4	7.4 ± 0.7	8.7 ± 0.7	–	–	0.30 ± 0.02
^{52}Fe	8.275h	cum	–	0.21 ± 0.02	0.17±0.05	–	1.8 ± 0.2	14.3 ± 1.0
^{51}Cr	27.704d	cum	29.3 ± 2.4	27.5 ± 2.8	32.0 ± 2.6	–	–	32.1 ± 5.0
^{49}Cr	42.3m	cum	2.2 ± 0.4	3.2 ± 0.5	3.8 ± 0.4	–	–	1.6 ± 0.2
^{48}V	15.9735d	cum	8.1 ± 0.9	11.2 ± 0.9	13.7 ± 1.0	–	–	2.8 ± 0.5
^{48}Cr	21.56h	cum	0.25 ± 0.03	0.51 ± 0.04	0.50 ± 0.05	–	–	–
^{48}V	15.9735d	ind	–	–	13.0 ± 2.9	–	–	–
^{48}Sc	43.67h	ind	0.97 ± 0.10	0.52 ± 0.05	0.78 ± 0.07	–	–	0.23 ± 0.10
^{47}Sc	3.3492d	cum	5.6 ± 0.5	3.1 ± 0.3	4.4 ± 0.4	–	–	0.36 ± 0.04
^{47}Ca	4.536d	cum	0.14 ± 0.03	0.030 ± 0.007	0.067 ± 0.015	–	–	–
^{47}Sc	3.3492d	ind	4.3 ± 0.5	3.0 ± 0.2	4.4 ± 0.3	–	–	–
^{46}Sc	83.810d	m+g	9.4 ± 0.8	7.1 ± 0.6	9.4 ± 0.9	–	–	–
^{44}Sc	3.927h	m+g	10.0 ± 1.6	12.4 ± 1.7	16.0 ± 3.4	–	–	–
^{44}Sc	3.927h	ind	5.4 ± 0.9	6.6 ± 0.9	8.5 ± 1.8	–	–	0.24 ± 0.05
^{43}Sc	3.891h	cum	4.2 ± 0.4	6.4 ± 0.5	5.5 ± 0.5	–	–	–
^{43}K	22.3h	cum	1.9 ± 0.2	1.19 ± 0.10	1.8 ± 0.2	–	–	–
^{42}K	12.360h	ind	4.4 ± 0.4	3.4 ± 0.3	4.5 ± 0.4	–	–	–
^{41}Ar	109.34m	cum	1.09 ± 0.09	0.54 ± 0.05	0.91 ± 0.07	–	–	–
^{39}Cl	55.6m	cum	0.57 ± 0.06	0.42 ± 0.06	0.53 ± 0.06	–	–	–
^{38}Cl	37.24m	m+g	1.6 ± 0.1	1.25 ± 0.89	2.0 ± 0.3	–	–	–
^{29}Al	6.56m	cum	–	–	2.5 ± 0.3	–	–	–
^{28}Mg	20.91h	cum	0.25 ± 0.02	0.18 ± 0.03	0.21 ± 0.02	–	–	–
^{27}Mg	9.462m	cum	–	–	1.27 ± 0.14	–	–	–
^{24}Na	14.959h	cum	2.0 ± 0.2	2.0 ± 0.2	2.2 ± 0.2	–	–	–
^{22}Na	2.6088y	cum	1.12 ± 0.28	1.51 ± 0.25	1.8 ± 0.9	–	–	–
^{7}Be	53.29d	ind	6.0 ± 0.6	6.2 ± 1.2	4.0 ± 0.4	–	–	–

Table 4: Experimental cumulative yields [mb] of the reaction product ground states for ^{209}Bi, ^{206,107,208,nat}Pb at Ep = 1.5 GeV and ^{209}Bi at 0.13 GeV. (The reaction yields obtained using the low-background spectrometer are labeled as:*)

				E_p=1.5GeV			E_p=0.13GeV
Nucleus	Half life	^{209}Bi	^{208}Pb	^{207}Pb	^{206}Pb	^{nat}Pb	^{209}Bi
^{207}Bi*	32.2 y	66.8 ± 8.6	–	–	–	–	–
^{206}Bi	6.243 d	31.5 ± 3.8	–	–	–	–	106 ± 11
^{205}Bi	15.31 d	29.4 ± 3.5	–	–	–	–	132 ± 28
^{204}Bi	11.22 h	30.3 ± 3.6	–	–	–	–	117 ± 14
^{203}Bi	11.73 h	23.3 ± 3.0	–	–	–	–	129 ± 16
^{202}Bi	1.67 h	13.2 ± 2.6	–	–	–	–	167 ± 18
^{201}Bi	108 m	–	–	–	–	–	103 ± 14
^{200}Bi	36 m	10.1 ± 1.2	–	–	–	–	74.4 ± 9.7
^{203}Pb	51.837 h	53.2 ± 5.9	40.2 ± 3.2	39.3 ± 3.2	50.5 ± 4.2	41.7 ± 3.4	278 ± 42
^{201}Pb	9.33 h	35.9 ± 6.0	24.1 ± 3.0	30.0 ± 3.1	39.6 ± 5.7	31.1 ± 3.2	168 ± 21
^{200}Pb	21.5 h	34.1 ± 4.0	22.1 ± 2.4	25.3 ± 2.3	24.6 ± 2.4	25.6 ± 2.5	147 ± 17
^{199}Pb	90 m	36.9 ± 7.0	22.5 ± 6.4	27.6 ± 4.7	39.5 ± 6.4	28.8 ± 6.3	136 ± 28
^{198}Pb	2.4 h	30.0 ± 6.0	–	–	–	–	24.1 ± 9.9
^{202}Tl	12.23 d	–	21.9 ± 1.7	19.8 ± 1.8	26.5 ± 3.4	21.1 ± 1.8	–
^{201}Tl	72.912 h	46.5 ± 5.6	49.3 ± 4.4	50.3 ± 6.5	68.9 ± 11.0	50.4 ± 4.5	200 ± 33
^{200}Tl	26.1 h	43.5 ± 5.0	32.3 ± 3.3	45.3 ± 3.7	45.8 ± 4.9	35.5 ± 3.0	130 ± 16
^{199}Tl	7.42 h	39.5 ± 5.4	36.2 ± 6.6	32.5 ± 4.8	47.8 ± 7.6	34.4 ± 5.5	122 ± 22
^{198}Tl	5.3 h	32.9 ± 5.5	37.4 ± 5.8	30.4 ± 4.6	44.0 ± 6.5	38.7 ± 5.6	26.6 ± 4.5
^{196}Tl	1.84 h	–	–	–	–	–	21.7 ± 6.4
^{194}Tl	33.0 m	13.7 ± 4.2	6.3 ± 2.3	7.0 ± 2.3	–	10.1 ± 3.7	
^{203}Hg	46.612 d	1.4 ± 0.1	6.0 ± 0.6	4.4 ± 0.7	5.5 ± 2.1	5.6 ± 0.6	
^{195}Hg	9.9 h	15.1 ± 4.6	–	–	–	–	
^{192}Hg	4.85 h	28.1 ± 4.3	27.2 ± 2.7	25.6 ± 3.6	37.7 ± 6.4	34.1 ± 4.4	
^{198}Au	2.696 d	0.55 ± 0.22	3.4 ± 0.6	2.4 ± 0.4	1.9 ± 0.3	2.2 ± 0.2	
^{195g}Au	182.9 d	–	–	51.6 ± 6.4	–	52.8 ± 8.0	
^{192}Au	4.94 h	36.8 ± 5.9	50.0 ± 5.5	46.9 ± 6.2	51.1 ± 7.5	51.5 ± 8.4	
^{191}Pt	2.9 d	24.3 ± 4.9	30.6 ± 6.0	27.4 ± 4.8	31.6 ± 4.9	31.2 ± 5.7	
^{189}Pt	10.87 h	–	25.8 ± 2.7	31.2 ± 3.0	28.5 ± 3.5	30.6 ± 6.5	
^{188}Pt	10.2 d	30.1 ± 3.5	36.9 ± 4.2	34.9 ± 3.1	43.6 ± 4.0	34.1 ± 4.0	
^{188}Ir	41.5 h	29.7 ± 3.4	–	–	–	–	
^{186}Ir	15.8 h	12.3 ± 2.2	11.6 ± 1.1	13.7 ± 1.5	11.7 ± 1.3	11.6 ± 1.4	
^{185}Ir	14.4 h	–	28.1 ± 7.1	38.3 ± 4.3	40.2 ± 6.3	33.7 ± 4.7	
^{184}Ir	3.02 h	19.7 ± 4.4	29.9 ± 2.6	25.4 ± 3.6	34.7 ± 3.1	35.4 ± 2.9	
^{185}Os*	93.6 d	33.9 ± 4.2	36.9 ± 3.8	37.6 ± 4.3	40.4 ± 4.1	41.9 ± 4.1	
^{182}Os	22.1h	28.1 ± 3.5	31.2 ± 3.4	32.3 ± 3.3	38.6 ± 3.8	34.8 ± 3.4	
^{183}Re	70.0 d	20.8 ± 3.5	32.0 ± 3.3	33.0 ± 3.9	38.1 ± 4.1	39.5 ± 4.1	
^{182}Re	12.7 h	31.6 ± 3.5	27.5 ± 2.7	36.9 ± 3.5	29.9 ± 3.4	32.8 ± 5.5	
^{181}Re	19.9 h	24.6 ± 5.4	35.6 ± 4.2	40.6 ± 6.0	38.4 ± 8.7	42.3 ± 6.6	
^{179}Re	19.7 m	19.7 ± 2.4	–	–	–	–	
^{176}Ta	8.08 h	27.1 ± 6.5	30.5 ± 6.8	34.2 ± 6.6	28.7 ± 7.1	35.8 ± 7.4	
^{174}Ta	1.18 h	18.7 ± 2.5	33.6 ± 3.3	25.4 ± 3.4	67.7 ± 6.7	55.8 ± 4.6	
^{173}Ta	3.14 h	20.2 ± 3.7	31.3 ± 4.2	22.0 ± 3.3	39.6 ± 6.9	36.7 ± 4.8	
^{172}Ta	36.8 m	7.9 ± 1.3	13.8 ± 1.7	7.3 ± 0.8	14.8 ± 1.6	10.0 ± 1.2	
^{173}Hf	23.6 h	30.7 ± 3.7	34.1 ± 4.0	36.7 ± 3.3	40.4 ± 6.4	41.5 ± 4.0	
^{172}Hf*	1.87 y	26.7 ± 3.0	23.8 ± 4.0	24.8 ± 2.1	26.2 ± 4.6	21.1 ± 2.9	
^{170}Hf	16.01 h	22.2 ± 3.1	22.8 ± 2.7	25.6 ± 2.7	27.3 ± 3.9	25.4 ± 3.0	
^{173}Lu*	1.37 y	26.9 ± 5.0	30.5 ± 5.5	29.0 ± 2.9	29.6 ± 6.3	48.1 ± 6.0	
^{171}Lu	8.24 d	26.9 ± 3.0	35.4 ± 5.4	31.3 ± 2.6	40.6 ± 4.9	32.3 ± 3.3	
^{170}Lu	2.00 d	–	24.4 ± 2.5	27.5 ± 2.6	22.8 ± 5.0	29.2 ± 3.0	
^{169}Lu	34.06 d	19.5 ± 3.2	22.8 ± 2.7	24.2 ± 3.3	25.3 ± 2.6	25.7 ± 3.3	
^{166}Yb	56.7 h	13.3 ± 1.6	13.9 ± 2.3	18.2 ± 1.8	21.3 ± 3.0	17.0 ± 1.7	
^{167}Tm	9.24 d	–	39.8 ± 6.7	33.2 ± 5.7	44.8 ± 7.5	33.2 ± 5.6	
^{160}Er	28.58 h	11.5 ± 1.3	15.9 ± 2.2	22.3 ± 2.9	21.1 ± 2.2	22.9 ± 4.3	
^{159}Er	36.0 m	–	15.5 ± 1.9	23.3 ± 2.8	21.6 ± 2.9	17.3 ± 2.5	
^{157}Dy	8.14 h	18.1 ± 2.2	19.9 ± 1.8	21.4 ± 1.9	25.3 ± 3.4	24.2 ± 2.3	
^{155}Dy	10.0 h	–	15.0 ± 1.3	16.8 ± 1.8	18.3 ± 1.8	17.5 ± 1.5	
^{155}Tb	5.32 d	–	15.9 ± 1.6	16.4 ± 1.6	19.6 ± 1.8	17.6 ± 1.8	
^{153}Tb	2.34 d	9.8 ± 1.3	13.7 ± 1.7	12.5 ± 1.3	15.3 ± 1.8	12.5 ± 1.4	
^{151}Tb	17.609 h	9.5 ± 1.1	10.8 ± 1.1	10.6 ± 1.0	9.3 ± 1.1	9.6 ± 1.7	
^{153}Gd*	241.6 d	10.1 ± 2.9	–	11.3 ± 1.1	13.5 ± 1.4	10.2 ± 1.2	
^{149}Gd	9.4 d	10.0 ± 1.1	9.0 ± 1.9	11.4 ± 2.0	12.8 ± 3.4	11.5 ± 1.5	
^{147}Gd	38.1 h	7.9 ± 1.1	7.1 ± 1.3	9.6 ± 1.5	7.7 ± 1.7	10.4 ± 1.5	
^{146}Gd	48.27 d	7.3 ± 0.8	6.2 ± 0.8	8.3 ± 0.7	9.5 ± 0.8	8.9 ± 0.8	
^{147}Eu	24.0 d	11.4 ± 1.4	–	10.2 ± 4.0	–	10.8 ± 2.3	
^{146}Eu	4.59 d	8.0 ± 0.8	7.4 ± 0.8	9.2 ± 0.7	10.8 ± 0.9	10.4 ± 0.9	

Table 4 (continued)

Nucleus	Half life	^{209}Bi	^{208}Pb	E_p=1.5GeV ^{207}Pb	^{206}Pb	^{nat}Pb	E_p=0.13GeV ^{209}Bi
^{145}Eu	5.93 h	4.6 ± 0.7	7.6 ± 0.7	5.5 ± 0.7	8.2 ± 1.5	6.8 ± 0.9	
^{143}Pm*	265 d	3.8 ± 1.2	–	6.7 ± 1.5	–	7.3 ± 0.7	
^{140}La	40.280 h	1.6 ± 0.2	–	–	–	–	
^{140}Ba	12.746 h	0.98 ± 0.13	–	–	–	–	
^{139}Ce	137.66 d	2.9 ± 0.5	4.3 ± 0.6	5.8 ± 0.7	6.8 ± 0.8	6.6 ± 0.7	
^{127}Xe	36.4 d	2.4 ± 0.2	4.1 ± 0.6	3.1 ± 0.6	3.0 ± 0.2	4.1 ± 0.3	
^{121}Te	17.78d	1.7 ± 0.4	1.50 ± 0.24	1.92 ± 0.30	1.78 ± 0.31	2.28 ± 0.40	
^{113}Sn	115.09 d	0.90 ± 0.14	–	0.82 ± 0.11	–	1.56 ± 0.38	
^{111}In	2.83 d	1.4 ± 0.2	2.28 ± 0.34	1.8 ± 0.2	1.93 ± 0.34	1.9 ± 0.2	
^{105}Rh	35.36 h	5.2 ± 0.6	3.4 ± 0.9	3.1 ± 0.6	4.8 ± 0.8	5.0 ± 0.9	
^{95}Tc	20.0 h	2.9 ± 0.6	2.05 ± 0.23	2.8 ± 0.4	2.50 ± 0.57	4.0 ± 0.7	
^{99}Mo	2.75 d	5.4 ± 0.7	5.6 ± 0.6	4.4 ± 0.4	3.5 ± 0.5	4.7 ± 0.5	
^{95}Nb	35.02 d	7.4 ± 1.1	8.7 ± 1.0	4.8 ± 0.5	5.7 ± 0.9	6.5 ± 0.6	
^{95}Zr	64.02 d	2.0 ± 0.3	6.4 ± 1.3	1.4 ± 0.5	1.9 ± 1.1	4.9 ± 0.7	
^{89}Zr	78.4 h	3.2 ± 0.5	2.2 ± 0.3	2.3 ± 0.2	2.6 ± 0.3	1.9 ± 0.3	
^{88}Zr	83.4 d	0.26 ± 0.04	–	–	–	2.6 ± 0.2	
^{88}Y*	106.61 d	3.2 ± 0.6	–	3.4 ± 0.4	–	3.7 ± 0.5	
^{87}Y	80.3 h	5.3 ± 0.6	4.8 ± 0.3	4.2 ± 0.4	6.6 ± 0.7	4.3 ± 0.5	
^{85}Sr	64.08 d	6.2 ± 1.0	4.0 ± 0.2	4.1 ± 0.4	5.4 ± 0.8	5.6 ± 0.6	
^{83}Rb	86.2 d	5.4 ± 1.1	–	5.2 ± 0.9	–	5.8 ± 0.8	

considered here to be the number of simulations within a 30% accuracy needed in applications [5].

Another parameter for comparing between the simulated and experimental data was proposed by R.Michel [8, 11] and used afterwords in our works [10, 12]. The parameter is a mean squared deviation factor

$$\langle H \rangle = 10^{\sqrt{\left\langle \left(lg\left(\frac{\sigma_{cal,i}}{\sigma_{exp,i}}\right)\right)^2 \right\rangle}}, \tag{1}$$

with its standard deviation $S(\langle H \rangle)$

$$S(\langle H \rangle) = 10^{\sqrt{a}}, \tag{2}$$

where

$$a = \left\langle \left(\left| lg\left(\frac{\sigma_{cal,i}}{\sigma_{exp,i}}\right)\right| - lg(\langle H \rangle)\right)^2 \right\rangle,$$

where $\langle\ \rangle$ designates averaging over all of the comparison events ($i = 1...N_S$ where N_S - number of experimental and simulated events used for comparison).

The mean squared deviation factor $\langle H \rangle$ with its standard deviation $S(\langle H \rangle)$ defines the interval $[\langle H \rangle / S(\langle H \rangle), \langle H \rangle \times S(\langle H \rangle)]$, which covers about two thirds of all the simulation-to-experiment ratios.

Table 6 presents information concerning the predictive power of each of the codes for high and low energies, namely, the total number of measured yields N_T, the number of the latter that was chosen to be used in the comparison with simulated data N_G, the total number of the simulated products that can be compared with the data N_S, the two numbers of "coincidences" between simulated and experimental values $N_{C_{1.3}}$, $N_{C_{2.0}}$, and the mean deviation $\langle H \rangle$ with its $S(\langle H \rangle)$ of simulation results from experimental data.

5. Conclusion

This study is the first step in our work on the non-fissible targets that are of interest for accelerator-driven facilities. In total, about 800 reaction data have been measured. Table 6

Table 5: Experimental independent yields [mb] of the ground states and independent and cumulative metastable states of ^{209}Bi, ^{208}Pb, ^{207}Pb,^{206}Pb, and ^{nat}Pb(p,x)-reaction products at E_p=1.5 GeV and 0.13 GeV, and cumulative yields [mb] for ^{208}Pb, ^{207}Pb,^{206}Pb for E_p=0.13 GeV. (The reaction yields obtained using the low-background spectrometer are labeled as:*)

Nucleus	Half life	Yield	^{209}Bi	^{208}Pb	^{207}Pb	^{206}Pb	^{nat}Pb
				E_p=1.5GeV			
^{208}Po	8.8 d	ind	4.0±0.6	–	–	–	–
^{206}Bi	6.243 d	ind	–	2.87 ± 0.35	2.52 ± 0.31	1.71 ± 0.31	3.12 ± 0.26
^{205}Bi	15.31d	ind	–	6.90 ± 0.75	7.3 ± 1.2	5.7 ± 2.8	7.9 ± 1.5
^{204m}Pb	67.2 m	ind	5.3±1.6	18.7 ±3.2	16.0 ± 2.5	21.3 ± 4.1	19.6 ± 2.3
^{204}Bi	11.22 h	g+m1+m2	–	4.23 ± 0.64	5.04 ± 0.52	7.8 ± 1.4	5.88 ± 0.85
^{203}Pb	51.837 h	g+m1+m2	31.1 ± 7.0	–	—	–	–
^{202}Tl	12.23 d	ind	5.8 ± 0.8	–	–	–	–
^{202m}Pb	3.53 h	ind	16.8 ± 2.5	13.0 ±1.1	12.8 ± 1.3	13.5 ± 2.3	17.6 ± 1.8
^{200}Tl	26.1 h	ind	9.4 ± 2.0	16.8 ± 1.5	25.9 ± 2.4	25.5 ± 3.1	20.9 ± 4.6
^{197m}Pb	44.6 m	cum	10.6 ± 3.0	10.4 ± 2.6	9.7 ± 1.9	13.8 ± 3.1	9.1 ± 2.5
^{196m}Tl	1.41 h	ind	19.1 ± 3.8	25.5 ± 3.8	23.4 ± 3.5	38.2 ± 8.5	32.9 ± 7.4
^{196}Au	6.183 d	g+m1+m2	0.96 ± 0.16	4.21 ± 0.34	3.1 ± 0.3	3.2 ± 0.2	3.7 ± 0. 3
^{194}Au	38.02 h	g+m1+m2	1.6 ± 0.3	5.4 ± 0.7	5.3 ± 0.6	4.7 ± 0.8	5.4 ± 0.6
^{194m}Tl	32.8 m	ind	5.3 ± 0.7	7.1 ± 1.1	4.92 ± 0.52	10.4 ± 1.0	7.1 ± 1.2
^{195m}Hg	41.6 h	ind	–	15.6 ± 2.1	15.4 ± 1.3	16.2 ± 2.2	17.2 ± 2.1
^{193m}Hg	11.8 h	ind	11.9 ± 1.7	15.6 ± 3.0	16.0 ± 2.9	14.5 ± 2.9	16.1 ± 3.6
^{183m}Os	9.9 h	cum	14.2 ± 2.2	14.3 ± 1.6	16.7 ± 1.6	15.7 ± 2.3	19.0 ± 1.9
^{150m1}Tb	3.48 h	ind	5.3 ± 1.2	6.3 ± 0.9	5.4 ± 1.0	–	5.5 ± 2.0
^{146}Eu	4.59 d	ind	0.71 ± 0.14	1.24 ± 0.24	1.04 ± 0.19	1.21 ± 0.16	1.56 ± 0.17
^{140}La	40.28 h	ind	0.54 ± 0.20	–	–	–	–
^{102}Rh*	2.9 y	ind	7.0 ± 1.2	–	–	–	–
^{101m}Rh	4.34 d	cum	2.2 ± 0.2	2.1 ± 0.3	1.6 ± 0.2	3.0 ± 0.3	2.2±0.4
^{95}Nb	35.02 d	ind	4.6 ± 0.6	2.2 ± 0.3	3.4 ± 0.4	3.9 ± 0.5	1.6 ± 0.4
^{90m}Y	3.19 h	ind	2.9 ± 0.5	4.1 ± 1.0	2.2 ± 0.2	5.0 ± 0.7	4.9 ± 0.4
^{82m}Rb	6.472 h	ind	3.0 ± 0.5	1.9 ± 0.6	2.8 ± 0.2	2.3 ± 0.6	–
^{96}Tc	4.28 d	g+m	1.2 ± 0.3	0.80 ± 0.07	1.08 ± 0.14	1.25 ± 0.22	1.08 ± 0.11
^{82}Br	35.3 h	g+m	3.8 ± 0.5	1.9 ± 0.3	2.4 ± 0.3	2.6 ± 0.2	2.8 ± 0.3
^{76}As	26.32 h	ind	4.4 ± 0.7	3.4 ± 0.6	3.2 ± 0.3	2.9 ± 0.5	
^{74}As	17.77 d	ind	2.5 ± 0.4	1.5 ± 0.2	2.6 ± 0.4	2.6 ± 0.5	2.2 ± 0.3
^{60}Co*	5.2714 y	g+m	2.0 ± 0.5	–	–	–	–
				E_p=0.13GeV			
^{207}Po	5.80 h	ind	29.6 ± 4.6	–	–	–	
^{206}Po	8.8 d	ind	53.8 ± 14.4	–	–	–	
^{206}Bi	6.243 d	ind	69.6 ± 7.8	–	–	–	
^{205}Po	1.66 h	ind	36.8 ± 4.5	–	–	–	
^{204}Po	3.53 h	ind	52.0 ± 6.3	–	–	–	
^{204m}Pb	67.2 m	ind	–	62.4 ± 7.3	59.3 ± 9.0	54.9 ± 23.7	
^{204}Bi	11.22 h	g+m1+m2	–	37.8 ± 5.7	39.3 ± 6.0	41.2 ± 10.5	
^{203}Bi	11.76 h	g+m	–	50.9 ± 7.7	50.9 ± 6.5	43.9 ± 7.5	
^{203}Po	36.7 m	ind	46.5 ± 10.7	–	–	–	
^{202m}Pb	3.53 h	ind	13.0 ± 2.8	39.6 ± 4.8	37.1 ± 4.1	28.7 ± 3.6	
^{202}Po	44.7m	ind	61.3 ± 8.4	–	–	–	
^{202}Bi	1.67 h	ind	–	51.8 ± 4.6	53.9 ± 4.2	60.9 ± 6.7	
^{201}Pb	9.33 h	ind	55.5 ± 14.4	–	–	–	
^{201}Bi	108 m	g+m	–	79.7 ± 6.8	90.4 ± 18.3	61.6 ± 14.2	
^{201}Pb	9.33 h	g+m	–	117.9 ± 17.5	113.2 ± 30.2	127.8 ± 28.9	
^{200}Bi	36.4 m	g+m	–	46.7 ± 4.3	50.6 ± 4.7	69.1 ± 6.8	
^{200}Tl	26.1 h	ind	18.6 ± 9.8	–	–	–	
^{198}Tl	5.3 h	ind	4.8 ± 3.6	–	–	–	
^{198}Bi	11.85 m	g+ m1+m2	–	39.8 ± 3.6	62.5 ± 5.7	66.1 ± 12.3	
^{197m}Pb	44.6 m	cum	16.2 ± 2.9	22.0 ± 5.7	81.6 ± 12.7	143 ± 20	
^{203}Pb	51.837 h	cum	–	217 ± 27	227 ± 25	256 ± 28	
^{201}Pb	9.33 h	cum	–	180 ± 20	171 ± 22	237 ± 26	
^{200}Pb	21.5 h	cum	–	203 ± 20	207 ± 24	197 ± 26	
^{199}Pb	90 m	cum	–	201 ± 36	247 ± 32	241 ± 46	
^{198}Pb	2.4 h	cum	–	107 ± 19	155 ± 26	188 ± 27	
^{201}Tl	72.912 h	cum	–	203 ± 27	288 ± 43	310 ± 49	
^{200}Tl	26.1 h	cum	–	207 ± 37	236 ± 22	188 ± 25	
^{199}Tl	7.42 h	cum	–	207 ± 23	217 ± 23	247 ± 28	
^{198}Tl	5.3 h	cum	–	123 ± 15	172 ± 25	175 ± 28	
^{197}Tl	2.84 h	cum	–	–	190 ± 39	263 ± 42	

Table 6: Statistics of simulation-to-experiment comparisons of the yields of the all presented reaction products.

Code	^{59}Co,^{63,65}Cu, E_p=0.13GeV N_T=40, N_G=34			^{59}Co,^{63,65}Cu, E_p=1.2,1.5GeV N_T=213, N_G=170		
	$N_{C_{1.3}}/N_{C_{2.0}}/N_S$	$\langle H \rangle$	$S(\langle H \rangle)$	$N_{C_{1.3}}/N_{C_{2.0}}/N_S$	$\langle H \rangle$	$S(\langle H \rangle)$
CEM95	10/23/31	2.10	1.73	38/101/155	2.18	1.65
LAHET	14/22/32	1.81	1.47	54/120/161	2.32	2.00
INUCL	9/16/34	2.60	1.87	28/96/163	2.42	1.76
HETC	3/9/25	5.29	3.03	19/45/96	4.07	2.75
CASCADE	3/12/32	3.40	1.91	20/66/160	3.53	2.14
ALICE(Fermi)	5/14/33	2.98	1.88	–	–	–
ALICE(Kataria)	11/19/34	2.21	1.65	–	–	–
YIELDX	9/17/34	2.58	1.81	74/150/169	1.61	1.36
NUCLEUS	9/13/31	2.82	1.92	16/53/95*	2.19	1.53
Foshina et al.	6/16/33	2.90	1.91	40/114/167	2.60	2.08
QMD	8/20/33	2.12	1.55	17/50/80*	2.38	1.74
Code	^{206,207,208}Pb, ^{209}Bi, E_p=0.13GeV N_T=94, N_G=82			^{206,207,208,nat}Pb, ^{209}Bi, E_p=1.5GeV N_T=454, N_G=397		
	$N_{C_{1.3}}/N_{C_{2.0}}/N_S$	$\langle H \rangle$	$S(\langle H \rangle)$	$N_{C_{1.3}}/N_{C_{2.0}}/N_S$	$\langle H \rangle$	$S(\langle H \rangle)$
CEM95	34/61/82	2.23	1.91	101/206/302	2.12	1.71
LAHET	40/73/82	1.70	1.52	79/273/396	2.35	1.81
INUCL	17/52/82	4.71	4.15	108/227/393	3.39	2.50
HETC	24/55/80	2.51	2.10	66/181/279	3.25	2.66
CASCADE	37/73/82	2.08	1.94	97/200/305	2.62	2.17
ALICE(Fermi)	45/74/82	1.87	1.75	–	–	–
GNASH	1/8/10**	1.98		–	–	–
YIELDX	38/77/82	1.50	1.28	60/173/390	3.52	2.29
QMD	16/43/82	2.39	1.65	92/242/394	2.67	2.01

* Here N_T = 124 and N_G = 98

** Simulations were made for 10 products

reflects the predictive power of the simulation codes used here.

At present, on analyzing the theoretical data, we come to the conclusion that the differences among some theoretical yields predicted by different codes can sometimes be very significant. This is a strong indication that all of the codes have to be further improved before they can become reliable predictive tools. Therefore, the relevant experiments have to be extended.

At the same time, it should be noted that we observed [13] several quite great discrepancies among some recent 0.13 GeV data measured at different laboratories. Further analysis of the uncertainties in the data and further reliable measurements are needed to be sure of the experimental database used as benchmark data to estimate the predictive power of the simulation codes.

6. Acknowlegements

The work was initiated under the ISTC Project # 017 and was completed under the Feasibility Study Stage of the ISTC Project # 839.

We thank C.H. Tsao for providing a latest version of the YIELDX code. F.E. Chukreev, V.A. Vukolov and N.V. Stepanov for useful co-operation in the work.

REFERENCES

[1] C. Rubbia, J.A. Rubio, S. Buono, F. Carminati, N. Fiétier, J. Galvez, C. Gelès, Y. Kadi, R. Klapisch, P. Mandrillon, J. P. Revol and C. Roche, CERN Report CERN/AT/95-44(ET) (1995).

[2] C.D. Bowman, in: Proc. Int. Conf. on Accelerator-Driven Transmutation Technologies and Applications, Las Vegas, NV, July 25-19, 1994, eds. E.D. Arthur, A. Rodriguez, and S.O. Schriber, AIP Conf. Proceedings 346 (1994) p. 22.; F. Vennery, " The impact of accelerator-driven transmutation of waste", IAEA Technical Committe Meeting an Feasibility and Motivation for Hybrid Concepts for Nuclear Energy Generation and Transmutation, Madrid, Spain, September 17-19, 1997.

[3] T.Mukaiyama, T.Ogawa, M.Mizumoto, T.Takizuka, R.Hino, and Y.Oyama, "OMEGA program and neutron science project for development of accelerator hybrid system at JAERI", IAEA Technical Committee Meeting on Feasibility and Motivation for Hybrid Concepts for Nuclear Energy Generation and Transmutation. Madrid, Spain. September 17-19, 1997.; T. Takizuka, T.Sasa, K.Tsujimoto, "Hybrid system concepts for nuclear waste transmutation", ibid.

[4] G.S. Bauer, "Research and development for Molten Salt Metal Target", Proc. of the 2nd Int. Conf. on Accelerator- Driven Transmutation Technologies and Applications" (1997) p.803;

[5] A.J. Koning Report ECN-C-93-005, Petten (January 1993);

[6] M.A. Lone, S. Cierjacks, J. Sisterson, E. Menapace, Y. Nakahara, S.M. Qaim, E. Ramström, H. Vonach, S. Pearlstein, R.C. Haight, "Intermediate Energy Nuclear Data Needed for Accelerators", INDC(NDS)-245, "Intermediate Energy Nuclear Data Needed for Applications", Proc. of the Advisory Group Meeting organized by the International Atomic Energy (1991) edited by N.P. Kocherov, p.177. Report ECN-C-93-041. Petten (June 1993).

[7] R. Michel, M. Gloris, H.-J. Lange, I. Leya, M. Lüpke, U. Herpers, B. Dittrich-Hannen, R. Rösel, Th. Sciekel, D. Filges, P. Dragovitsch, M. Suter, H.-J. Hoffmann, W. Wölfli, P.W. Kubik, H. Bauer and R. Wieler, Nucl. Instr. and Meth. B. 103 (1995) 183.

[8] R. Michel and P. Nagel, International Codes and Model Intercomparison for Intermediate Energy Activation Yields, NEA/OECD, Paris, 1997, NSC/DOC(97)-1.

[9] O.V. Shvedov, Yu.E. Titarenko et al., Experimental and calculating research of deep spallation reaction on ^{59}Co induced by 1.2GeV, ITEP PrePrints 1993-81 and 1994-30; Yu.E. Titarenko et al., in: Proc. Int. Workshop on Nucl. Methods for Transmutation of Nuclear Wastes: Problems, Perspectives, Cooperative Research, Dubna, Russia, May 29-31, 1996, eds. M.Kh. Khankhasayev, Zh.B. Kurmanov and H.S. Plendl (World Scientific, Singapore, 1997) p. 207; Yu.E. Titarenko et al., in: Proc. Second Int. Conf. on Accelerator-Driven Transmutation Technologies and Applications, Kalmar, Sweden, June 3-7, 1996, ed. H. Condé (Uppsala University Press, 1997), Vol. 2, p. 585; Yu.E. Titarenko et al., in: Proc. Int. Sem. on Precise Measurements in Nucl. Spectrometry "TIYaS-XI", September 2-5, 1996, Sarov (Arzamas-16), Russia, Voprosy Atomnoi Nauli i Tekhniki, Seriya: Fizika Yadernykh Reaktorov, TIYaS-XI, 1997, p. 184 (in Russian).

[10] Yu.E. Titarenko, et al., Expreimental and computer simulation study of the radionuclides produced in thin ^{209}Bi targets by 130 MeV and 1.5 GeV protons, LANL Preprint LA-UR-97-3787, submitted to Nucl.Instr.Meth.

[11] R. Michel, R. Bodermann, H. Busemann, R. Daunke, M. Gloris, H.-J. Lange, B. Klug, A. Krins, I. Leya, M. Lüpke, S. Neumann, H. Reinhardt, M. Schnatz-Büttgen, U. Herpers,

Th. Sciekel, F. Sudbrock, B. Holmqvist, H. Condé, P. Malmborg, M. Suter, B. Dittrich-Hannen, P.W. Kubik, H.-A. Synal and D. Filges, Nucl. Instr. and Meth. B. 129 (1997) 153 and references theirein.

[12] Yu.E.Titarenko et al., "Experimental Study and Theoretical Simulation of Radionuclide Production in ^{99}Tc irradiated by protons of intermediate energies" Int. Conf. on Nuclear Data for Science and Technology, May 19-24, 1997, Trieste, Italy.

[13] Yu.E.Titarenko, et al. "Experimental Study and Computer Simulation of the Yields of Radioactive Product Nuclei in Thin Targets ^{65}Cu, ^{63}Cu Irradiated by 1.5 and 0.13 GeV Protons and ^{59}Co Irradiated by 1.2 and 0.13 GeV Protons", to be published in Nucl.Instr.Meth.

[14] K.K. Gudima, S.G. Mashnik and V.D. Toneev, Nucl. Phys. A 401 (1983) 329; S.G. Mashnik, Izv. Akad. Nauk. Ser. Fiz. 60 (1996) 73 [Bull. Russian Ac. Sci.: Physics, 60 (1996) 58]; S.G. Mashnik, A.J. Sierk, O. Bersillon and T. Gabriel, Los Alamos National Laboratory Reports LA-UR-97-2905 and LA-UR-97-3176 (1997); http://t2.lanl.gov/publications/publications.html; LANL e-print archive nucl-th/9709014; to be published in *NIM*.

[15] V.S. Barashenkov, Le Van Ngok, L.G. Levchuk, Zh.Zh. Musul'manbekov, A.N. Sosnin, V.D. Toneev and S.Yu. Shmakov, JINR Report R2-85-173, Dubna (1985); V.S. Barashenkov, F.G. Zheregi and Zh.Zh. Musul'manbekov, Yad. Fiz. 39 (1984) 1133 [Sov. J. Nucl. Phys. 39 (1984) 715]; V.S. Barashenkov, B.F. Kostenko and A.M. Zadorogny, Nucl. Phys. A 338 (1980) 413.

[16] G.A. Lobov, N.V. Stepanov, A.A. Sibirtsev and Yu.V. Trebukhovskii, ITEP Preprint ITEP-91, Moscow (1983); A.A. Sibirtsev, N.V. Stepanov and Yu.V. Trebukhovskii, ITEP Preprint ITEP-129, Moscow (1985); N.V. Stepanov, ITEP Preprint ITEP-81, Moscow (1987); N.V. Stepanov, ITEP Preprint ITEP-55-88, Moscow (1988) (in Russian).

[17] T.W. Armstrong and K.C. Chandler, Nucl. Sci. Eng. 49 (1972) 110.

[18] R.E. Prael and H. Lichtenstein, Los Alamos National Laboratory Report LA-UR-89-3014 (1989).

[19] P.G. Young, E.D. Arthur and M.B.Chadwick, Los Alamos National Laboratory Report LA-12343-MS (1992); M.B. Chadwick and P.G. Young, Phys. Rev. C 47 (1993) 2255.

[20] M. Blann, Phys. Rev. C 54 (1996) 1341.

[21] Phys. Rev. C52 (1995) 2620; K. Niita, S. Chiba, H. Takada, and T. Maruyama, Proc. of the Third Workshop on Simulating Accelerator Radiation Environments, KEK Proceedings 97-5 (1997) edited by H. Hirayama, p.1.

[22] T. Nishida, Y. Nakahara, T. Tsutsui: "Development of a Nuclear Spallation Simulation Code and Calculations of Primary Spallation Products", JAERI-M 86-116, (1986), [in Japanese].

[23] C.H. Tsao, priv. comm., R. Silberberg, C.H. Tsao, Astrophys. J. 220 (1973) 315; 335.

[24] M. Foshina, J.B. Martins, O.A.P. Tavares, and V.Di Napoli, Radiochimica Acta 35 (1984) 121-131.

Appendix I: Program of the Third Specialists' Meeting on High Energy Nuclear Data

Program of
3rd Specialists' Meeting on High Energy Nuclear Data
March 30-31, 1998 at JAERI, Tokai, Ibaraki-ken, Japan

[Presentation Time: Talk + Discussion]

Mar. 30 (Mon.)
13:30 – 13:40
1. Opening Address A. Hasegawa (JAERI)

13:40 – 14:00
2. Project of High Energy File Production Chairman: T. Fukahori (JAERI)
2.1 Role of Task Force on JENDL High Energy File Integral Test [15+5]
Y. Oyama (JAERI)

14:00 – 16:00
3. Experiments Chairman: S. Tanaka (JAERI)
3.1 Searching Results of Neutron Induced Differential Experimental Data [30+10]
M. Baba (Tohoku Univ.)
3.2 Searching Results of Proton Induced Differential Experimental Data [30+10]
Y. Watanabe (Kyushu Univ.)
3.3 Experimental Results Performed at Satune [30+10]
S. Meigo (JAERI)

16:00 – 16:20 Coffee Break

16:20 – 17:40
4. Status of Evaluation and Reviewing Method
Chairman: T. Kawano (Kyushu Univ.)
4.1 Status of JENDL High Energy File – Evaluation Method, Tools, etc.) [30+10]
T. Fukahori (JAERI)
4.2 Recommendation of Common Reviewing Method [30+10]
N. Yamano (SAE)

18:00 – 20:00 Reception (Akogi-ga-Ura Club)

Mar. 31 (Tue.)
9:10 – 10:30
5. Processing and Transport Calculation Method
Chairman: K. Ueki (SRI/MOT)
5.1 Results of User Research and Recommendation of New Method [30+10]
A. Hasegawa (JAERI)
5.2 Present Status of Processing Method [30+10] K. Kosako (SAE)

10:30 – 10:40 Coffee Break

10:40 – 12:00
6. Benchmark Tests Chairman: K. Hayashi (Hitachi Eng.)
6.1 Searching Results of Benchmark Experiments [30+10]
H. Nakashima (JAERI)
6.2 Results of Benchmark Test with MCNP Code [30+10]
F. Maekawa (JAERI)

12:00 – 13:00 Lunch

13:00 – 14:30
7. International Trend Chairman: A. Hasegawa (JAERI)
7.1 Review of LANL Activity [20+5] S. Chiba (JAERI)
7.2 Program of High Energy File Preparation in Korea [30+10]
J. Chang (KAERI)
7.3 Intercomparison of Evaluated High Energy Files [20+5]
Y. Lee (KAERI)

14:30 – 14:50 Coffee Break

14:50 – 16:30
7.4 Status of Measurement of High Energy Neutron Induced Fission Cross Section up to 200 MeV [30+10] O.A. Shcherbakov (KRI)
7.5 Neutron-induced Fission Cross Sections of Uranium Isotopes up to 40 MeV [15+5]
V.M. Maslov (RPCPI)
7.6 Experimental and Computer Simulation Study of the Radionuclide Yields from the ADT materials irradiated with Intermediate Energy Protons [30+10]
Y. Titarenko and V.F. Batyaev (ITEP)

16:30 – 16:45
8. Summary Talk M. Kawai (KEK)

Appendix II: List of Participants for the Third Specialists' Meeting on High Energy Nuclear Data

Participant's Names	Affiliations
ARUGA, Takeo	Japan Atomic Energy Research Institute
ASAMI, Tesuo	Data Engineering Inc.
BABA, Mamoru	Tohoku University
BATYAEV, V.F.	Institute for Theoretical and Experimental Physics
CHANG, Jonghwa	Korea Atomic Energy Research Institute
CHIBA, Satoshi	Japan Atomic Energy Research Institute
FOMITCHEF, A.	V.G. Khlopin Radium Institute
FUKAHORI, Tokio	Japan Atomic Energy Research Institute
HASEGAWA, Akira	Japan Atomic Energy Research Institute
HAYASHI, Katsumi	Hitachi Engineering, Co., Ltd.
IWAMOTO, Osamu	Japan Atomic Energy Research Institute
KATAKURA, Jun-ichi	Japan Atomic Energy Research Institute
KAWAI, Masayoshi	High Energy Accelerator Research Organization
KAWANO, Toshihiko	Kyushu University
KONNO, Chikara	Japan Atomic Energy Research Institute
KOORI, Norihiko	Tokushima University
KOSAKO, Kazuaki	Sumitomo Atomic Energy Industries Ltd.
KUROSAWA, Masayoshi	Japan Atomic Energy Research Institute
LEE, Young-Ouk	Korea Atomic Energy Research Institute
MAEKAWA, Fujio	Japan Atomic Energy Research Institute
MAKI, Koichi	Hitachi, Ltd.
MASLOV, V.	Radiation Physics and Chemistry Problems Institute
MATSUNOBU, Hiroyuki	Data Engineering Inc.
MEIGO, Shin-ichiro	Japan Atomic Energy Research Institute
MURATA, Toru	Aitel, Co.
NAKAJIMA, Yutaka	Research Organization for Information Science and Technology
NAKASHIMA, Hiroshi	Japan Atomic Energy Research Institute
NARITA, Tsutomu	Japan Atomic Energy Research Institute
OYAMA, Yukio	Japan Atomic Energy Research Institute
SASA, Toshinobu	Japan Atomic Energy Research Institute
SHCHERBAKOV, O.A.	Petersburg Nuclear Physics Institute
SHIBATA, Keiichi	Japan Atomic Energy Research Institute
SOUKHOVITSKI, E.	Radiation Physics and Chemistry Problems Institute
TANAKA, Susumu	Japan Atomic Energy Research Institute
TERADA, Akihiko	Mitsui Engineering & Shipbuilding Co.,LTD.
TITARENKO, Yu. E.	Institute for Theoretical and Experimental Physics
UEKI, Kotaro	Ship Research Institute
YAMANO, Naoki	Sumitomo Atomic Energy Industries Ltd.
WADA, Masayuki	Japan Atomic Energy Research Institute
WATANABE, Takashi	Kawasaki Heavy Industries Co. Ltd.
WATANABE, Yukinobu	Kyushu University

国際単位系 (SI) と換算表

表1　SI基本単位および補助単位

量	名称	記号
長さ	メートル	m
質量	キログラム	kg
時間	秒	s
電流	アンペア	A
熱力学温度	ケルビン	K
物質量	モル	mol
光度	カンデラ	cd
平面角	ラジアン	rad
立体角	ステラジアン	sr

表2　SIと併用される単位

名称	記号
分，時，日	min，h，d
度，分，秒	°，′，″
リットル	l，L
トン	t
電子ボルト	eV
原子質量単位	u

1 eV = 1.60218 × 10^{-19} J

1 u = 1.66054 × 10^{-27} kg

表3　固有の名称をもつSI組立単位

量	名称	記号	他のSI単位による表現
周波数	ヘルツ	Hz	s^{-1}
力	ニュートン	N	m·kg/s^2
圧力，応力	パスカル	Pa	N/m^2
エネルギー，仕事，熱量	ジュール	J	N·m
工率，放射束	ワット	W	J/s
電気量，電荷	クーロン	C	A·s
電位，電圧，起電力	ボルト	V	W/A
静電容量	ファラド	F	C/V
電気抵抗	オーム	Ω	V/A
コンダクタンス	ジーメンス	S	A/V
磁束	ウェーバ	Wb	V·s
磁束密度	テスラ	T	Wb/m^2
インダクタンス	ヘンリー	H	Wb/A
セルシウス温度	セルシウス度	℃	
光束	ルーメン	lm	cd·sr
照度	ルクス	lx	lm/m^2
放射能	ベクレル	Bq	s^{-1}
吸収線量	グレイ	Gy	J/kg
線量当量	シーベルト	Sv	J/kg

表4　SIと共に暫定的に維持される単位

名称	記号
オングストローム	Å
バーン	b
バール	bar
ガル	Gal
キュリー	Ci
レントゲン	R
ラド	rad
レム	rem

1 Å = 0.1 nm = 10^{-10} m

1 b = 100 fm^2 = 10^{-28} m^2

1 bar = 0.1 MPa = 10^5 Pa

1 Gal = 1 cm/s^2 = 10^{-2} m/s^2

1 Ci = 3.7 × 10^{10} Bq

1 R = 2.58 × 10^{-4} C/kg

1 rad = 1 cGy = 10^{-2} Gy

1 rem = 1 cSv = 10^{-2} Sv

表5　SI接頭語

倍数	接頭語	記号
10^{18}	エクサ	E
10^{15}	ペタ	P
10^{12}	テラ	T
10^{9}	ギガ	G
10^{6}	メガ	M
10^{3}	キロ	k
10^{2}	ヘクト	h
10^{1}	デカ	da
10^{-1}	デシ	d
10^{-2}	センチ	c
10^{-3}	ミリ	m
10^{-6}	マイクロ	μ
10^{-9}	ナノ	n
10^{-12}	ピコ	p
10^{-15}	フェムト	f
10^{-18}	アト	a

（注）

1. 表1～5は「国際単位系」第5版，国際度量衡局 1985年刊行による。ただし，1 eVおよび1 uの値はCODATAの1986年推奨値によった。
2. 表4には海里，ノット，アール，ヘクタールも含まれているが日常の単位なのでここでは省略した。
3. barは，JISでは流体の圧力を表わす場合に限り表2のカテゴリーに分類されている。
4. EC閣僚理事会指令ではbar，barnおよび「血圧の単位」mmHgを表2のカテゴリーに入れている。

換　算　表

力	N(=10^5 dyn)	kgf	lbf
	1	0.101972	0.224809
	9.80665	1	2.20462
	4.44822	0.453592	1

粘度　1 Pa·s(N·s/m^2) = 10 P(ポアズ)(g/(cm·s))

動粘度　1 m^2/s = 10^4 St(ストークス)(cm^2/s)

圧力	MPa(=10 bar)	kgf/cm^2	atm	mmHg(Torr)	lbf/in^2(psi)
	1	10.1972	9.86923	7.50062 × 10^2	145.038
	0.0980665	1	0.967841	735.559	14.2233
	0.101325	1.03323	1	760	14.6959
	1.33322 × 10^{-4}	1.35951 × 10^{-3}	1.31579 × 10^{-3}	1	1.93368 × 10^{-2}
	6.89476 × 10^{-3}	7.03070 × 10^{-2}	6.80460 × 10^{-2}	51.7149	1

エネルギー・仕事・熱量	J(=10^7 erg)	kgf·m	kW·h	cal(計量法)	Btu	ft·lbf	eV
	1	0.101972	2.77778 × 10^{-7}	0.238889	9.47813 × 10^{-4}	0.737562	6.24150 × 10^{18}
	9.80665	1	2.72407 × 10^{-6}	2.34270	9.29487 × 10^{-3}	7.23301	6.12082 × 10^{19}
	3.6 × 10^6	3.67098 × 10^5	1	8.59999 × 10^5	3412.13	2.65522 × 10^6	2.24694 × 10^{25}
	4.18605	0.426858	1.16279 × 10^{-6}	1	3.96759 × 10^{-3}	3.08747	2.61272 × 10^{19}
	1055.06	107.586	2.93072 × 10^{-4}	252.042	1	778.172	6.58515 × 10^{21}
	1.35582	0.138255	3.76616 × 10^{-7}	0.323890	1.28506 × 10^{-3}	1	8.46233 × 10^{18}
	1.60218 × 10^{-19}	1.63377 × 10^{-20}	4.45050 × 10^{-26}	3.82743 × 10^{-20}	1.51857 × 10^{-22}	1.18171 × 10^{-19}	1

1 cal = 4.18605 J（計量法）

= 4.184 J　（熱化学）

= 4.1855 J　（15 °C）

= 4.1868 J（国際蒸気表）

仕事率　1 PS（仏馬力）

= 75 kgf·m/s

= 735.499 W

放射能	Bq	Ci
	1	2.70270 × 10^{-11}
	3.7 × 10^{10}	1

吸収線量	Gy	rad
	1	100
	0.01	1

照射線量	C/kg	R
	1	3876
	2.58 × 10^{-4}	1

線量当量	Sv	rem
	1	100
	0.01	1

（86年12月26日現在）